

05

"Made available under NASA sponsorship
in the interest of early and wide dis-
semination of Earth Resources Survey
Program information and without liability
for any use made thereof."

249032

III
E7.4-10.692
CTR-139225

CALIFORNIA COAST NEARSHORE PROCESSES STUDY
FINAL REPORT
ERTS-1 EXPERIMENT #088

Douglas M. Pirie
Principal Investigator, User ID #DE324
U. S. Army Engineer District, San Francisco
100 McAllister Street
San Francisco, California 94102

David D. Steller
Co-Investigator
Geoscience Division
Geosource International Incorporated
2201 Seal Beach Boulevard
Seal Beach, California 90740

May 1974

Original photography may be purchased from
EROS Data Center
10th and Dakota Avenue
Sioux Falls, SD 57198 color

Final Report

Prepared for:

Goddard Space Flight Center
Greenbelt, Maryland 20771

ORIGINAL CONTAINS
COLOR ILLUSTRATIONS

1088A
RECEIVED

AUG 13 1974

SIS/902.6

Reproduced by
NATIONAL TECHNICAL
INFORMATION SERVICE
U S Department of Commerce
Springfield VA 22151

1. REPORT NO.	2. GOVERNMENT ACCESSION NO.	3. RECIPIENT'S CATALOG NO.
4. TITLE AND SUBTITLE CALIFORNIA COAST NEARSHORE PROCESSES STUDY ERTS-1 EXPERIMENT #088 FINAL REPORT		5. REPORT DATE MAY 1974
		6. PERFORMING ORGANIZATION CODE ERTS-1-III
7. AUTHOR(S) Pirie, Douglas M., DE324 and Steller, David D.		8. PERFORMING ORGANIZATION REPORT #
9. PERFORMING ORGANIZATION NAME AND ADDRESS U. S. Army Engineer District, San Francisco 100 McAllister Street and Geoscience Division San Francisco, CA 94102 Geosource International Inc. Seal Beach, CA 90740		10. WORK UNIT NO.
		11. CONTRACT OR GRANT NO. S-70257-AG
12. SPONSORING AGENCY NAME AND ADDRESS Mr. Fredrick Gordon, Jr., Code 430 Technical Monitor Goddard Space Flight Center Greenbelt, Maryland 20771		13. TYPE OF REPORT & PERIOD COVERED ERTS TYPE III Aug. 1972 - May 1974
15. SUPPLEMENTARY NOTES Prepared in cooperation with Geoscience Division, Geosource International Incorporated, Seal Beach, California.		14. SPONSORING AGENCY CODE
16. ABSTRACT This study analyzes the nearshore processes along the California coast utilizing ERTS-1 imagery. Findings were confirmed using U-2 photography, low altitude aircraft remote sensing and sea truth data. The major objectives include the interpretation of nearshore currents, sediment transport, river discharge and estuarine surface characteristics. Current direction in the coastal area is detectable in such detail that it is now being used in coastal protection, harbor development and ocean engineering projects along the California coast. The surface current characteristics for the three ocean seasons (Oceanic, Davidson and Upwelling) and for each month were plotted. The majority of the information was interpreted from ERTS-1 MSS band 4 (5000-6000 Å). Band 5 (6000-7000 Å) also supplied much useful insight into the location and dynamic characteristics of the main sediment plumes. It is possible to determine river discharge characteristics including offshore plumes, pulsing effect, direction of sediment transport and general location of deposition. A detailed analysis of the Santa Barbara Channel indicated a close correlation between ERTS-1 image density and suspended sediment concentrations. Enhancement of NASA-supplied 70 mm transparencies and magnetic tapes for subtle nearshore features was successfully accomplished. Flying spot scanner density expansion and computer compatible tapes processing provided much useful information. Results of this study are now being utilized in U. S. Army Corps of Engineers operational coastal programs.		
17. KEY WORDS California coast Computer processing Sediment transport Photographic processing Coastal currents Coastal processes		18. DISTRIBUTION STATEMENT Original photography may be purchased from EROS Data Center 10th and Dakota Avenue Sioux Falls, SD 57198 color
19. SECURITY CLASSIF. (of this report) Unclassified	20. SECURITY CLASSIF. (of this page) Unclassified	21. NO. OF PAGES 168
		22. PRICE 11.50

PREFACE

This Type III Final Report for the California Coast Nearshore Processes Study, Contract S-70257-AG, is submitted to the Goddard Space Flight Center for the period August 1972 to May 1974. The report was prepared by the U. S. Army Engineer District, San Francisco, and the Geoscience Division of Geosource International Incorporated, Seal Beach, California. The Geoscience Division of Geosource is an affiliate of Rockwell International Corporation. Prior to October 1, 1973, it was identified as the Earth Resources Programs Group of Rockwell International's Space Division.

The objectives of this study were to analyze nearshore currents, sediment transport and estuarine and river discharges along the California coast through the use of synoptic, repetitive imagery from the Earth Resources Technology Satellite (ERTS). During ERTS-1 overpasses, airborne and sea truth data were collected for comparing and confirming details of nearshore processes that were detected on ERTS imagery. Four test sites along the California coast (San Francisco, Monterey Bay, Santa Barbara Channel, and Los Angeles) were emphasized during the interpretation of the overall ocean surface dynamic structure.

The major conclusion of this study is that the feasibility of utilizing satellite imagery for analyzing littoral and nearshore processes has been proven. The ocean seasons surface dynamics were analyzed and several techniques were developed for interpreting subtle nearshore features. To date the ERTS-1 imagery has been utilized in several Corps operational projects including the study of river mouths. Dredging and groin placement programs alone costs the Corps over \$7 million a year in the California coastal area. The effectiveness of these expenditures can be improved if the scientist and coastal engineer gain a more complete understanding of the natural processes concerned. The use of ERTS-1 information in this understanding is just now being incorporated into coastal analysis programs. Because of the transitory seasonal nature of near-shore processes this study must be continued over an extended time period in order to gain maximum benefit for the Corps operational programs. Benefits are expected to result in reduction in maintenance and engineering costs for shoreline and harbor protection facilities and in reducing storm damage costs due to better engineering of coastal structures.

In this final report the major processing techniques and nearshore parameters that were determined are detailed as follows: (1) distinct seasonal and monthly patterns for sediment transport as a function of ocean current systems and coastal morphology have been identified; (2) large-scale sediment plumes for intermittent streams and rivers extend offshore to heretofore unanticipated ranges as shown on the ERTS-1 imagery. Areas where these plumes contain possible contamination from on-land activities can be traced in detail. This is true of the Santa Clara River - Anacapa Island area;

(3) Computer generated contouring of radiance levels from NASA-CCT's resulted in charts usable for the determination of surface and near-surface suspended sediment distribution; (4) flying spot scanner enhancements resulted in details of sediment features; (5) use of film characteristic curves were successful when photographically processing for maximum contrast in the density range of suspended sediment; (6) data from this study are providing significant information for coastal planning and construction projects.

Recommendations resulting from this study include: (1) continuation of this study so the transitory seasonal nearshore processes can be better understood for use in operational Corps projects; (2) expansion of the dynamic range of the ERTS-1 signal for ocean and nearshore observations; (3) processing of computer compatible tapes so investigators can order single channel tapes; and (4) improvement of ERTS-1 imagery resolution so more precise interpretations can be made.

ACKNOWLEDGEMENTS

In conducting the programs described in this report, the authors have been greatly assisted by several individuals. We wish to express our thanks and gratitude to the following persons who either provided essential inputs to this report or showed special interest in the results.

J. W. Jaman	USACE	Program direction
Col. J. L. Lammie	USACE	Program direction
H. E. Pape	USACE	Program direction
M. J. Murphy	USACE	Data reduction
T. E. Harrowby	Geoscience	Program direction
D. T. Hodder	Geoscience	Sediment transport analysis and overall study advisement
L. V. Lewis	Geoscience	Development of flying spot scanner enhancement development and photography
J. F. Niebla	Geoscience	Computer compatible tape, program development and enhancement techniques
M. G. Ghobadi	Geoscience	Computer compatible tape processing
P. J. Stevens	Geoscience	Photographic processing and aerial photography
S. P. Davis	Geoscience	Typing editing and figure formulating
H. R. Lazar	Geoscience	Figure editing and drafting
E. L. Cohn	Geoscience	Aerial photography and data playback

Thanks is also expressed to the following sources of sea truth, aircraft and interpretation data.

R. Kolpack, Ph.D.	University of Southern California
S. VonderHear	University of Southern California
M. Silver, Ph.D.	California State University, Santa Cruz
A. Margozzi	NASA/Ames Research Center
M. Kolipinski, Ph.D.	National Park Service, San Francisco
H. Baldwin	Photometrics, Inc., Lexington, Massachusetts
F. Parsons	Photometrics, Inc., Lexington, Massachusetts
D. Robinson	National Park Service, Oxnard, California
G. Robertson	National Park Service, Oxnard, California
R. Ecker	USACE, San Francisco, California
M. Knutson	NASA/Ames Research Center, Earth Resources Aircraft Project
Earth Science Department,	California State University, Fullerton

TABLE OF CONTENTS

<u>Section</u>	<u>Page</u>
1.0 INTRODUCTION AND SUMMARY	1
2.0 NEARSHORE PROCESSES	11
3.0 ENHANCEMENT TECHNIQUES	31
3.1 FLYING SPOT SCANNER (FSS) ENHANCEMENTS	31
3.1.1 Analog Preprocessing Technique	32
3.1.2 Hybrid Digital/Analog Technique	36
3.1.3 FSS Modifications and Improvements	37
3.2 COMPUTER PROCESSING CCT'S	39
3.2.1 Products	39
3.2.2 CCT's Processing Step	42
3.2.3 Software Processing	42
3.3 MULTI-CHANNEL COMPUTER PROCESSING	53
3.4 PHOTOGRAPHIC OPTICAL PROCESSING	54
4.0 CALIFORNIA COASTAL CURRENTS	65
4.1 GENERAL HISTORICAL DESCRIPTION	67
4.2 CURRENT SUMMARY	67
4.2.1 Oceanic Current Period	68
4.2.2 Davidson Current Period	79
4.2.3 Upwelling Period	85
5.0 SUSPENDED SEDIMENT ANALYSIS	115
5.1 APPROACH TO ERTS DENSITY VS. SUSPENDED SEDIMENT CONCENTRATION	115
5.2 SURVEY OPERATIONS FOR SEDIMENT QUANTIFICATION	123
5.3 EXPERIMENT ANALYSIS OF 1973 SEDIMENT DATA	129
5.4 CONCLUSIONS	137

TABLE OF CONTENTS (Continued)

<u>Section</u>	<u>Page</u>
6.0 CONCLUSIONS	139
7.0 RECOMMENDATIONS	143
8.0 REFERENCES	145
APPENDIX A - SUMMARY OF FLIGHT OPERATIONS	149
APPENDIX B - ANCILLARY SUPPORT EQUIPMENT	155
APPENDIX C - ERTS DATA UTILIZATION	159
APPENDIX D - ATMOSPHERIC EFFECTS	163

LIST OF ILLUSTRATIONS

<u>Figure</u>		<u>Page</u>
1-1	Cape Mendocino - January 1, 1974	5
1-2	Northern Test Cell Outlined	6
1-3	Southern Test Cells Outlined	7
1-4	Crescent City Area High Altitude Infrared Color	8
1-5	Santa Cruz - Monterey Bay	9
2-1	Eel River - Cape Mendocino	12
2-2	Pt. Conception - Santa Barbara	13
2-3	Bolinas Bay	17
2-4	Santa Barbara Channel - 1109-18073-4	18
2-5	Humboldt Bay - U-2 Photography	21
2-6	Humboldt Bay - Effluents	23
2-7	San Francisco - U-2 Photography (NASA)	25
2-8	Humboldt Bay	26
2-9	San Francisco - Monterey Bay	27
2-10	San Francisco Bay - Infrared Color	28
2-11	Russian River-Bodega Head High Altitude False Color	29
2-12	Southern California 1180-18015-4	30
3-1	San Francisco FSS Enhancement, Scene 1130-18235-4	33
3-2	San Francisco FSS Enhancement, Scene 1130-18235-5	34
3-3	Signal Limiter	35
3-4	FSS Enhancement of ERTS Frame 1234-18021	38
3-5	Decimal Equivalent Plot - Santa Barbara Channel	40
3-6	Isodensity Contour Analysis of Santa Barbara Channel, Scene 1234-18021-4	41
3-7	FSS Enhancement of Monterey Bay	43
3-8	Processing Flow Chart - Bulk and Precision CCT	44
3-9	Precision CCT Processing Flow Chart	45
3-10	Bulk CCT Processing Flow Chart	46
3-11	Contouring Program Flow Chart	49
3-12	Digital Dump of Monterey Bay Contour Map, Scene 1183-18182-4	50
3-13	Contour of Santa Barbara Channel	51
3-14	Santa Barbara - Anacapa, Scene 1234-18021	55
3-15	Ratioing of Scene 1234-18021, Santa Barbara - Anacapa Area	56
3-16	Subtraction of Scene 1234-18021, Santa Barbara - Anacapa Area	57
3-17	Characteristic Curve	58

LIST OF ILLUSTRATIONS (Continued)

<u>Figure</u>		<u>Page</u>
3-18	Characteristic Curve for Kodak 2430 (Kodak, 1969)	60
3-19	ERTS-1 Characteristic Curve Enhancement	62
3-20	San Francisco Area Kodak 2575 Film	63
4-1	Summary of ERTS Imagery Useful to Nearshore Processes	66
4-2	California Coastal Currents Summary - ERTS-1	69
4-3	Summary of Inshore Currents from ERTS-1	70
4-4	Summary of Offshore Currents from ERTS-1	71
4-5	Oceanic Current Plot - Northern California	73
4-6	Oceanic Current Plot - Southern California	74
4-7	Oceanic Period Mosaic (May-November 1973)	75
4-8	Oceanic Current Period (May-November 1973)	76
4-9	Davidson Current Plot - Northern California (November 1972-January 1973)	80
4-10	Davidson Current Plot - Southern California (November 1972-January 1973)	81
4-11	Davidson Current Period Mosaic	82
4-12	Davidson Current Period Mosaic (November 1972-January 1973)	83
4-13	Upwelling Current Plot - Northern California	87
4-14	Upwelling Current Plot - Southern California	88
4-15	Upwelling Period Mosaic	89
4-16	Upwelling Period Mosaic (March-April 1973)	90
4-17	Southern California Coastal Currents - January 1973	91
4-18	Northern California Coastal Currents - January 1973	92
4-19	Southern California Coastal Currents - February 1973	93
4-20	Northern California Coastal Currents - February 1973 and 1974	94
4-21	Southern California Coastal Currents - March 1973	95
4-22	Northern California Coastal Currents - March 1973	96
4-23	Southern California Coastal Currents - April 1973	97
4-24	Northern California Coastal Currents - April 1973	98
4-25	Southern California Coastal Currents - May 1973	99
4-26	Northern California Coastal Currents - May 1973	100
4-27	Southern California Coastal Currents - June 1973	101
4-28	Northern California Coastal Currents - June 1973	102
4-29	Southern California Coastal Currents - July 1973	103
4-30	Northern California Coastal Currents - July 1973	104
4-31	Southern California Coastal Currents - August 1973	105
4-32	Northern California Coastal Currents - August 1972 and 1973	106
4-33	Southern California Coastal Currents - September 1973	107
4-34	Northern California Coastal Currents - September 1972 and 1973	108
4-35	Southern California Coastal Currents - October 1972 and 1973	109
4-36	Northern California Coastal Currents - October 1972 and 1973	110

LIST OF ILLUSTRATIONS (Continued)

<u>Figure</u>		<u>Page</u>
4-37	Southern California Coastal Currents - November 1972 and 1973	111
4-38	Northern California Coastal Currents - November 1972	112
4-39	Southern California Coastal Currents - December 1972 and 1973	113
4-40	Northern California Coastal Currents - December 1973	114
5-1	Mugu Lagoon & Ocean Water Sediment Loads and Spectral Transmittance	117
5-2	Film Density Vs. Sediment Load & Optical Extinction	118
5-3	Calibration Curve for Sediment Load Vs. Film Density in Median California Coastal Waters (Fi	119
5-4	Attenuation of Blue-Green Light Vs. Sediment Loading	120
5-5	Tentative Mapping of Near-Surface Suspended Sediment from ERTS Imagery	121
5-6	Sea Truth Stations - November 21, 1973	125
5-7	Sea Truth Stations - December 9, 1973	126
5-8	Flight Lines - November 21, 1973 ERTS Underflight Altitude 3048 Meters	127
5-9	Flight Lines - December 9, 1973 ERTS Underflight Altitude 3048 Meters	128
5-10	Airborne Photo Evidence of Nearshore Sediment Inhomogeneity	131
5-11	Comparison of Unnormalized ERTS Film Density Sediment Load and Extinction Depth, 9 December 1973	132
5-12	Comparison of Unnormalized ERTS Film Density Sediment Load and Extinction Depth, 21 November 1973	133
5-13	Comparison of Available Light Spectrum - Ventura	134
5-14	Clearest Waters ERTS Scene Normalized Density Vs. Sediment Load (10/9 and 11/21/73) Average of all Values	135
5-15	Normalized ERTS Density Values Vs. Suspended Sediment Load (Bands 4 and 5, 11/21/73 and 12/9/73)	136
A-1	ERTS-1 Underflights - Geoscience	153
B-1	EDP Scan - Santa Barbara Area	158
C-1	X-Band Side Looking Radar Image of Monterey Bay and the Carmel Carmel Basin	
C-2	Unenhanced ERTS-1 MSS Channel 5 for 1/22/73, Monterey Bay and the Carmel Basin	162
C-3	Analog Derivative and Thresholding of MSS Channel 5	162
D-1	ERTS-1 Strip 1, Block 1, Frame 1235-18075-4 and -5	164

LIST OF TABLES

<u>Table</u>		<u>Page</u>
2-1	Nearshore Processes Detectable from ERTS-1 Imagery	15
5-1	Recalibration Data	122
5-2	Sea Truth Data	124
A-1	ERTS-1 Underflights - Geoscience	152

INTRODUCTION AND SUMMARY

The objectives of this Earth Resources Technology Satellite (ERTS) study have been to analyze nearshore currents, sediment transport, estuary surface characteristics and river discharges along the California coast. During selected ERTS-1 overpasses, high altitude aircraft photography, low altitude aircraft photography, and sea truth data were collected for comparing and confirming details of nearshore processes that were detected on ERTS imagery. Four test sites along the California coast (San Francisco, Monterey Bay, Santa Barbara Channel and Los Angeles) were emphasized during the interpretation of the entire coastal ocean surface dynamic structure. Several techniques for extracting information from the ERTS transparencies and magnetic tapes were successfully applied. This information is being incorporated into U. S. Army Corps of Engineers (Corps) ongoing operational projects. The benefits from using ERTS-1 in these projects are expected to result in more efficient utilization of Corps maintenance and engineering funds. Each shoreline and harbor protection facility requires a detailed analysis of coastal processes and local study before management decisions can be made on the project construction and financing. In addition, the results of constructed facilities require continuous monitoring. Periodically, modifications, repairs, and additions to shoreline structures maintained by the Corps are required. In each of these instances it is necessary to obtain the most current available data on the ocean forces acting on the structures. The ERTS-1 imagery presents a source of continually updated information which can be applied to these ongoing operational problems.

Besides the use of standard photographic interpretation methods, flying spot scanner (FSS) enhancements and various computer compatible tape (CCT) processing techniques were utilized in this study. These procedures were used in the enhancement of subtle nearshore features that were difficult or impossible to interpret without processing. It was possible to plot the currents monthly and seasonally for three major California coastal current periods (Oceanic, Davidson, and Upwelling) utilizing a combination of these methods. Using the information from these three plots as background, detailed test site studies were carried out by the Corps of Engineers as partial fulfillment of their operational requirements. These analyses were done primarily using ERTS-1 MSS Band 4 data supplemented by Band 5.

In studying currents, sediment transport, river discharges and estuaries, it is necessary that a detectable trace material be present in the nearshore waters as shown in Figure 1-1. During the majority of the year, sufficient material is provided by river and stream discharge supplemented by coastal erosion by storm action and littoral currents. This is true along the northern California coast throughout this year. Along southern California, the lack of rainfall from about May until fall results in little runoff presenting some problem in studying nearshore processes. During a majority of the ERTS-1 overpasses, however, wave action and littoral currents have resulted in sufficient

suspended sediment along the coast for at least limited detection of currents and transport direction. During the time of large storms, when great volumes of runoff and sediment are discharged into coastal water, sediment plumes remain for over 18 days on repeat ERTS-1 orbits.

The boundaries of the test cells that were originally defined are shown on Figures 1-2 and 1-3. Once the ERTS-1 imagery arrived and analysis commenced, it became apparent that limiting study to these boundaries would not result in valid findings. As current and sediment patterns often originated outside the test sites, it was decided to investigate the entire coastal current pattern and related nearshore processes.

The primary scientific result is a collection of up to date information on the nearshore environment of California. At many California coastal locations there is unpredictable seasonal sediment deposition or erosion. Changes occur in the source of material, nearshore currents and transport characteristics. The general process is very complex and not thoroughly understood. Using the sea truth and aircraft surveys as calibration, however, the analysis of ERTS-1 imagery yields the following information: (1) definition of the source of sediments being transported, (2) the location of nearshore eddies and gyres, (3) nodal points of coastal water surface motion, (4) basic sediment patterns from season to season, (5) differential California water penetration capability, and (6) the effect of wind and coastline shape on nearshore subsurface deposition and erosion. It is also possible to emphasize the various sediment layers within a riverine discharge lobe utilizing contrast enhancement of aircraft and satellite collected magnetic tape data. Flying spot scanner enhancements have proven to be especially useful in detecting subtle suspended sediment distributions. The suspended sediment distribution detection combined with water penetration analysis is particularly applicable to the problem of boundary definition and has definite possibilities in the continuing analysis of the various water bodies associated with estuarine flushing.

Operational projects of the Corps are where these scientific results are being applied. These projects include protecting and developing the California coastal area. The feasibility of satellite imagery for analyzing littoral and nearshore processes has been proven during this ERTS-1 program. The ocean season surface dynamics were analyzed and several techniques developed for interpreting subtle nearshore features. To date the ERTS-1 imagery has been utilized in several Corps operational projects including the study of river mouths.

The following descriptions of proposed studies are preliminary, but the basic scopes of work are known and have typical direct requirements for ERTS-1 type data:

- (a) Crescent City, California - The Corps study of approximately \$30,000 will define the littoral current, and wave climate between Crescent City and Point Saint George. Field surveys are required and computer program analysis of wave energy is possible. ERTS-1 type imagery can input the majority of nearshore current data required for this study.
- (b) Moss Landing, California - This \$50,000 engineering study will evaluate the littoral and nearshore environment of Moss Landing Harbor and define the corrective measures necessary to restrict erosion and accretion of sand in the harbor. ERTS-1 data can aid in corrective inputs for computerized sand transport analysis of wave energy, as well as circulation in Monterey Bay. The costs for construction of the project could be approximately \$4 million.

During the study, high altitude aircraft photographic missions were flown along the coast by NASA-Ames Research Center. These flights, usually from 19812 m (65,000 feet), supplied a number of valuable oblique images which were used to confirm ERTS-1 interpretations. The swath width of almost 30 km provided detail, resolution and areal coverage which was significant in the overall interpretations. A number of these images are included with this report to demonstrate the impressive capabilities of the NASA high altitude remote sensing platform.

The most useful techniques for nearshore processes analyses were found to be flying spot scanner (FSS) enhancements, processing of computer compatible tape (CCT) data and orbit-by-orbit interpretation of photographically enhanced imagery. The FSS was utilized to amplify the small portion of the density range which represented the nearshore processes features of interest. This expansion took place prior to recording and film playback so the film could be used directly in interpretation. These same techniques were used in conjunction with dual channel ratioing and subtraction for studying quantitative sediment concentrations and distributions. The CCT multispectral scanner (MSS) data was processed for interpretation using three basic techniques: discrete point density analysis; isodensity contour analysis; and mass concentration image analysis. Each of these methods proved useful in sediment distribution and concentration analysis as described in Section 3.0, Enhancement Techniques.

The photographic methods utilized during this study varied from standard enlargement and printing to precision variations of exposures, film type and processing. In each case, the ultimate goal was enhancement of nearshore features. The use of negative prints was determined to be most useful, as was the use of highly sensitive Kodak 2575 duplicating film. Each of these techniques resulted in pictures of ERTS images showing more detail than the original imagery since they provided better contrast for viewing.

The quantitative distribution of the suspended material in the nearshore area was studied in detail at several test sites, including the Santa Barbara Channel and the Los Angeles area. This was possible when ocean surveys which collected water samples

or transmissometer measurements allowed for the determination of sediment concentrations. It was necessary that this data be collected simultaneously with an ERTS-1 overpass and low altitude aircraft underflights on a clear day. Data from several surveys provided sufficient information for interpretation. It was deemed possible to correlate changes in sediment concentrations from ocean stations with film density recorded by ERTS. This technique must be refined and expanded over a much larger test area, however, before accurate sediment budgets can be predicted.

The feasibility of using satellite imagery in conjunction with low altitude aircraft imagery for analyzing oceanic and nearshore processes has been proven during this study. Benefits are already being realized by the Corps of Engineers in several operational projects, including the study of river discharge sediment distribution characteristics. This information is used by the Corps in developing methods of coastal protection and in improving coastal engineering knowledge. Specific nearshore data from ERTS-1 are presently being applied to the Russian River Comprehensive Study, Salinas Wastewater Study, as well as various coastal studies concerned with littoral drift, dredging, and river discharges of sediment. Because of the transitional nature of the features being studied it is now essential that this type of analysis continue. In that way, it will be possible to develop the historical background information on coastal processes that can provide the Corps operational units with cost effective data to support their design, construction and maintenance responsibilities.

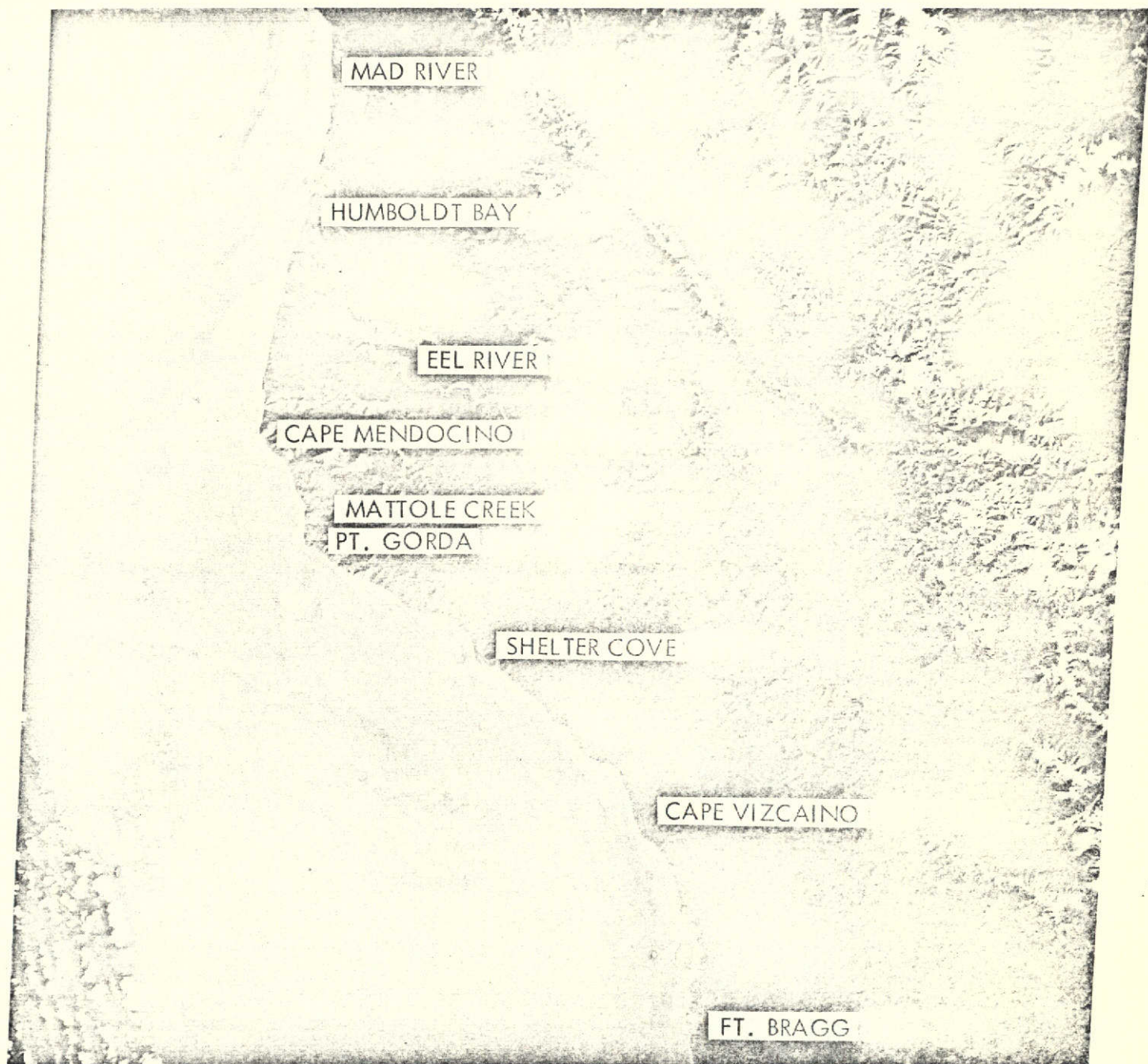


Figure 1-1. Cape Mendocino - January 1, 1974

This channel 4 (5000-6000 Å) ERTS-1 image of the Northern California coast graphically illustrates the affect of coast currents on discharging suspended sediments. The current is to the south transporting material from the Mad and Eel Rivers and a number of creeks. In the offshore area several lobes of material are visible. Off Cape Vizcaino a reverse gyre has formed as a result of a northwest moving current. This picture represents 185 x 185 km.

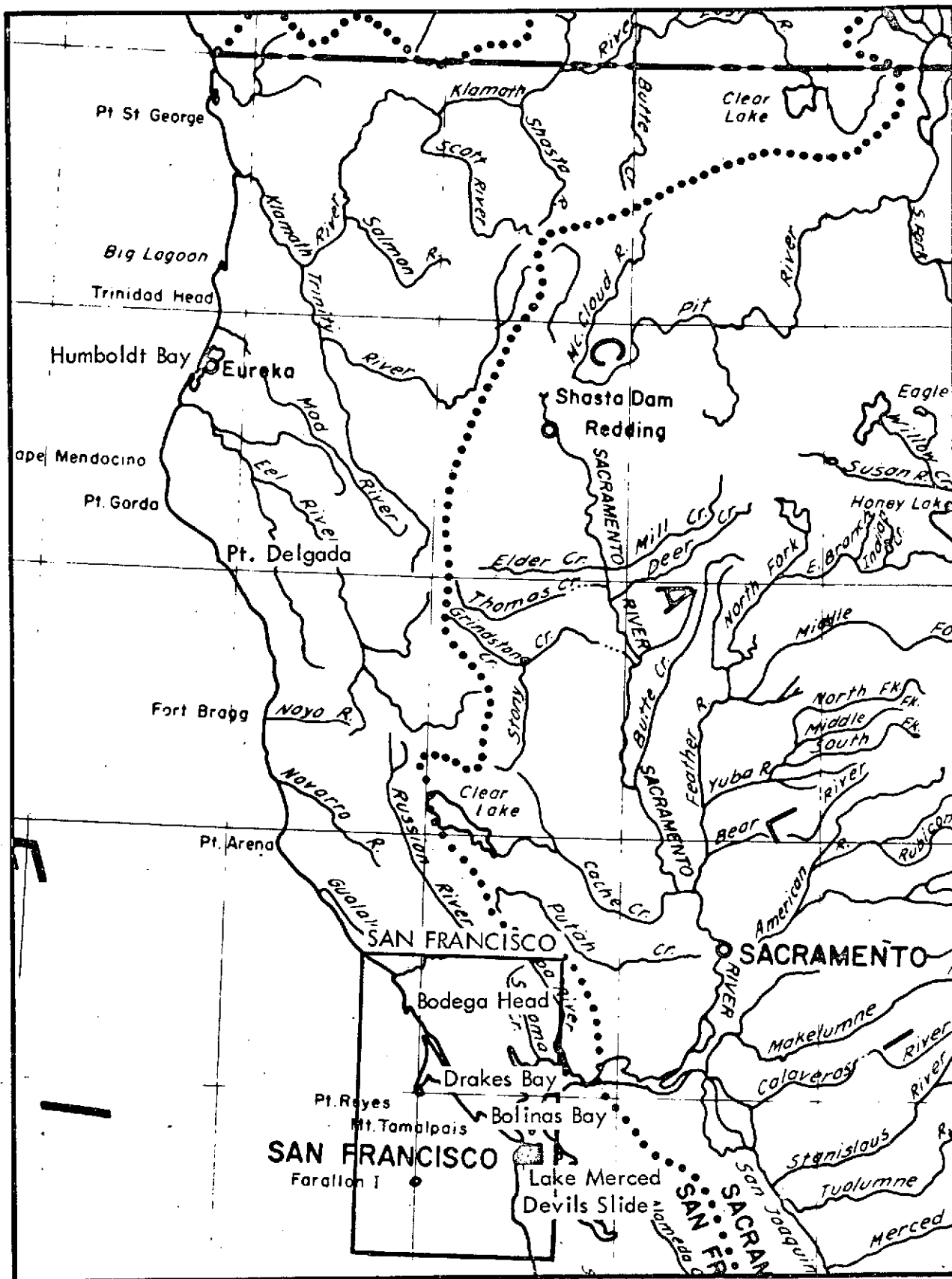


Figure 1-2. Northern Test Cell Outlined

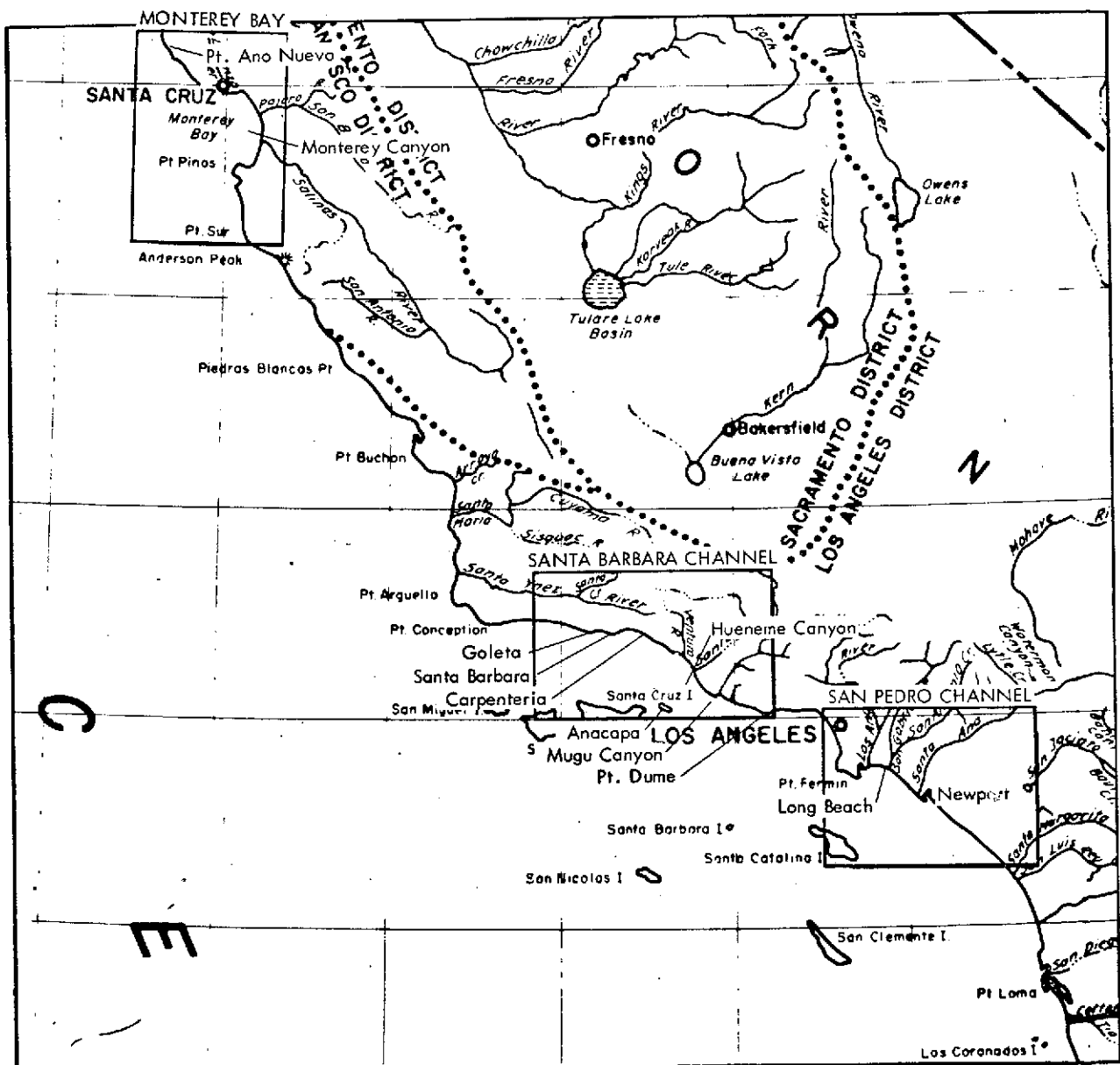




Figure 1-4. Crescent City Area High Altitude Infrared Color. The picture was taken from approximately 19812 meters during the Davidson Current Period. Crescent City, California is just east (left) of Pt. St. George in the center of the picture. The oblique view is southeast along the California coast. A gyre is set up off Pt. St. George moving sediment from the Smith River (foreground) counterclockwise toward Crescent City. Rock wakes are visible south of the St. George Reefs. Large amounts of suspended sediment is being discharged from the Klamath River seen south of Crescent City. The dominant current in the area is the southward California Current.

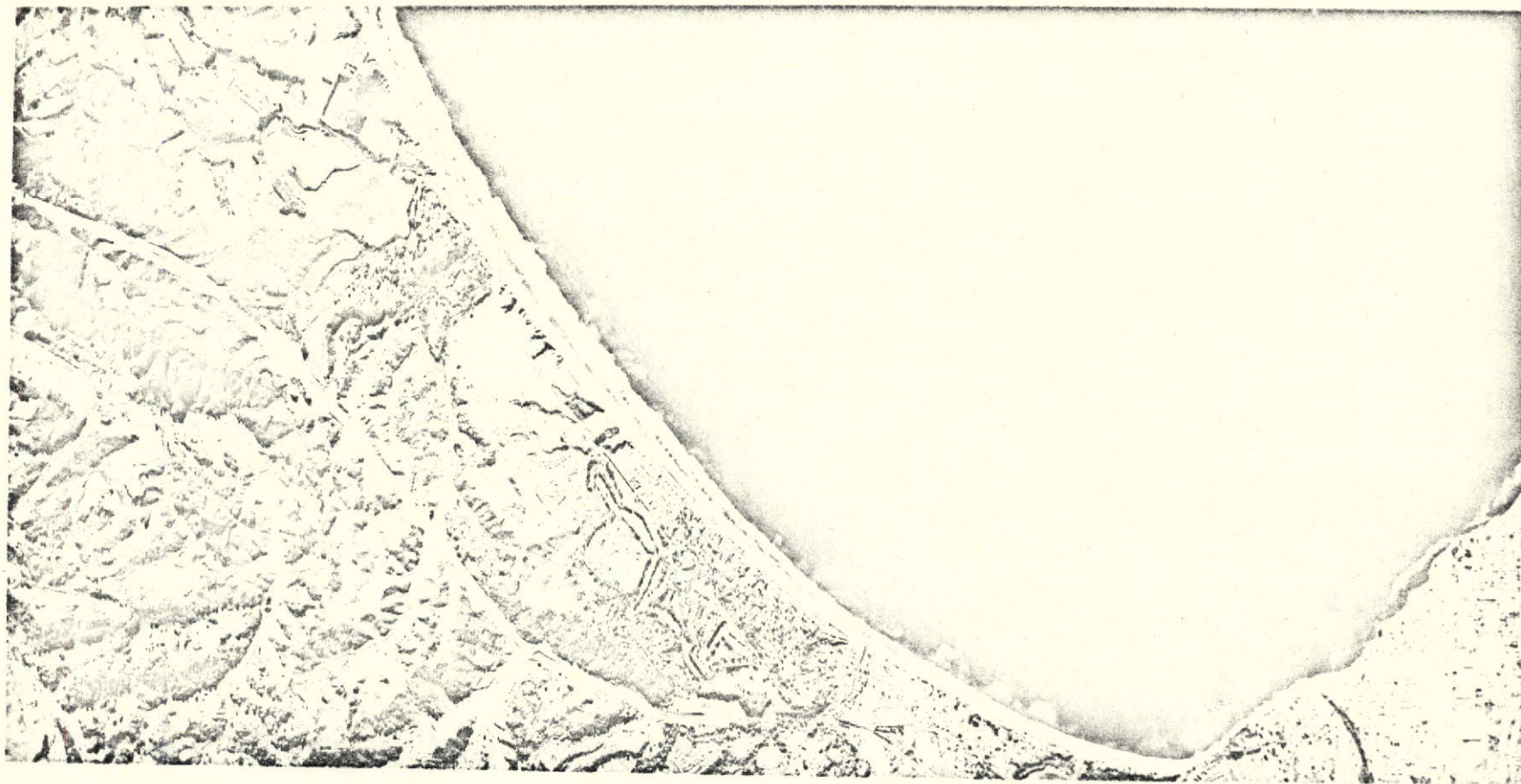


Figure 1-5. Santa Cruz - Monterey Bay

This color infrared picture illustrates the sediment transport in Monterey Bay. The shoreline west of Santa Cruz (top) is eroding critically (NSS, 1971). The original of this picture was taken by NASA on a 228 x 456 mm (9 x 18 in.) format. The Santa Cruz coastal area is being studied for shore protection facilities.

2.0 NEARSHORE PROCESSES

ERTS-1 imagery contains information of significant value for coastal engineering studies. In this analysis, it has been possible to view the parameters affecting sediment transport, nearshore currents, riverine discharge and estuarine flushing under a variety of seasonal and tidal periods. Precipitation, run-off, wind, waves, surface current, bottom contours, temperature, water column dynamics and salinity all have variable effects on these processes. It was impossible to monitor all of these variables in detail, but they were considered and utilized as available. The interpretations that were made utilized a combination of standard photographic and automatic processes described in detail in other sections of this report. Included with the following brief descriptions of the main study objectives are exemplary figures that illustrate the features. The ERTS information analysis and the interpreted seasonal variations have been monitored throughout the 18-month study period, and the resulting analyses are being utilized in ongoing Corps studies.

Sediment Transport

The transported sediment that was monitored includes suspended particulate matter being moved by currents and sand particles transported mainly by littoral drift. The importance of the sediment is that it acts as the tracer which is visible in the satellite imagery. The technique for detecting the location and distribution is discussed in detail in Sections 3.0, 4.0 and 5.0. The FSS enhancements and the suspended sediment measurements represent valuable processes that were used in this study. In some cases, wind blown particles deposited in the nearshore zone are also of significance. The smaller silt and clay stay in suspension because of the upward component action of the current velocity. Temperature, salinity and the resulting density differences in varying water bodies act in concert with ocean dynamics to keep particles in suspension. Suspended sediments are eventually deposited due to settling and flocculation. Sand particles which have been thrown into suspension by the turbulence of the breaking waves are moved by littoral drift. The direction and amplitude of a wave attack determine the direction and magnitude of the littoral draft at a given time. Figures 2-1 and 2-2 are examples of the detailed sediment transport detectable from ERTS.

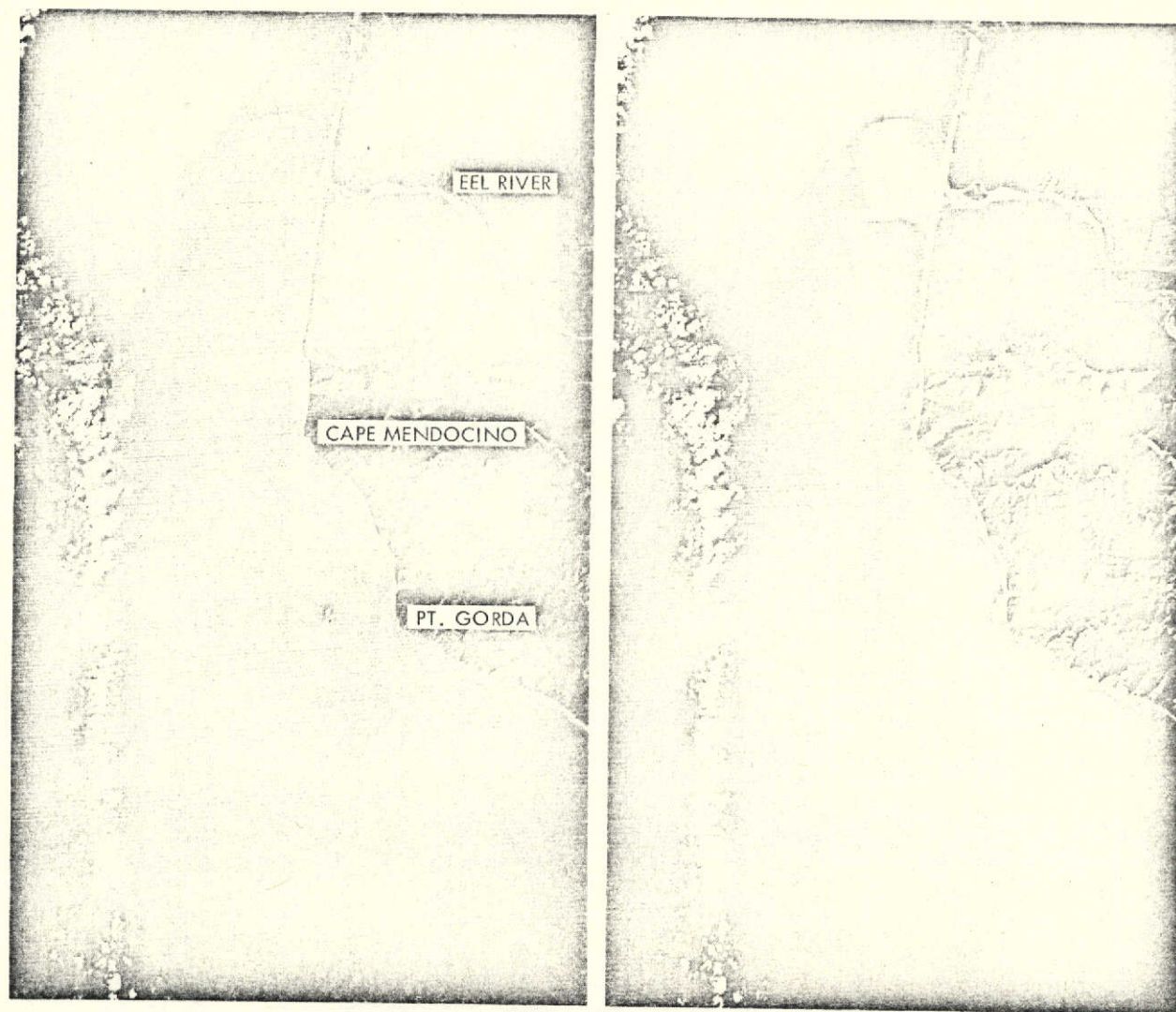


Figure 2-1. Eel River - Cape Mendocino

Riverine discharge and sediment transport as affected by the California current moving southward. The Eel River, which draws the fastest eroding basin in the United States, is visible top center. The Mattole Creek, at Pt. Gorda is also discharging a large volume of suspended material into the Pacific Ocean. Layering in the offshore sediment pattern and several large gyres are clearly visible. The channel 4 imagery defines the outer boundary of the sediment discharge and nearshore erosion. This image was collected on January 2, 1974.

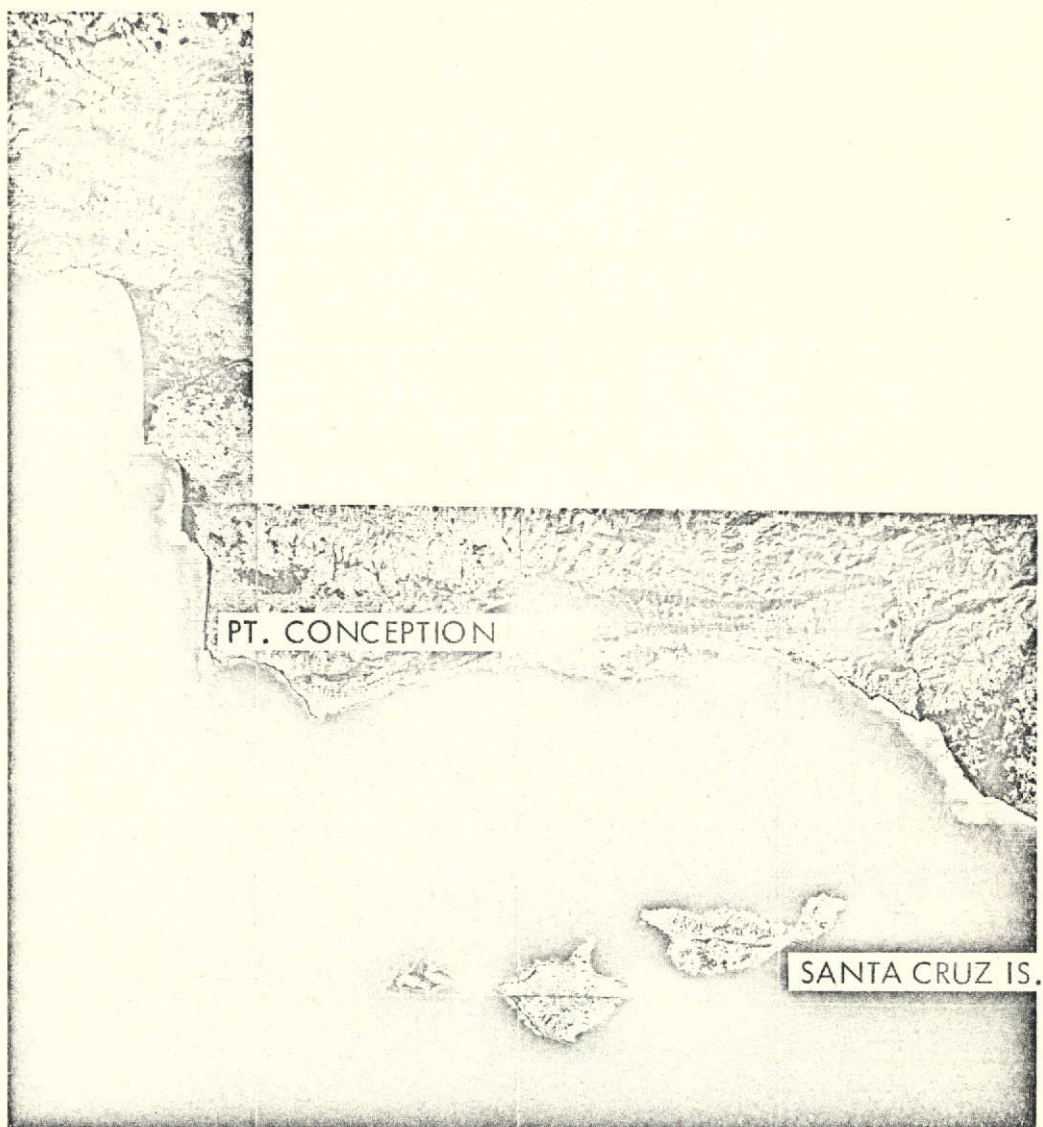


Figure 2-2. Pt. Conception - Santa Barbara. This flying spot scanner enhancement (medium gain) of the Santa Barbara Channel shows a distinct counterclockwise gyre off Pt. Conception. On March 15, 1973, when this image was collected, the north-northwest moving Davidson Current was still affecting the coastal currents. A large lobe of material is moving northward adjacent to Santa Cruz Island.

Nearshore Currents

The nearshore currents are directly related to the sediment transport problem in that the suspensates act as the current pattern tracers which are viewed from the satellite remote sensor platform. The flow pattern set up by nearshore currents is quite different from day to day as seen in the current charts in Section 4.0. The nearshore currents are definitely detectable from ERTS data present on photographic prints and CCT magnetic tapes. The various dynamic changes within the current structure can be enhanced using FSS techniques and magnetic tape processes to emphasize subtle features, see Section 5.0. In analyzing ERTS-1 imagery, it is possible to view currents and related tracer features ranging from the relative large-scale Anacapa current in the Santa Barbara channel down to gyres found off Bolinas Lagoon and the Russian River and pollution off Humboldt Bay, Figures 2-3 through 2-8.

Estuarine Flushing

The study area encompasses several estuary type water bodies of sufficient size to be monitored by satellite imagery (i.e., Humboldt Bay, San Francisco Bay, Bolinas Lagoon, Newport Bay). Although Bolinas Lagoon and Newport Bay receive no fresh water during part of the year, they are included because of their size and importance. Each of these areas is surrounded by a population which has a variety of demands on the water body ranging from recreation to sewage outfalls. As indicated in Figures 2-9 and 2-10, it is possible to trace water movement patterns in estuaries by utilizing sediment as a tracing medium. There are inherent problems such as interference patterns from wind shear and shallow water features which must be accounted for in using the visible patterns as dynamic pattern indicators. These problems are partially compensated for, however, in that the satellite imagery provides a synoptic, repetitive coverage, and also a reasonable resolution capability.

The South Bay of San Francisco Bay estuary is a good example of a water body which requires continual monitoring. In the South Bay, phosphate content increases because of the lack of flushing during certain seasons of the year. The phosphate is due to discharge into South Bay from a number of communities. The phosphate concentration is controlled by the flow of fresh water from the Sacramento River which is seasonal.

Riverine Discharge

Large quantities of sediment are brought into the nearshore area by riverine discharges. As the suspended sediments and fresh river water mix with the saline ocean water, a decrease in velocity causes settling of the larger particles (i.e., sand). Flocculation also causes further deposition. The sediments discharged from the rivers are affected by a new set of forces including the longshore currents, tidal currents and the complex dynamics of movement of sand along beaches. The supply, or lack of supply, of these sediments and their movement greatly affect the entire nearshore processes picture. Thus, they represent a most important link in this overall study. It has been found by reviewing the ERTS-1 imagery that the direction and effect of coastal currents on riverine suspended sediment loads can be clearly seen. The major rivers (Eel, Klamath, Russian, Sacramento, San Joaquin, Ventura, Santa Clara, Los Angeles, San Gabriel, and Santa Ana), which empty into the test cells, act as a continuous source of tracer material for use in analyzing sediment transport, nearshore currents and estuarine flushing as seen in Figures 2-10 to 2-11. Since the sediment source varies greatly, it is necessary to monitor riverine discharges for several seasons to acquire sufficient temporal data for possible forecasting.

The detectability of nearshore processes is the result of the combination of the feature characteristics, the sensor specification and resolution, and the ability to enhance the image signal. Although ERTS was not designed specifically for nearshore or oceanographic feature detection, investigation has shown that this imaging obstacle can be sufficiently overcome. Below is a summary list of nearshore processes and coastal features along with their detectability from ERTS.

TABLE 2.1 Nearshore Processes Detectable from ERTS-1 Imagery

O - Observable, NO - Not Observable			
Gyres	-	O	Normally associated with promotories
Beach Width	-	O	Possible for large changes (i.e., between summer and winter)
Cliff Erosion	-	O	Effects seen as suspended sediment
Crescent Beaches	-	O	Seasonal changing beaches
Current Speed	-	NO	Must be confirmed by Sea Truth
Depth Variations	-	NO	This is possible but need further confirmation to prove results
Estuary Water Surface Characteristics	-	O	Depends on size and suspended sediment
Island Wake	-	O	Channel Islands show examples
Kelp	-	O	Can be located - help define bathymetry and bottom characteristics
Longshore Currents	-	O	Tracer turbidity necessary

TABLE 2.1 (Continued)

O - Observable, NO - Not Observable			
Pollution	-	O	Dispersion of pollutants from large effluent discharge, i.e., Humboldt Bay
Red Tide	-	NO	Possible but needs further confirmation
Rip Currents	-	NO	Must be very large and transporting large volume of suspensates, possible future
River Stages	-	O	Dispersion characteristics, sand discharge, initial flooding
Sediment Transport	-	O	Detail detectable, see Section 4
Sediment Transport Quantification	-	O	This is possible by a large-scale ocean station sampling necessary for confirmation
Tidal Variations	-	O	Estuaries, back bays
Wave Phenomena	-	NO	Effects seen on longshore currents
Wind Blown Dust	-	O	Off canyons, tails from islands

The above table gives a brief summary of the nearshore features, some of which are described in detail in Section 3.0 - 5.0.

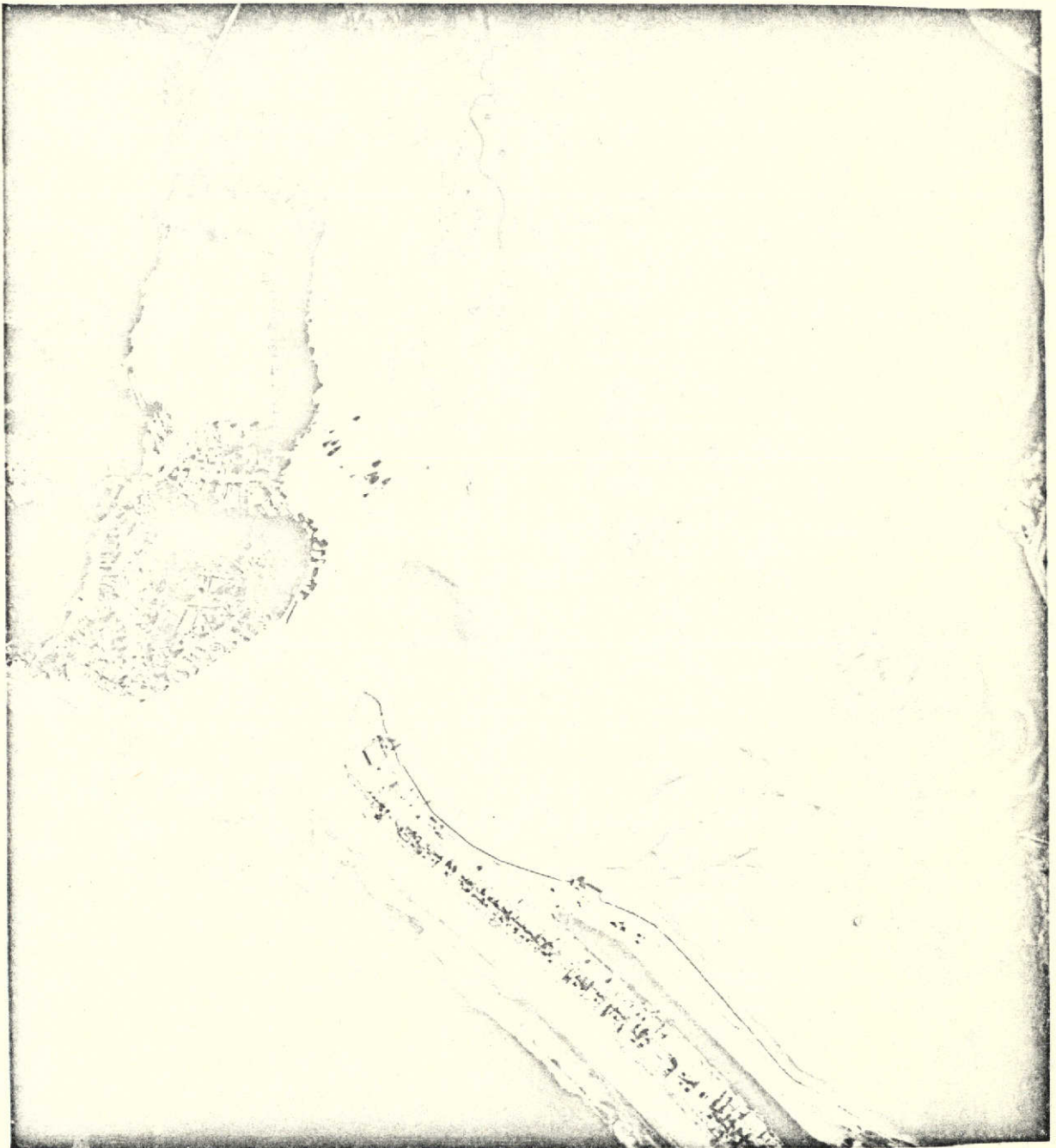


Figure 2-3. Bolinas Bay

Wave refraction is visible at bay entrance. Critical erosion is taking place at the base of the cliff on the northwest (left) side of the bay entrance. The tide is ebbing.

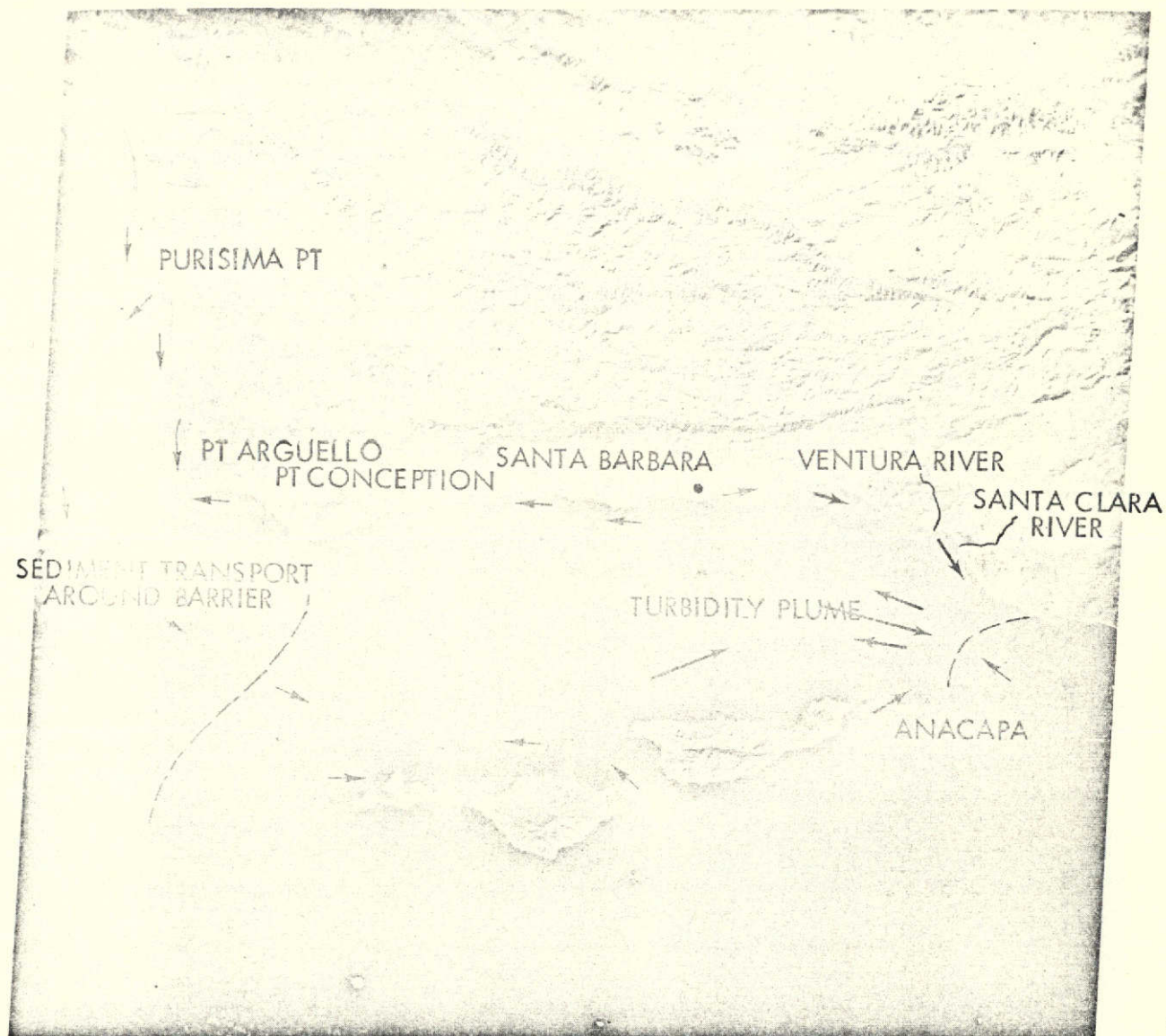


Figure 2-4. Santa Barbara Channel 1109-18073-4

The MSS-4 band provides definition of the maximum extent of suspended sediment. Current direction is indicated by arrows. Sediment gyres and eddies around the coastal points and barrier headlands reveal transfer of sediment between the commonly assumed typical California coastal sediment cells with discrete fluvial or mass wasting sources and a down drift sink (submarine canyons). The Anacapa Current effect is clearly evident between Anacapa Island and the Santa Clara River moving sediment in the NE direction. Along the coast east of Santa Barbara southeastward moving nearshore sediment transport is visible. A large lobe of material moving seaward from the Santa Clara and Ventura Rivers is also evident. The California Current is moving sediment around Pt. Conception into the Santa Barbara Channel in a large concave pattern visible out to 48 Km off the coast. North of Pt. Conception complex nearshore sediment movement is also clearly evident around Purisima Pt. and Pt. Arguello.

Figure 2-5. Humboldt Bay - U-2 Photography. Offshore effluent patterns and several boundaries caused by longshore currents are visible in detail in this picture. Humboldt Bay and Eureka, California, are located in the right center of this photograph which was taken at 19,812 meters on 3 April 1973 at 0930. The current is moving at 2.4 knots in a southern direction as evidenced by the effluent dispersion at points 1 and 2. This material, which comes from industrial plants, is being transported to within 1 mile of the entrance to Humboldt Bay. Dissipation of this material accounts for loss of visible indication of its further movement. Three distinct NE-SW suspended sediment boundaries are present paralleling the coast at points 3, 4 and 5. Their respective distances from the coast are: 2 km (3), 4 km (4) and 13 km (5). Boundary 3 appears to result from a combination of longshore sediment movement and bottom topography. Rip currents at 6 are moving through the breaker zone. Several wave defraction patterns are visible inside the entrance to Humboldt Bay and two sand spits built up by these patterns are visible at 7 and 8. At point 9, an apparent small upwelling is bringing clearer subsurface waters to the surface where they are being moved southwest.

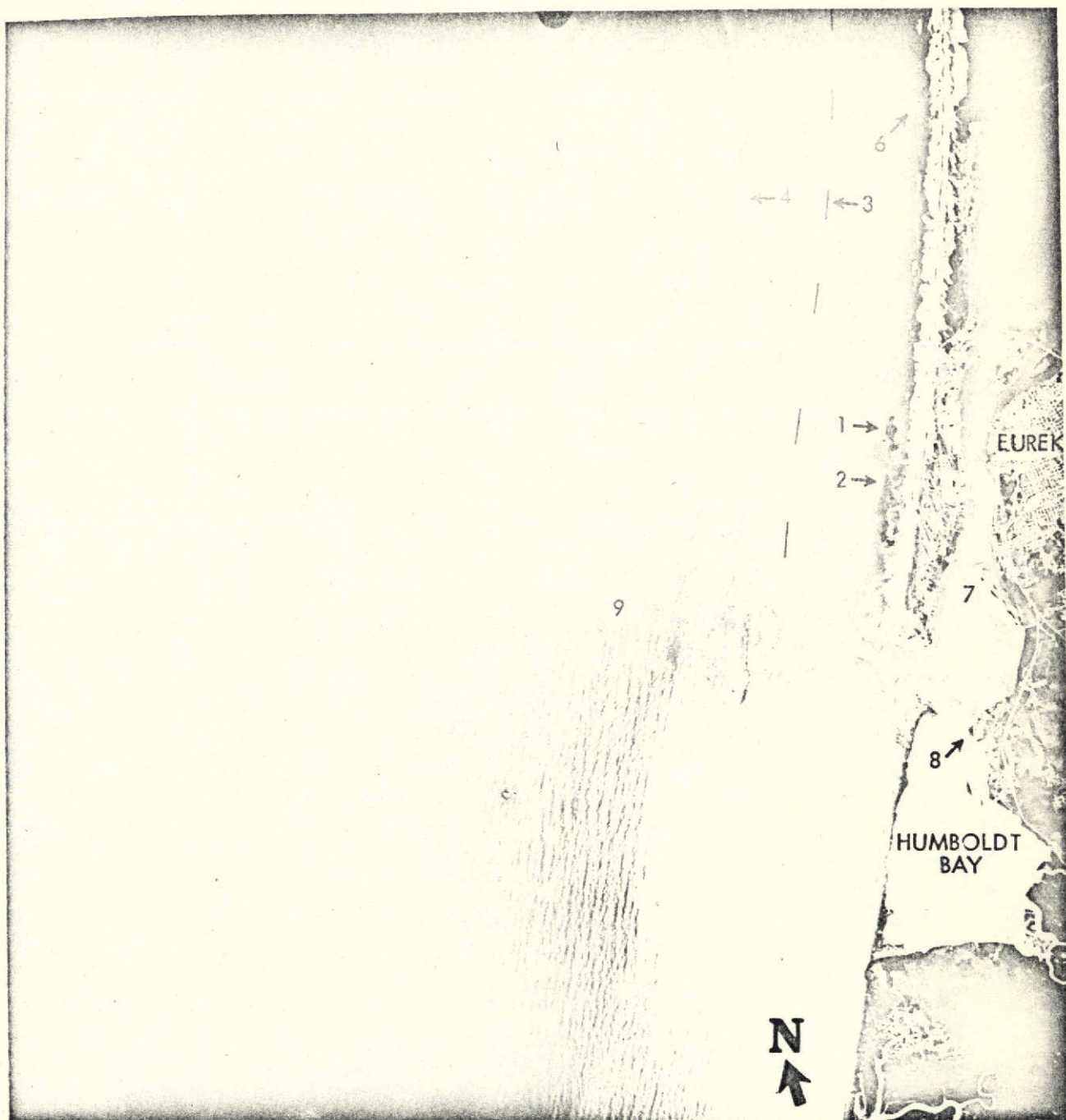


Figure 2-5. Humboldt Bay - U-2 Photography

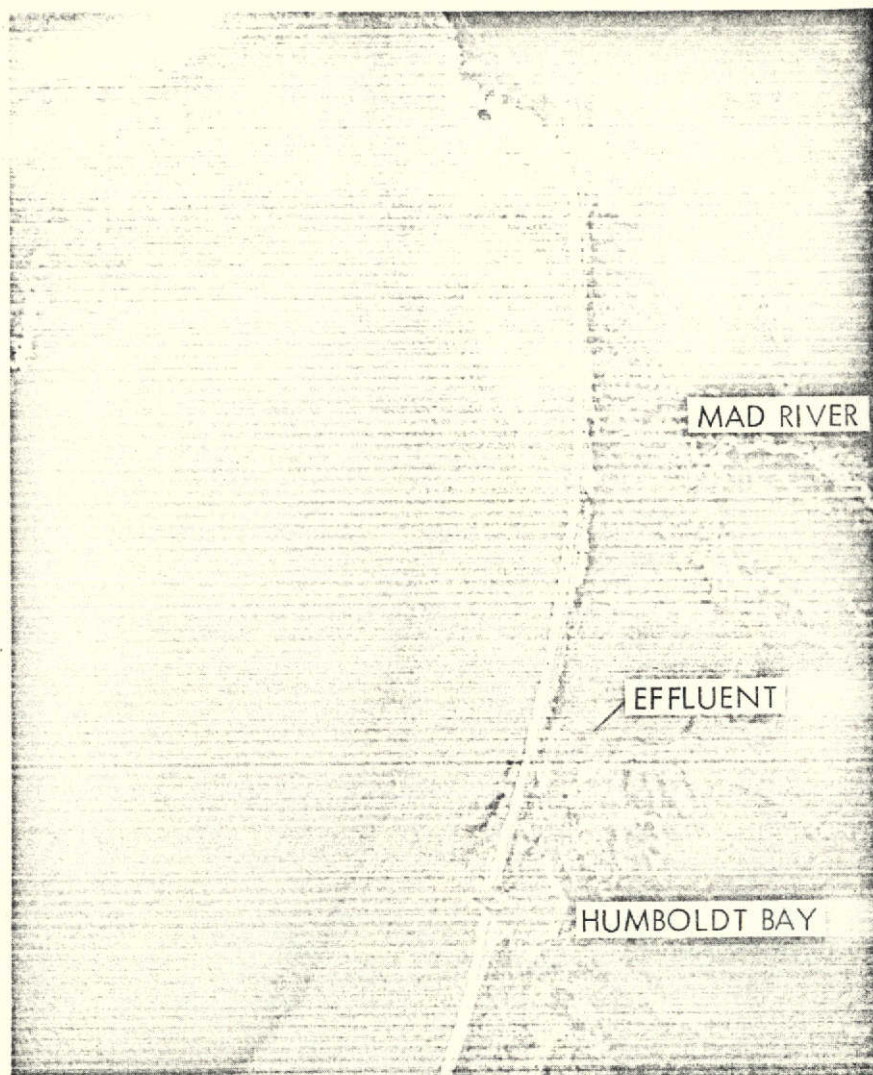


Figure 2-6. Humboldt Bay - Effluents

This enlargement of ERTS frame 1528-18304-4 was made to illustrate the effluents discharging into the coastal waters just off Humboldt Bay. During ebb tide, material from this source has been found to enter the bay. This January 2, 1974, image illustrates the south moving near-shore sediment transport.

Figure 2.7. San Francisco - U-2 Photography. This photograph was taken on 3 April 1973 at an altitude of 19,812 meters. Sediment transport and current activity in the Gulf of the Farallones are shown in detail. The wake of the ship at Point 1 shows clearer subsurface waters being mixed with the thin layer of sediment-laden surface water. The gyre of material in the Gulf of the Farallones indicated by the dashed line, Point 2, is approximately 9 km across and is moving in a clockwise direction. The location of this gyre on the photography confirms findings determined during this study and measurements made by the U. S. Army Corps of Engineers (1971). The movement of this material reflects the influence of the upwelling period. During the March through July period, the coastal currents and the littoral drift regime in the vicinity of the San Francisco Bar are directed up-coast along the outside contour of the Bar. The San Francisco Bar forms an arc approximately 8 km in diameter off the outer entrance to San Francisco Bay. At the Golden Gate Bridge, the current is moving into San Francisco Bay at 3.7 knots and is within one hour of maximum flood. At a distance of 500 meters off Pt. Bonita (Point 3) and 400 meters off Pt. Lobos (Point 4), sharp boundaries between the sediment laden flood waters and the clearer near-shore waters is evident. To the north along the coast, the clearer waters appear to be a result of an upwelling. To the south of the entrance, this boundary is a result of wind drift, wave-induced current and changes in the depth and gradient of the Bar. To the west (left), a definite boundary is present which separates the lighter coastal sediment laden water and darker "open ocean" waters. Several wave train directions are also visible, trending N-S, NE-SW and E-W. Wave refraction is clearly visible at the Bay entrance and south along the San Francisco coast. The sun glitter pattern emphasizes the wave direction. A wake is presently adjacent to Mile Rock off Pt. Lobos (right of Point 4) as a result of the high current velocity. This type of imagery is used as background in the ERTS data analysis.

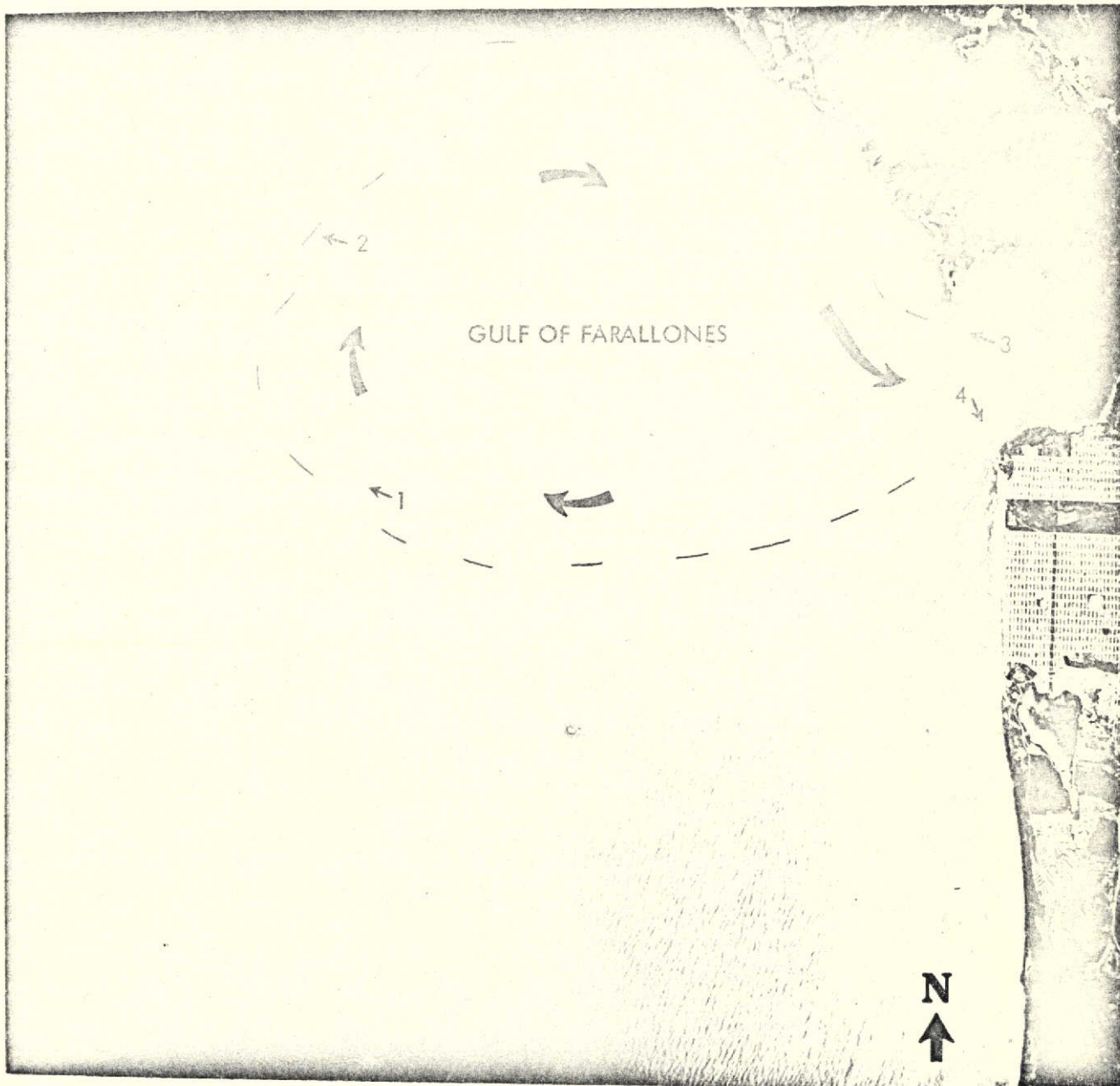


Figure 2-7. San Francisco - U-2 Photography (NASA)

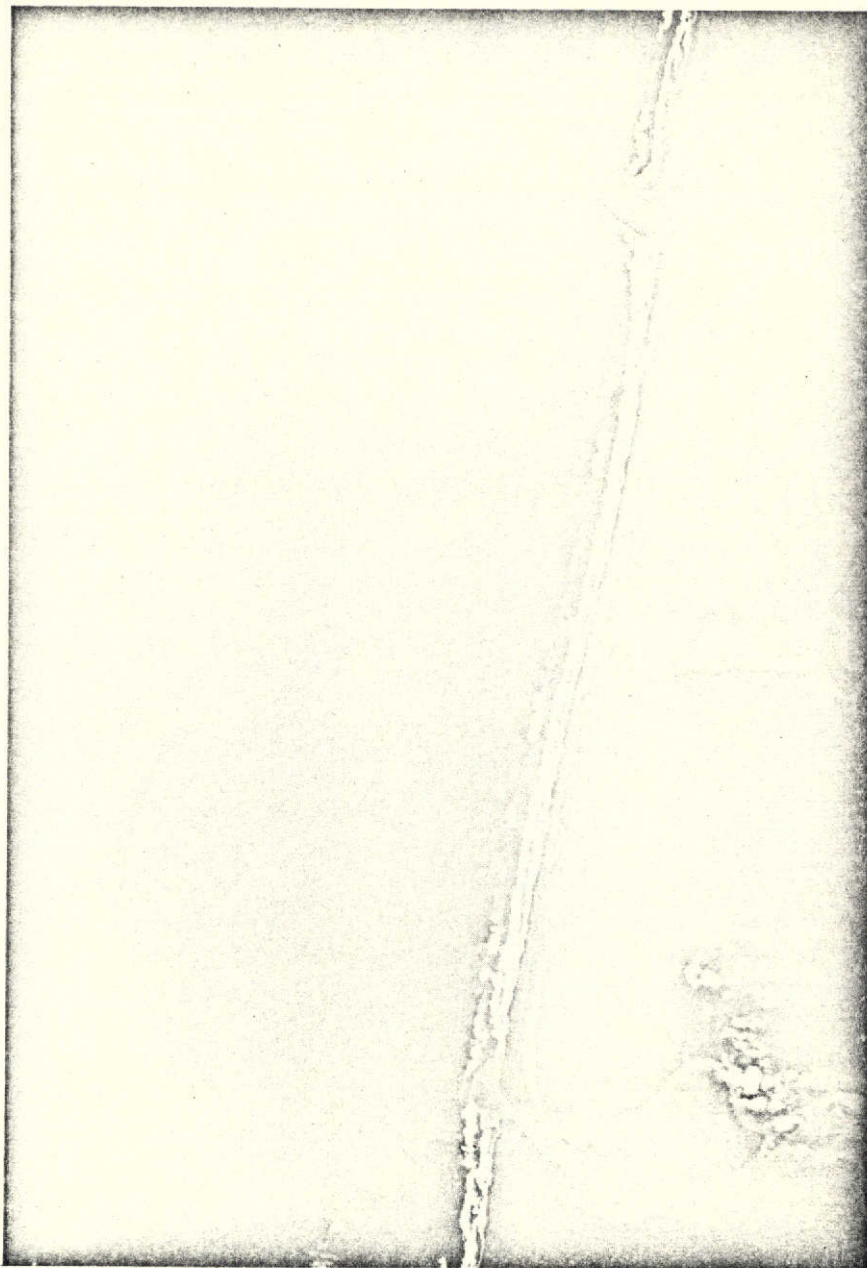


Figure 2-8. Humboldt Bay

U-2 photograph taken December 18, 1973 from 19,812 meters. The Eel River mouth is visible near the bottom of the picture and entrance to Humboldt near the top. Coastal currents are directed northward. Lobing and mixing patterns are present off the Eel River mouth.



Figure 2-9. San Francisco - Monterey Bay. Flying spot scanner enhancement (medium gain) of coastal sediment transport and currents taken on May 27, 1973. Features of interest include an offshore gyre at Duxbury Pt., an eddy of the Golden Gate Bridge, erosion at Devils Slide and offshore movement at Pt. Ano Nuevo. ERTS-1 scene 1291-18182-4.

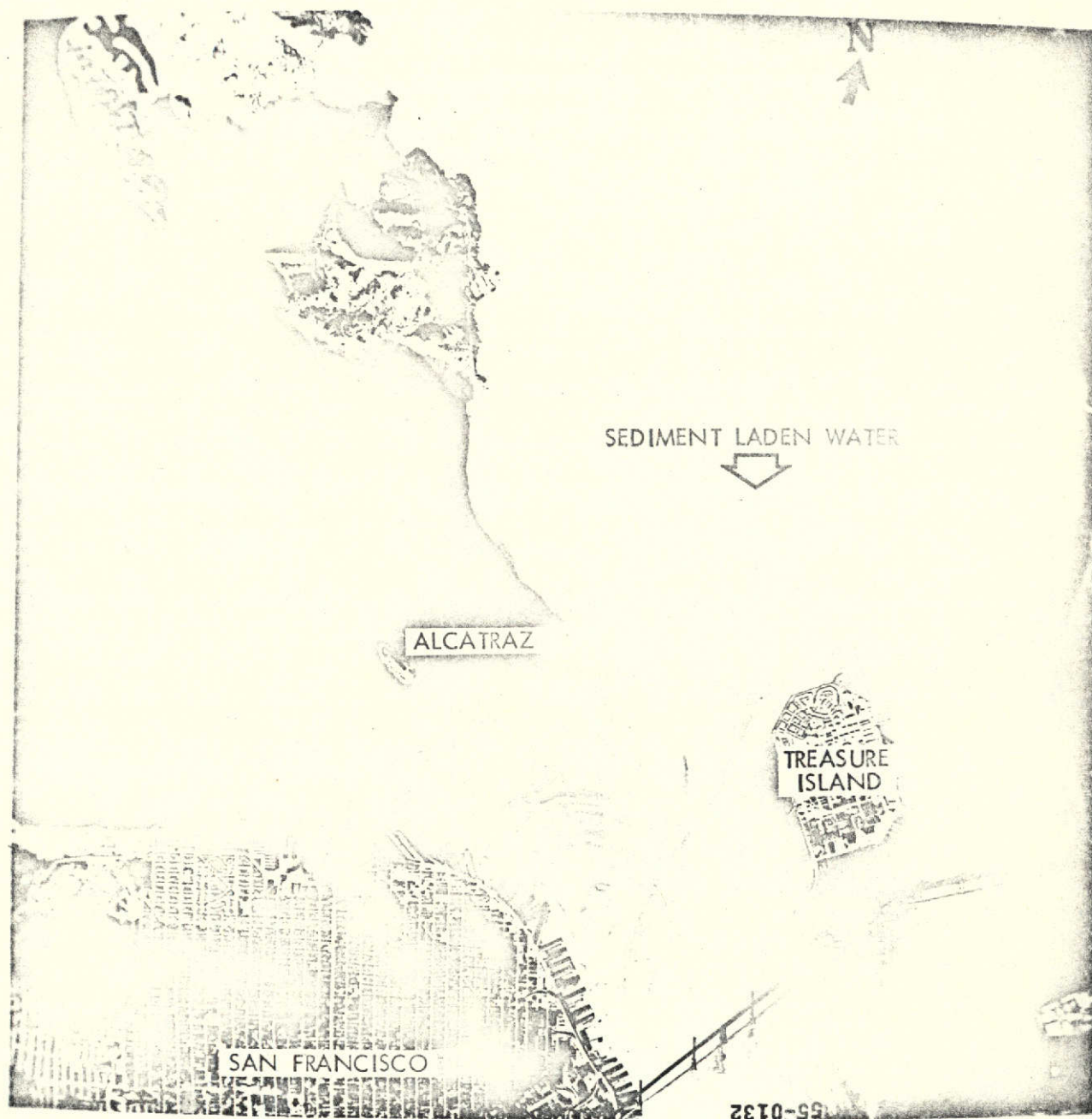


Figure 2-10. San Francisco Bay - Infrared Color

This infrared photograph is of northern San Francisco, Angel Island, Alcatraz and Treasure Island. Details of the complex eddies and currents west of Alcatraz are clearly visible. Sediments from the northern San Pablo Bay and the Sacramento-San Joaquin River discharge is flowing into the south bay at a relatively rapid velocity. The island wake and lee effect of Treasure Island is clearly apparent. The high reflectivity of the near-surface sediments in this infrared color photograph made them clearly visible. This picture was taken on January 22, 1973, one hour before maximum current, current speed was 2.5 knots at the Golden Gate when this picture was taken.

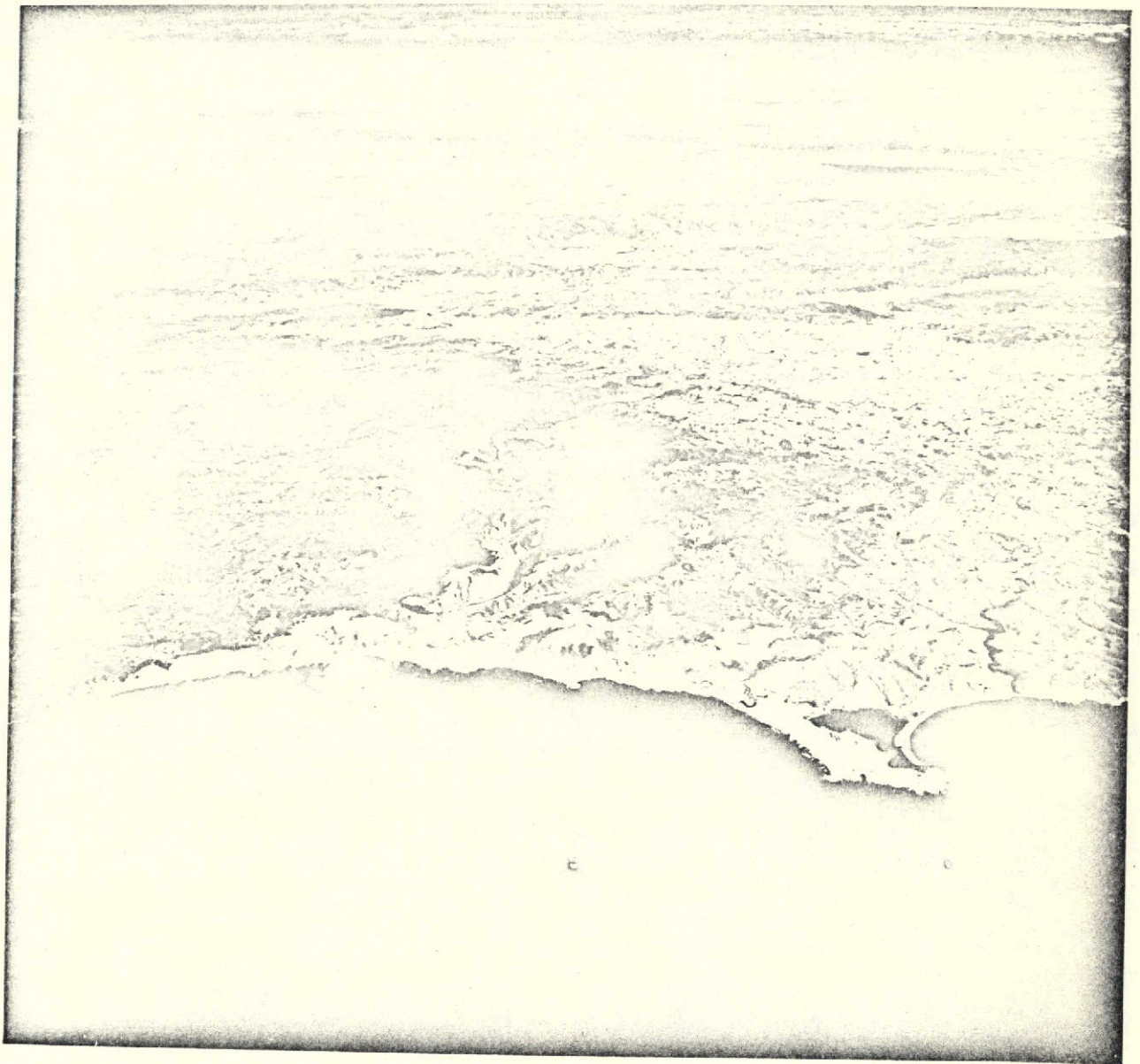


Figure 2-11. Russian River - Bodega Head High Altitude False Color. Looking east across the Russian River mouth (left) and Bodega Head (right) toward the Sierra Nevada Mountains (horizon). Discharging sediment from the Russian River is moving offshore in visible lobes then northward. The Davidson Current effect is clearly seen. This oblique picture was taken at 19,812 meters.

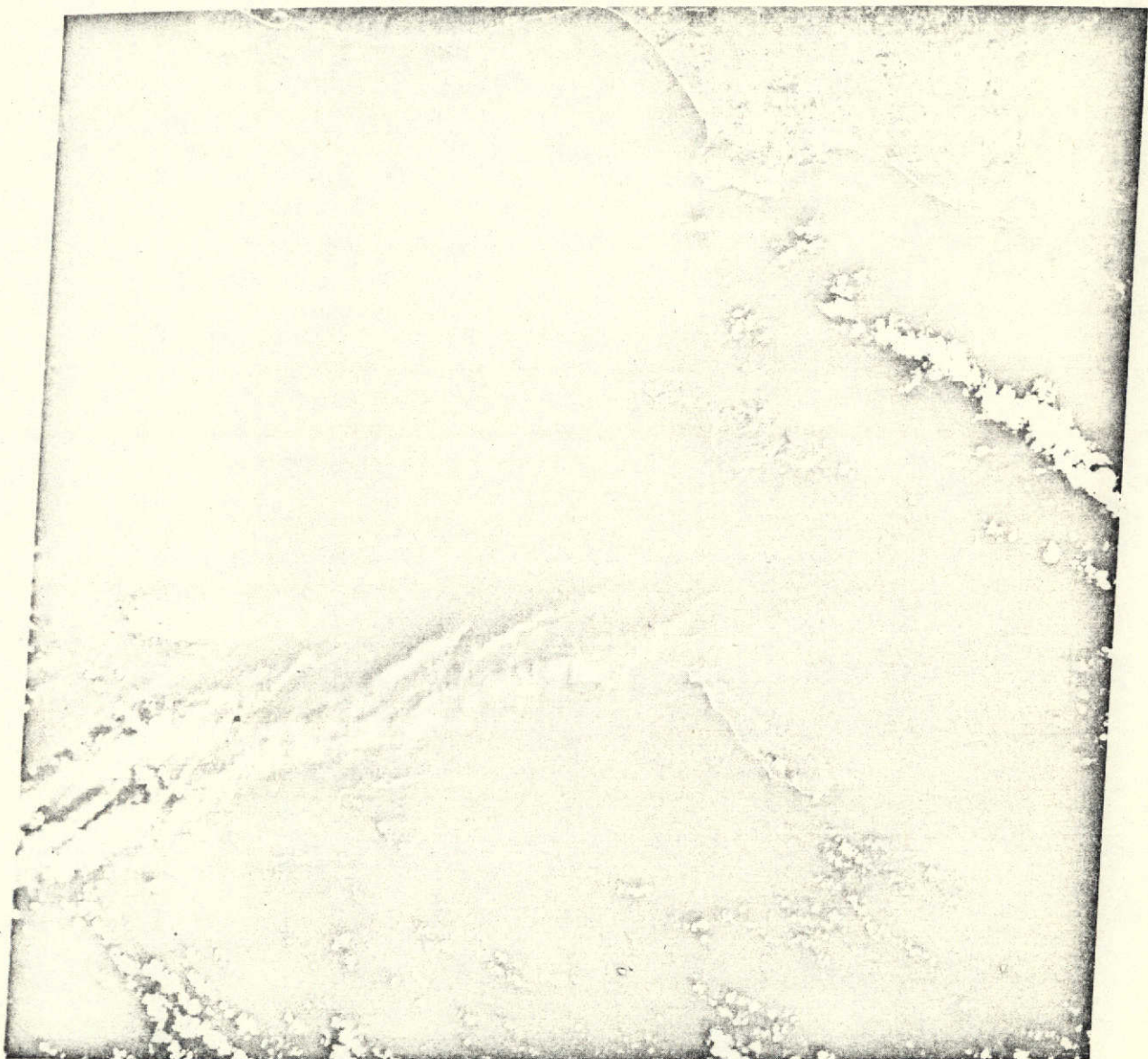


Figure 2-12. Southern California 1180-18015-4

Sediment discharge from the Los Angeles Basin is evident in the nearshore area. The affect of the Los Angeles breakwater can be clearly seen southeast of Los Angeles. The beach along Newport is classified as critically eroding. This image was taken on January 19, 1973.

3.0 ENHANCEMENT TECHNIQUES

This section describes the enhancement techniques other than standard photographic processing that were used in this study. Two major sources of NASA-supplied ERTS data were used: 70 mm negative transparencies and MSS bulk and precision computer compatible tapes (CCT). A flying spot scanner (Section 3.1) was used to expand the ERTS-1 density ranges which represented the suspended sediment and nearshore processes of interest on both data sources. CCT's were processed (Section 3.2) and used for discrete point density analysis, isodensity contour analysis, and mass concentration image analysis. After the CCT techniques were mastered, they were applied to multi-channel computer processing (Section 3.3). The results of subtraction and ratioing of bands 4 and 5 are discussed. Although all three of these techniques were successful, they were time consuming with respect to personnel and computer. Section 3.4 on Photographic Optical Processing gives examples of techniques which were used to supplement the other processes.

3.1 FLYING SPOT SCANNER (FSS) ENHANCEMENTS

Imagery, enhanced and improved for nearshore sediment detection and delineation, is recorded on film from NASA computer compatible tapes (CCT). A modified flying spot scanner system is used to convert NASA digital data to hard copy film. This film writing/reading system uses a high resolution CRT as a light source for data processing. A spot size of 0.7 mils can be achieved when normal brightness and signal levels are employed.

Data on a 9-track 800 BPI tape is directly applied to the system at a real time rate. Recorder playback clocks are used to discretely position the CRT spot through one of five fixed digital rasters.

Horizontal and vertical deflection is provided from two 12-bit digital to analog converters (DAC's), and the Z-axis modulation of the CRT's intensity is performed after digital to analog conversion of the video. Video gain and level manipulation are controlled through a wide bandwidth video amplification stage to provide signal levels yielding optimum film gamma for every scene.

Enhancement Technique

Original NASA bulk imagery displays a scene's dynamic range within the film's available gamma range. Typically, however, the sediment features which are of particular interest to this study are represented in only a small portion of this gamma or density range. Thus, sediment features have a relatively low contrast as compared with that which could be achieved during film recording. Figures 3-1 and 3-2 portray a typical example of how the contrast of sediment features are enhanced. Parts (a) of the two figures are direct prints from MSS band 4

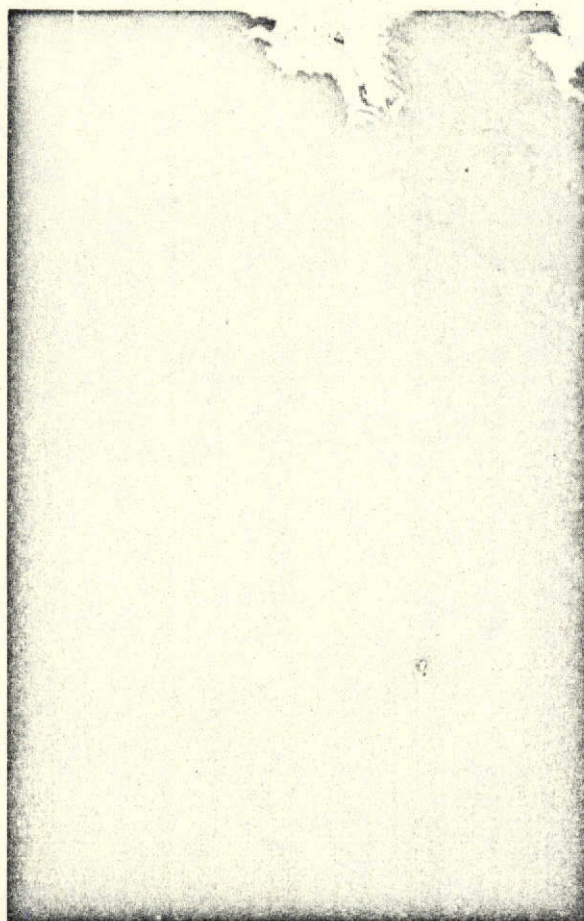
and 5 negatives. The scenes display a nominal contrast with white or light clouds in the northeast corner and a dark density or black in the ocean regions. These prints were exposed on poly contrast Kodak paper with a No. 3 filter to increase the contrast of offshore sediment features.

The (b) parts of the two figures are prints from the negatives recorded on the FSS using the analog preprocessing technique. A comparison between the two matching images immediately illustrates the advantages of controlled playback exposures. NASA imagery must be recorded on film in such a way that all signal levels are within the film's density range. It would not be practical or desirable for NASA to generate negatives with exposures optimized for only selected portions of any scene's signal range. However, for special features of interest, such as offshore suspended sediment, the signal range is limited and relatively small.

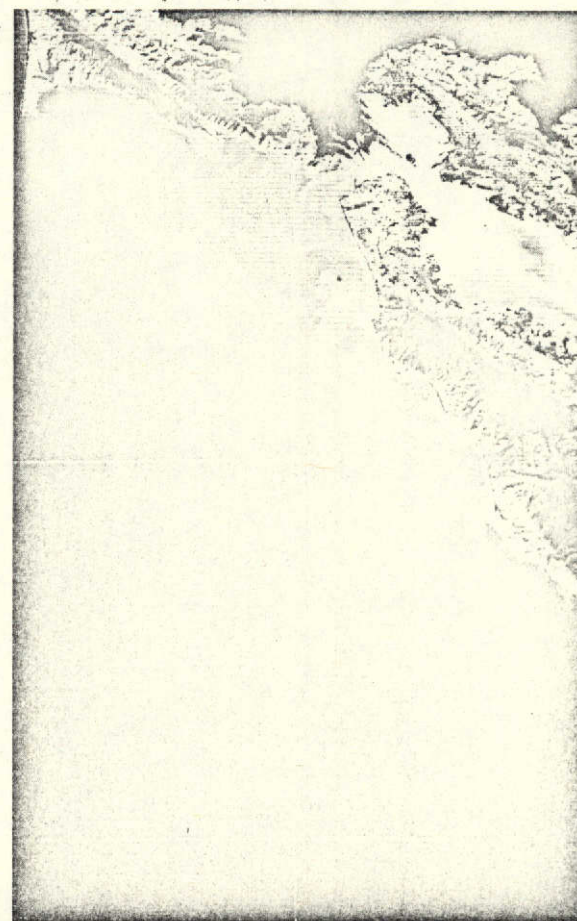
To contrast enhance features within any scene, two signal processing techniques are available in the FSS system. One method employs standard analog amplification methods (Analog Preprocessing Technique) to control the signal's gain and DC level setting. The alternate method is a hybrid digital/analog technique. In this method, the eight-bit parallel digital data is shifted at the input to the digital-to-analog converter (D/A) to achieve the appropriate gain. By this second method, discrete steps in gain of 2/1 can be applied to the input signals. The D/A output is then fed through a unit gain analog amplifier where DC offset is controlled. In the application of either of these techniques for enhancing ERTS scenes, particular problems may present themselves. Thus, a more detailed discussion of these techniques in a total system context is presented below.

3.1.1 Analog Preprocessing Technique

The exposure of the FSS negatives is a function of numerous parameters and systems settings (CRT voltage or brightness, signal levels, scan rate and raster size, lens aperture, and film characteristics, etc.). To reduce the effect and randomness of these variables, an analysis of FSS system performance was undertaken as they applied to ERTS data reduction. The results of this study are presented in a following section. However, it is necessary to understand that all parameters and settings have been standardized or fixed for the ERTS data task. This approach of formulating a standard system configuration and data reduction procedure was necessary so that consistent optimum high quality products could be produced. Additionally, the processing time was reduced to a minimum. All other parameters being fixed, the film exposure is now only a function of the signal levels present at a system monitoring point. This point is in the video chain at the output of the analog video preprocessing amplifier prior to being input to the electron beam video drive amplifier. A signal swing from 0 to 0.5V results in a log film density of 0.41 to 2.25.



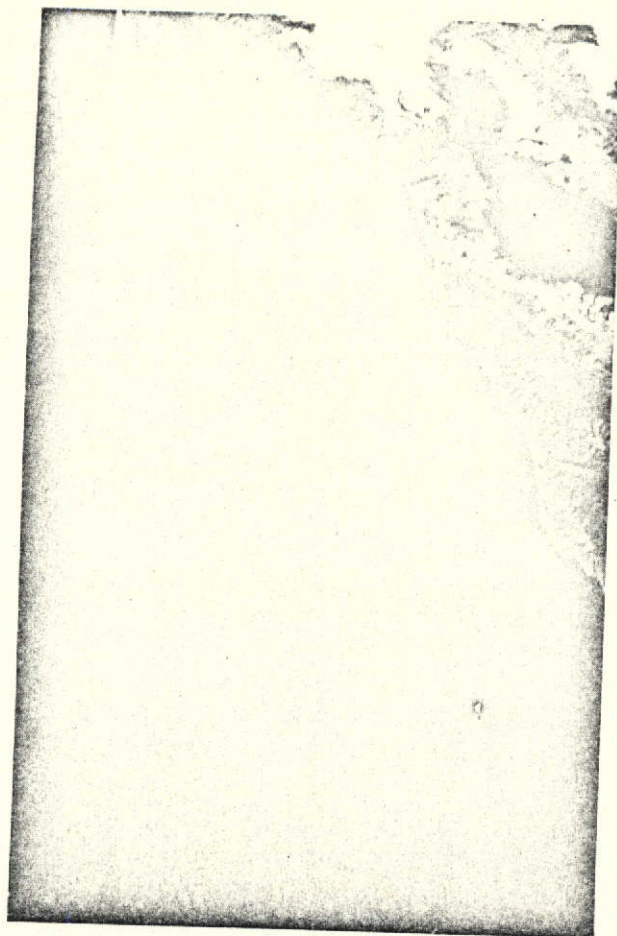
(a)
1130-18235-4 ORIGINAL



(b)
1130-18235-4 FSS

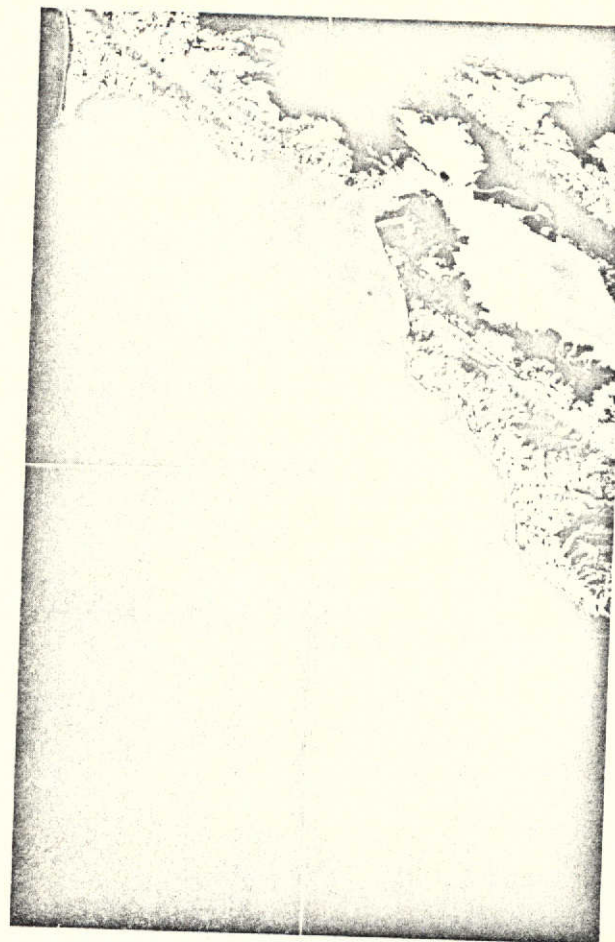
Figure 3-1. San Francisco FSS Enhancement
Scene 1130-18235-4

Note gyre in the Gulf of the Farallones and offshore sediment movement south of Half Moon Bay (in b).



(a)

1130-18235-5 ORG



(b)

1130-18235-5 FSS

Figure 3-2. San Francisco FSS Enhancement
Scene 1130-18235-5

Surface sediment distribution is shown. Gyre and offshore movement
near Devils Slide and Half Moon Bay are emphasized (in b).

The digital data from the tape deck is converted to analog signals for preprocessing prior to film recording. The video amplifiers are used to control the signal gain and DC level so that the signal levels are within the 0 to 0.5 volt range. For a normal exposure, the total signal range of any scene is adjusted so that it is within this voltage window. To enhance the contrast of sediment features, the signal levels are increased by virtue of the analog gain controls so that the video signals representing sediment features swing from 0 to 0.5 V. As noted above, the application of this analog gain to enhance features presents an additional problem. This problem is that signals from other features, such as land, beach, etc., have also been amplified. These signal levels are larger than the maximum desirable signal level of 0.5 V. Recording of this amplified full dynamic range signals would result in poor imagery, as well as presenting potential damage to the CRT. The large signal levels present two problems. Firstly, these larger signals could saturate the post amplification stages of the video amplifiers, thus causing holdover of the video signals in regions of land-water interfaces. Secondly, and more important, the excessive signal level will overdrive the CRT brightness. This would result in an increased CRT spot size, internal light scattering, and thus fogging of the imagery. To eliminate these problems, a signal limiter was incorporated into the video chain (Figure 3-3).

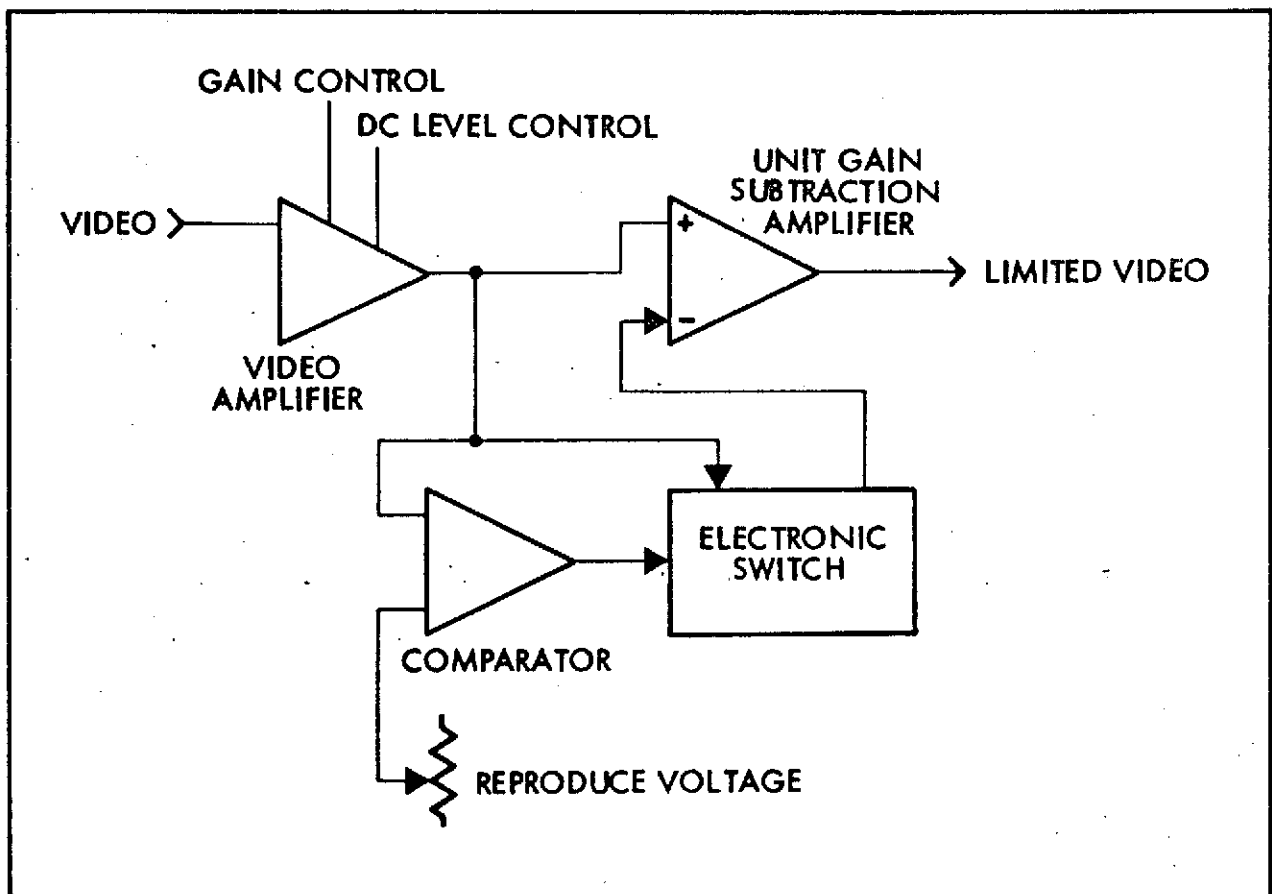


Figure 3-3. Signal Limiter

This block diagram illustrates the electronic limiting function necessary for applying contrast enhancement.

The conditioned video is applied to an analog comparator, a subtraction amplifier, and a series of electronic switches. When the signal levels are less than the reference voltage, the video switch is off so the video is passed through the subtraction amplifier unaltered. However, when the signal level increases and exceeds that reference level, the comparator switches on so that the video is passed to the minus (-) side of the subtraction amplifier, thereby subtracting the video from itself. The limited video output for this condition is then 0 V. This post-processing electronics effectively limits the video levels to the desirable dynamic range of 0 to .5 V. Gain can be applied to the video signal, but the output signal range is fixed to 0 to 0.5 V. This amount of enhancement is a function of the gain applied. Figures 3-1 and 3-2 reveal the results.

3.1.2 Hybrid Digital/Analog Technique

The second preprocessing technique available for contrast enhancement employs all the capabilities and system settings as described in the analog discussion. The single exception is digital gain. It must be remembered that to perform contrast enhancement, one must control signal levels and this must be done within system constraints, i.e., a limiter function. In the analog case, the gain is continuously controllable from 0 to 10 degrees. Thus, it is difficult to repeat amplified settings, or to specify differences between settings. This is not to say that the system cannot be calibrated to get such information. However, additional steps are required. The digital techniques allow us to apply gain in discrete multiples of two. This technique then yields the same results, signal gain, but in known multiples. The procedure is simple and straightforward assuming a basic knowledge of digital-to-analog converters. However, a discussion may serve to clarify the technique. A digital word consists of 8 bits (labeled 2 degrees to 2^7 for reference). A weighting or significant level is associated with each bit. The significance of 2^7 bit is less (by a factor of 2) than 2^6 bit which is less (by a factor of 2) than the 2^5 bit, etc. This is also true with respect to the more significant bits (2^1 and 2^0). Now when normally converting a digital word to analog level each bit either adds or doesn't add its associated significant level to the output levels, depending on whether or not its digital bit is a "1" or a "0". Now if one understands the normal operation involved in digital-to-analog conversion, imagine shifting each bit up towards its adjacent more significant position. Each bit would now add in twice the level as in the normal case. The 2 degrees bit would not be used. Digital words which were using this most significant bit in the normal case, however, would be decoded as a lesser value than in the normal case. All other words would be increased in value by a factor of two. This shifting can be continued in discrete increments until the signal of interest is appropriately enhanced.

The two techniques described above are those used to control signal gains. Other techniques are available for application to the analog signal. These include non-linear amplification, thresholding and differentiation. Each technique yields an enhanced image, however, for sediment detection and delineation contrast enhancement seems to yield the optimum results.

3.1.3 FSS Modifications and Improvements

Throughout the program an attempt was made to continuously improve the data product as recorded on our FSS system. Continuing analyses were directed towards isolating problem areas in the FSS system which early in the program prevented producing imagery displaying resolution that improved on prints from NASA original negatives. The FSS system has been used to generate imagery with enhanced sediment features (i.e., gain control was used to increase the contrast of the sediment anomalies). This resulted in isolating three major problem areas: (1) CRT dynamic focus; (2) the recording lens; and (3) the recording film. The dynamic focus power supply was readjusted so that the CRT spot remains focussed at all points on the CRT face. Additional shaping circuits were incorporated and a complete adjustment made to yield an optimum dynamic waveform. Secondly, a new recording lens was installed into the system. The result was an increase in the modulation transfer function of the optics. Care was taken during installation to achieve a critical focus in the image plane. The third problem area was the film used for recording. Additionally, the recording procedure was standardized to reduce the time required to playback an image. Candidate films were reviewed based on their characteristic curves, granularity, and spectral sensitivity. Also, a requirement for red light insensitivity, for ease of handling, was imposed. The film selected was Kodak TRI-X Ortho type 4163*. Test exposure and processing times were experimentally varied to determine a standardized procedure. This resulted in a relationship between input voltage levels and film densities. The following table shows this relationship:

<u>Input Voltage Level</u>	<u>Log Film Density</u>
0	0.41
0.1	1.03
0.2	1.50
0.3	1.93
0.4	2.15
0.5	2.23

*Processed in D-19 at 68°F for 7 minutes.

Data from CCT of frame 1183-18105-4 were used during the first test runs. These runs produced another problem. If the signal levels of interest are between signal levels, both above and below their levels, the signals larger than those of interest became too large as gain was applied to the signal. These signal levels actually become large enough to damage the CRT phosphor or the light level increase to a point which results in fogging of adjacent data. To remedy this problem, a signal limiter was incorporated into the video section of the FSS. This is displayed on the imagery as a fold-over condition as illustrated by the black clouds in Figures 3-1b and 3-2b. As the signal's level increases to this safety threshold, the film image is increasing in density. Once the signal increases past this level, the resulting density is folded over to clear and remains there until the signal level falls below the safety threshold level.

The incorporation of the above modifications and procedures resulted in improved FSS imagery. The new imagery displays resolution approaching that of NASA originals. Thus, enhanced data can be recorded with little reduction in resolution. The format size of data produced via the FSS system is 35 mm X 63.5 mm. An image being comprised of 1024 lines of 872 pixels each. This correlates to above 16.4 lines/mm. As explained in the Digital Processing Section, an ERTS frame was originally broken into 8 blocks (1024 lines X 872 pixels) and 4 blocks, 292 lines X 872 pixels. The resolution of the FSS system and recording film is sufficient to write more data into the above format. Thus, the ERTS frame was blocked differently (2048 lines X 1744 pixels). The line spacing was effectively reduced, resulting in a better product. Figure 3-4 illustrates the image quality which can be achieved via the FSS system during the enhancement process.

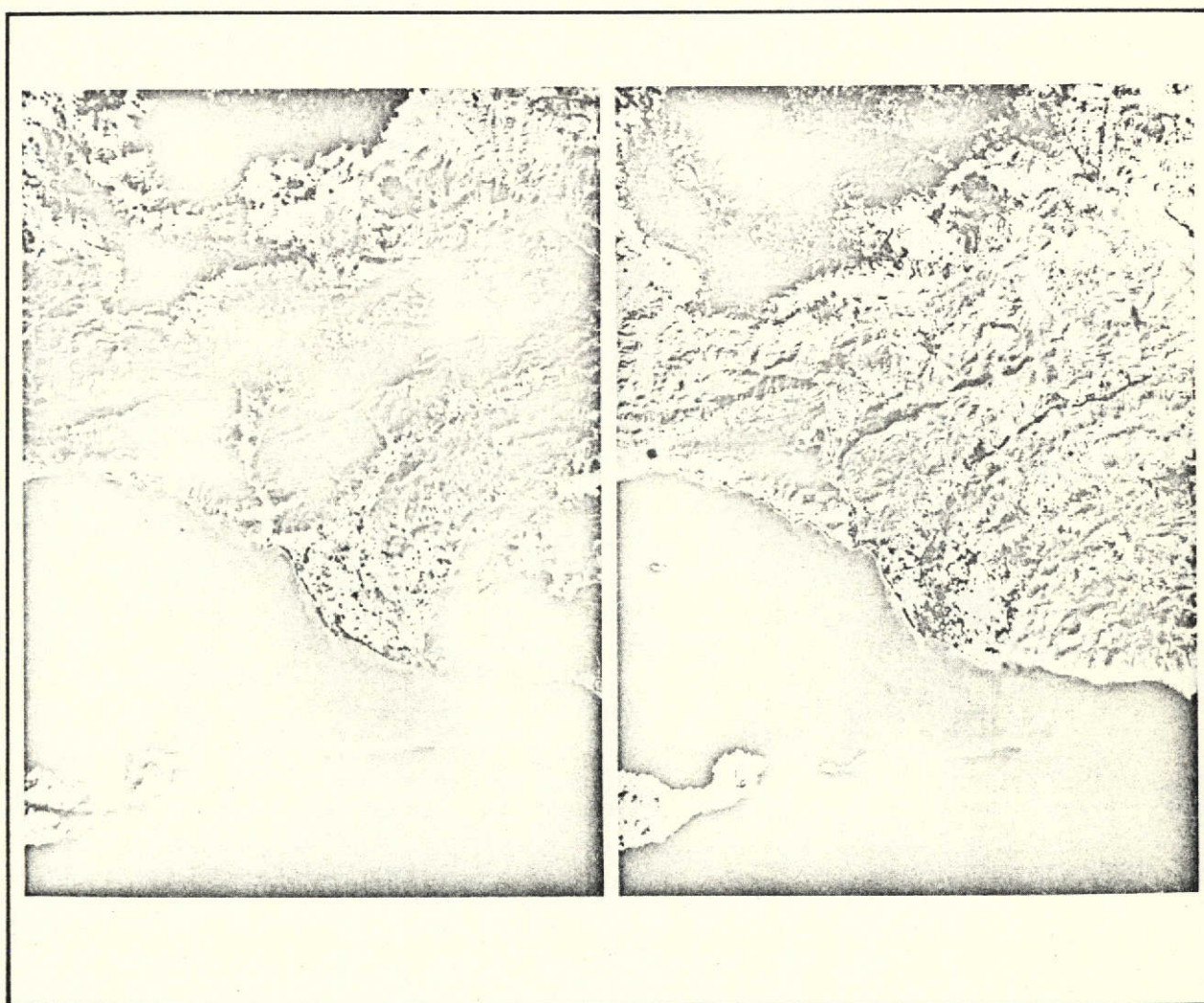


Figure 3-4. FSS Enhancement of ERTS Frame 1234-18021.

The scene is a 91 km x 153 km area of the total ERTS image. This subset of data was reformatted or blocked from the NASA CCT's via an IBM 370 computer. This technique will be described in the following section.

3.2 COMPUTER PROCESSING CCT'S

The computer processing activity associated with this study was oriented towards developing techniques for the use of the ERTS precision and bulk computer compatible tapes provided by the NASA. Three basic techniques were utilized in analyzing ERTS CCT data: discrete point density analysis; isodensity contour analysis; and mass concentration image analysis. The products used in the above analyses are described below, 3.2.1, and are followed by a discussion of the processing steps, 3.2.2, the CCT characteristics of interest, conventions adopted, and the software processes, 3.2.3, used for the present effort. Two computers were used for this project, an IBM 370, and a Raytheon 706 minicomputer. The digital processes discussed in this section produced output in three formats, i.e., tabular listings, graphical image and photographic images. Specific characteristics and uses of the specified analytical techniques and their products are as follows:

3.2.1 Products

Discrete Point Density Analysis

Sediment analysis from conventional photographic reproductions is dependent upon the density differentiation abilities of the human eye. This is a severe limitation since the initial experimental runs made on precision CCT's indicated that the total range of water density variations of MSS band 4 ranged from 0.634 to 0.758.

A printout of the point-by-point density of the lines of areas of interest will circumvent this visual limitation since the printout will show up to single count variations. Software programs were developed to enable the investigator to printout the actual count of each point on a selected scan line segment or an alpha-numeric code designating the various density levels in an area of interest. The line printouts can then be plotted for multiple bands, as shown in Figure 3-5, for detailed analysis of sediment concentrations and for comparisons of reflectivity characteristics of sediment in the different spectral bands.

The area density level printouts may be used in conjunction with conventional photographs to make accurate measurements of the degree of density variations within a given area.

Isodensity Contour Analysis

The area discrete point density printouts discussed previously are useful as a quick and relatively inexpensive method for obtaining accurate numerical values of the density levels. The generation of isodensity contour lines is, however, a more useful technique for analysis of sedimentation patterns. This technique combines the characteristics of pictorial representations and numerical printouts. Figure 3-6 shows a contour-plot around the Santa Barbara Channel. The large geographic features such as shorelines, peninsulas, and islands are clearly distinguishable. These provide a good location reference

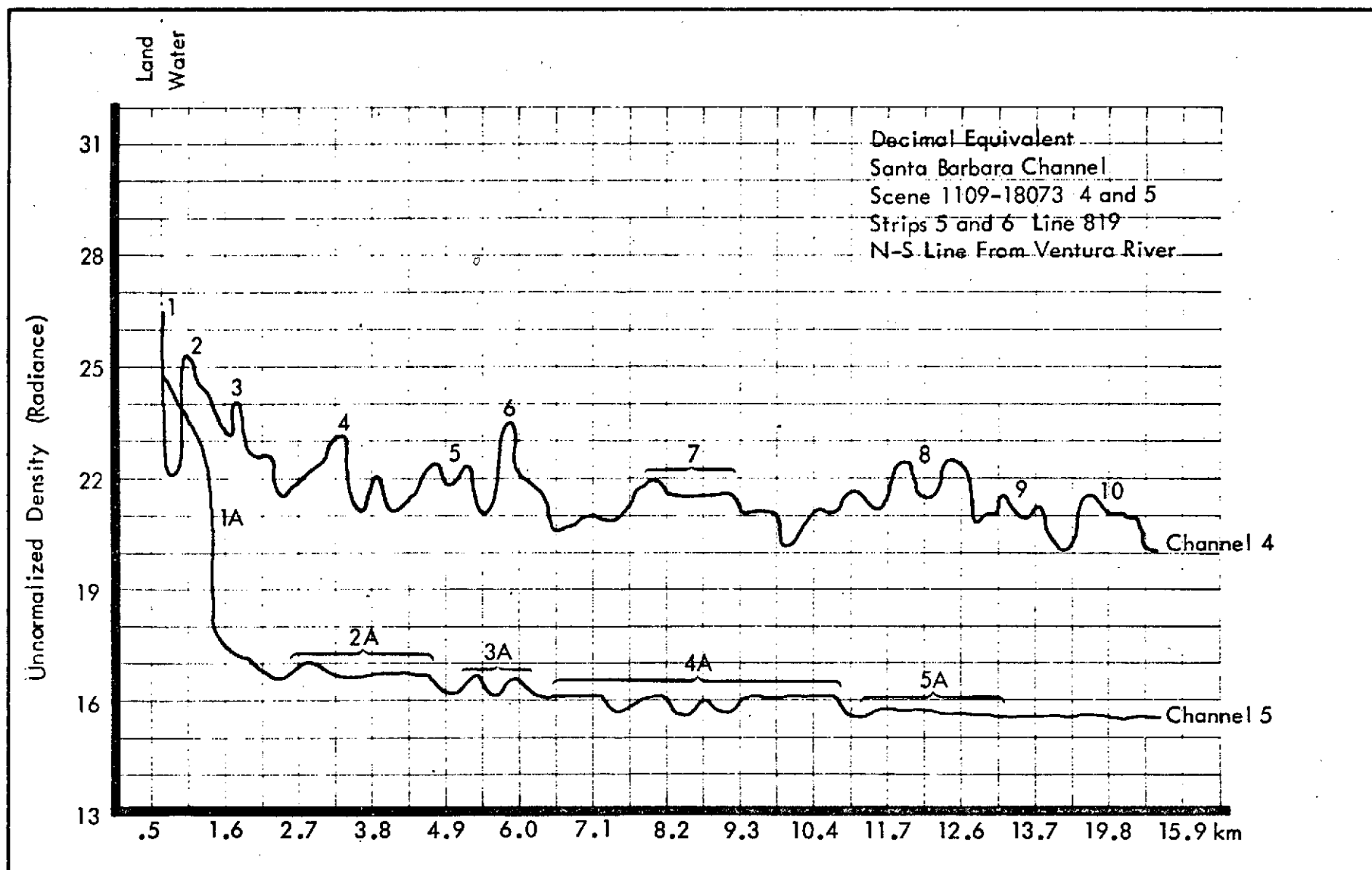


Figure 3-5. Decimal Equivalent Plot - Santa Barbara Channel

The density differences along line 819 of the ERTS computer compatible tape 1109-18073 4 and 5 are shown to a distance of about 13 km offshore from the Ventura River. The upper graph, representing Channel 4, contains ten major amplitude changes, which can be directly related to increases in density levels related to increase amounts of suspended sediment. The lower graph, which represents Channel 5, has five major and minor amplitude changes, all of lower density value. The greater water penetration capability of Channel 4 is indicated by the higher density levels and amplitude changes in the Channel 4 graph. This information is used in interpreting nearshore sediment transport.

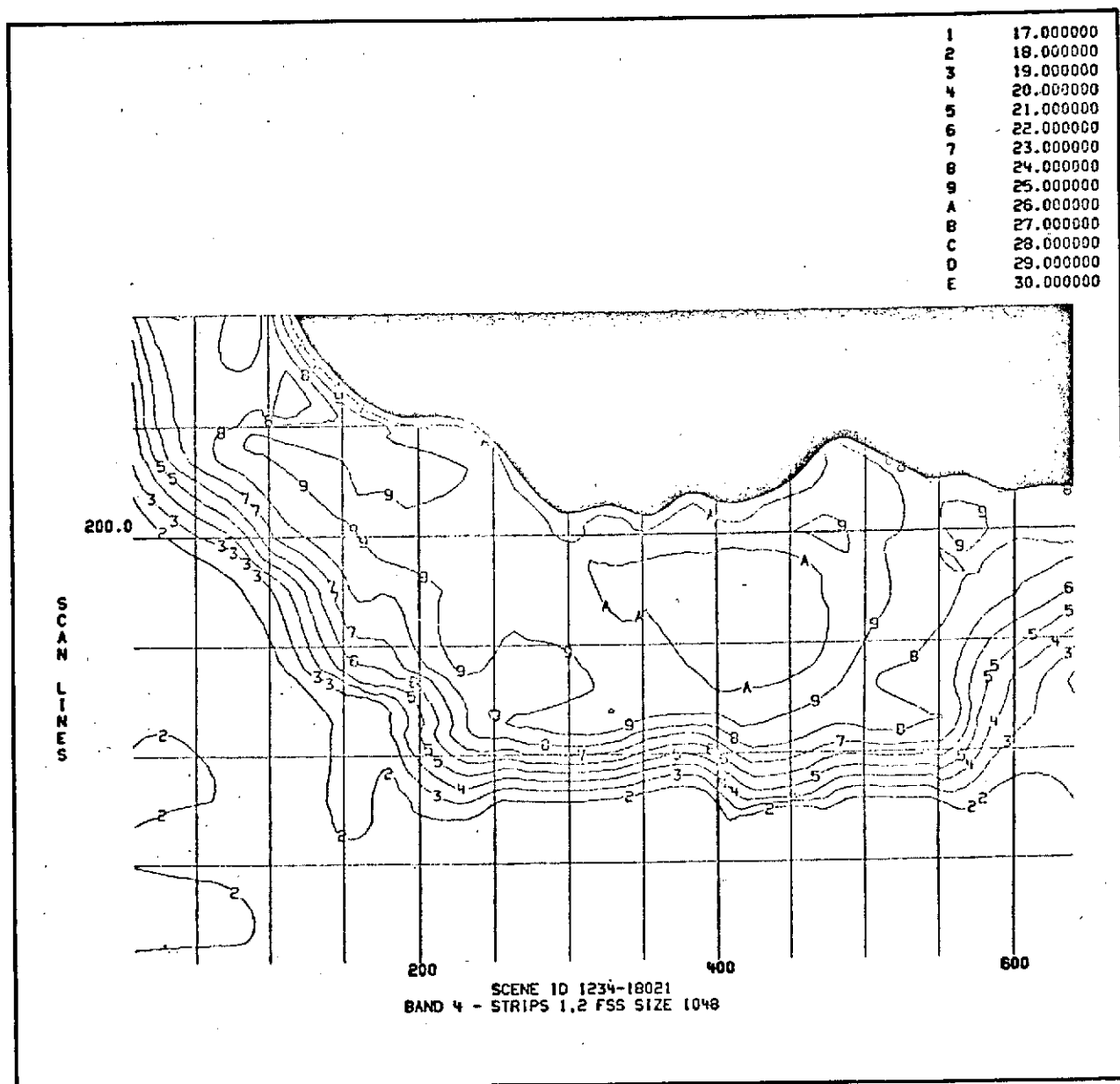


Figure 3-6. Isodensity Contour Analysis of Santa Barbara Channel, Scene 1234-18021-4.

which may not always be easily distinguishable on numerical printouts. At the same time, contour plots do show the exact numerical value of the density levels contained within the area of interest. More importantly, however, these plots show sediment distribution and patterns in a more clearly understood graphical representation, namely by showing the isodensity contour lines.

Mass Concentration Analysis

The third application in which the ERTS CCT's were used was in the generation of digital tapes compatible with the Flying Spot Scanner imaging system (FSS). Several options were included in the process which generated these tapes. Basically, these options provide the capability to obtain cross-spectral mathematical and logical combinations of selectable areas. The results of these combinations (e.g., add, subtract, mask) are formatted onto a digital tape such that it can be played back and through the analog front end of the FSS to produce an enhanced image on a photograph or transparency. Figure 3-7 is a reproduction of a picture produced in this manner.

3.2.2 CCT's Processing Step

Both the precision and bulk computer compatible tapes supplied to ERTS users were processed and used to generate the types of data described previously. Since the format of the NASA-supplied precision and bulk tapes are significantly different, it was necessary to provide some flexibility in the processing system during the initial phases when the various output products were being evaluated for use by the Principal Investigator. This was achieved in two ways: first, a hands-on computer policy using assembly language coding was adopted; and secondly, precision tapes were preprocessed to provide precision data on tape formats somewhat similar to the bulk tape format. The general processing flow for both precision and bulk tapes are illustrated in Figure 3-8 and described below.

Precision Tape Preprocessing and Reformatting

ERTS MSS computer compatible precision tapes are organized into a group of four tapes which depict a scene approximately 185 km square. These tapes are processed and converted to an FSS compatible format, as illustrated in Figure 3-9. Two computer programs are involved in this conversion:

De-Stack. Processing with De-Stack will split the data files in the NASA-supplied tapes such that a separate tape is produced for each strip. Note that the source tapes (Format A) include two strips of data per file while the target tapes (Format B) include only one strip per file.

AREA OF SOUTH
MONTEREY
PENINSULA
CONTOUR MAP

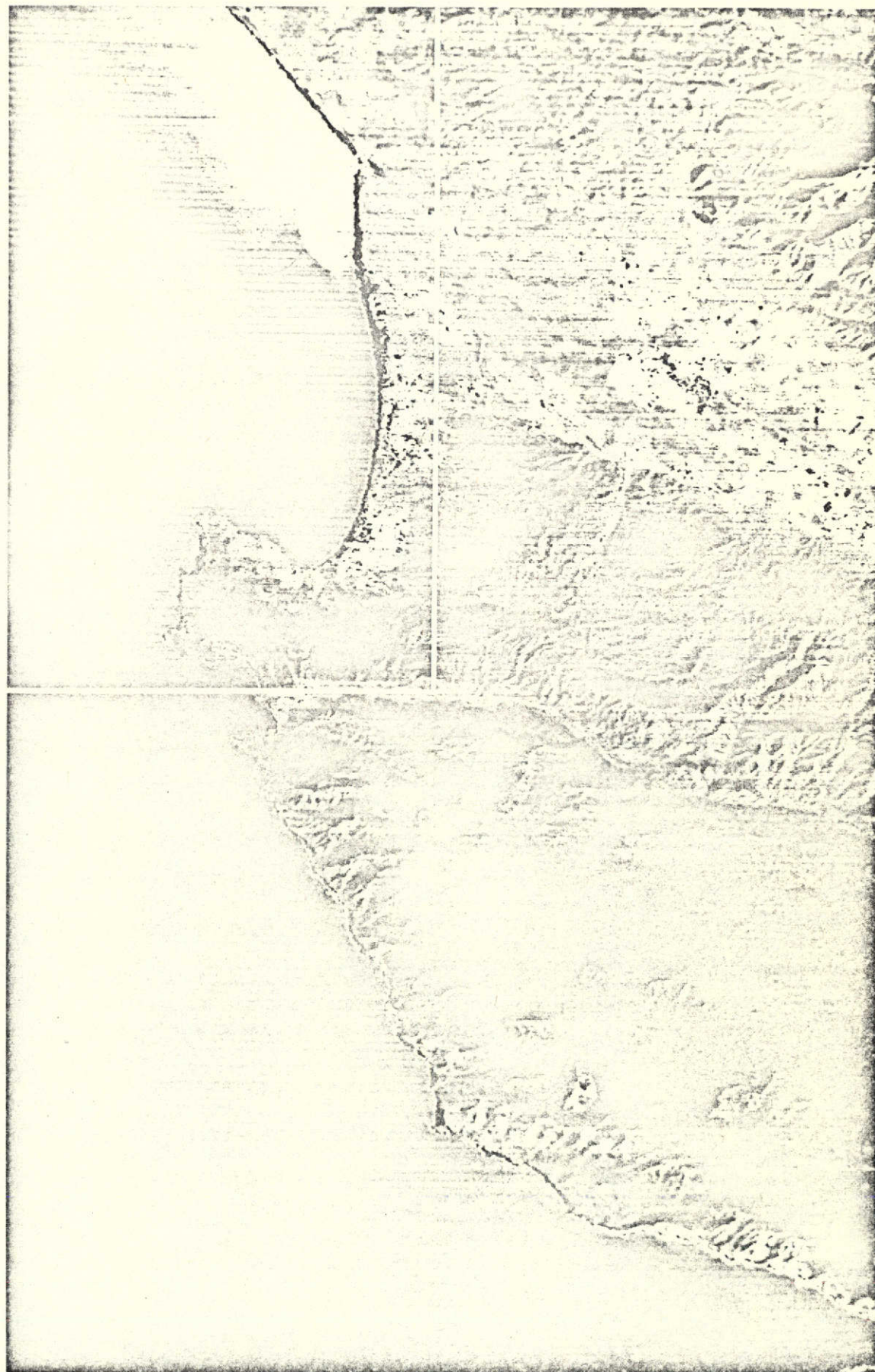


Figure 3-7. FSS Enhancement of Monterey Bay
Area of digital dump Figure 3-12 - Scene 1183-18182-4. January 22, 1973.

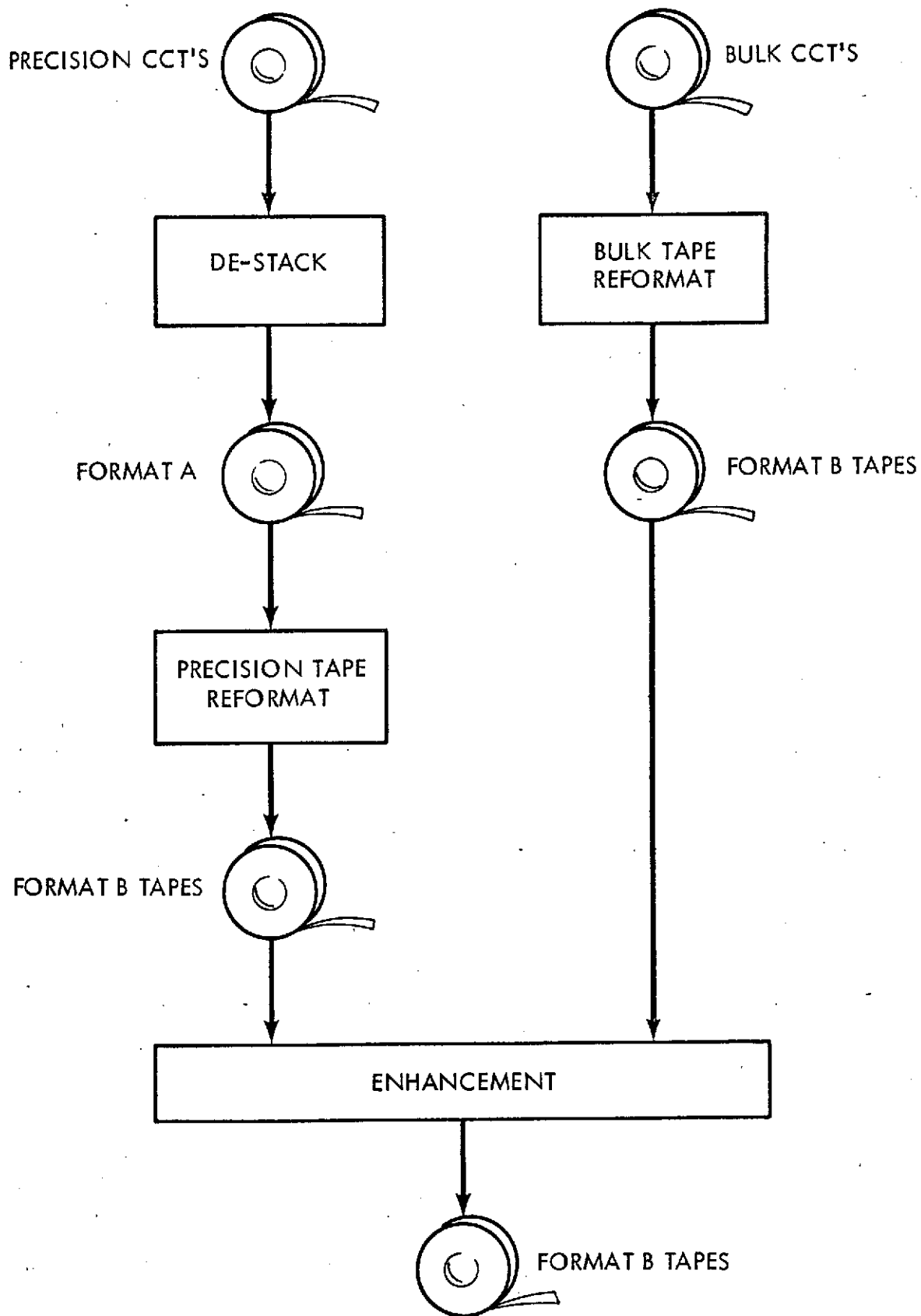


Figure 3-8. Processing Flow Chart - Bulk and Precision CCT

FSS Block Gen. Once the Format B tapes have been produced, it is possible for the investigator to select any two adjacent strips to be processed utilizing the FSS Block Gen Program. This program will convert the two strips into four FSS compatible digital data blocks (Format C) consisting of 1024 X 1024 elements.

Depending on the processing to be done during the subsequent image enhancement phase, the investigator may elect to process one or more of the spectral bands and generate an FSS compatible tape for each band.

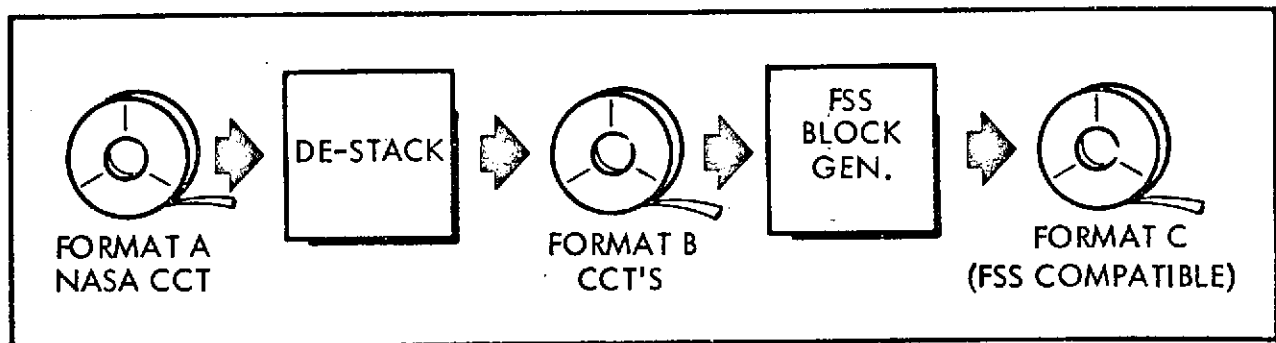


Figure 3-9. Precision CCT Processing Flow Chart

These new tapes, designated Format A, are then reformatted to a format compatible with the existing hardware and software systems of Geoscience. This final format is designated Format C.

Format C tapes contain selected scenes and spectral bands in data blocks of 1024 byte records in files 1024 records long. This corresponds to a 46 x 46 km area when derived from a precision tape. In this format, the data can be read directly into the FSS to produce enhanced images under control of the analog system operator. A significant amount of work using digital tapes was done in precisely this mode. Additional work, however, was done using digital techniques for extracting information from the data, as detailed in other sections of this report.

Bulk CCT Preprocessing and Reformatting

ERTS MSS computer compatible tapes are also organized into groups of tapes which depict a scene approximately 185 km square. There are four tapes per scene which contain information depicting a strip 46 km wide x 185 km long in each of four spectral bands.

Reformatting of the bulk tapes to Format B was handled in one step but required the adoption of the conventions illustrated in Figure 3-10. The insertion of dummy data was necessary to render these tapes compatible with the FSS input

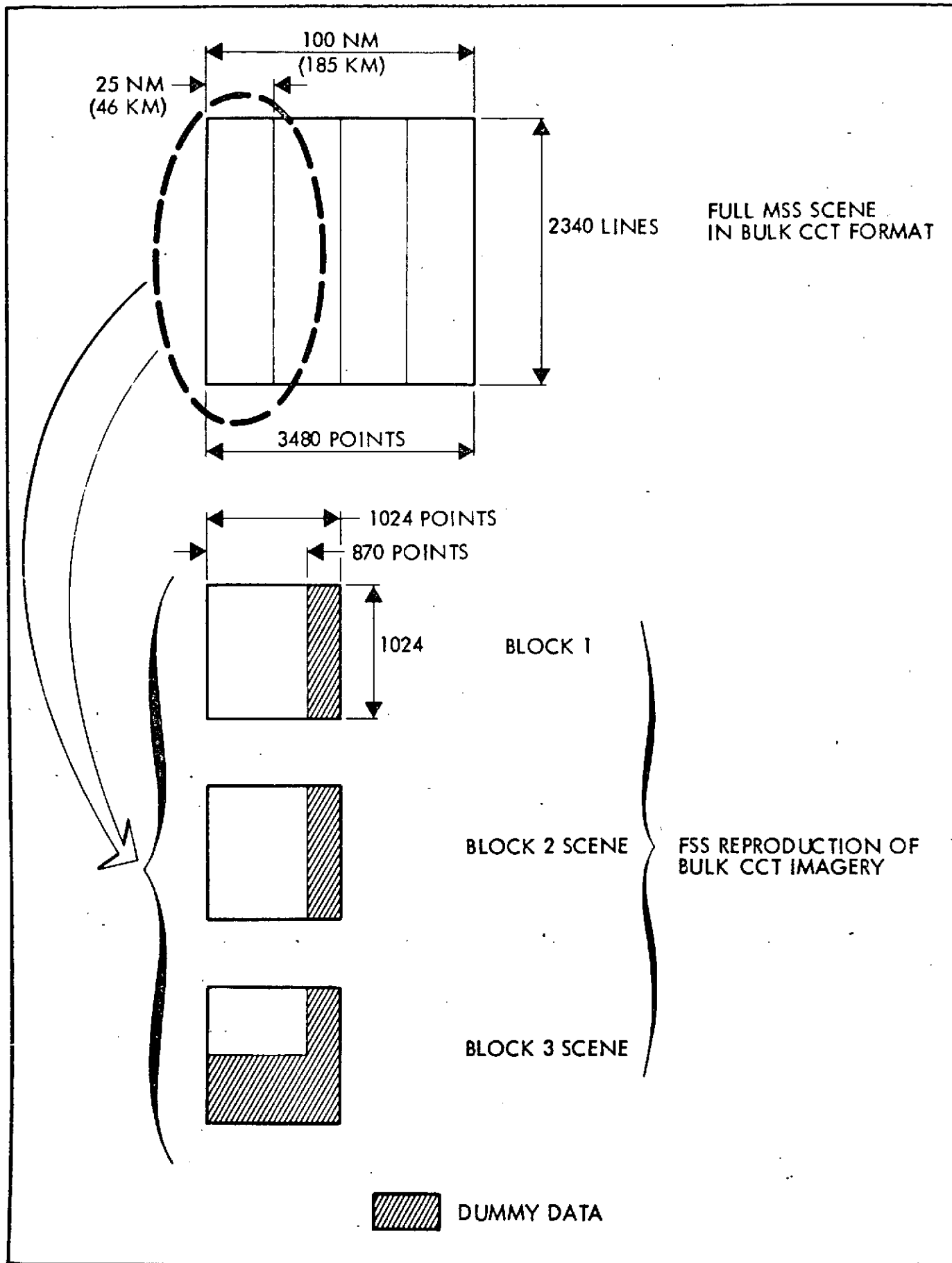


Figure 3-10. Bulk CCT Processing Flow Chart

data specification which limits scanning and line contours in the imaging system to be selectable only in binary steps of 256, 1024, 2048, and 4096. Since the 46 km strip from the bulk tape only contains around 870 points (bytes), it is necessary to insert enough dummy points (bytes) per line to total 1024. Similarly, the length of each strip of bulk data is 2340 lines and not an even multiple of 1024; it was therefore decided that when processing complete strips, they would be separated into two 1024 line blocks and one short block with dummy lines added to total 1024.

3.2.3 Software Processing

The processing techniques described below are equally applicable to preprocessed precision and bulk ERTS MSS tapes. Both types of CCT's were processed and analyzed in support of this program. It was soon decided, however, that the better radiometric accuracy of the bulk tapes was more valuable to the study of nearshore processes than the geometric accuracy of the precision tapes; attention was shifted, therefore, from precision tapes and only bulk tapes were processed during the latter phases of the study. The conventions adopted and other details of the digital processing techniques used are detailed in the following paragraphs.

Discrete Point Density Analysis

Starting with a 1024 X 1024 point Format B tape, there are several options available to the investigator:

Area Density Printout. The precise N-S line crossing a feature of interest can be located by requesting this formatted printout. Large geographical features such as islands, peninsulas and bays can be located by noting the sudden density changes of transitions from water to land. Then since the number of the first line and first column on the printout is known, it is a rather routine matter to locate the exact number of the line or column of interest. Typically, this would be a line that crosses two reference points, i.e., an island and a peninsula, and also a sediment deposit. Additional and more detailed studies can then be made by exercising the other program options.

Single Line Printout. A single N-S or E-N line can be selected for printout or graphical display from one or more spectral bands. These displays give the exact density values of every point and can be useful in conjunction with ground truth data in determining the correspondence between sediment load and reflectivity for the various spectral bands.

Multispectral Line Combinations. The multispectral N-S or E-W lines selected in the previous option can then be analyzed by using various mathematical techniques such as weighted arithmetical combinations of two or more spectral bands or cross-spectral correlational analysis of these lines.

Isodensity Contour Analysis

While most of the computer work done during the early phases of this study was performed on the Raytheon 706 computer system, it was necessary in the latter phases to utilize an IBM 370-165 system. This was primarily necessary because of core-size limitations, e.g., the Geoscience Earth Resources Contouring Program requires 300 K bytes of core. The steps involved in applying the Earth Resources Contouring Program to the ERTS data and the various options available are depicted in Figure 3-11.

First, the raw data contained in the bulk tapes is analyzed on a point-by-point basis to determine its micro-characteristics. Figure 3-12 is a computer dump of the data which represents the California coast around the Monterey Peninsula. Each number corresponds to a pixel and the specific value is representative of the reflectivity recorded for that point. Due to the scattering effect caused by small reflectivity variations, a smoothing operation is performed on the data prior to the generation of the contour map. More specifically, the following steps are taken:

Spectral Channel Selection. A specific rectangular area within the 1024 x 1024 scene is selected during the sampling process. The contouring program is sized to accept a maximum of 4900 data points.

Area Size Selection. By appropriately designating the sampling rate, areas of various sizes can be selected for contouring. For example, a 1024 x 1024 block represents a 46 x 46 km area. Therefore, a square array of data points (64 points long on each side $64 \times 64 = 4096$) can represent the full scene (46 km x 46 km) 1/4th (23 km x 23 km), 1/8th (11.5 km x 11.5 km), 1/16th (5.7 km x 5.7 km) or 1/32nd (2.8 km x 2.8 km) depending on whether a sampling rate of 16, 8, 4, 2, or 1 is selected. For the present application, a sampling rate of 8 was found to yield the most satisfactory results. This allows contouring in 11.5 km x 11.5 km geographical blocks as illustrated in Figure 3-13.

Digital Dump Selection. The data points representing the area selected are punched on data cards and may also be dumped on the line printer for verification.

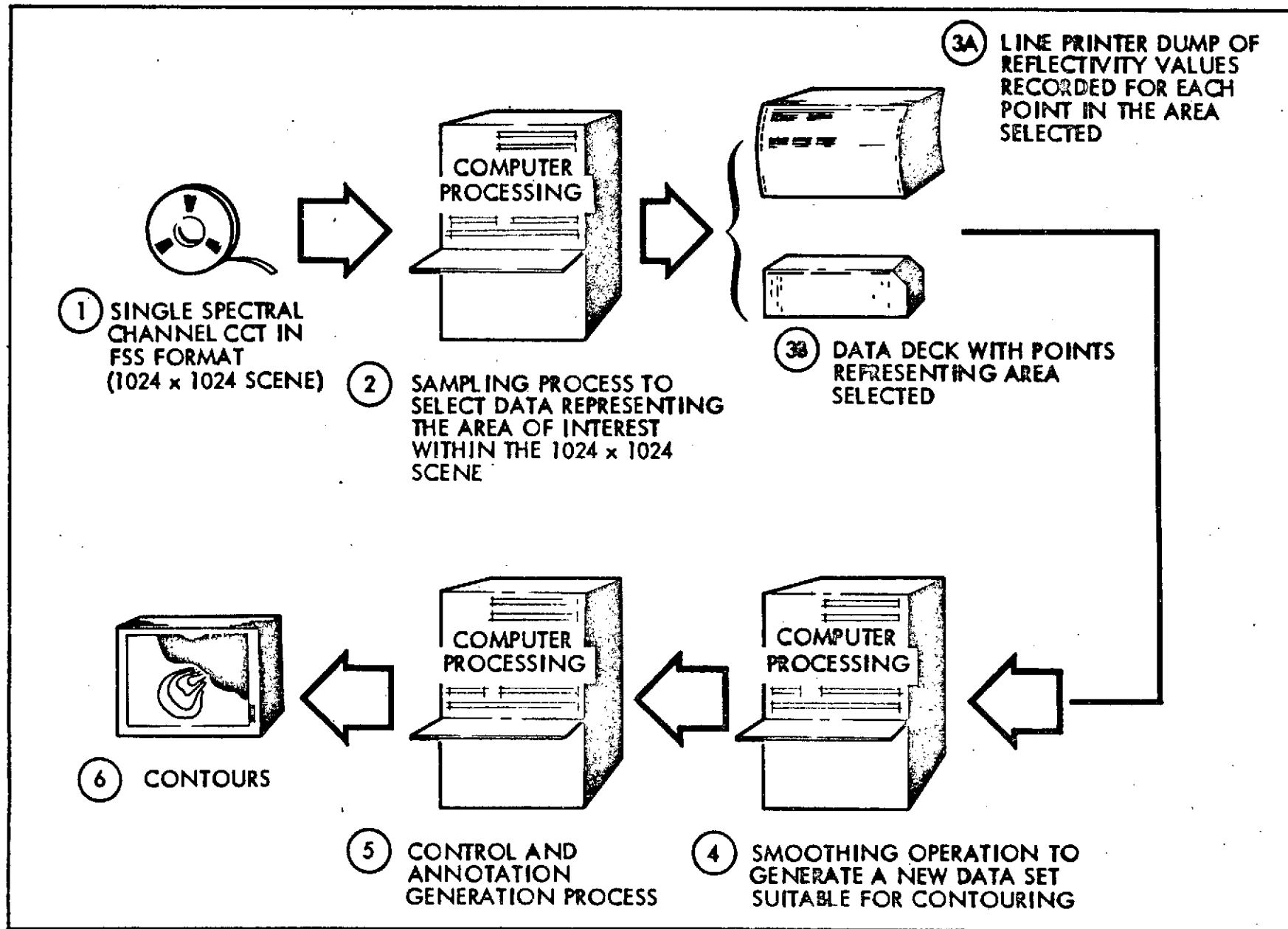


Figure 3-11 . Contouring Program Flow Chart

Figure 3-12. Digital Dump of Monterey Bay Contour Map
SCENE 1183-18182-4

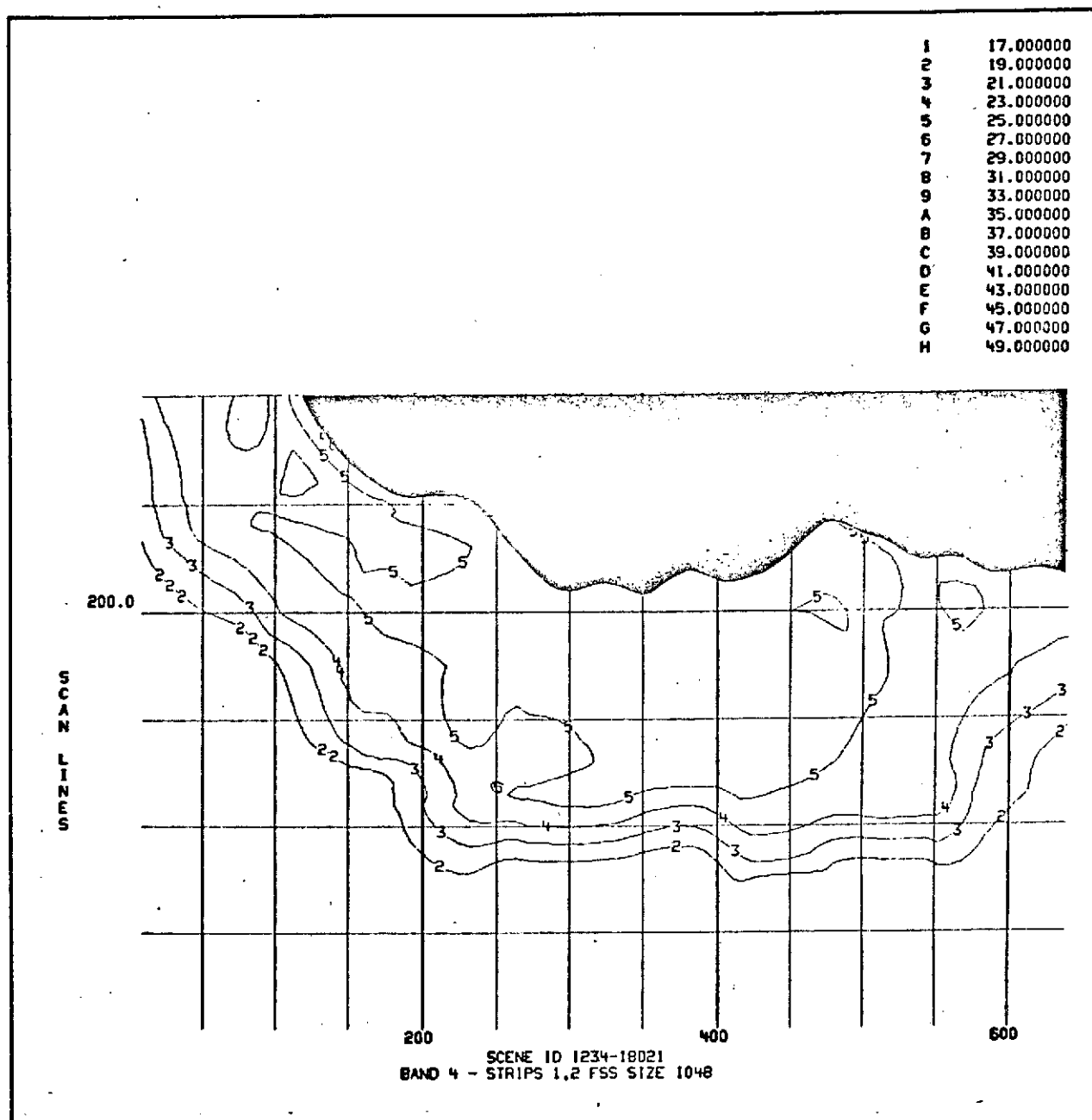


Figure 3-13. Contour of Santa Barbara Channel

Data Smoothing. Once a specific data block has been selected, a smoothing program is used to operate on the data. This involves using multiple regression surface fitting technique that eliminates scattering in the data values. This approach yields a set of data values which, when contoured, will reflect large area sedimentation patterns rather than localized variations.

Annotation Selection. During the contouring and annotation process, several formatting parameters can be specified: (a) a grid is superimposed on the contours and may be located to represent latitude and longitude lines; (b) the ratio of physical distance covered by equal number of points in the X and Y directions may be specified; this is useful in working with bulk data since 185 km in the X direction is represented by 3480 points while only 2340 points represent 185 km in the Y direction. This distortion may be corrected in the contoured plot by simply specifying this ratio.

A step external to the above process was incorporated in the generation of the contours shown in the figure. This consisted of using MSS spectral band 7 (near IR) as a reference to generate the shoreline. The characteristics of this band are such that the reflectance levels of land features are significantly lower in value than reflectance levels of water features (typically, water reflectivity value range is 0 to 3 and land reflectivity values range from 11 to 15); therefore, the shoreline can be easily discerned. A digital printout of band 7 was used to locate the shoreline on a similar printout of the identical area in band 4. The land mass was then masked and assigned a large reflectance value that would produce a distinct contour in the final output.

Mass Concentration Image Analysis

An important tool in the conduct of this study was the FSS analog image processor and its ability to generate enhanced images from digital tapes with data in the described Format B.

All of the digital processes that output area information can be made to generate a Format B digital tape which can then be played through the FSS system to generate an enhanced photograph. The digital system operates in these instances as a preprocessor to the analog processing techniques discussed in other sections of this report. Some of the options that can be exercised in generating the FSS tapes are as follows:

Block Selection. Specific 1024 X 1024 blocks can be selected from any scene and spectral band for reproduction on the FSS.

Block Combination. Any four adjacent 1024 X 1024 blocks can be digitally combined to generate a 1/4 scale image of a larger area.

Multispectral Combinations. Special effects such as masking can be achieved in the output image by combining data from two spectral bands such that if the data exceeds a pre-established threshold in one band, then the data on the other band is saturated. This technique is particularly useful in defining shorelines in a fashion similar to that used in the contouring process where band 7 is used to mask and mark the transition from water to land.

3.3 MULTI-CHANNEL COMPUTER PROCESSING

The multi-channel computer processing takes place on the IBM 370 computer. This technique is used to enhance water density differences between various MSS channels in order to enhance suspended sediment and current features. The IBM 370 is advantageous because larger amounts of data can be processed under control of a single program. The first step is to produce a FSS compatible tape as described in Section 3.2.2. A program option allows the operator to select a portion of a single strip from one CCT or combine strips from two CCT's into a single frame. The resulting displays cover 46 km or 92 km wide areas, respectively.

The next step was to manipulate the data from different bands in order to obtain digital enhancement of certain features. A program was written to allow up to 10 arithmetic operations to be performed on each reformatted set of spectral data. Constants may be added, subtracted, multiplied or ratioed with array elements. Original and/or resultant data arrays may be manipulated together through a sequence of operations specified by the user. The resultant data set is formatted for graphical display on the FSS. ERTS frame number 1234 - 18021 was selected and processed through the above program. First, the original band 4 and band 5 data sets were converted into FSS compatible formats. The digital levels of two specific features (open ocean water and high suspended sediment concentration) were determined. These numbers establish the values of constants, as well as the optimum arithmetic operation to be applied to the raw data sets. These initial operations function as a preprocessing. Such operations are necessary to insure that signal range produced by additional interband processing will result in real meaningful data that can be recorded through the FSS system. When performing such inter-band operations as subtracting or ratioing, the probability of generating values less than one, or, in fact, less than zero exists. These data values are not acceptable. Preprocessing reduces this possibility. For the above ERTS frame, the measured values are shown below:

<u>Spectral Band</u>	<u>Open Water</u>	<u>Maximum Suspended Sediment</u>
4	7	14
5	14	28

Two interband manipulations were performed: (1) ratioing the band 4 array by band 5; and (2) subtracting the band 5 array from band 4.

The extent and boundary of sediment anomalies detected by band 4 greatly exceeded those visible in band 5 data. A typical ERTS scene can be thought of in terms of three regions. The first region contains suspended sediment features which were detected in both band 4 and 5. These features are common. The second area or region contains sediment which is visible in band 4, but not detected by band 5. The details of these features are of key importance to a proper interpretation since this suspended material is in the subsurface water. Lastly, the open water area is that region where sediment features were not detected by either band. The anticipated results on any inter-band manipulation is an enhancement of those features described by the second condition. To successfully apply inter-band processing, the nominal brightness levels of the three regions were considered. The above table lists this information for frame 1234 - 18021. As shown, the levels associated with open water and sediment features were higher in band 5. Thus, both raw data arrays had to be preprocessed. The type and extent of conditioning varied for ratioing and subtraction, respectively.

The ratioing process was designed to normalize the common regions (open water and regions of high sediment concentration). The uncommon feature would be divided by a level correlating no sediment in band 5. The result would be an enhancement of the uncommon feature along with suppression of those which were common. The original NASA frames are shown in Figure 3-14. In Figure 3-15, the results of ratioing using the multi-channel computer processing is illustrated. The details of the nearshore sediment plumes are brought out. Possibly more important, the southeast directed lineation south of Anacapa Island is brought out in this process. A number of other similar features are also emphasized. When viewing the original, many of these features are invisible.

The subtraction method was also designed to enhance the uncommon sediment feature. For this technique, the band 4 array was from multiplication by 2. This brought the brightness levels of specific feature within bands 4 and 5 to a common base. The differencing resulted in a suppression of common features and an enhancement of the uncommon data. The processed image is shown in Figure 3-16.

3.4 PHOTOGRAPHIC OPTICAL PROCESSING

In making interpretations from NASA-supplied negatives, it was necessary to use photographic optical processing to bring out subtle features. For a specific film emulsion, there exists a relationship between resulting film density and exposure when making contact transparencies of ERTS-1 imagery. This relationship is well documented and supplied by the manufacturer (known as the Characteristic Curve). The significance of this curve will be explained in the following text. At

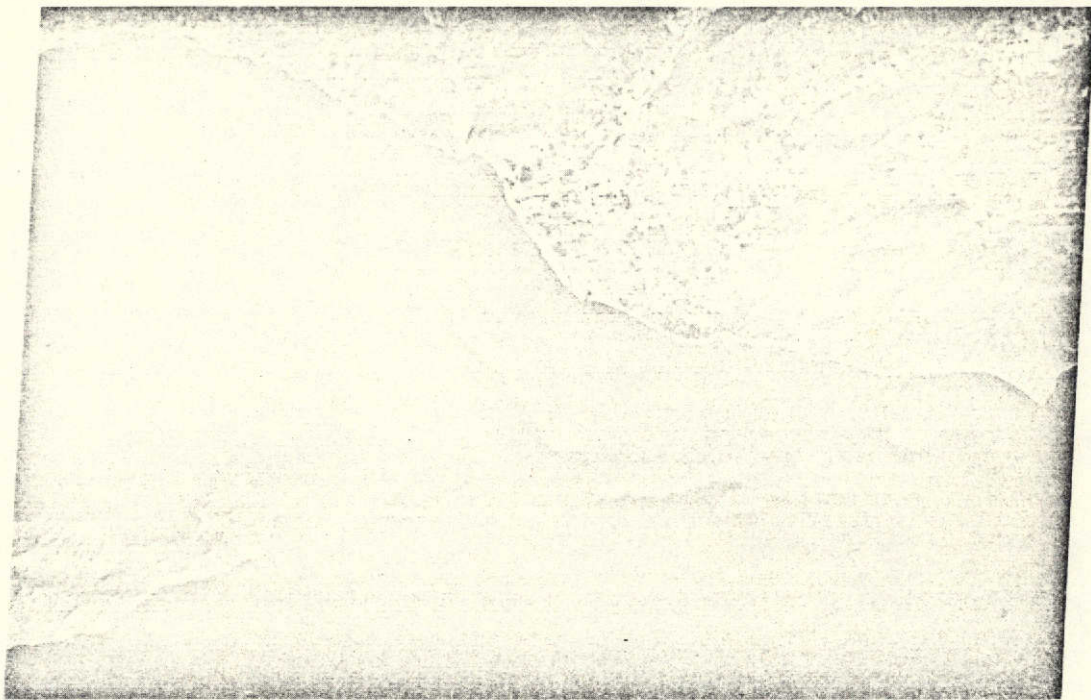
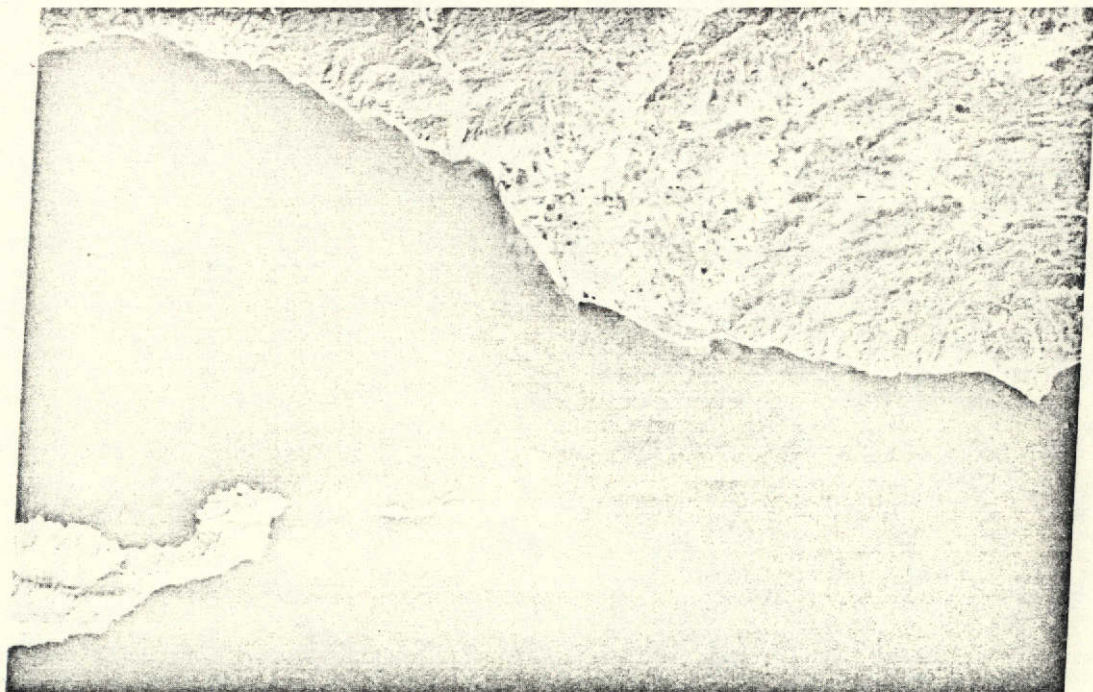


Figure 3-14. Santa Barbara - Anacapa, Scene 1234-18021
(Original MSS band 4 top, band 5 bottom)



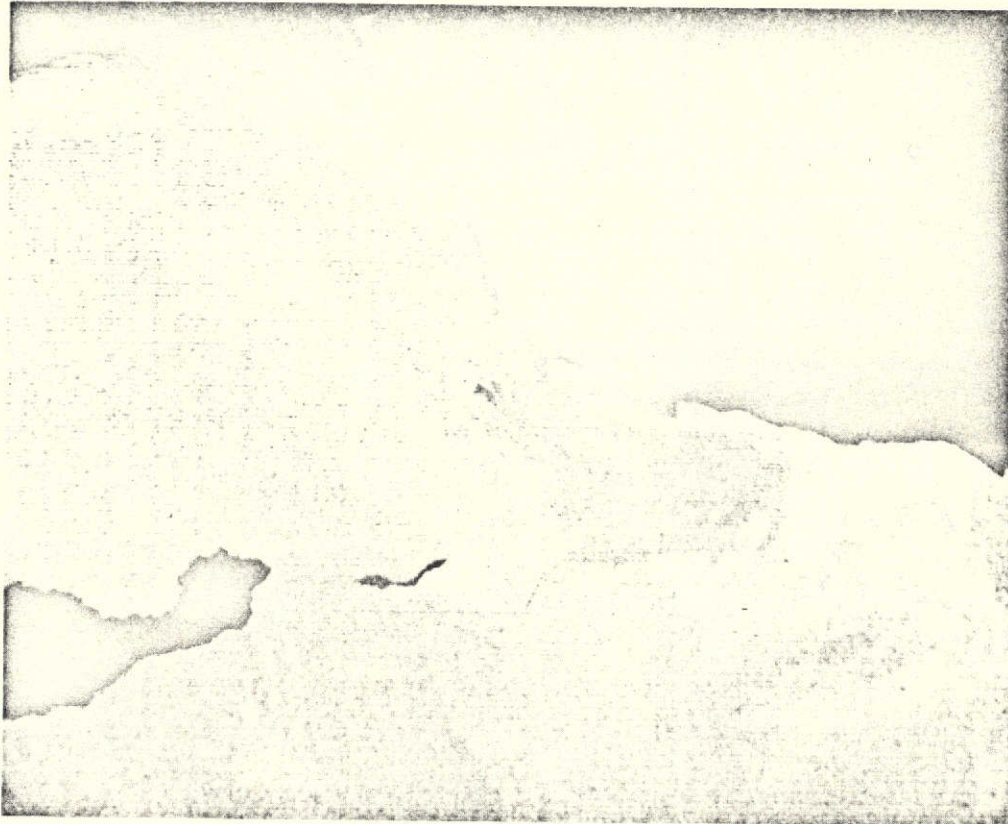


Figure 3-15. Ratioing of Scene 1234-18021, Santa Barbara - Anacapa Area
 Formula used - Ratio = 5 (band 4)/(band 5).
 Positive (above), Negative (below).





Figure 3-16. Subtraction of Scene 1234-18021, Santa Barbara - Anacapa Area
 Formula used - Subtraction = 2 (band 4)/(band5).
 Positive (above), Negative (below).



this point, however, some basic definitions will serve to clarify the theory of this method.

Contact printing of ERTS bulk film chips was accomplished by placing a developed negative over and in direct contact with an unexposed film and exposing. The light source used for our experiment was provided from an Omega D-2 Enlarger. The intensity of the incident light is referred to as I_0 . The intensity of light which is transmitted through the image is referred to as I_T . For the purpose of explanation, we will consider a small portion of the ERTS image such that the density within this bound area is constant and homogeneous. Density is defined as:

$$\text{Density} = \log_{10} \frac{I_0}{I_T} \quad (1)$$

Thus, the light which is transmitted through an ERTS negative and exposes the over-exposed film can be called I_0' where,

$$I_0' = I_T = \frac{I_0}{\log_{10} (\text{Density})} \quad (2)$$

The unexposed film is now exposed to an intensity equal to I_0' . The exposure level (E), however, is a function of not only I_0' , but also time. Thus,

$$E = I_0' \times (\text{time}) \quad (3)$$

With the above definitions in mind, the Characteristic Curve can be presented. Below is a typical Characteristic Curve, relating resultant film density to log exposure level:

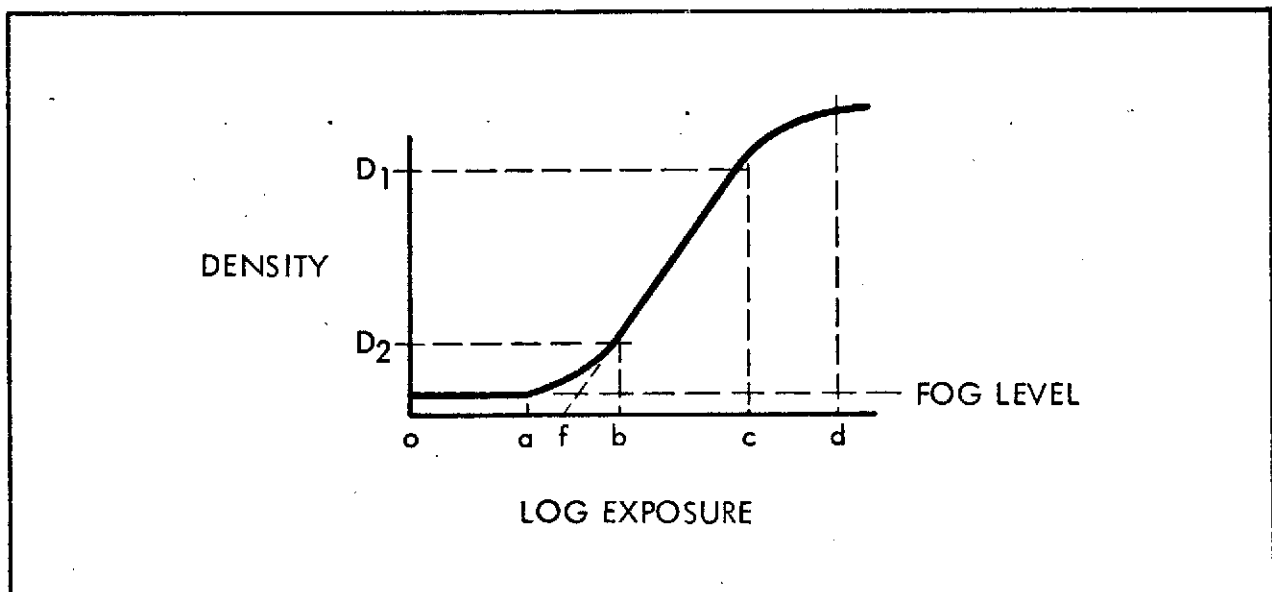


Figure 3-17. Characteristic Curve

One should note that the relationship is an "S" shaped curve. For exposures between "0" "a", the resultant density doesn't change with exposure. This, typically, is referred to as the film's fog level. As the exposure is increased from "a" to "b", the resultant density increases in a non-linear manner. This portion of the Characteristic Curve represents "under exposure." Exposures from "b" to "c" will result in a linear increase in density. Again, the exposure scale is plotted as a log. For exposures between "c" and "d", one gets a slight increase in density for increased exposure. This region is generally known as "overexposure." The slope of the curve's linear segment (b to c) is referred to as film gamma (γ), where:

$$\gamma = \frac{D_1 - D_2}{c - b} \quad (4)$$

Since we have been considering a small area within an ERTS image with a uniform density, the exposing light intensity transmitted through the image onto the unexposed film was a constant. Thus, we varied our exposure level by increasing the exposure time. Now consider the nearshore sediment feature as viewed from ERTS film data. The sediment is represented as a density range contained within total density range of the image. When contact printing these features, this density range relates first to transmitted light, then to an exposure range along the log E axis of the Characteristic Curve. This exposure range then relates through the curve to a resultant density range on the printed image. One can see if you could change the slope or γ of this curve, the resultant density range for a given exposure range will change. Thus, contrast enhancement could be achieved.

In practice, different films have Characteristic Curves with different γ 's. Also, the γ of a specific film is not unique, but can be controlled by varying the parameter used in the film processing method. These parameters include: (1) the type of developing solution; (2) time of processing; and (3) temperature of developer.

Approach

The contrast in a contact printed transparency can be controlled. However, a number of changing parameters must be considered. The approach used attempted to minimize these changes. The first parameter considered was the intensity of the exposing light source. As mentioned above, an Omega D-2 Enlarger provided the light which was transmitted through the ERTS negative and exposed the unexposed film. The intensity of this light is a function of: (1) the lens f-number; and (2) the format size of the projected light. These parameters were optimized and held fixed. Thus, the exposure became a function of time only.

A MacBeth Spot Densitometer was used to measure the densities on a Kodak step wedge. This wedge was then contact printed onto Kodak fine grain aerial duplicating film 2430. The resultant densities on the contact transparency were measured. The film processing parameters were selected to correlate with the

3-minute characteristic curve contained within the family of curves shown below.

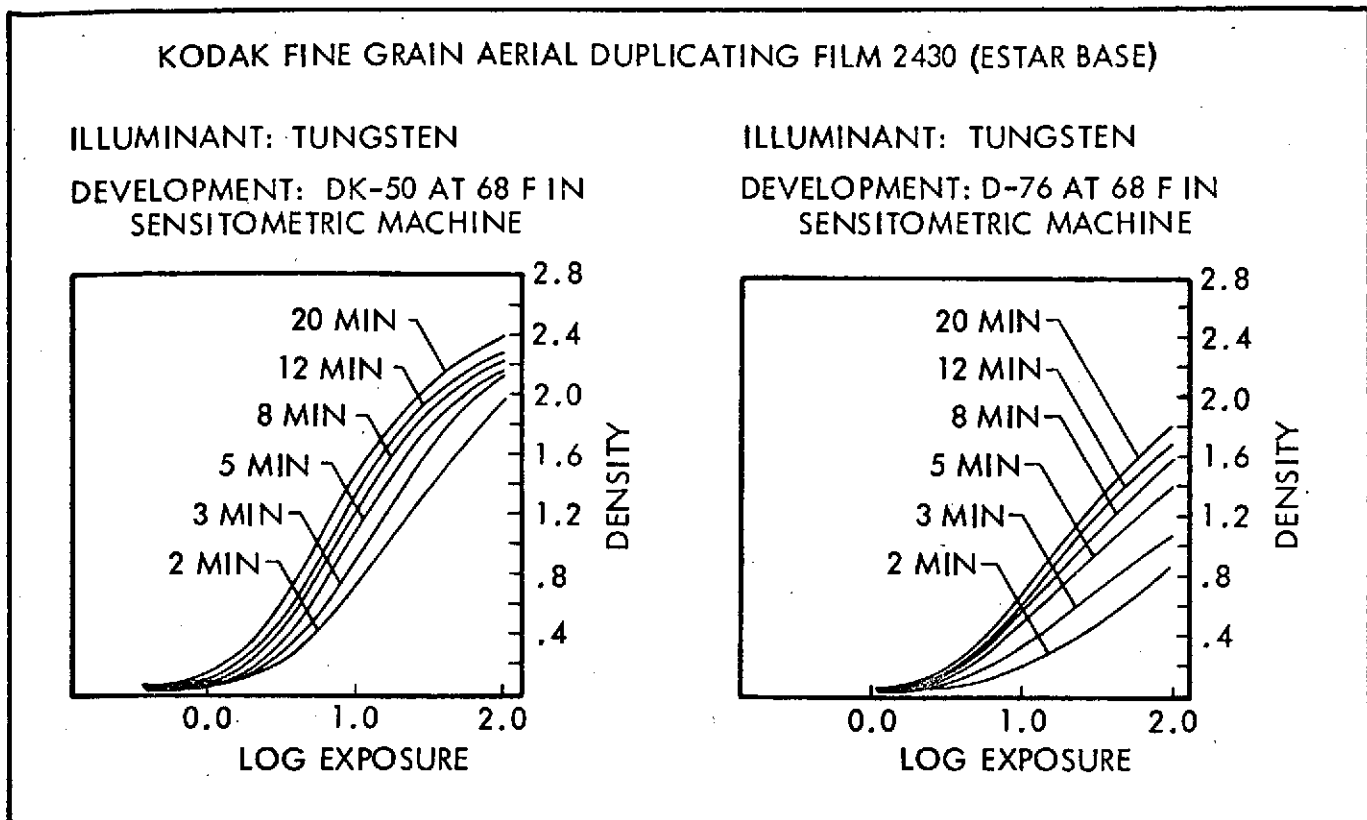


Figure 3-18. Characteristic Curve for Kodak 2430 (Kodak, 1969)

By locating a resultant density on the density axis, the log exposure number that relates to that density can be determined. Now from equations (2) and (3), I_0 (intensity of incident light) can be determined.

$$I_0 = \frac{\log_{10}^{-1}(\log E) \times \log_{10}^{-1}(\text{Density})}{\text{Time}} \quad (5)$$

Knowing I_0 , you can measure the lightest and darkest densities contained in a sediment anomaly (minimum intensity is open ocean water). Given I_0 as a constant, the minimum and maximum transmitted light intensities can be determined using equation (2). Knowing $I_0'_{\min}$ and $I_0'_{\max}$, it is now possible to determine an exposure time which correlates to the linear segment of any one of the family of Characteristic Curves. Selecting that curve will give the maximum contrast for the determined exposure range established above.

Experiment and Results

Using a spot densitometer, the diffuse density of three features in ERTS-1 frame No. 1562 - 18191 -4 measured as shown on the next page.

<u>Feature</u>	<u>Density</u>
Open Water	1.40
Concentrated Offshore Sediment	1.66
Inter-bay Sediment	1.74

These density values correlated to steps 8 through 11 on the standard Kodak calibrated step wedge. Using the procedure described above, this portion of the wedge was contact printed at three exposure times and then processed in accordance with the 3-minute curve in Figure 3-18. The resultant densities are tabulated below.

<u>Step No.</u>	<u>Exposure Time (sec)</u>	<u>Density of Steps</u>	<u>Resultant Density</u>
8	5	1.25	.32
9	5	1.40	.25
10	5	1.55	.19
11	5	1.70	.14
8	15	1.25	.58
9	15	1.40	.49
10	15	1.55	.39
11	15	1.70	.30
8	30	1.25	.80
9	30	1.40	.66
10	30	1.70	.44
11	30	1.70	.44

The above data and the 3-minute Characteristic Curve was then used to calculate the intensity of our light source, using equation (5). This number is necessary so that one can determine the optimum exposure time when processing the film to a new and different gamma. The intensity was determined to be 22. This light, however, is transmitted through the ERTS negative and attenuated by the film's density during the printing process. The intensities transmitted through a density correlating to open water and concentration offshore sediment, respectively, were calculated using equation (2) to be .88 and .44.

Since contrast enhancement is of major interest, the film was processed to the gamma curve with the greatest slope. Inspection of Figure 3-19B shows that the 20-minute characteristic curve is optimum. The linear portion of this curve is bound by log exposure numbers from .95 to 1.5. From equation (3) and knowing the minimum intensity of the exposing light, the optimum exposure time was determined:

$$\text{time} = \frac{\log^{-1}(\log \exp N_0)}{I_0} \quad (6)$$

The optimum exposure time was determined to be 13 seconds. This exposure time is only optimum when the film is processed to the 20-minute Characteristic Curve.

Figure 3-19 shows the results obtained. Image A was printed and processed to a lesser gamma than Image B. One can immediately see the increased contrast displayed in Image B.

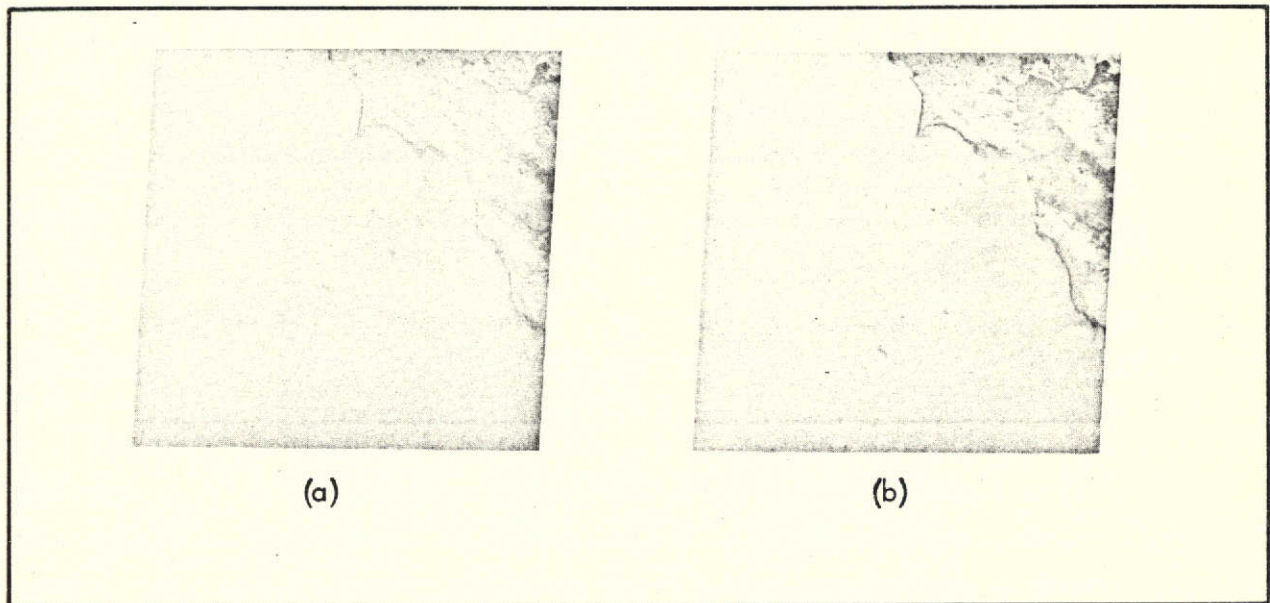


Figure 3-19. ERTS-1 Characteristic Curve Enhancement

These two pictures were taken using the techniques described in Section 3.4. Image A was printed and processed to a lesser gamma than Image B. The increased contrast in Image B emphasizes the nearshore and offshore suspended sediment in greater detail. This is a valuable assist to the investigator looking for subtle changes. This picture was taken February 5, 1974, and shows San Francisco Bay, Pt. Reyes, and the San Francisco Peninsula.

As stated, different films have Characteristic Curves with different γ 's. The initial approach was to control the slope or γ of a specific film's Characteristic Curves (Kodak type 2430 Aerial Duplicating Film). This was accomplished by varying the processing procedures. An alternate approach was to select a film whose characteristics were more tailored to the contrast enhancement application. A literature search resulted in the selection of Kodak type 2575 as an optimum emulsion. This film displays an increased gamma for shorter processing times, thus simplifying the data processing task. Figure 3-20 shows the band 4 enhancement of scene 1562 - 18191 which resulted.

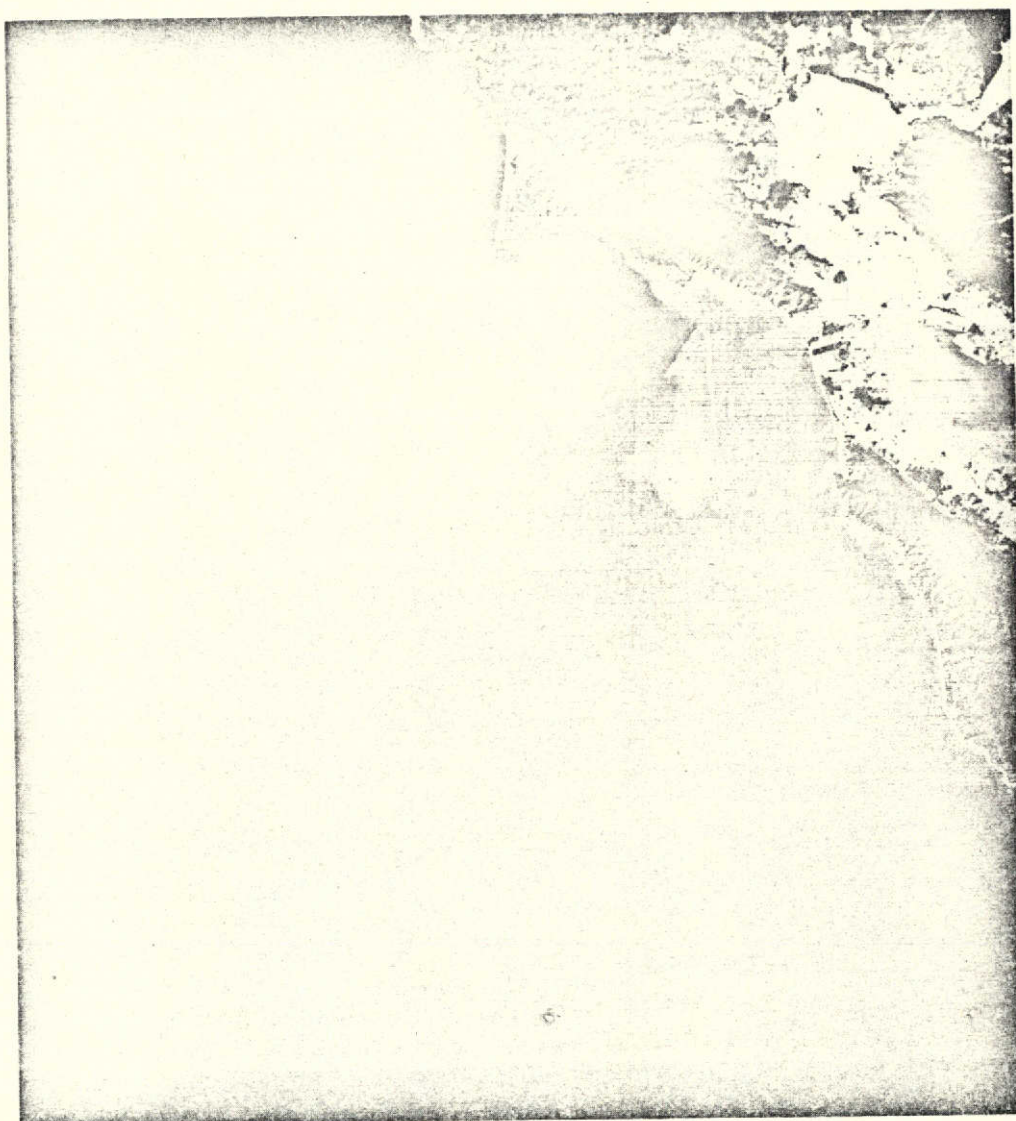


Figure 3-20. San Francisco Area Kodak 2575 Film

This print illustrates the use of film with characteristics which emphasize contrast in the densities corresponding to suspended materials. This is scene 1562-18191-4 taken February 5, 1974.

4.0 CALIFORNIA COASTAL CURRENTS

The ability to analyze the California coastal currents from ERTS-1 has been demonstrated in detail as evidenced by the enclosed seasonal and month-by-month current charts. During this study, it became apparent that background literature concerning precise surface currents on much of the nearshore area was either lacking or incomplete. This was not necessarily the case near oceanographic institutions or in the calmer southern California waters but north of Pt. Conception the detailed information was often seasonal. The ERTS data which defines surface dynamics supplies an important source of data on the California coastal current system. The transitory nature of the currents makes their study both time consuming and expensive when using ocean station information. The combination of ERTS imagery analysis with confirmation by aircraft data and sea truth spot checks has added an important dimension to the study of coastal processes.

Originally this study was to be confined to four test cells (San Francisco, Monterey, Santa Barbara Channel and San Pedro Channel) as shown on the map, Figures 1-2 and 1-3. It soon became apparent that it was impossible to abide by these limiting boundaries. The interaction of the entire coastal current system was necessary for analysis. For this reason, the test cells were used for operational examples only. The new boundaries were defined as the geographic limits of the coast of California. In some cases, this limit was not even sufficient (i.e., the California currents splitting into northern and southern moving components near Capo Colnett in Baja California; however, the majority of the discussion applies to the waters off California.

In analyzing the ERTS-1 imagery, Channel 4 (5,000-6,000Å) was found to be the most useful in current studies. Channel 5 (6,000-7,000Å) was excellent for showing the areas of high suspended sediment concentration. Although Channel 6 (7,000-8,000Å) not used extensively, in several cases it was utilized to illustrate the immediate outline of riverine discharges with the highest sediment concentration. The infrared Channel 7 (8,000-9,000Å) clearly delineated the shoreline and provided good haze penetration.

Throughout the study period (July 1972 - May 1974), the usefulness of the ERTS-1 imagery varied as determined by weather, run-off, haze and image quality. A summary of the imagery usefulness in the study of nearshore processes is presented in Figure 4-1. It should be noted that several months are supplemented by aircraft data. Out of the 480 possible images represented on this summary, 142 or 30% were useful for sediment transport and current analysis. An additional 35 images represented high quality pictures but for seasonal or lack of run-off were not useful in this study. Once the image quality was improved in the fall of 1972, the usefulness of the data became fairly consistent. With the exception of February 1973, the only extended period of low % image usefulness was during the fall months of 1973. This was due primarily to the coastal fog and haze which often remains over the coast past the ERTS overpass time of about 10:00 AM.

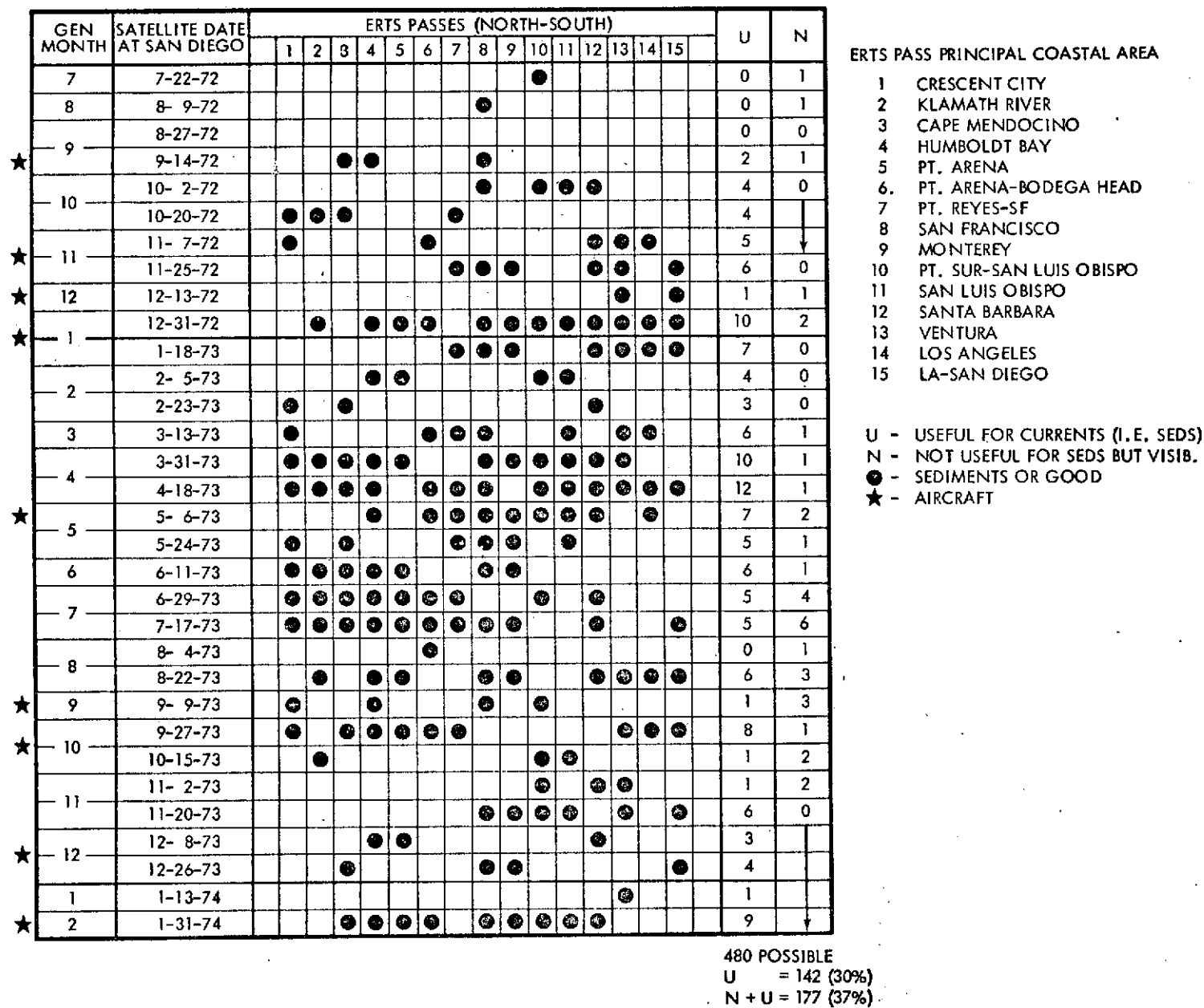


Figure 4-1. Summary of ERTS Imagery Useful to Nearshore Processes

4.1 GENERAL HISTORICAL DESCRIPTION

The California Current which has the dominant effect on the California coast was described by Sverdrup, et. al., 1942. Analysis at that time was based on periodic ocean station information. For the detail presented from these sketchy sources, it is remarkable in its content. Modifications of this California Current due to seasonal wind and supplemental currents was described. During the period of March through July, north-northwest winds cause various upwelling to occur. Toward the end of summer, upwelling gradually ceases, and a more or less regular pattern of currents flowing generally south occurs. This is called the Oceanic Current Period as described by Skogsberg (1936) in his detailed study of Monterey Bay. In the fall, the surface layers of water are affected by a countercurrent moving generally northward. This Sverdrup called the Davidson Current. It runs north during November to January or February until upwelling and the nearshore California Current again break up this pattern. The detailed eddies, upwellings and countercurrents set up by these transitory patterns are described in detail in sections on these currents - Oceanic 4.2.1, Upwelling 4.2.2 and Davidson 4.2.3. These discussions are based on the ERTS mosaics which, in turn, are based on Sverdrup and Skogsberg's original current season definitions.

Recent publications on the California coastal processes and currents include discussions by Kolpack, 1971, SCCWRP (Southern California Coastal Water Research Project, 1972), and Inman and Brush, 1973. Kolpack's report deals mainly with the Santa Barbara oil spill site, but the overall temperature, salinity, and current plots he presents are most useful as background in the understanding of the southern section of the current system. The SCCWRP report emphasizes the water environment and pollution in the Southern California Bight and includes several sections on currents and suspended sediment distribution. The Inman, Brush, 1973 article is one in a long series authored or co-authored by Inman. This publication titled the "Coastal Challenge" gives a detailed description of the dynamic coastal zone environment and the impact of man's intervention on this zone. Since this is one of the primary concerns of the U. S. Army Corps of Engineers, the included information was most pertinent.

4.2 CURRENT SUMMARY

Analysis of all the available ERTS-1 imagery, NASA/Ames, U-2 photography, low altitude aircraft imagery and sea truth data resulted in the following series of current plots. In most cases, the NASA supplied 70mm Channel 4 transparencies and subsequent photographic enlargements were used in these plots. Where details of the suspended sediment patterns were needed, CCT tapes were used; and contrast stretching of the available signals were carried out (Section 3.0). At times, however, weather, fog, or imagery contrast resulted in little or no usable ERTS information. In these cases, the U-2 photography was essential for continuing the month-by-month current analysis. The U-2 data which also covers many of the periods when good ERTS imagery was available, was also excellent for detailed nearshore sediment transport, current patterns and wave parameters.

The low altitude aircraft flights are described in Appendix A, plus the log of resulting 70mm photography, thermal imagery, multispectral photography, and multispectral scanner data which were utilized as background information for this study. Numerous sources of sea truth were also obtained as available. The most useful came from: U. S. Army Corps of Engineers, National Park Service, University of Southern California, California State University Santa Cruz and U. S. Geological Survey.

A number of current plots are presented in this section to show seasonal and monthly changes in the transitory surface current pattern. Figure 4-2 is a summary of all of these plots while Figure 4-3 and 4-4 illustrate current changes in the inshore and offshore current pattern, respectively. Where north or south currents are dominant the current direction is indicated by an arrow. During the transition months, however, the composite of all available information resulted in the need to plot either a gyre or a mixture pattern. This is especially evident (Figure 4-2) during the fall months when the south-moving California Current is being overcome by the north moving Davidson Current in the nearshore areas. In the Santa Barbara area, the California Countercurrent, which is present to various degrees throughout the year, causes the variable patterns indicated. At several locations, isolated south-moving currents are plotted in the middle of a general north current pattern. Investigation of these isolated features indicates that in each case a headland, cape or point is protruding into the coastal current stream causing gyres, eddies and current reversals.

The inshore (Figure 4-3) and offshore (Figure 4-4) current plots are in general agreement with a few significant exceptions. In the southern California Bight, the north-northwest moving current stays in effect in the inshore area long after the offshore currents have reversed. Again, this is caused by the complex California Countercurrent in the Southern California Bight. The California Current is moving southward offshore long before (about 3 months) its effect is felt inshore. In viewing these three figures by themselves, the promontories and bights along the coast can be picked out by noting current reversals. This is because of the current changes caused by the changing coastline. These major contributing coastal features are from north to south: Pt. St. George, Patrick's Point, Cape Mendocino, Pt. Gorda, Pt. Delgada, Pt. Arena, Pt. Reyes, Duxbury Pt., Pt. Ano Nuevo, Monterey Bay, Pt. Sur, San Luis Obispo Bay, Pt. Conception, Southern California Bight, Pt. Dume, Palos Verdes Peninsula, Dana Pt. and Pt. Loma.

Current plots for the three ocean seasons are presented on Figures 4-5 to 4-16 and the monthly plots for both northern and southern California on Figures 4-17 to 4-40.

4.2.1 Oceanic Period

The California Current system dominates the nearshore surface current patterns during the Oceanic Period from July to November. In the offshore area, this current is the driving force of open ocean waters throughout the year. In this offshore area, the surface currents are driven and affected by gravity, friction, forces due to pressure gradients and Coriolis acceleration. Nearshore water movements, however, which overlie the continental shelf are affected to a greater degree by wind, tidal forces,

EXPLANATION

SOUTH CURRENTS
NORTH CURRENTS

▲ = UP COAST
▼ = DOWN COAST
○ = GYRES
• = MIXTURE

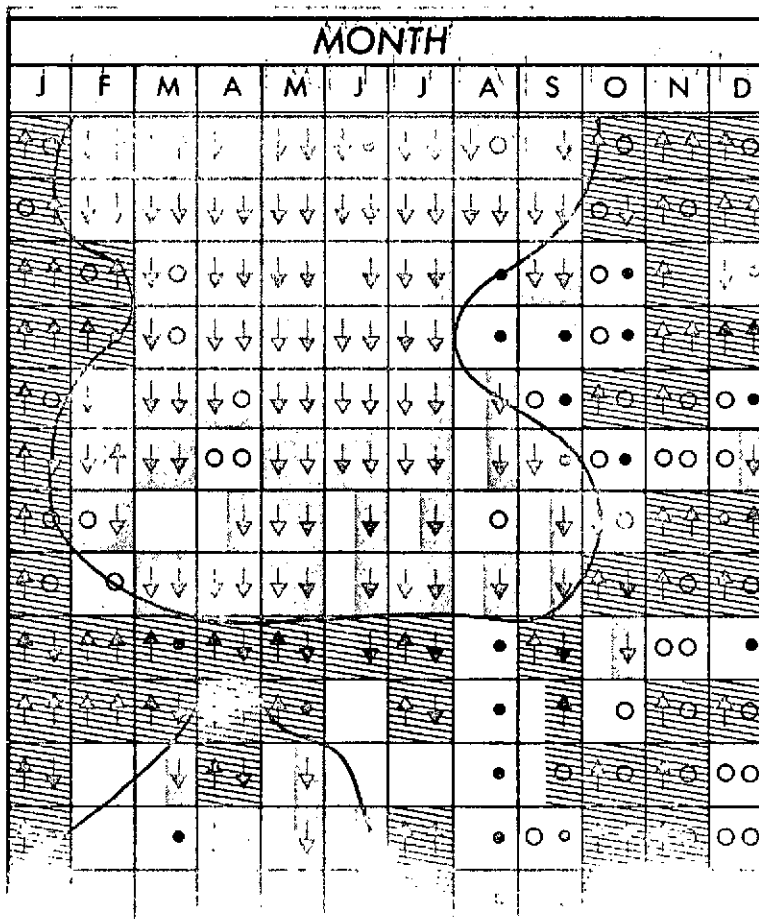
▲ = INSHORE ~1-5 KM
▲ = OFFSHORE ~30 KM

LATITUDE (°N) LONGITUDE (°W)

MONTH

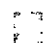
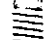
REACH

41-42	124-125
40-41	124-125
39-40	123.5-124.5
38-39	123-124
37-38	122-123
36-37	121.5-122.5
35-36	121-122
34.5-35	120.5-121
34-34.5	119.5-120.5
34-34.5	119-120
33.5-34	118.5-119
33-33.8	118-118.5
33-33.5	117-118



CRESCENT CITY
CAPE MENDOCINO
FT. BRAGG
PT. ARENA-BODEGA HEAD
SAN FRANCISCO
MONTEREY
PT. SUR-SAN LUIS OBISPO
SAN LUIS OBISPO
SANTA BARBARA
VENTURA
LOS ANGELES
LONG BEACH
OCEANSIDE

EXPLANATION

 SOUTH CURRENTS
 NORTH CURRENTS

 - UP COAST
 - DOWN COAST
 - GYRES
 - MIXTURE

 - INSHORE ~1-5 KM
 - OFFSHORE ~30 KM

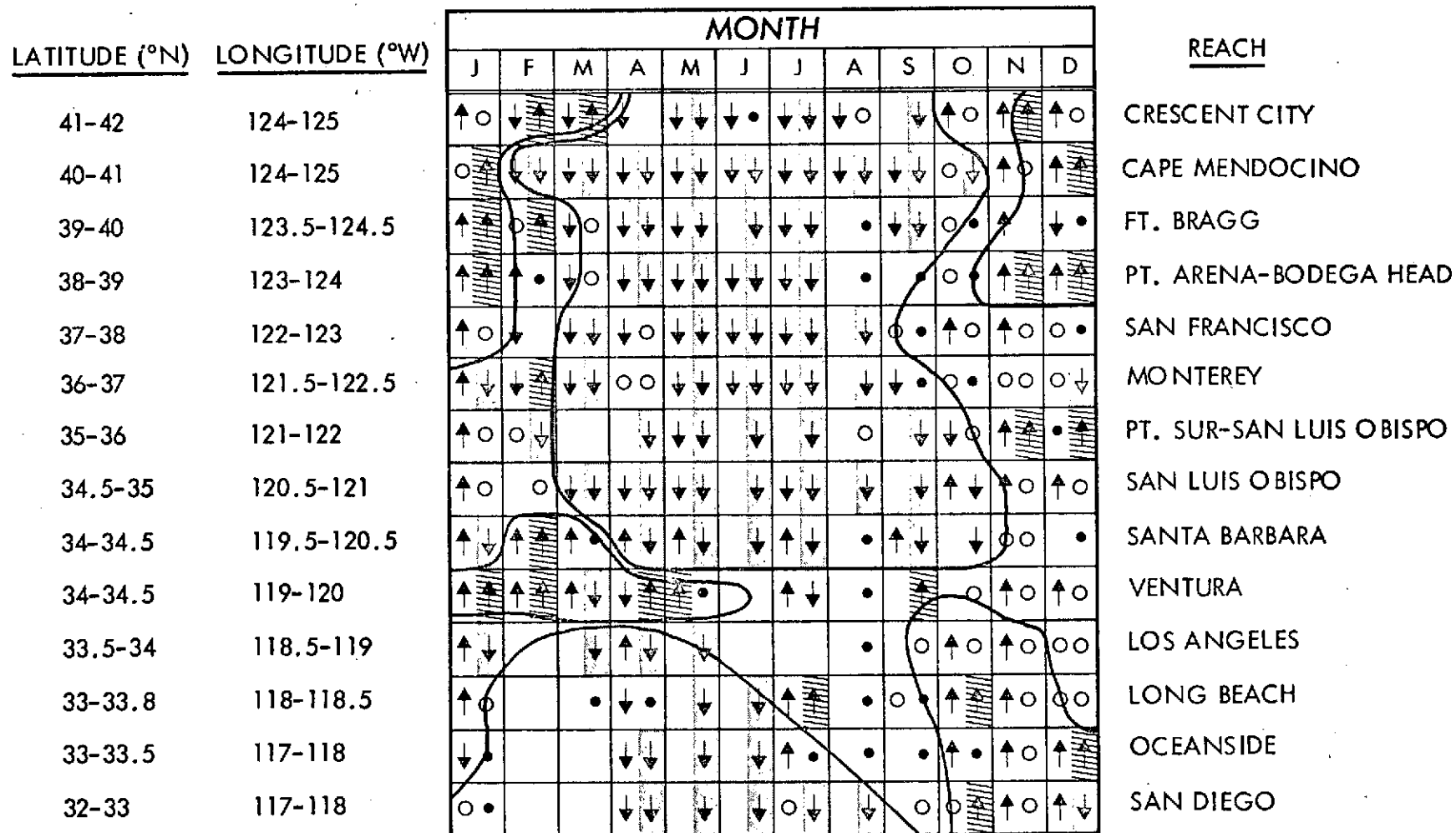




Figure 4-3. Summary of Inshore Currents from ERTS-1

EXPLANATION

 SOUTH CURRENTS
 NORTH CURRENTS

▲ - UP COAST
 ▼ - DOWN COAST
 ○ - GYRES
 • - MIXTURE

▲ - INSHORE ~1-5 KM
 ▲ - OFFSHORE ~30 KM

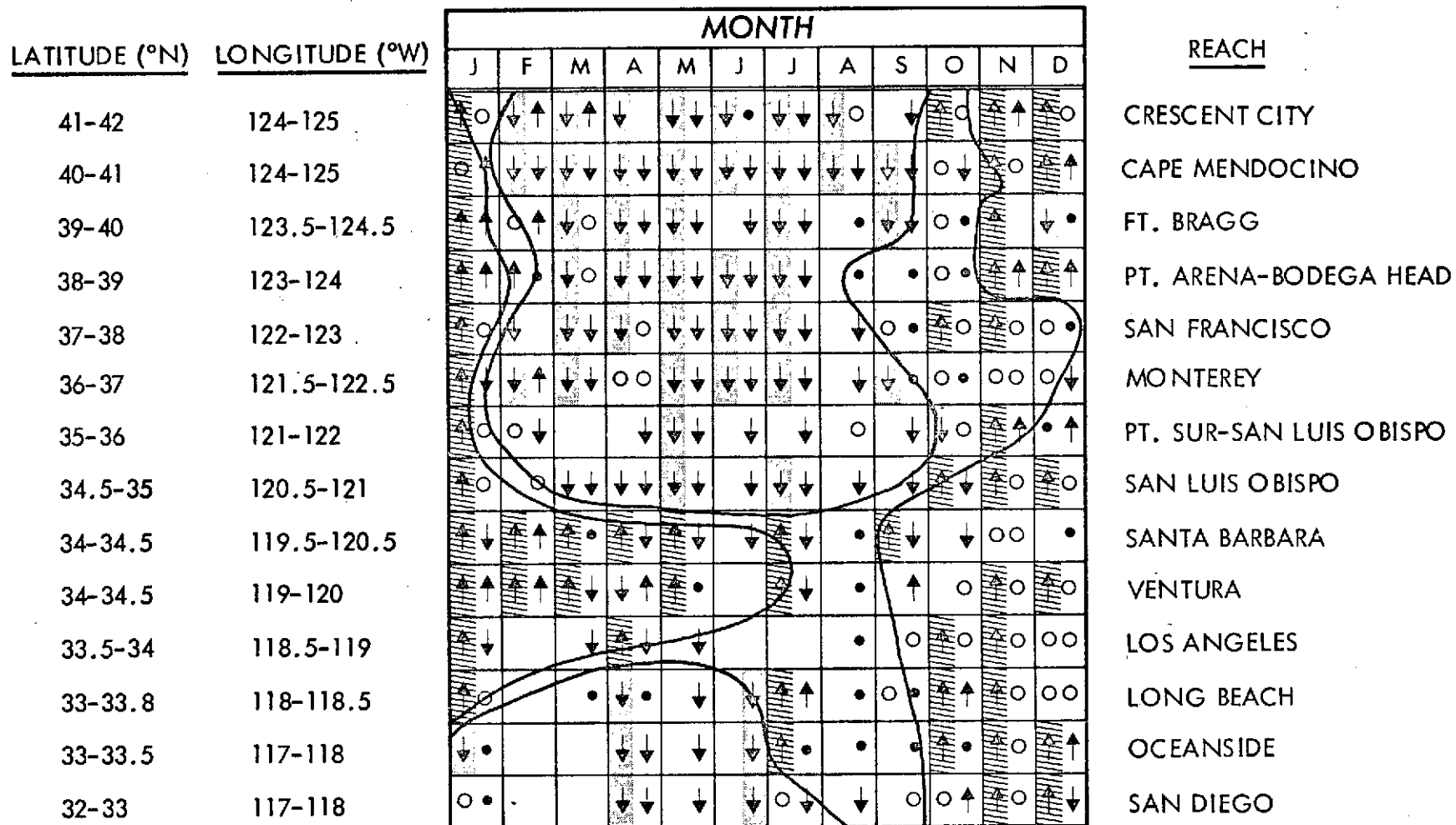


Figure 4-4. Summary of Offshore Currents from ERTS-1

internal waves and irregularities in the ocean bottom. The features which are of particular interest in this study and which are often visible on ERTS imagery, lie within this zone. Before the advent of ERTS, it was often found during studies of local currents that these effects combined with seasonal run-off often distorted the nearshore currents to such a degree that it was difficult to determine the regional circulation. ERTS graphically illustrates the California Current as well as the nearshore surface currents, when suspended material acts as a detectable tracer. The California Current has a continuous effect offshore even during the Davidson and Upwelling Current Periods.

The local current effects during the Oceanic Period and the source ERTS imagery are shown on Figures 4-5 and 4-8. The mosaic was made from Channel 4 (5,000-6,000Å) imagery. The California Current is the south-moving component of the clockwise circulation of the North Pacific Ocean. As this current slowly moves southward at speeds generally less than .25 m/sec, it becomes warmer under the influence of the sun and by mixing with the warm waters to the west. On the inshore side of the current, the numerous local disturbances, which are of major interest in this study, are found.

The California Current which moves southward past Point Conception continues to a point off Baja California, where the main portion of the current turns eastward. This is mentioned because of the major influences of this movement on Southern California nearshore processes. As the flow approaches land it splits into two branches. One branch which eventually forms part of the Southern California Countercurrent turns northward and flows through the Channel Islands. The second branch turns southward and continues down the coast to Baja California.

With this brief description of the California Current as background, let us now pursue the study of ERTS imagery in analyzing the complex dynamic surface movements of the Oceanic Period. In these discussions, all geographic locations not noted on plots are presented on the detailed California maps, Figures 1-2 and 1-3.

In the Crescent City area, off Point St. George, a large gyre is visible moving offshore from the sandy beaches and then south for a distance of approximately 40 km. This feature includes the moving of sediment off the critically eroding beach (National Seashore Study, 1971) 4 km north of Crescent City. Some of the transported material from north of Point St. George is moving back onshore south of Crescent City after bypassing this critically eroding beach. At times a gyre is found around this point causing the nearshore currents at Crescent City to be northward. During this type of current movement, accretion within the Crescent City Harbor takes place at the east and west ends of the harbor (Roberts, et. al., 1970).

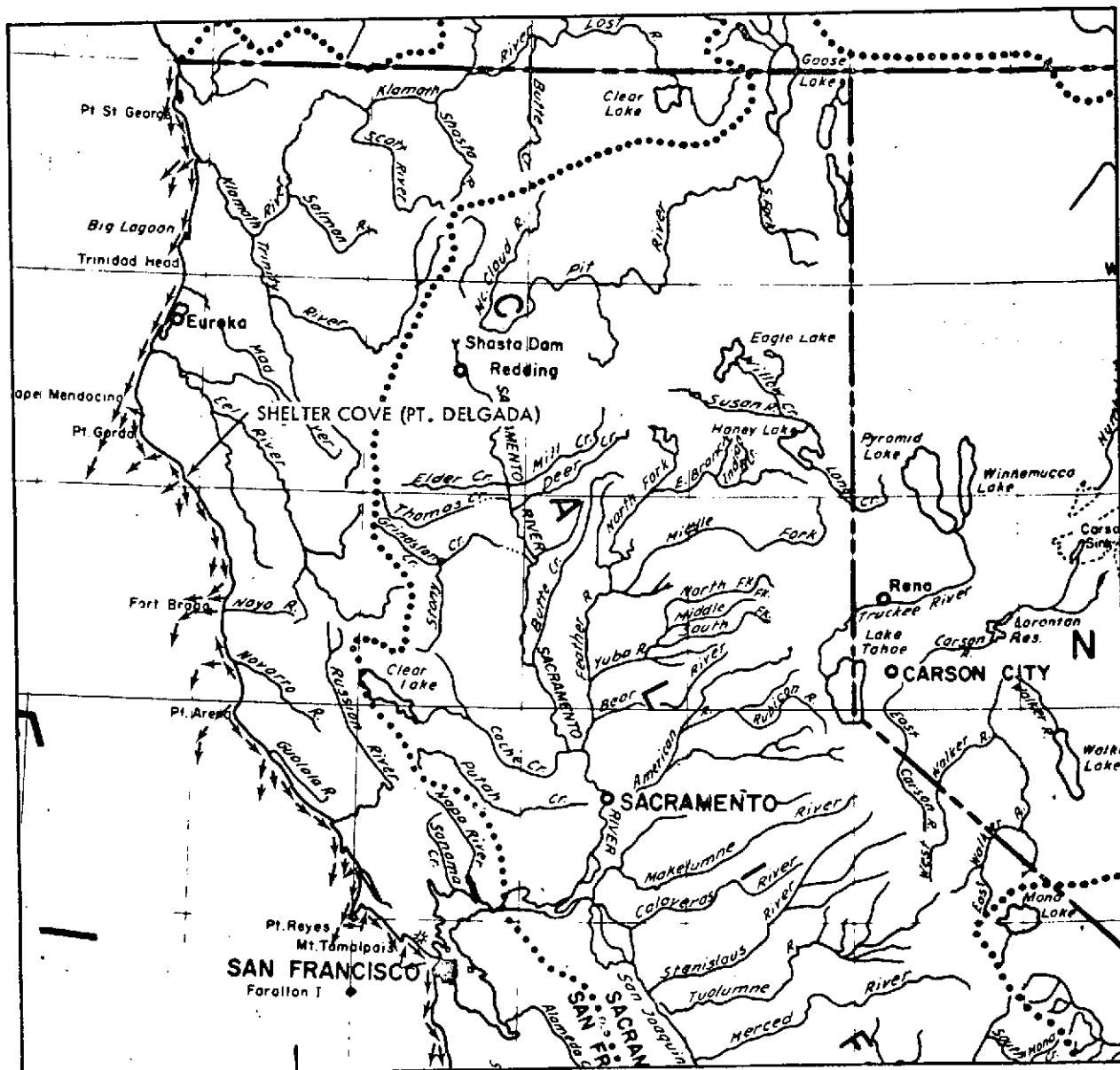


Figure 4-5. Oceanic Current Plot - Northern California.

Nearshore and coastal currents determined from ERTS and aircraft photography, May-November 1973.

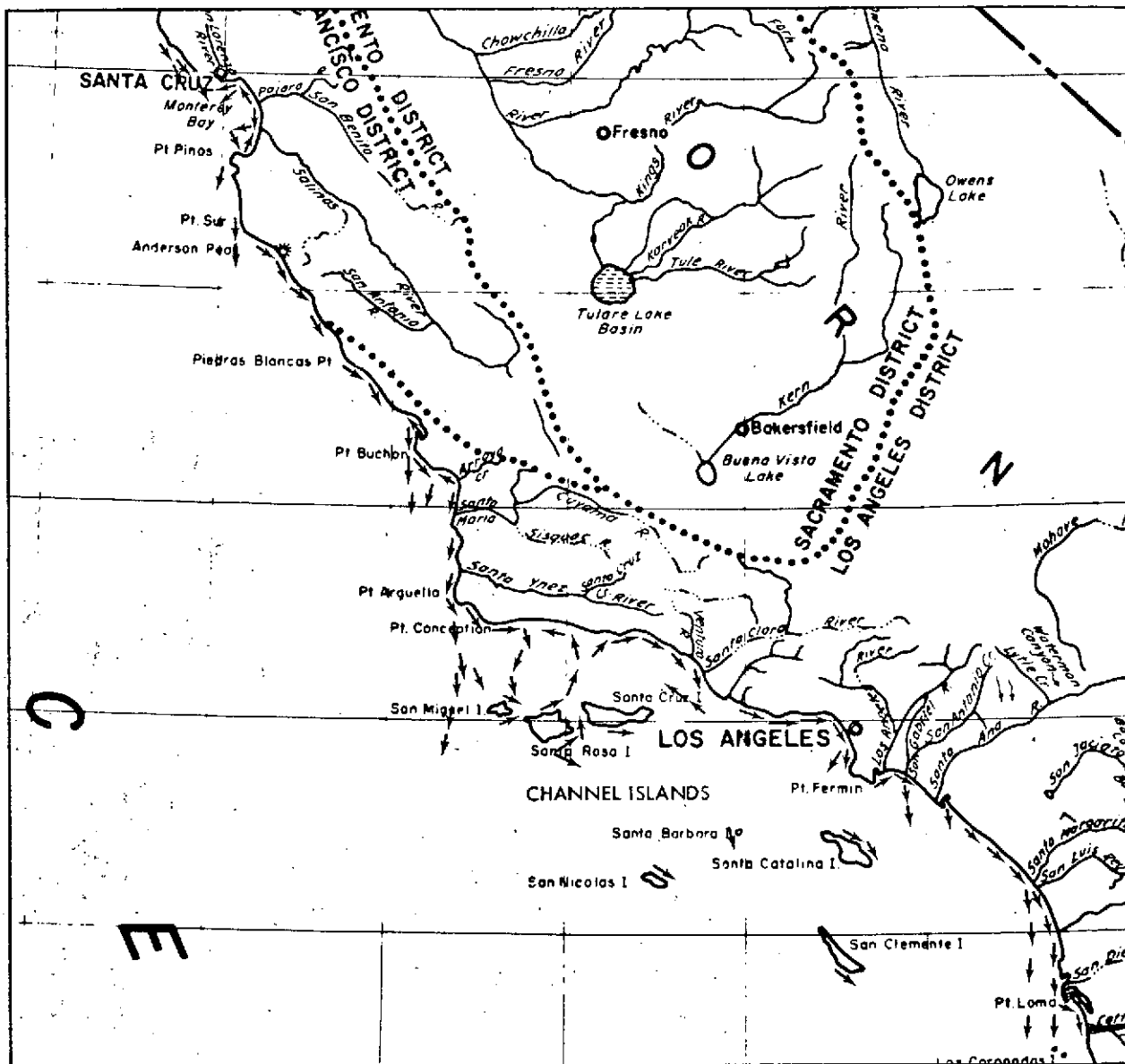


Figure 4-6. Oceanic Current Plot - Southern California.

Nearshore and coastal currents determined from ERTS and aircraft photography, May-November 1973.

CALIFORNIA COAST NEARSHORE PROCESSES
ERTS-A
MULTISPECTRAL SCANNER CHANNEL 4
MAY-NOVEMBER 1973

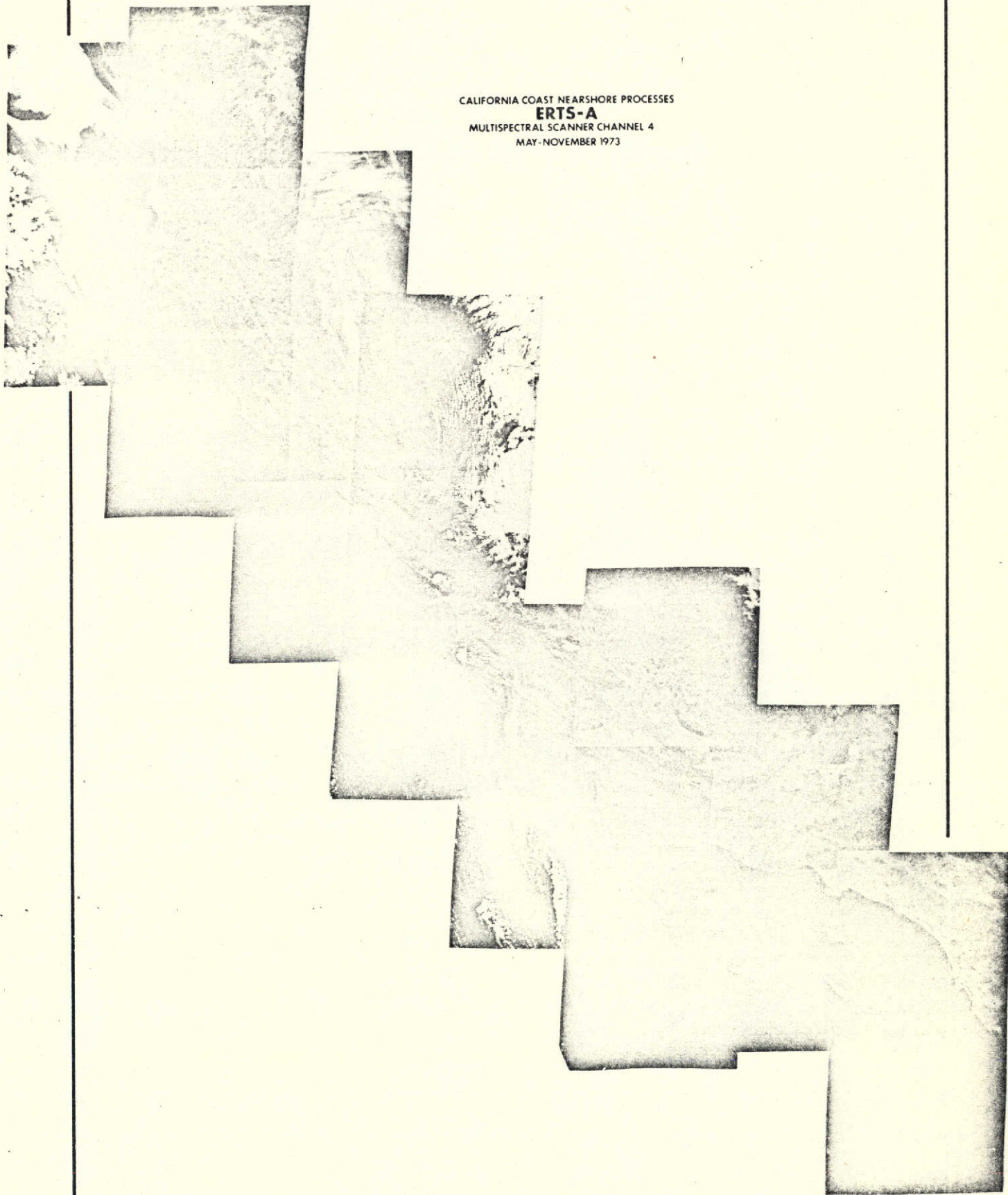


Figure 4-7. Oceanic Period Mosaic (May-November 1973)

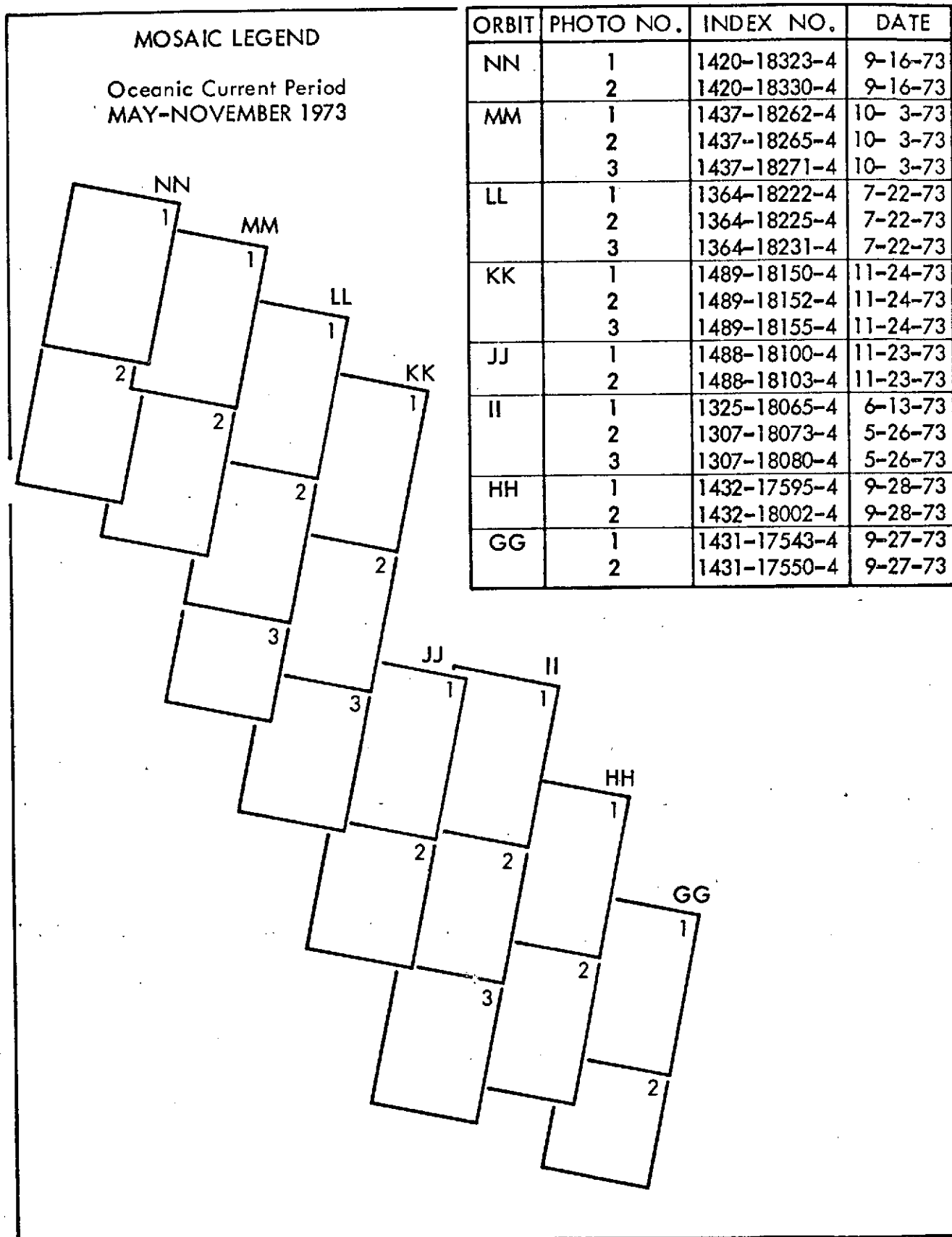


Figure 4-8.

In the Humboldt Bay area the sediment being transported mainly from the Mad and Eel Rivers is visible moving southward and offshore to a distance of 100 km from the entrance to Humboldt Bay. At times throughout the years the effluent issuing from several plants along the Humboldt Bay spit are visible on ERTS. This material is generally moved offshore but under certain current and wind conditions there is transport of material into the harbor. Further to the south in the lee of Cape Mendocino a small eddy is usually present. This eddy is clearly visible on the Oceanic Period mosaic and appears to be contributing to the critically eroding shoreline 8 km southeast of Cape Mendocino. The erosion is affecting the stability of the coast highway along this stretch of coast.

Between Cape Mendocino and the San Francisco Bay entrance a number of sediment gyres are set up moving material directly offshore. At Point Arena a linear plume of material is moving westward for a distance of about 25 km. The first 5 km of this feature appears to be heavily laden with sediment. Further offshore settling and mixing of the material causes the gradual decrease in this visible pattern. The fact that this feature is able to move offshore into the California Current appears to be the result of a clockwise gyre set up north of Point Arena. Similar processes are present off Shelter Cove and Anchor Bay.

At Bolinas Bay, about 15 km northwest of the Golden Gate, a number of estuary improvement proposals have been initiated. The predominant direction of littoral drift past the entrance of this bay is from east to west. Reinforcement of drift occur during storms when the wind and waves are from the southeast and during the Davidson Current period. Since the shoreline adjacent to the Bolinas Lagoon entrance periodically erodes critically, currents and sediment transport studies are essential in this area. To date, all plans for construction of breakwaters at the lagoon entrance have concluded that downcoast erosion would result (USACE, 1966). This ERTS study has illustrated the Bolinas area transport of sediment in detail. Actually, a clockwise gyre is often present off the San Francisco Bay entrance (USACE, 1971) which brings sediment from the Bay system northward into the Bolinas area. Currents moving southeast are visible past Duxbury Point, on which is located the city of Bolinas. During this type of current movement, the material is transporting away from the area, and erosion appears to be taking place. This is part of the overall Gulf of the Farallones current and transport cell.

Some of the most complex local currents occurring along the California coast take place near the entrance to San Francisco Bay. They result from high current velocities during flood and ebb tide, variations in bottom topography and highly variable wind drift all imposed on the coastal currents. The transitory nature of the local currents make them impossible to monitor on the 18 day cyclic ERTS imagery. What is shown, however, are surface details of this area at various instances of time throughout the year. In piecing this information together, valuable insight into the nearshore processes taking place is possible. It should also be noted that rough water conditions which are often present in the Gulf of the Farallones have always made detailed survey ship operations difficult. This is another reason why the ERTS analysis will be useful to future survey operations in this area especially.

As the clockwise current movement transports material southward past San Francisco a definite contact appears between sediment laden waters and clearer ocean water. This feature forms a 20 km long triangular break in the sediment gyre that is spreading from the Golden Gate area. This clear water feature is probably the result of upwelling along the coast from San Francisco south to about the Devil's Slide area. About halfway between the Golden Gate entrance and Devil's Slide a nodal point in the littoral drift pattern is evident. The littoral currents north of this point appear to be moving northward and littoral currents south appear to be moving southward. This is noted to emphasize one of the many complex detailed surface patterns that can be detected on the ERTS imagery.

In Monterey Bay the entire offshore area out to about 3 km contains suspended sediment which forms a crescent shaped pattern similar to the contour of the bay. Two breaks occur in this pattern, however. The first 8 km north of Monterey and the second over the Monterey Submarine Canyon. These breaks appear as areas of clear water in the nearshore suspended sediment pattern. The Monterey Submarine Canyon is the location of numerous upwellings which are indicated by lower temperature lenses which move to the north and south of the canyon itself (CCOFI, 1958). The feature 8 km north of Monterey appears to be a divergence or nodal point between a small sediment gyre in the southern end of the bay and the suspended sediment issuing from the Salinas River. This feature is adjacent to a critically eroding beach at Fort Ord (National Seashore Study, 1971).

The coastline between Pt. Conception and the Mexican Border is herein considered as a single system which has been described as the Southern California Bight. It is the sharp eastern break of the coast to the south of the point and the resulting indentation that extends for 575 km to Cabo Colmett on the Baja California coast. This Bight interrupts the southern flow of the dominating California Current. The hydrodynamic discontinuity forms a return eddy and a semi-independent system of water circulation within the Bight. This is called the Southern California Countercurrent and is a combination of converging southern, western, northern and upwelling waters.

The surface currents and sediment transport in the Bight, as viewed from ERTS, forms a complex dynamic system. For the first time, however, it is possible to view the entire Bight in one look (the entire Bight is imaged in two consecutive days by ERTS). What is generally seen during the Oceanic Period in the Bight is a counterclockwise gyre which passed northward through the eight Channel Islands. This is combined with southern moving water along the coast from the Santa Monica Bay - Palos Verdes Peninsula area.

In the Oceanic Period mosaic (Figure 4-7) a small plume of suspended material is moving south and southeast around Pt. Conception - Pt. Arguello. This represents the split between the south moving California Current and the material entering the California Countercurrent gyre in the western Santa Barbara Channel. This counterclockwise movement is apparent along the Channel Islands and then coastward to a point between Pt. Conception and Goleta Pt. East of Santa Barbara to Port Hueneme; however, the nearshore sediment transport is to the east. The Mugu and Hueneme Submarine Canyons

appear to be capturing material at these points. Within the Santa Monica Bay, the currents and sediment transport are clockwise along the coast to Palos Verdes. Very little material is rounding the peninsula because of the combination of the Santa Monica Submarine Canyon sediment capture and the offshore sediment movement.

South of the Palos Verdes Peninsula all of the nearshore transport is to the south. In the Los Angeles Harbor area, the effect of the Federal breakwater on offshore current is visible. At the harbor entrance, several lobes of material are visible. South of Long Beach transport is south and southeast. In the vicinity of Newport, Dana Point and Oceanside current transport is offshore to about 3 km then southeast. Although the waters off San Diego contain little suspended sediment the transport is obviously southward.

4.2.2 Davidson Current Period

The complex movements of the various surface currents which occur during the Davidson Current Period are illustrated in Figures 4-9 and 4-10. The information for this plot comes from repetitive ERTS coverage, several aircraft flights and sea truth sources. Figure 4-11 is a mosaic of Channel 4 (5,000-6,000Å) ERTS imagery, which includes scenes judged to most clearly delineate the relative concentrations and dispersal of suspended sediment. The time period covered by these figures is mid-November 1972 - February 1973, and the imagery utilized is shown in Figure 4-12. Normally, the main influencing current on the coast is the California Current (Section 4.2.1), which is a part of the great clockwise circulation of the North Pacific Ocean; however, during the period of approximately November to February each year, the Davidson Current, a north-moving countercurrent, is the dominant inshore transporter of water and suspensates.

The Davidson Current is generally a deep countercurrent below 200 meters which flows to the northwest along the coast from Baja California to some point beyond Cape Mendocino. It brings warmer, more saline water great distances northward along the coast. When the north winds are weak or absent in late fall and early winter this countercurrent forms at the surface, well on the inshore side of the main stream of the California Current. The evidence for this current is visible on the mosaic and indicated by the temperature contours and current measurements collected from this area. The temperature contours in the eastern Pacific bend to the north along the coast during the height of the Davidson Current activity with the most dramatic changes taking place in February.

In general, the Figure 4-11 mosaic of this period illustrates the greatest concentration of nearshore northern moving sediments offshore to a distance of 4 to 8 km. At several points along the coast the movement is blocked by large gyres which appear to carry significant volumes of sediment off-coast where they are then transported southward by the California Current. At Pt. Conception a relatively small blockage takes place, but off Pt. Lopez 67 km south of Monterey an extensive offshore movement of sediment takes place. Initial transport here is in the southwest direction to a point about 96 km off the

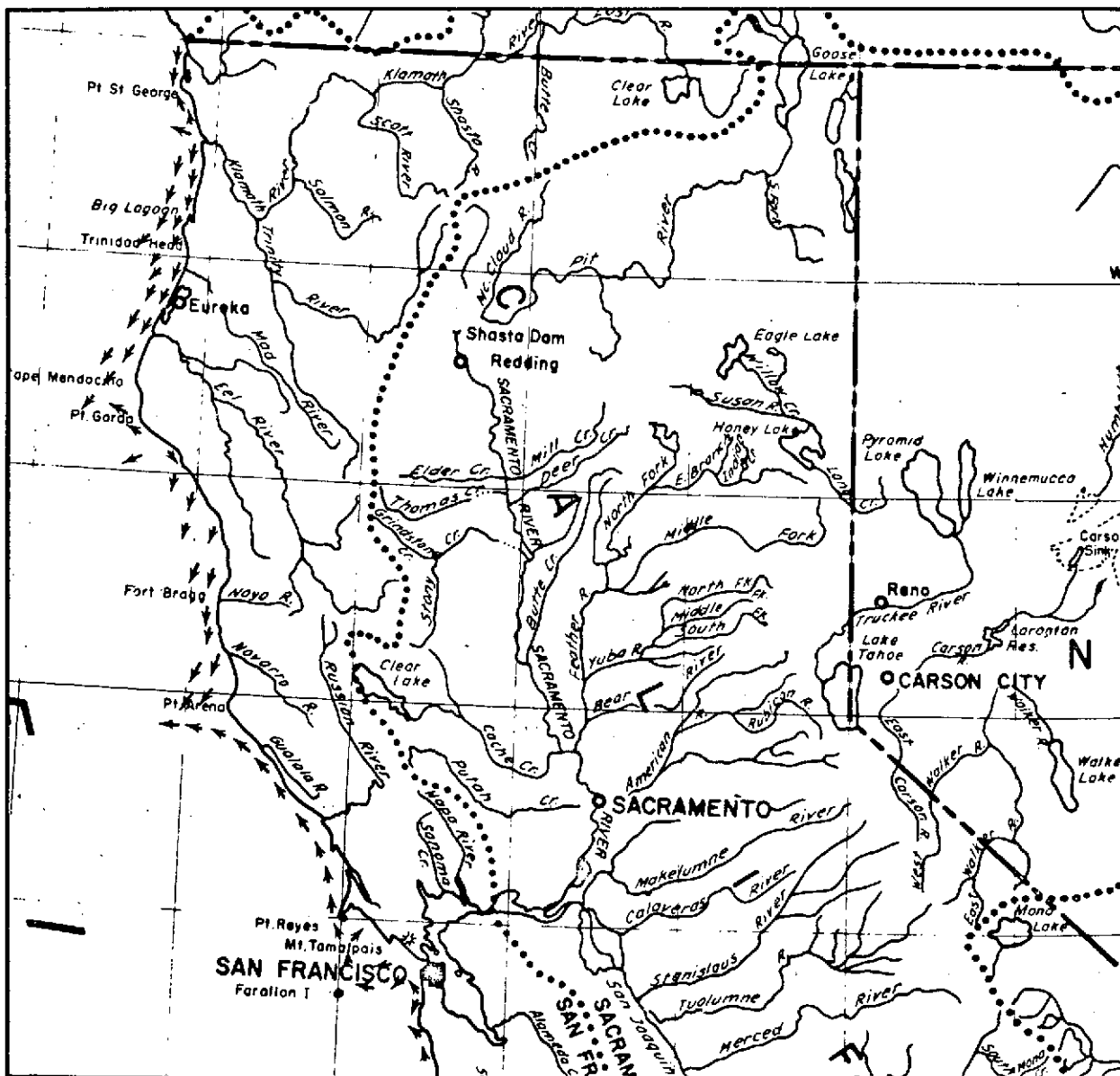


Figure 4-9. Davidson Current Plot - Northern California (November 1972-January 1973)

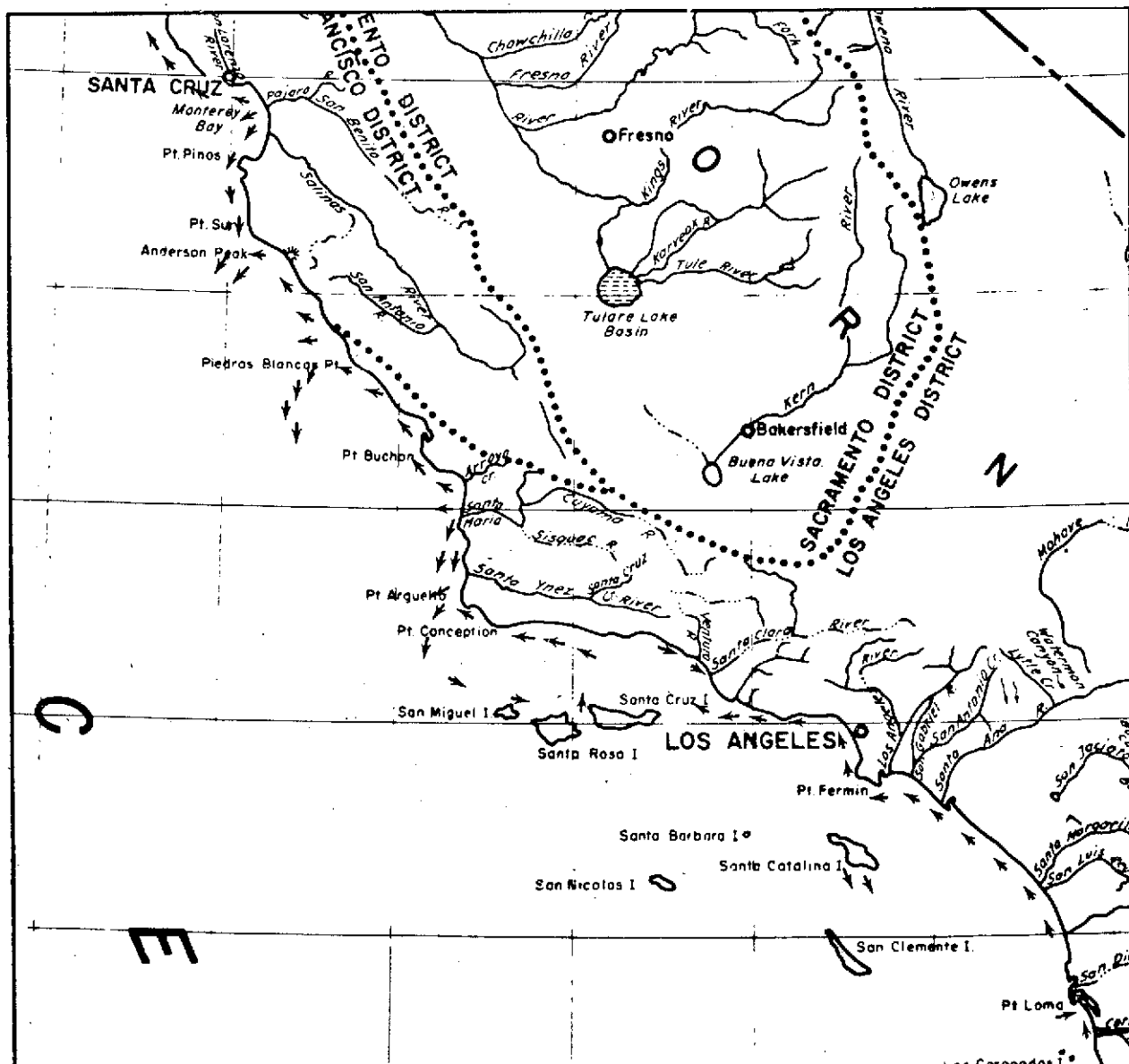


Figure 4-10. Davidson Current Plot - Southern California (November 1972-January 1973)

CALIFORNIA COAST NEARSHORE PROCESSES

ERTS-A

MULTISPECTRAL SCANNER CHANNEL 4

NOVEMBER 1972-JANUARY 1973

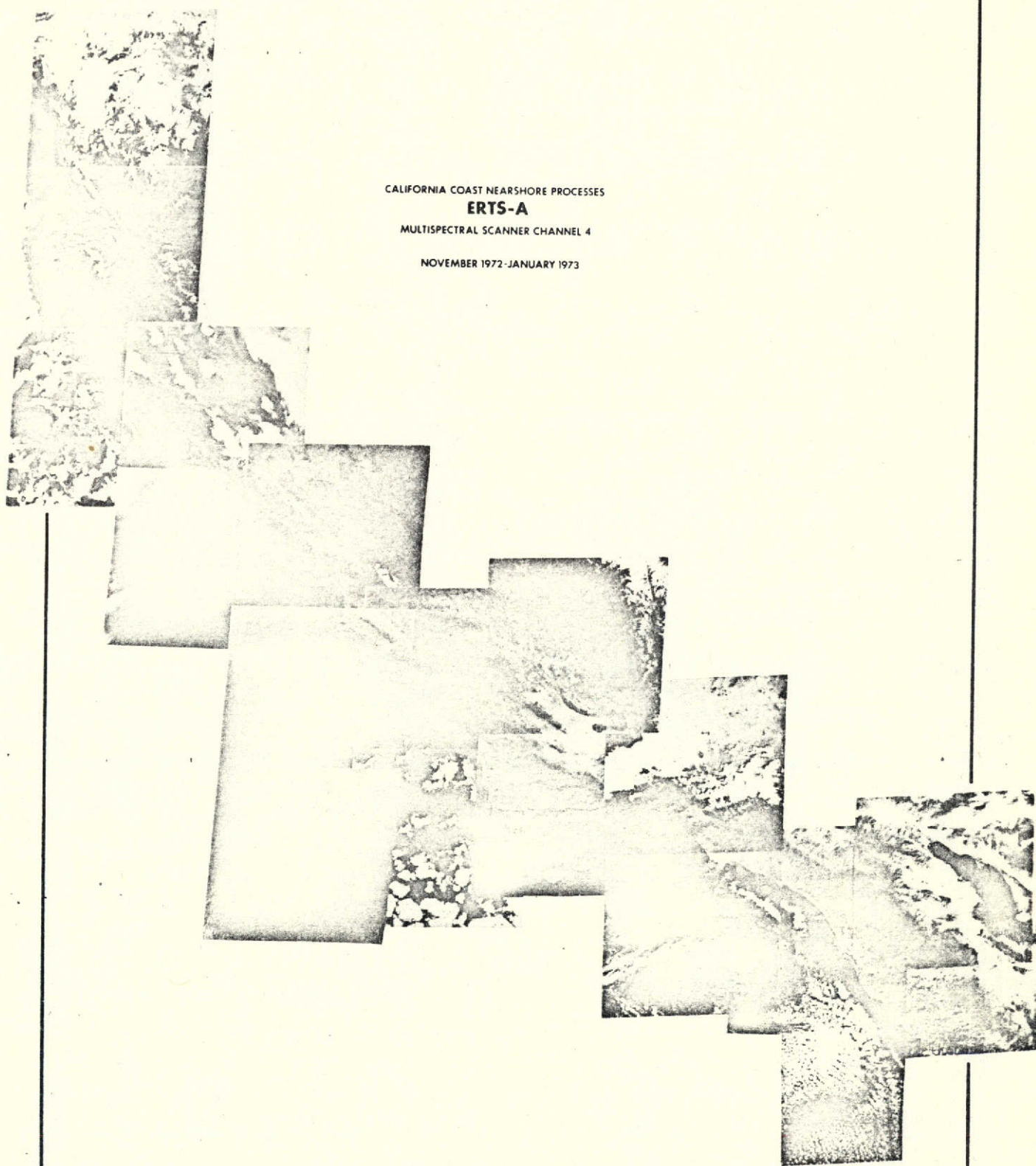


Figure 4-11. Davidson Current Period Mosaic

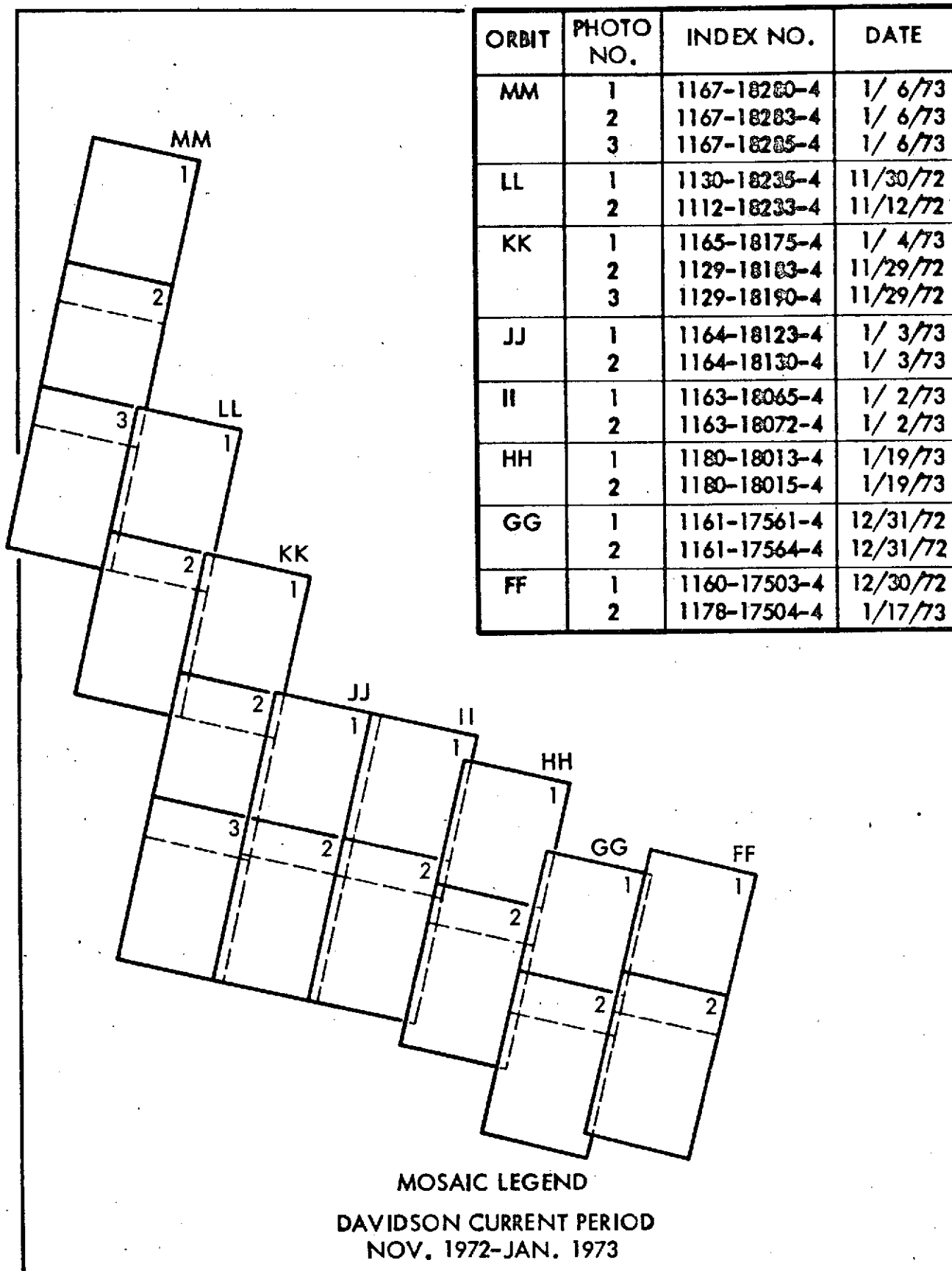


Figure 4-12

coast where movement changes to the south. From that point this plume of sediment is detectable being moved 250 km to the south to the edge of the presently available imagery. At its southern extent this plume is 56 km wide. The total area of this feature is approximately 3400 square km. Similar gyres on smaller scales are present near Pt. Ano Nuevo, Devils Slide, Pt. Arena, Pt. Delgada, and off Humboldt Bay. In each case, a counterclockwise gyre is present which carries north-moving nearshore sediments offshore into the south-moving California Current. No attempt has been made to estimate the significant amount of offshore sediment movement occurring during the Davidson Current period.

In the Los Angeles Harbor area material from the Los Angeles, San Gabriel and Santa Ana Rivers are being moved offshore and westward by the influence of the Davidson Current. Inside the harbor itself an east-southeastward current is in effect. Once outside the Los Angeles breakwater a slow moving westward current appears to dominate the nearshore sediment movement. Off Santa Catalina Island, however, transport is in the southeast direction indicating a surface current reversal in the San Pedro Channel. Suspended sediments in Santa Monica Bay ring the bay with a 4 to 8 km wide border. This ring of sediment appears to be escaping the bay area to the westward around Pt. Dume. This agrees with the general Davidson Current pattern.

In the Santa Barbara Channel between Port Hueneme and the Anacapa Islands the westward current domination is observed. The pattern, with minor modifications, continues to west of Carpinteria. A counterclockwise gyre is present just east of Santa Barbara which is moving sediment offshore 6 to 8 km where they are again moved to the west. Off Pt. Conception the California Countercurrent in the area between the mainland and the Channel Islands, as described by Drake (1972), appears to pick up these suspended particles and transports them offshore in a complex pattern where they are influenced by the California Current.

The Monterey Bay surface waters are reported to be exceedingly uniform during the Davidson Current period (CCOFI, 1958). The temperature difference between any pair of stations averages a little less than (0.25°C). No regular pattern of temperature distribution is discernible. The general northern trend of the suspended sediment, however, appears to continue in Monterey Bay as noted on the ERTS imagery. From the area of the Elkhorn Slough north and northwest to Santa Cruz a large gyre of material is present. Little of this material appears to be escaping the confines of the Bay. The suspensate movement from the Bay appears to be blocked by the counterclockwise gyre activity that is present off Pt. Ano Nuevo.

In the Gulf of the Farallones, which encompasses the majority of the San Francisco test cell, a complex surface current and sediment transport system is present. A large clockwise gyre is present off the Golden Gate Bridge reaching from the Lake Merced area northwest to the vicinity of Duxbury Pt. Near Lake Merced a nodal point is present separating the large gyre just mentioned from a smaller gyre present off the Devil's Slide. From Duxbury Pt. toward Drakes Bay the current appears to be moving sediment in a northwest direction. Near Drakes Bay this current meets a counterclockwise moving current which generally moves around Pt. Reyes. Just north of Pt. Reyes at the mouth

of the Russian River the distinct northern effect of the Davidson Current is illustrated. The majority of the movement takes place within 5 to 6 km of the coast.

The overall affect of the current along the California coast can be viewed in detail on the ERTS imagery. Although the general changes in current direction have been known for some years the complexities within the general currents are not recorded in detail. Near the coast the effect of the irregular coastline and varying depth governs detailed transport and current direction. This topography and the winds, which sometimes reinforce and sometimes oppose the current, and the significant vertical motion in the region of upwelling and the oscillations of internal waves, all combine to make the measurement of current complex. The synoptic ERTS view of currents as indicated by sediment tracers presents a unique capability to the coastal investigator.

4.2.3 Upwelling Period

The Upwelling Period is a markedly seasonal phenomena which takes place generally from mid-February to July. An Upwelling Period Current Plot, Figures 4-13, 4-14 resulted from analyzing the ERTS imagery mosaic, Figure 4-15, for the March-April 1973 period. This mosaic is assembled from ERTS channel 4 (5000-6000A) frames (Figure 4-16). The imagery was picked for clarity and visible suspended sediment content which is utilized as a tracer for studying current movement.

During the Upwelling Period winds parallel to the coast move surface waters offshore allowing deeper ocean water to surface. This effect seems to be intensified above submarine canyons south of capes and points which extend out into the current stream. On the current plot, the process of upwelling is illustrated at Crescent City, Cape Mendocino and south of Pt. Conception, Half Moon Bay and Monterey Bay. These colder upwelling waters are often rich in nutrients with the additional result that plankton blooms often accompany this period. This often increases the fish population, which is obviously of great interest to the fishing industry.

During the April 16-30, 1973, period, gradual warming of surface waters was taking place along the coast with the exception of the Cape Mendocino area. An extensive upwelling extended from Crescent City to south of San Francisco forming a variation in the general warming trend. Similar features on a more local scale were detectable by studying offshore tonal changes on the ERTS imagery. Confirmation of coastal processes during this period resulted from aircraft and sea truth measurements similar to the Davidson Current Period.

As in the Davidson Current mosaic, the major features visible are large offshore transport cells which joint the south moving California Current. The largest transport cell is visible off Pt. Conception. This feature stretches for 210 km off the coast to the edge of the available ERTS imagery. This Pt. Conception feature (imagery date 3/15/73) is 170 km further south along the coast from the parallel "Lopez Point" transport cell (imagery date 11/29/72) noted on the Davidson Current mosaic.

In addition, a number of smaller offshore transport systems are also present. They include features off: Half Moon Bay, Humboldt Bay, the Eel River and Pt. St. George. The total volume of offshore sediment movement during this Upwelling Period appears to be a significant loss in the California coast sediment budget.

In the Monterey Bay, suspended sediment from the Salinas River is moving northward to the vicinity of the Pajaro River. Upwelling above the Monterey Canyon is resulting in the shoreward transport of sediment adjacent to Moss Landing.

The effect that upwelling has on the nearshore coastal sediment transport is emphasized and illustrated on the ERTS imagery mosaic. In reviewing historical data on upwelling, it is noted that the exact location of these features are not predictable. The importance of this information to understanding of the nearshore processes and to the fishing industry is apparent.

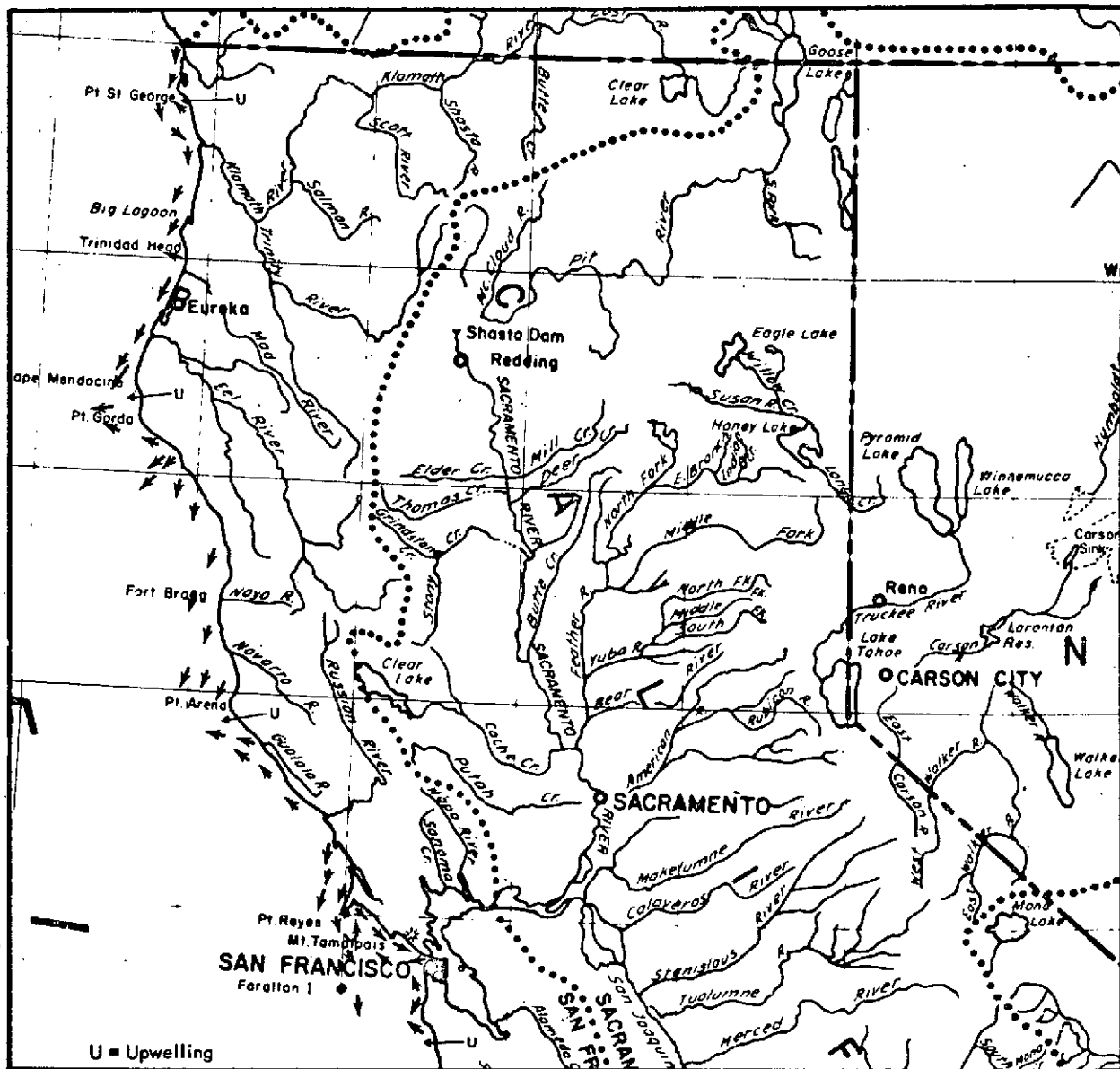


Figure 4-13. Upwelling Current Plot - Northern California

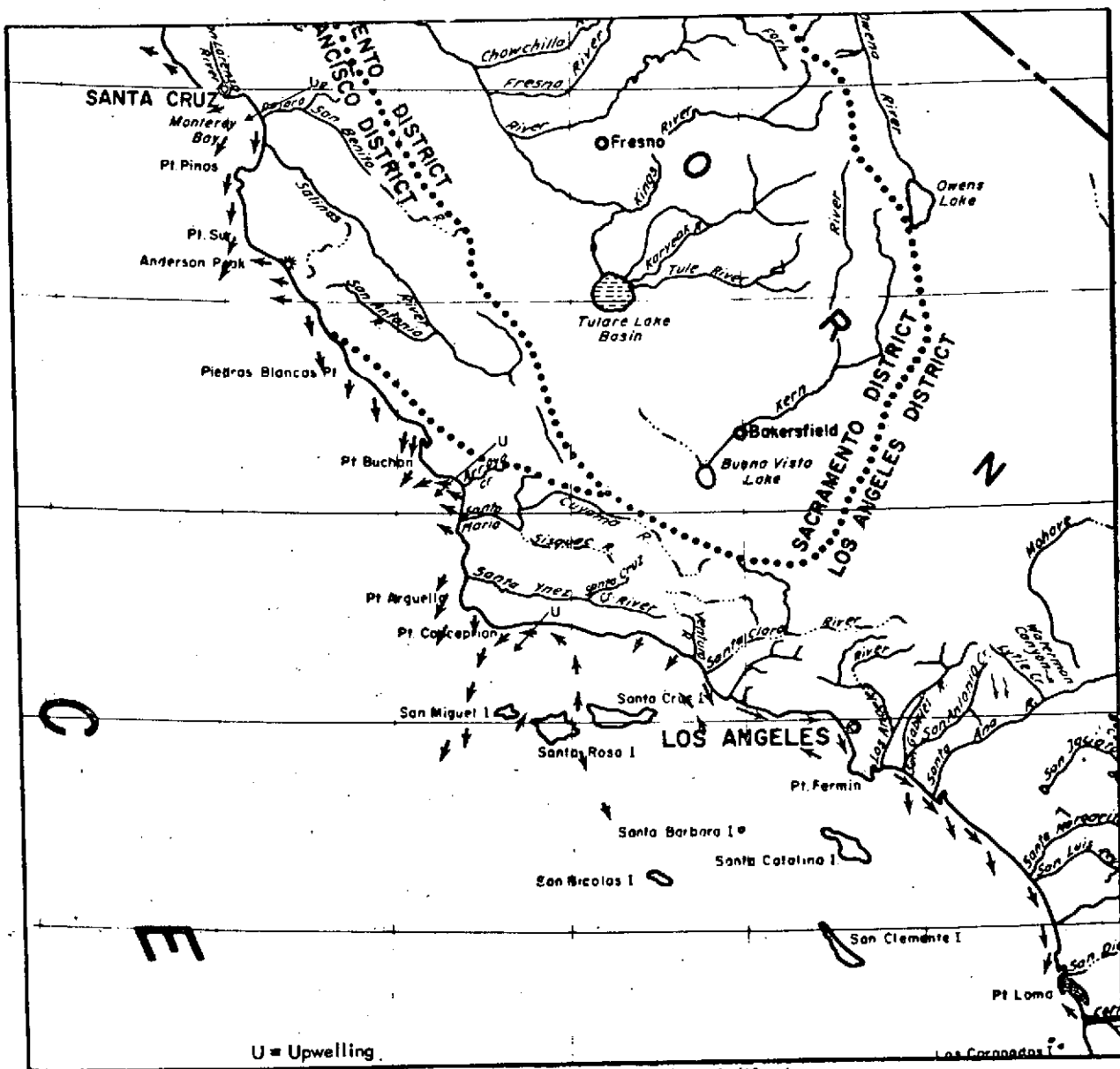


Figure 4-14. Upwelling Current Plot - Southern California

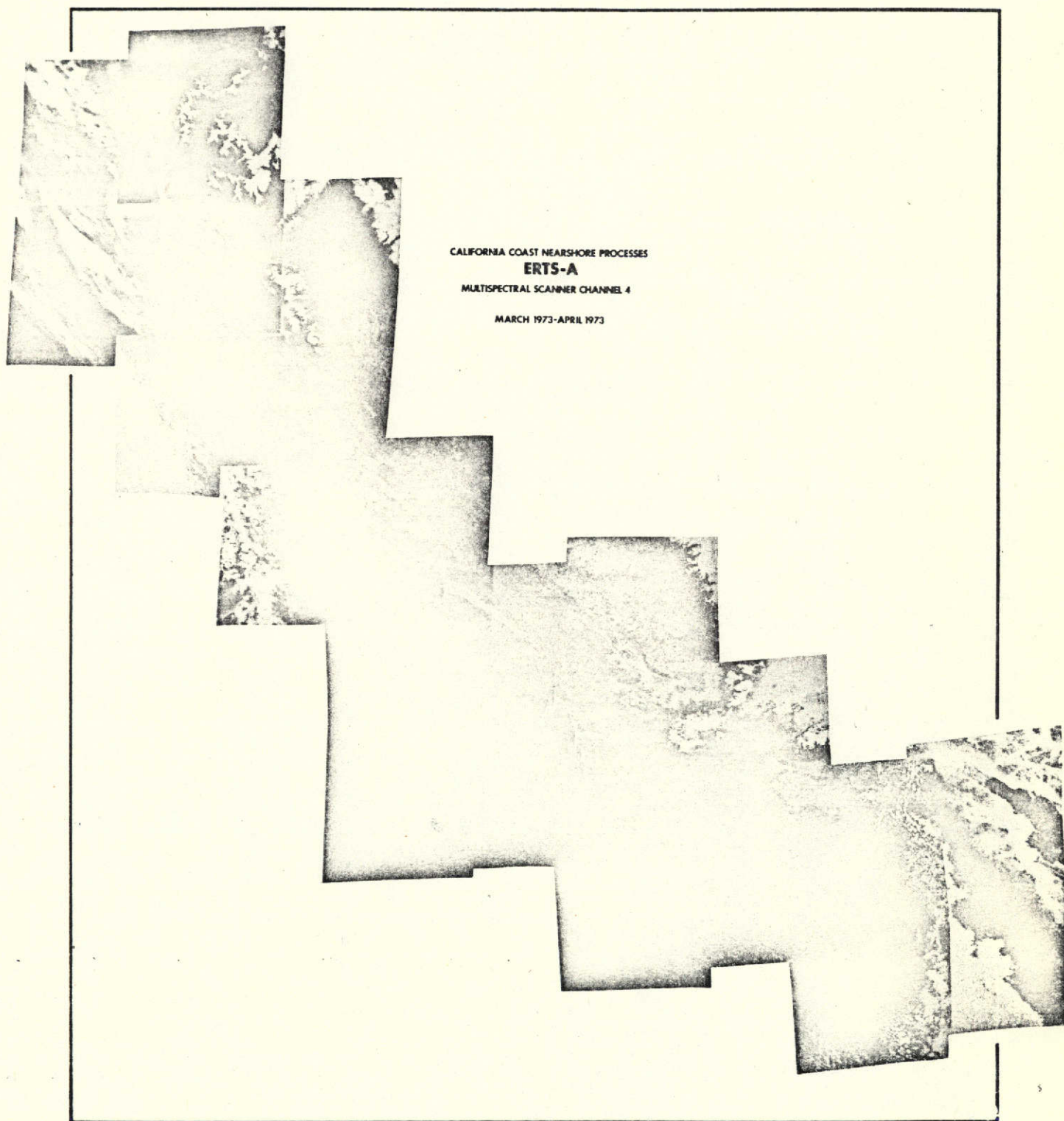


Figure 4-15. Upwelling Period Mosaic

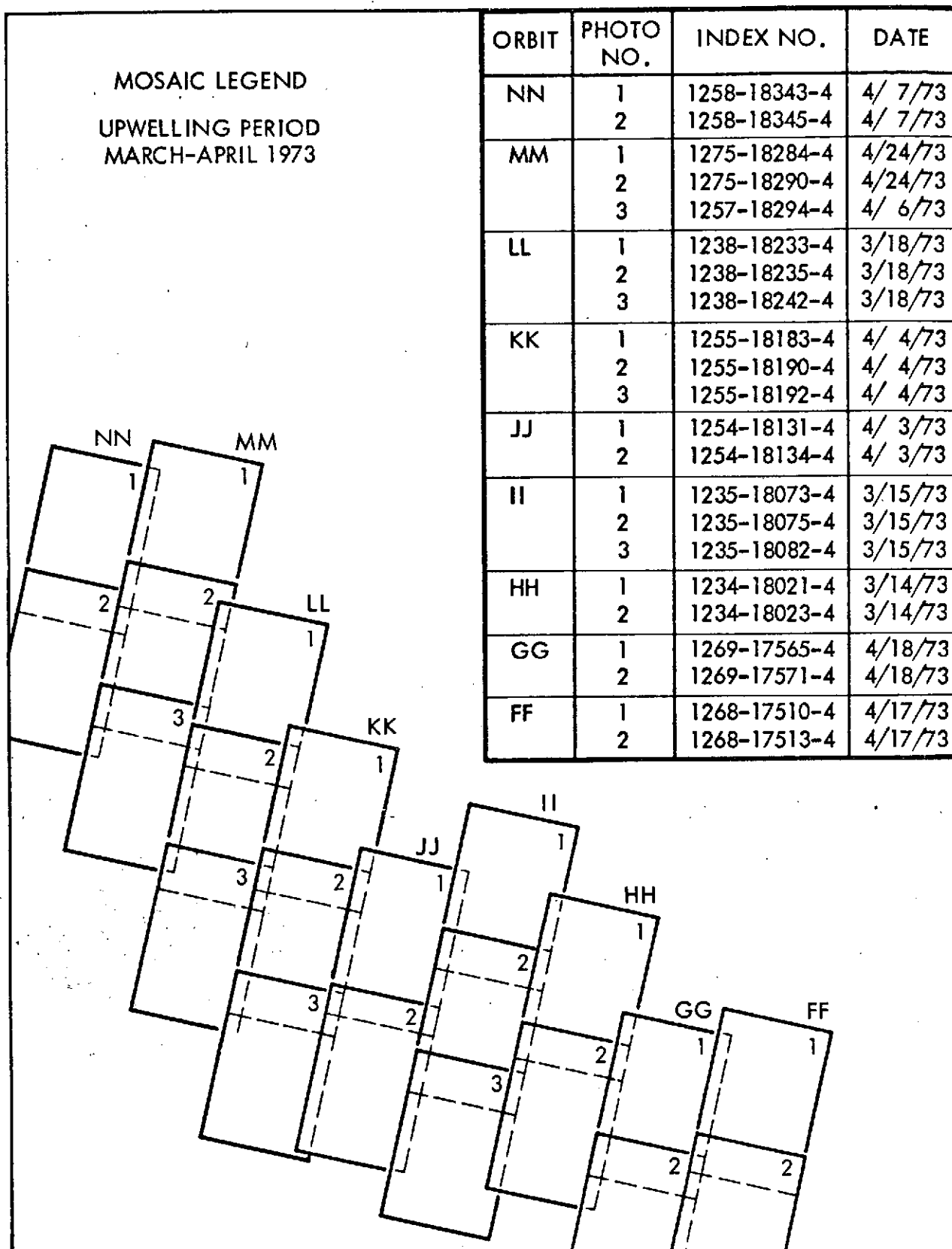


Figure 4-16

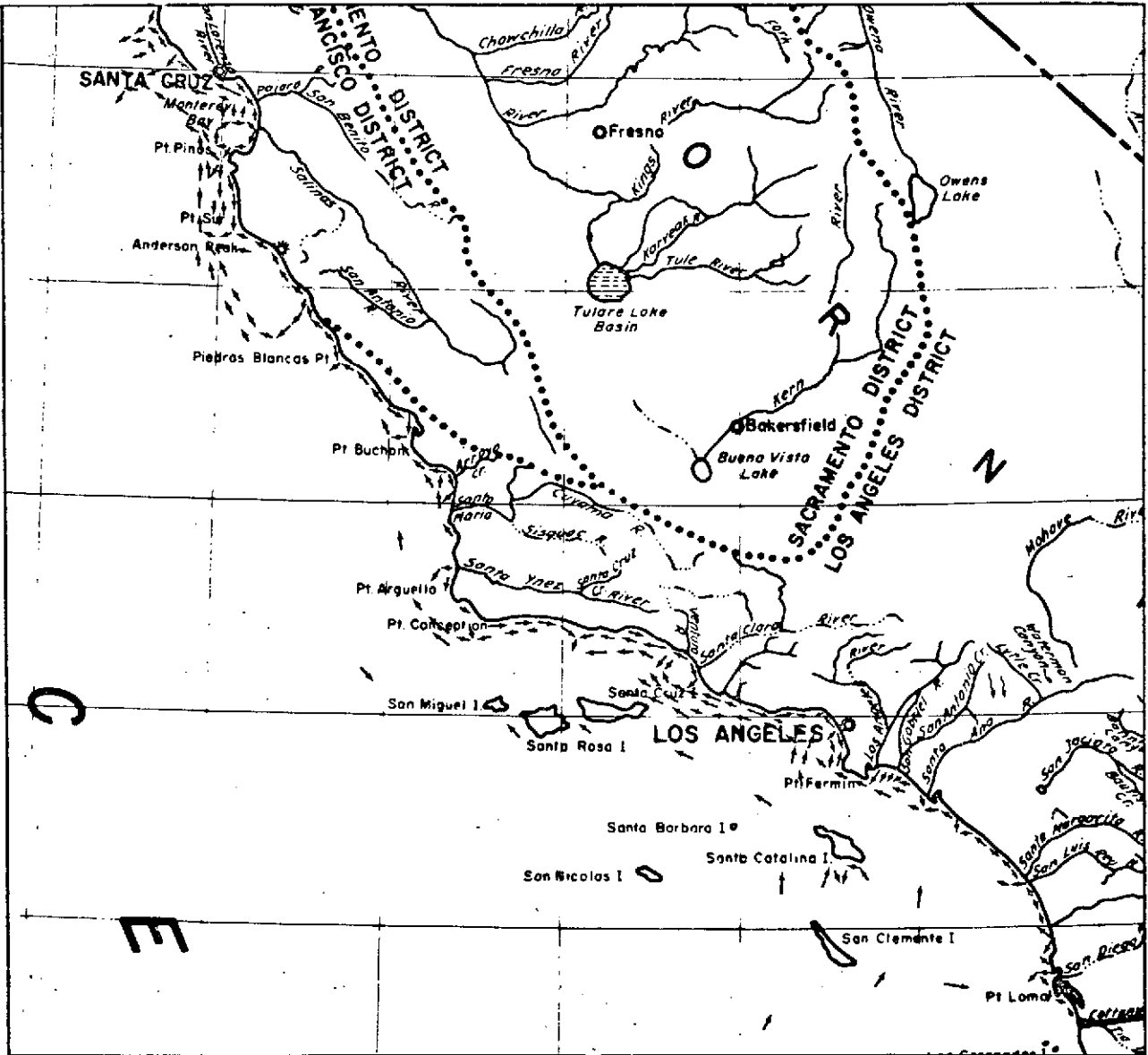
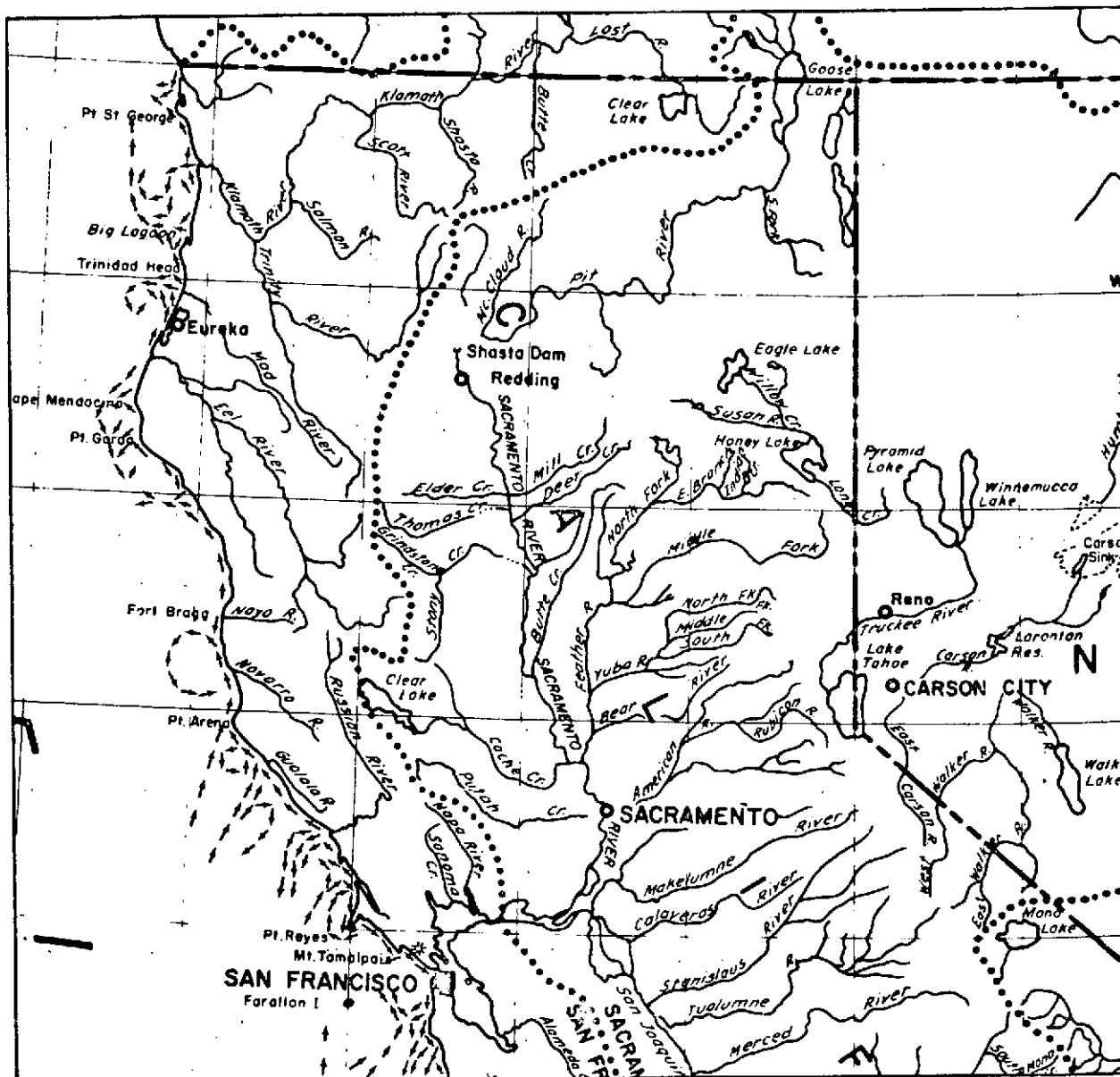


Figure 4-17. Southern California Coastal Currents - January 1973



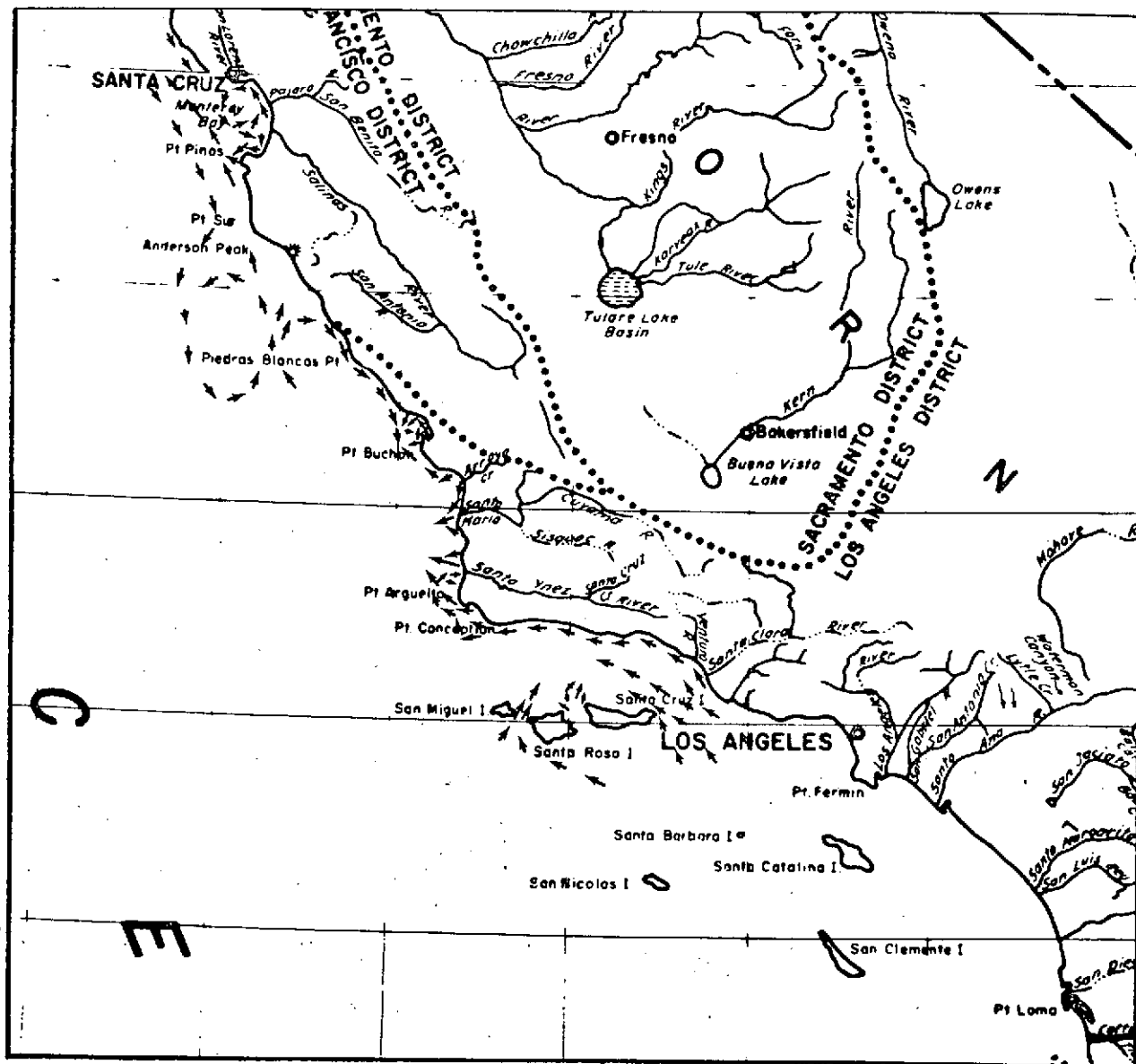


Figure 4-19. Southern California Coastal Currents - February 1973

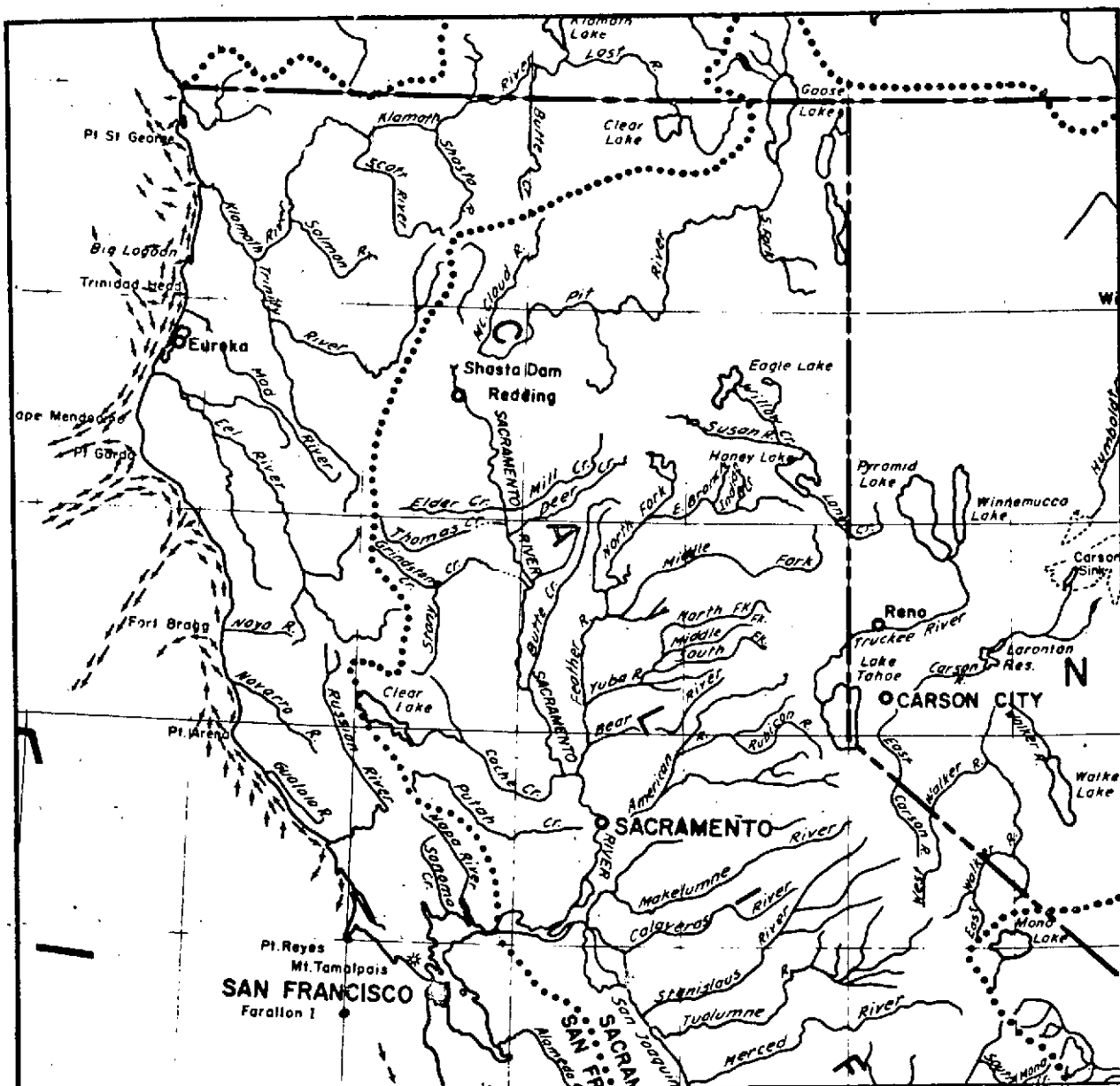


Figure 4-20. Northern California Coastal Currents - February 1973 and 1974.

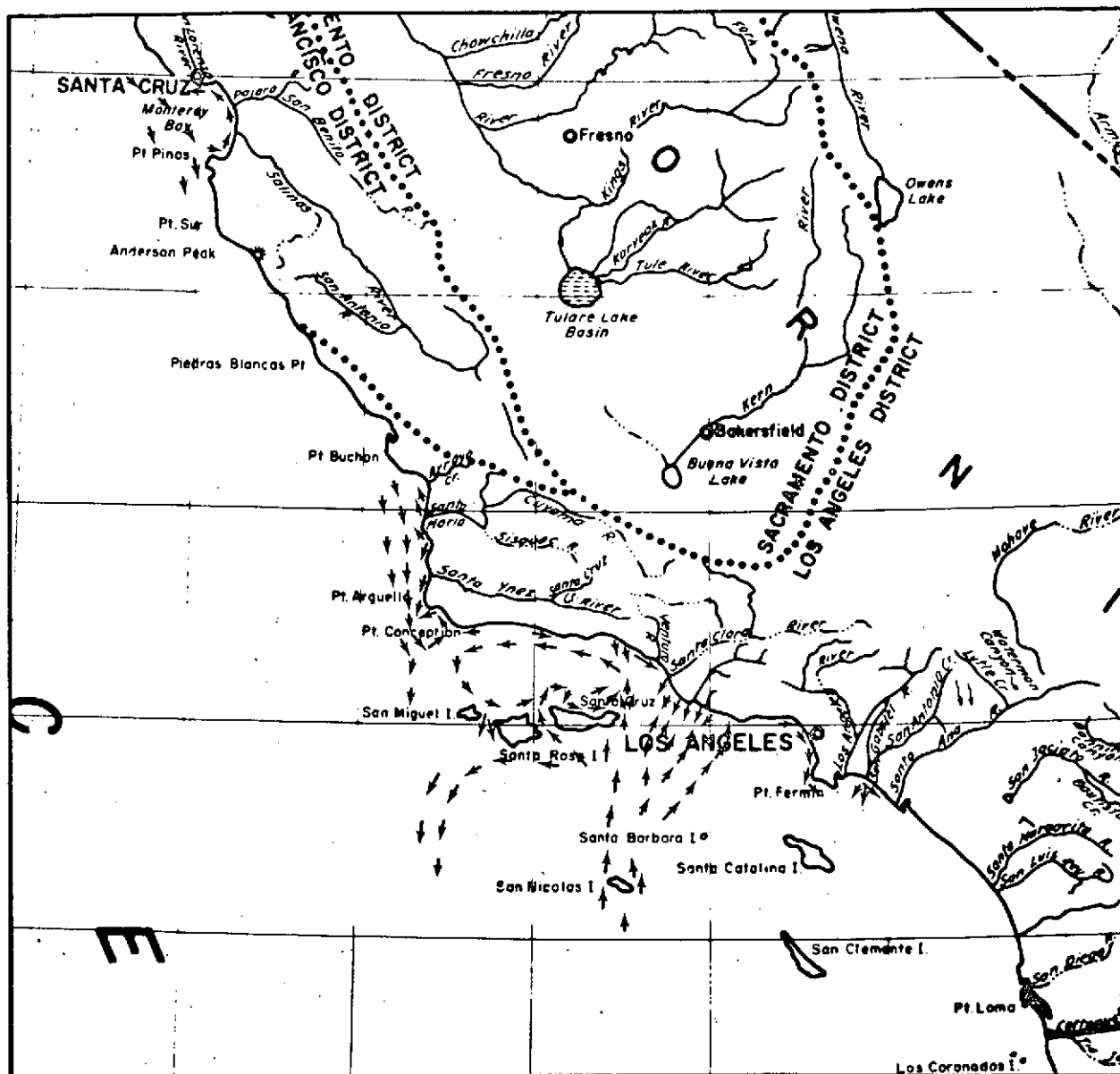
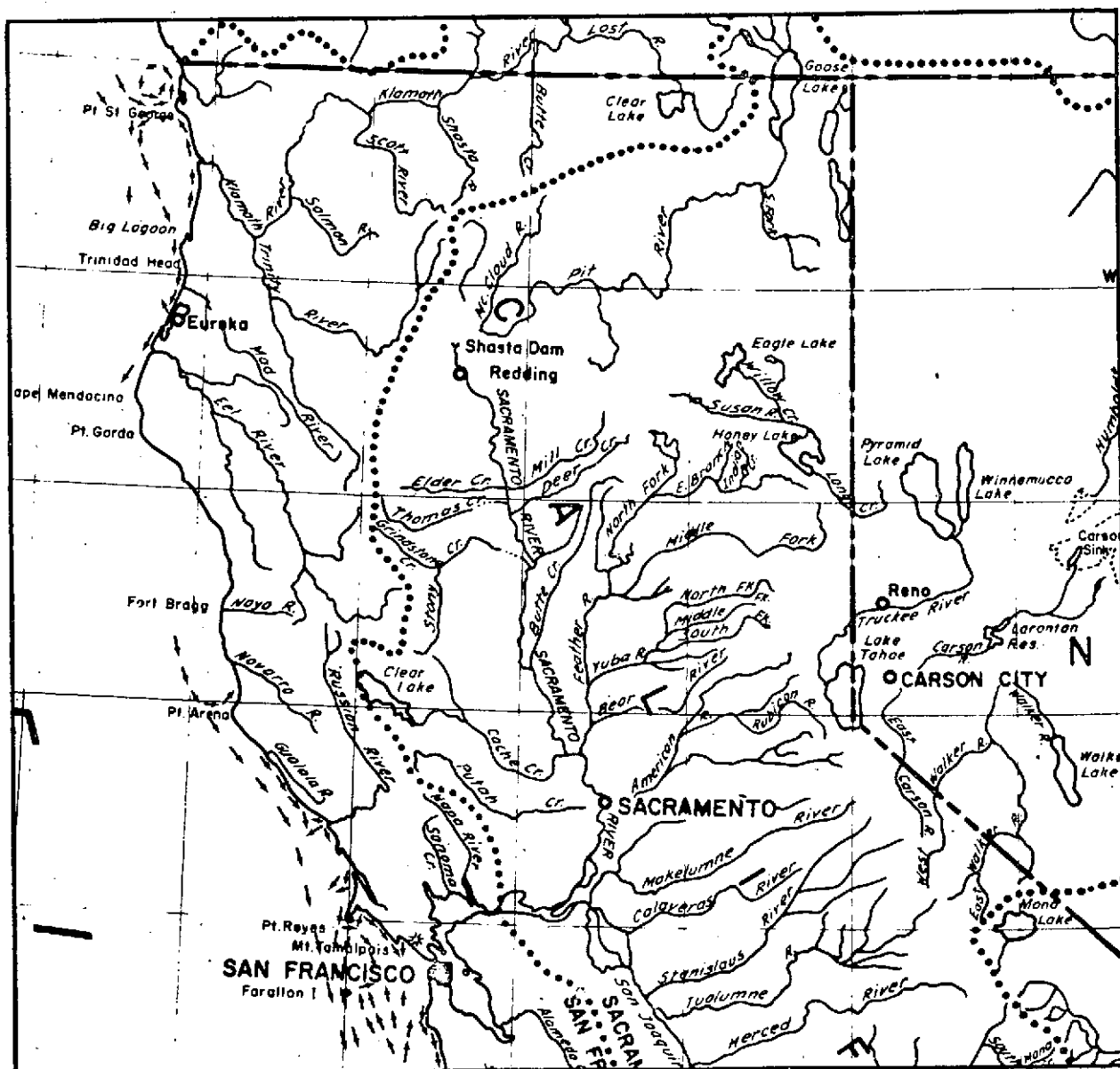


Figure 4-21. Southern California Coastal Currents - March 1973



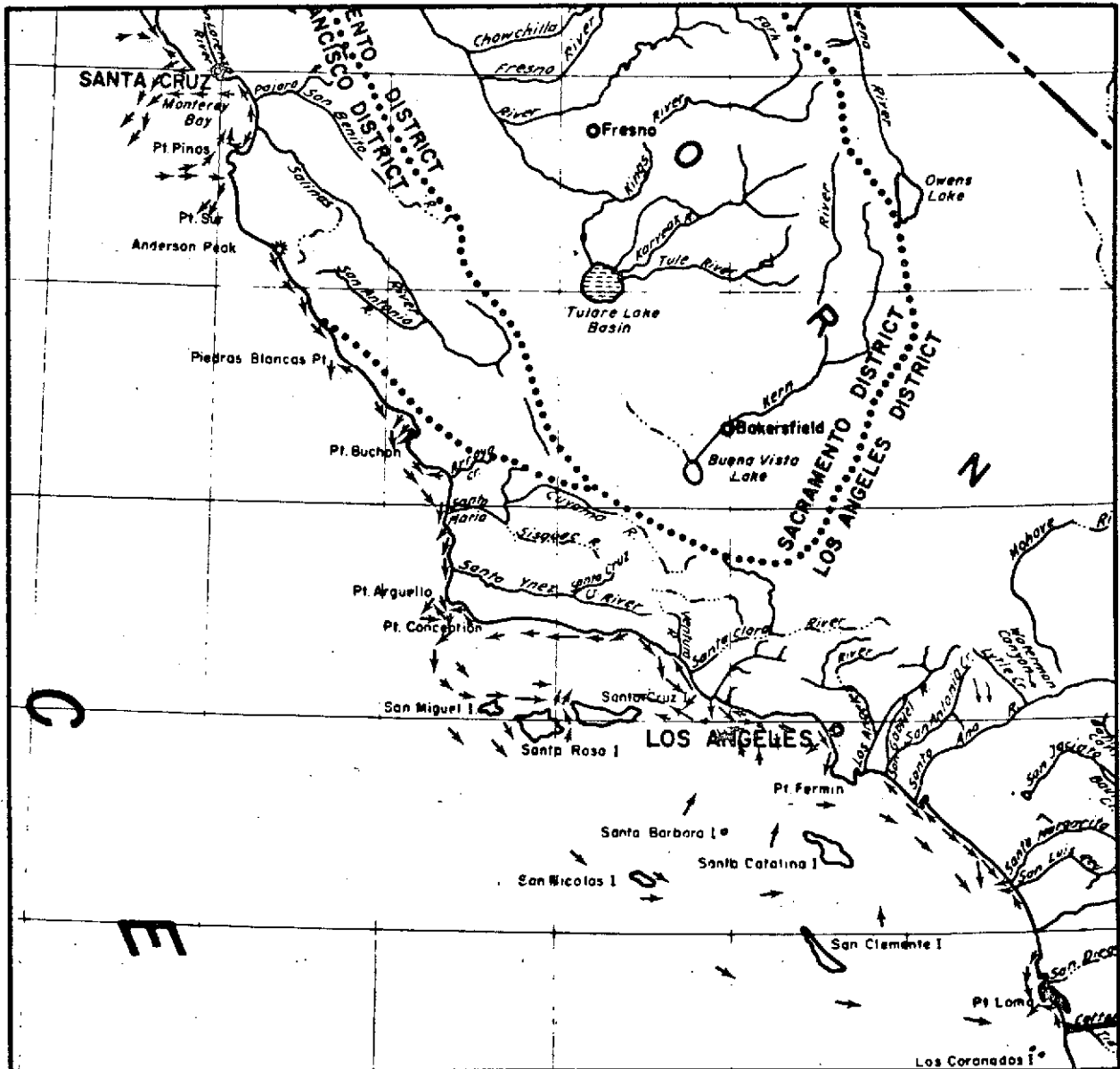
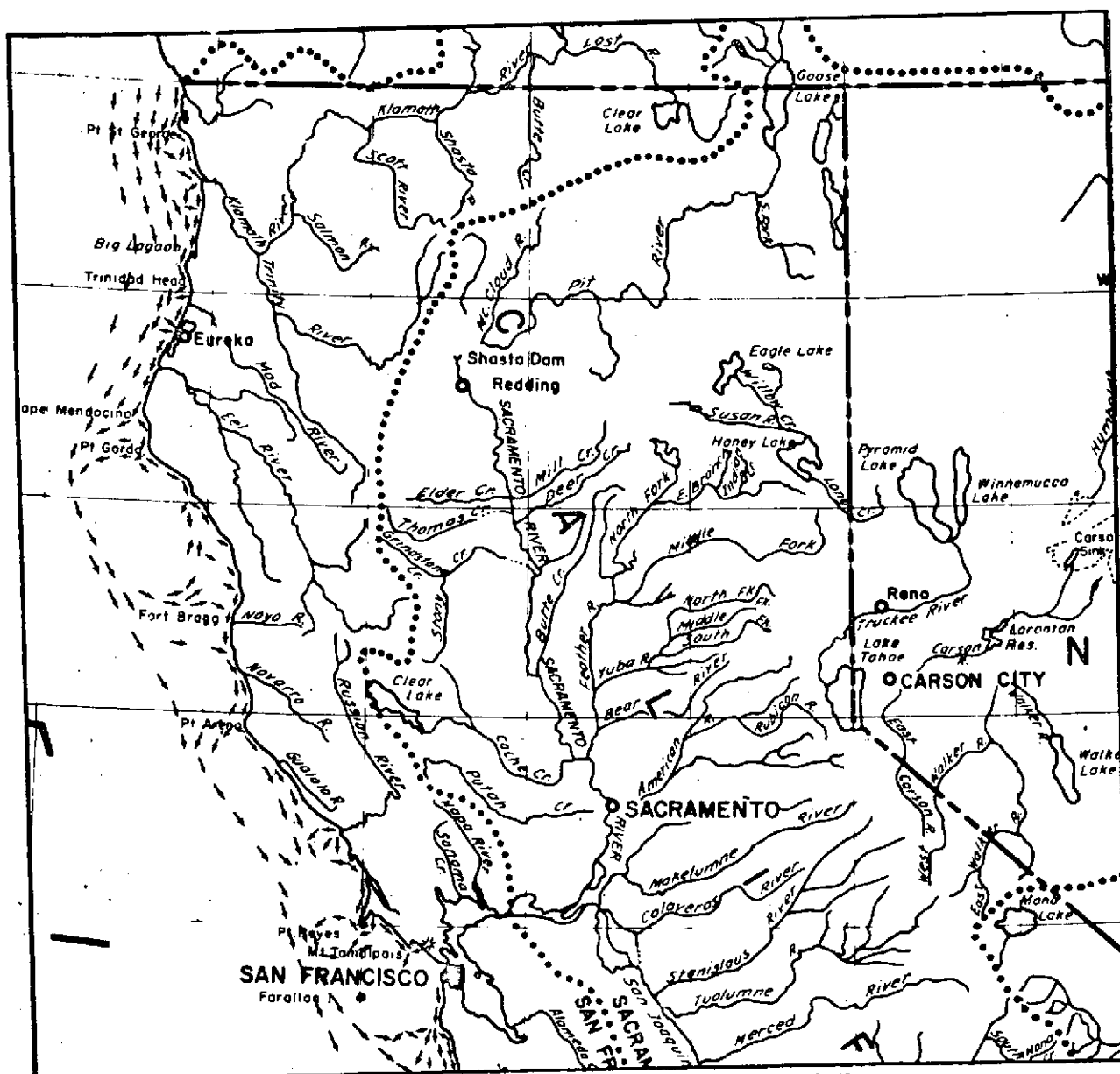


Figure 4-23. Southern California Coastal Currents - April 1973



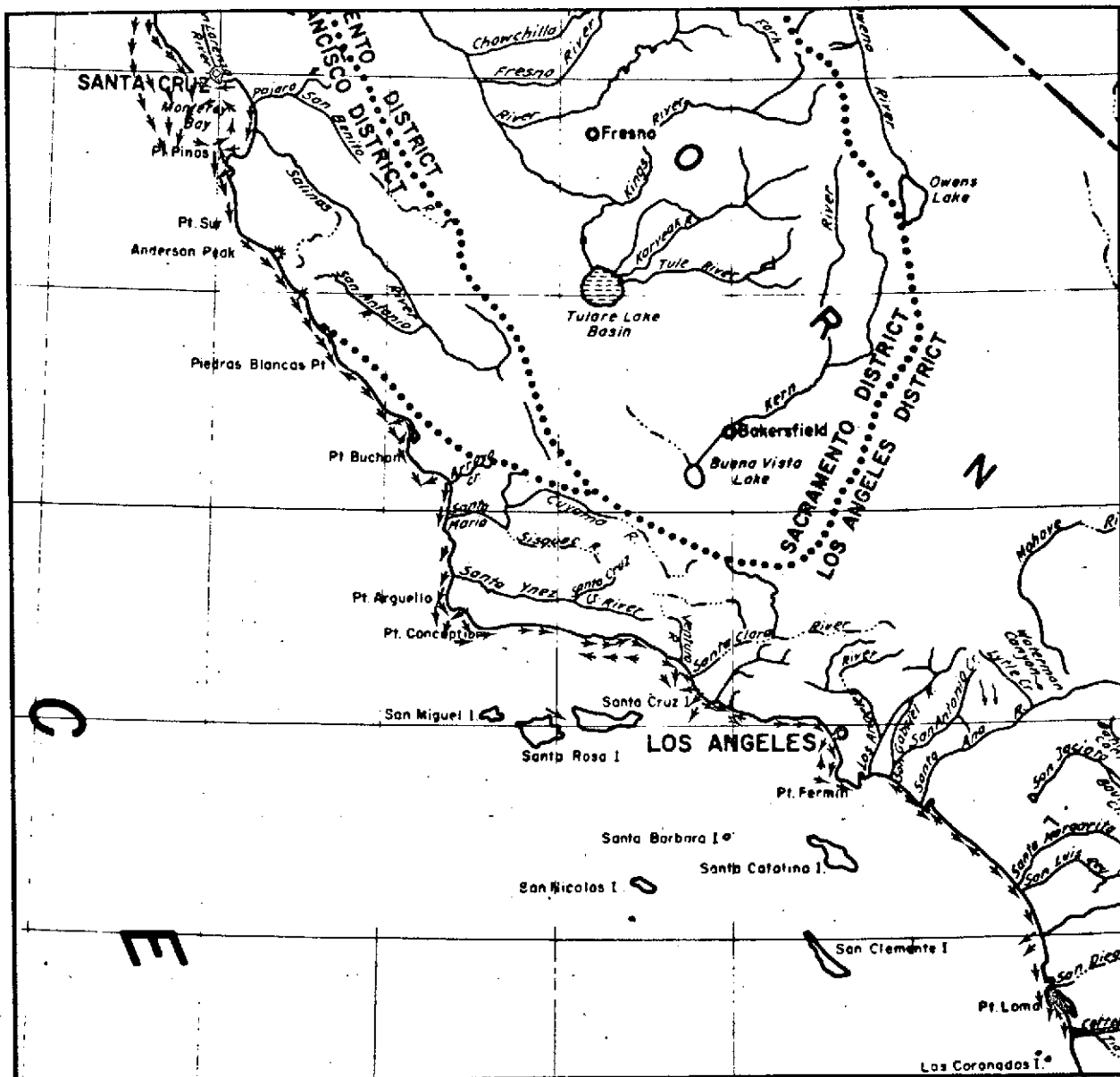
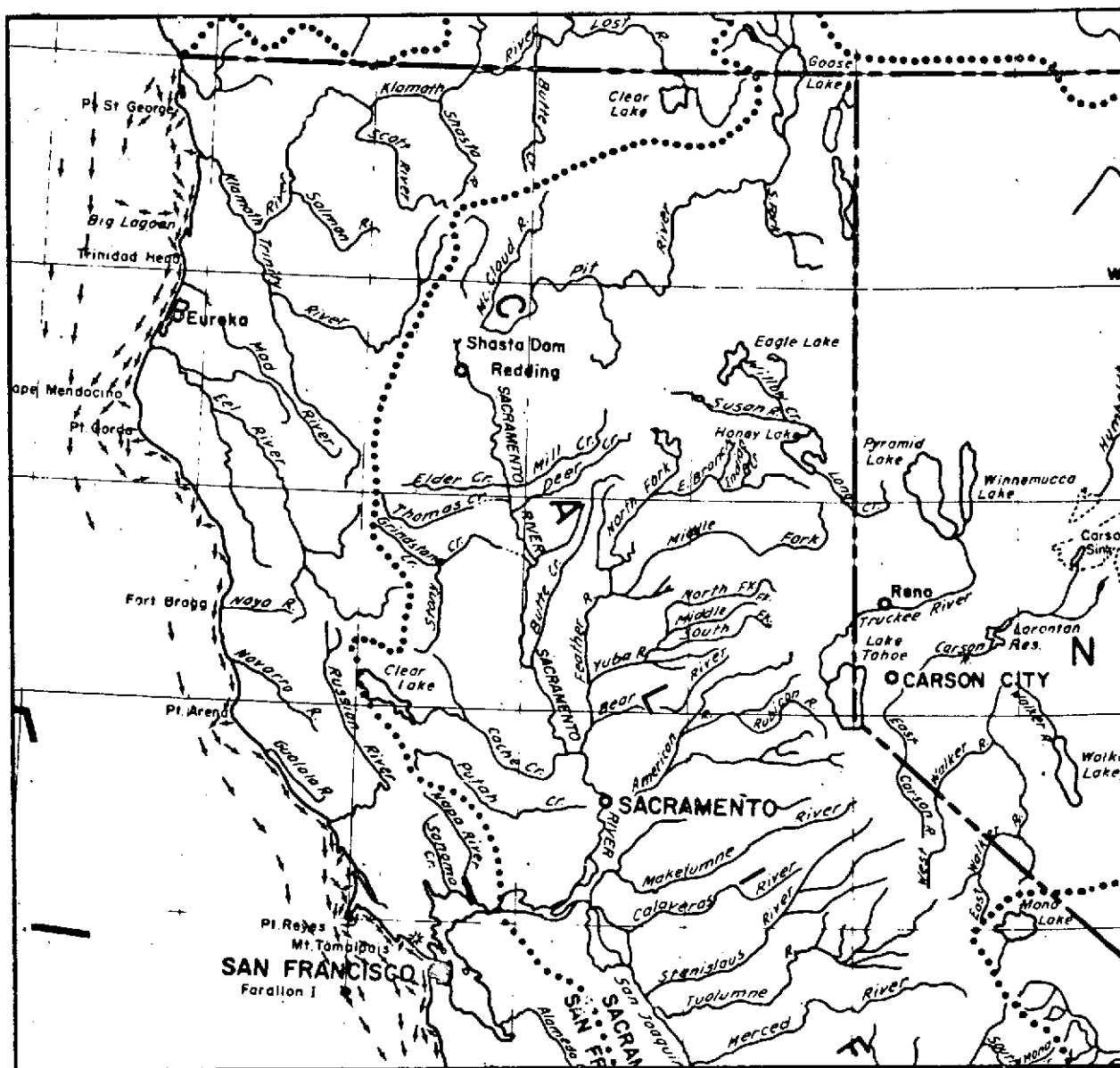


Figure 4-25. Southern California Coastal Currents - May 1973



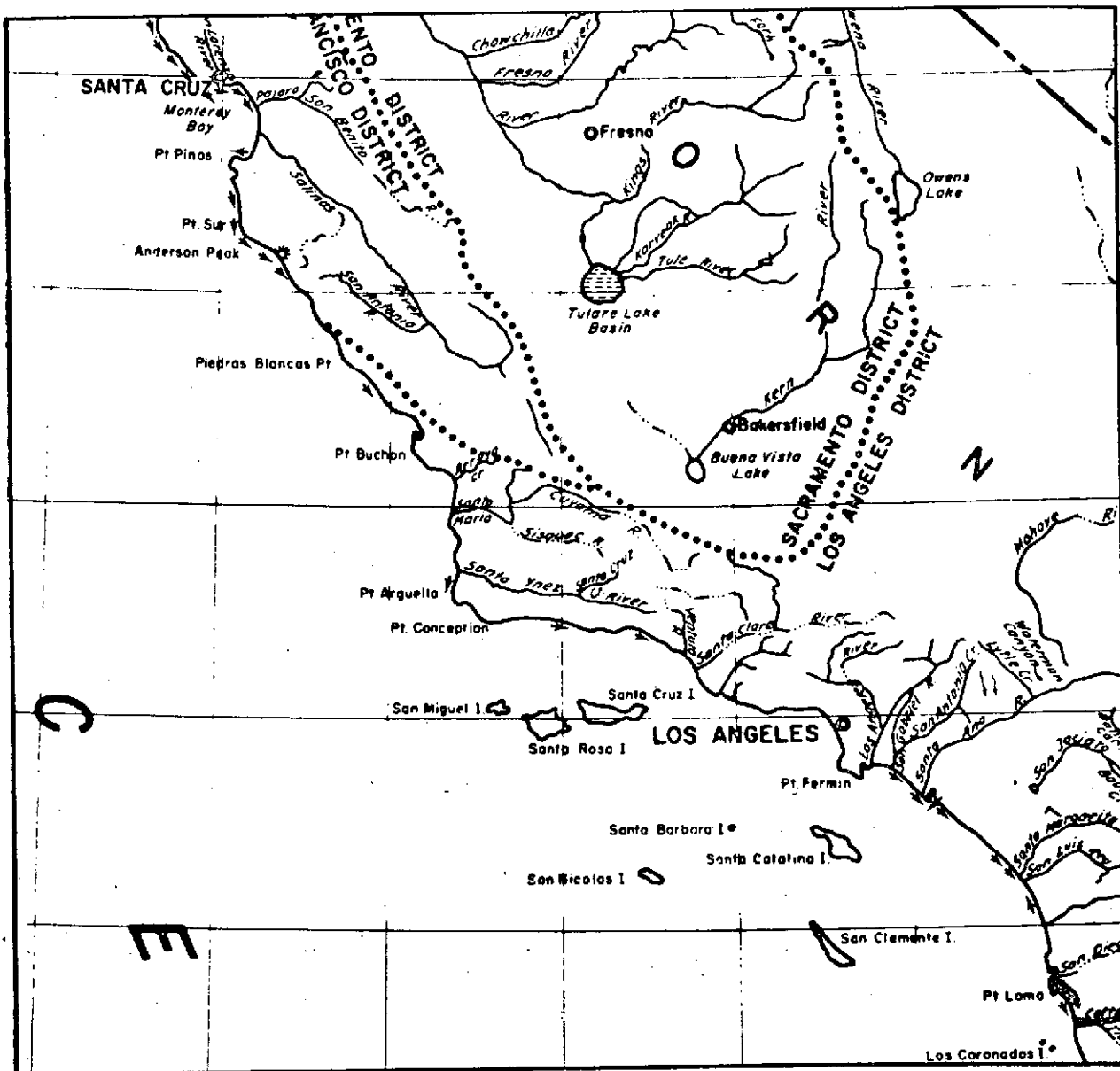
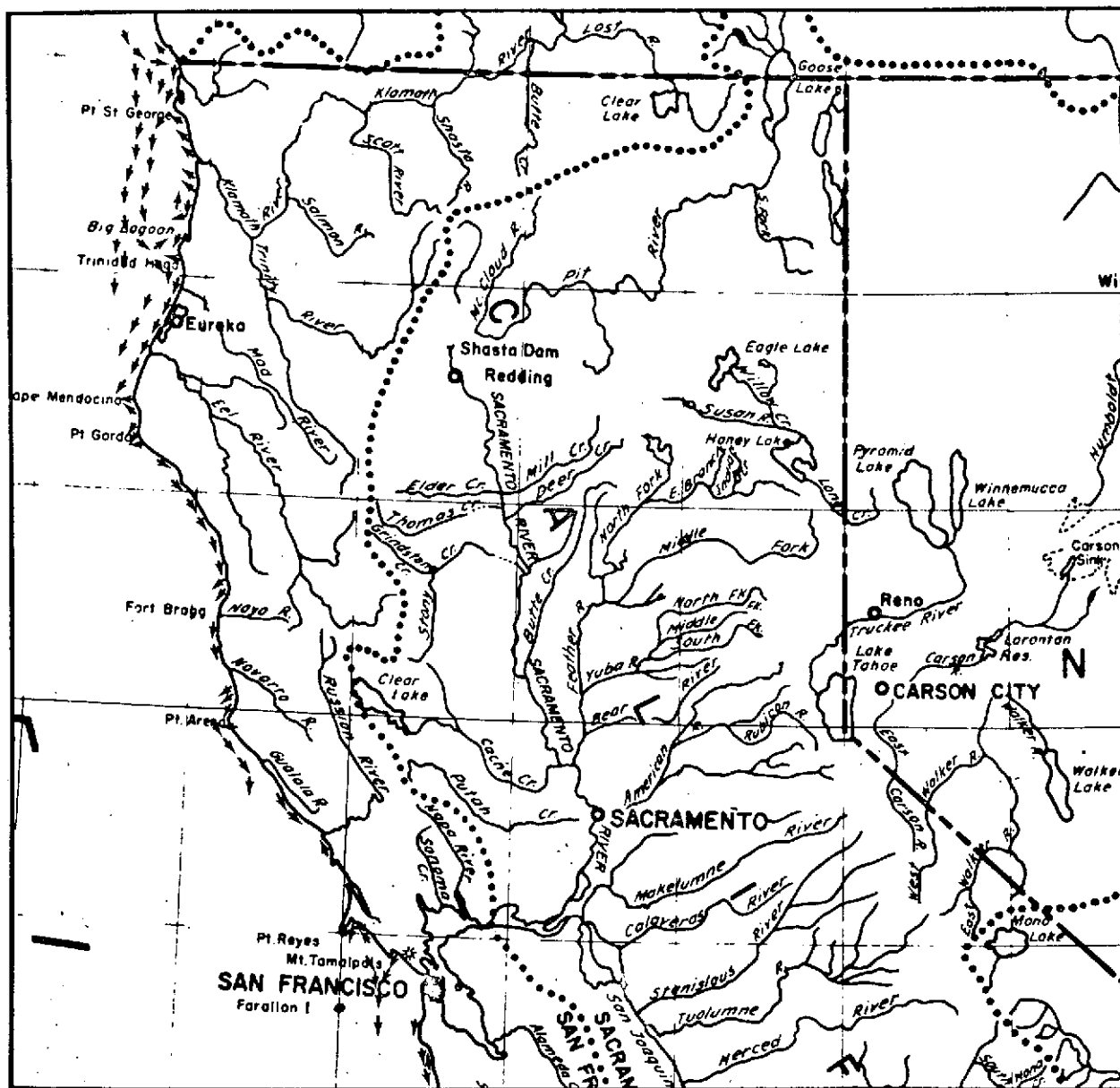


Figure 4-27. Southern California Coastal Currents - June 1973



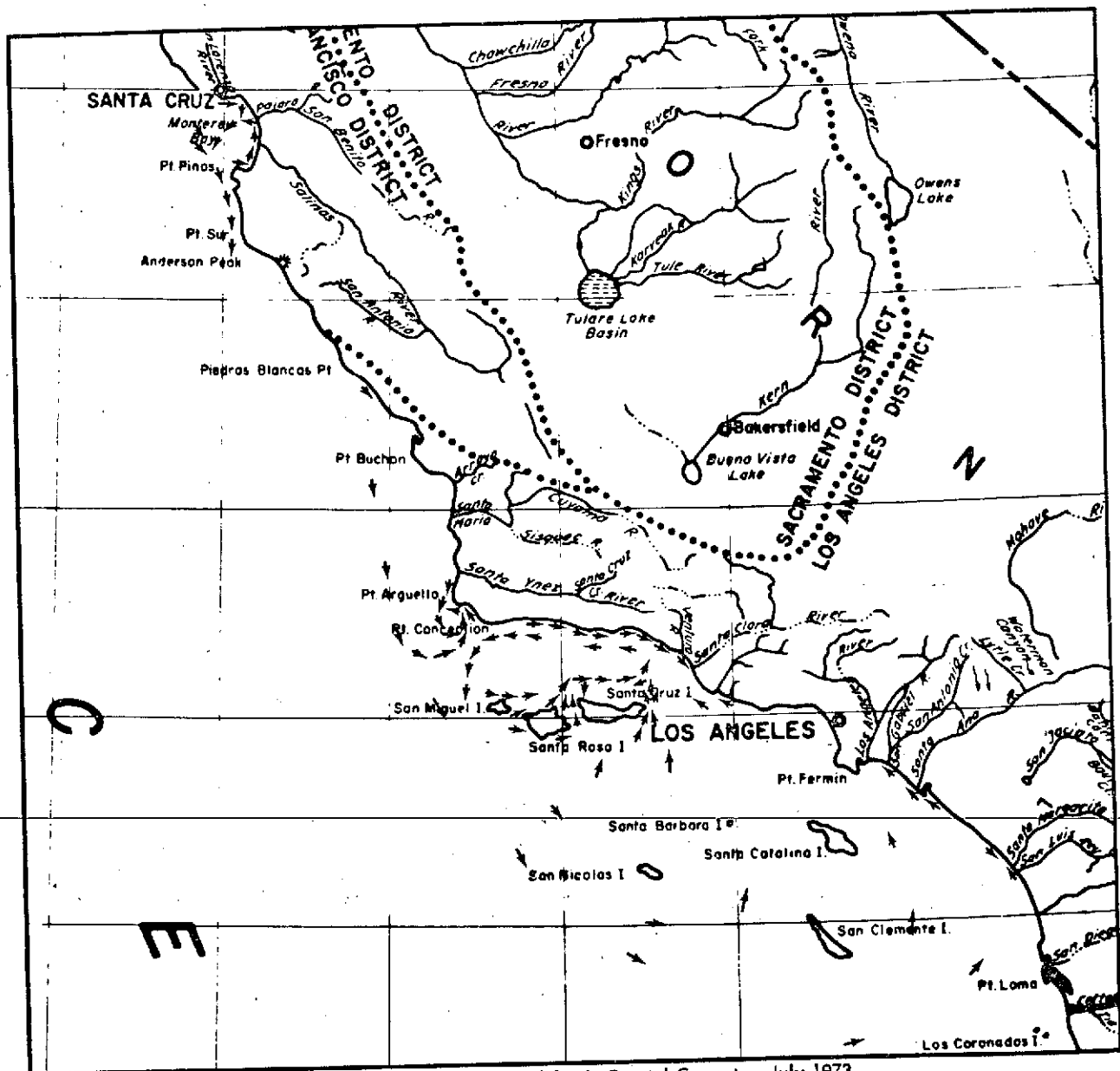
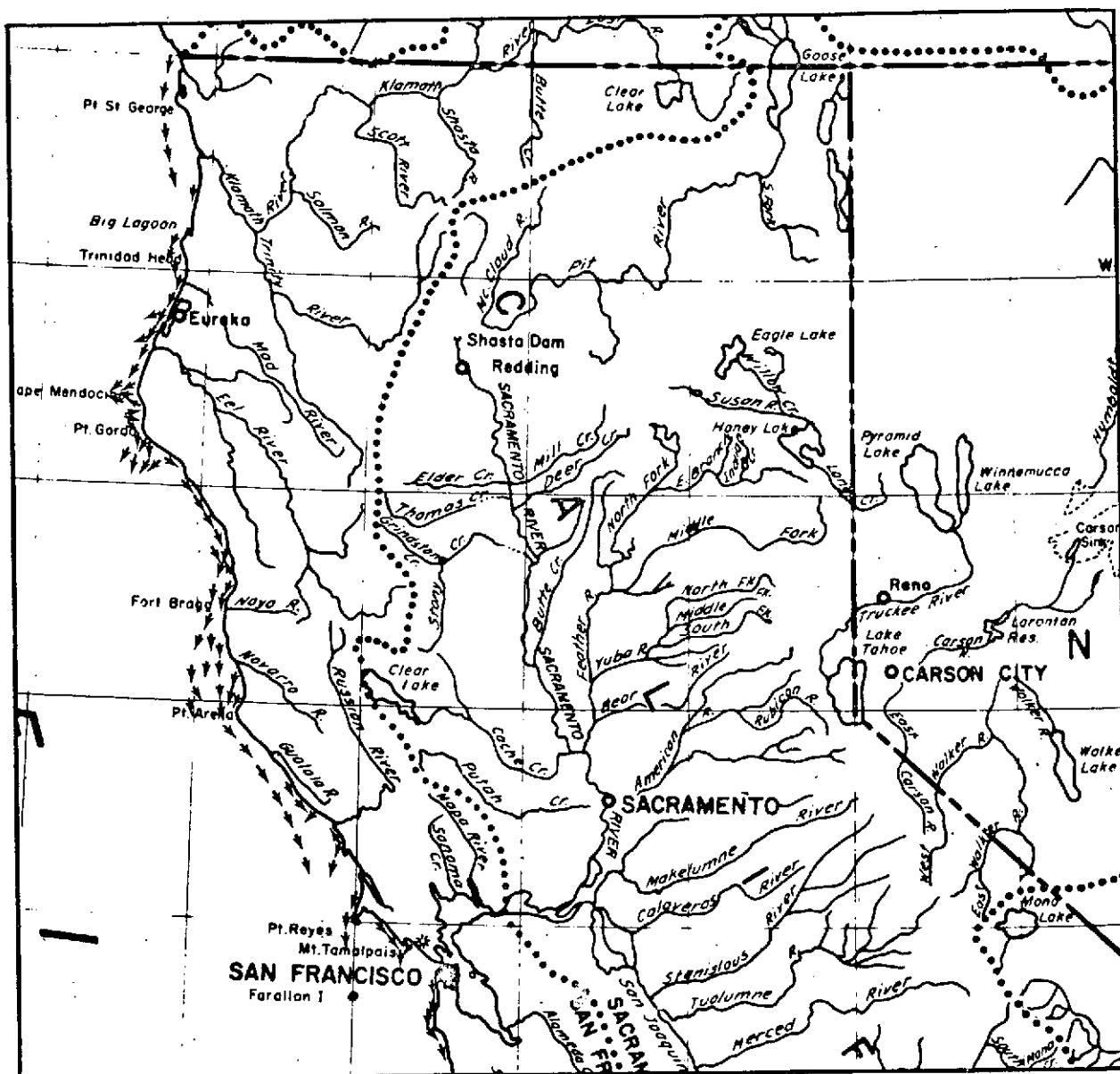


Figure 4-29. Southern California Coastal Currents - July 1973



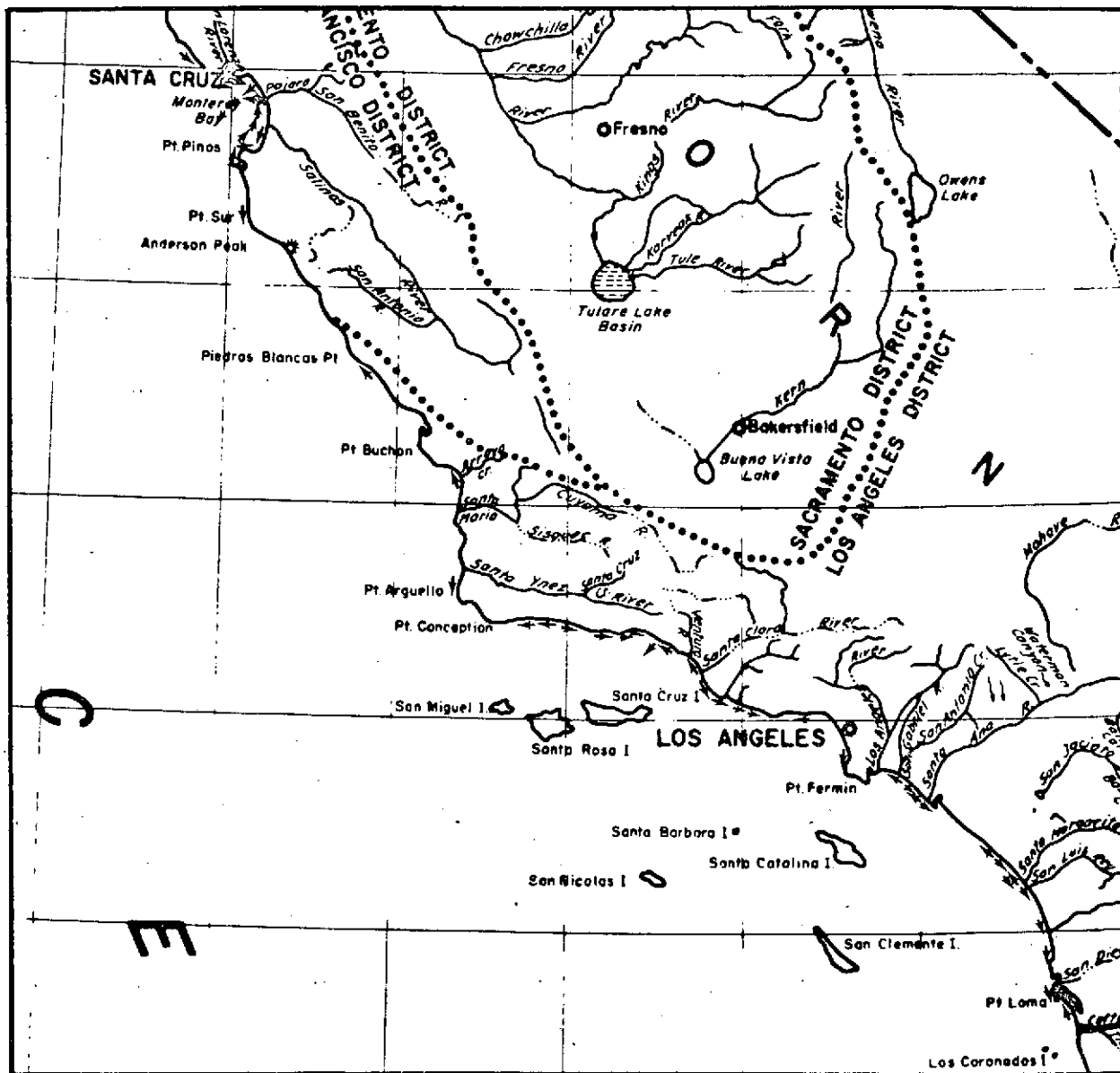
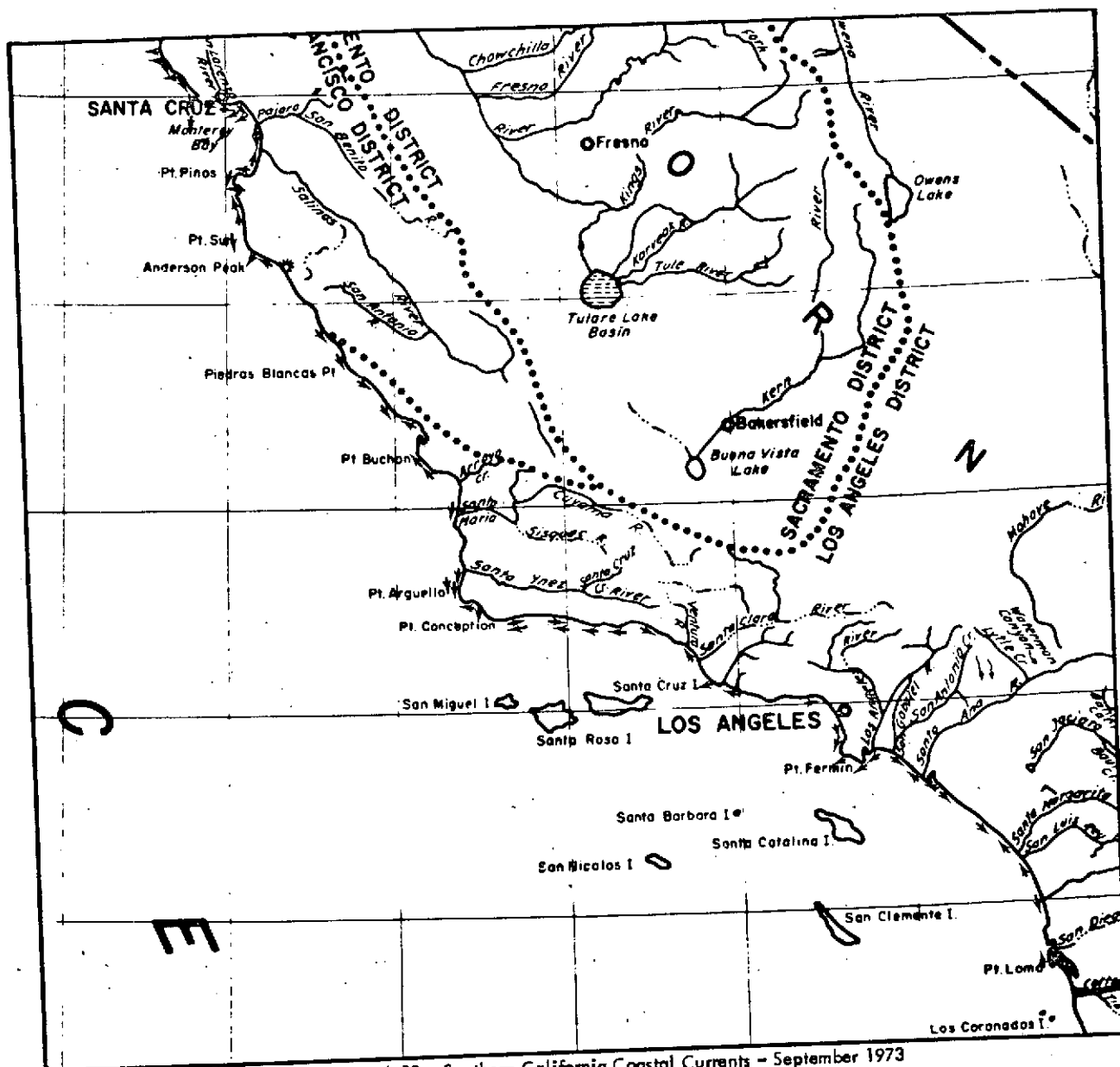


Figure 4-31. Southern California Coastal Currents - August 1973



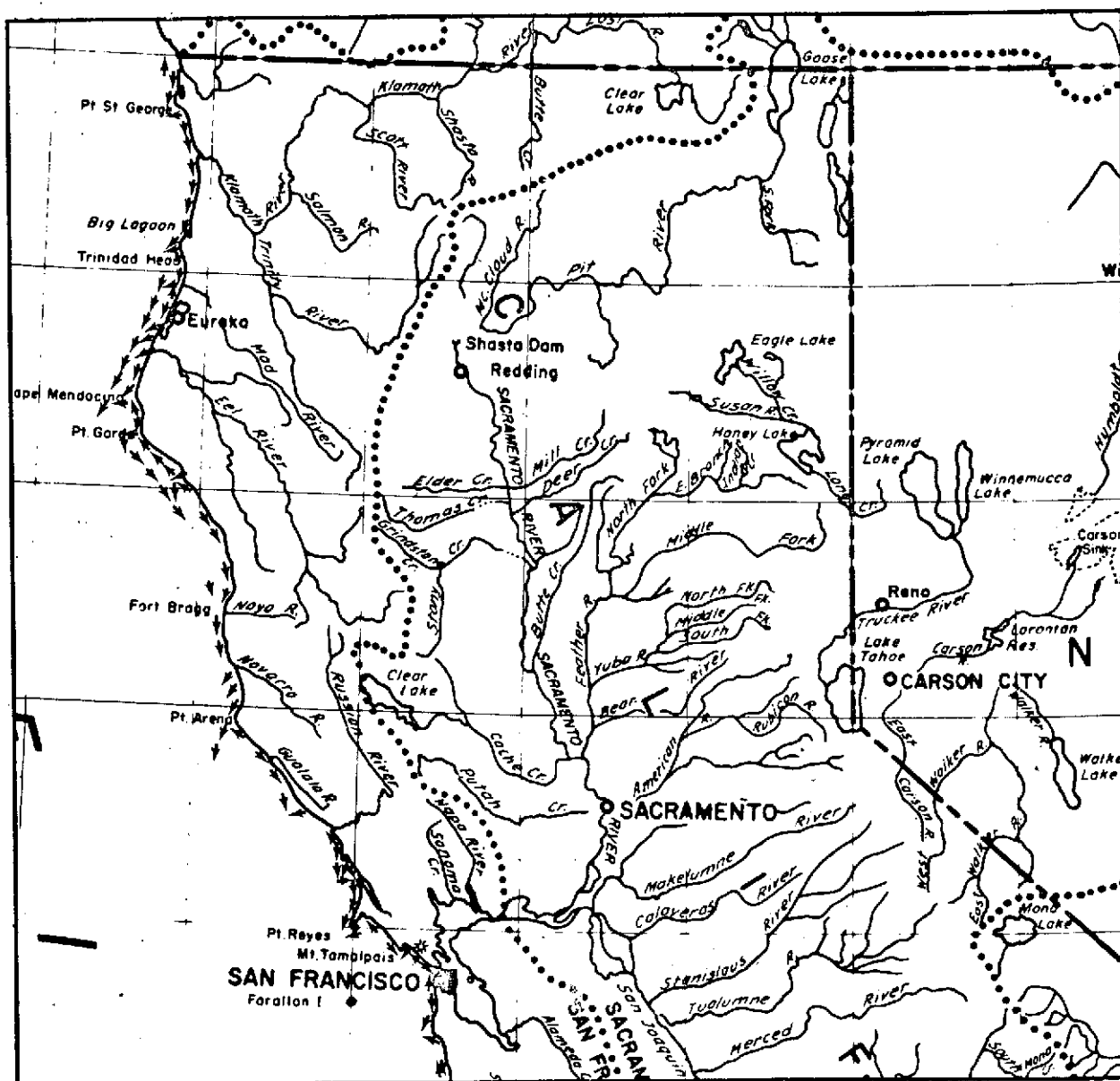


Figure 4-34. Northern California Coastal Currents - September 1972 and 1973

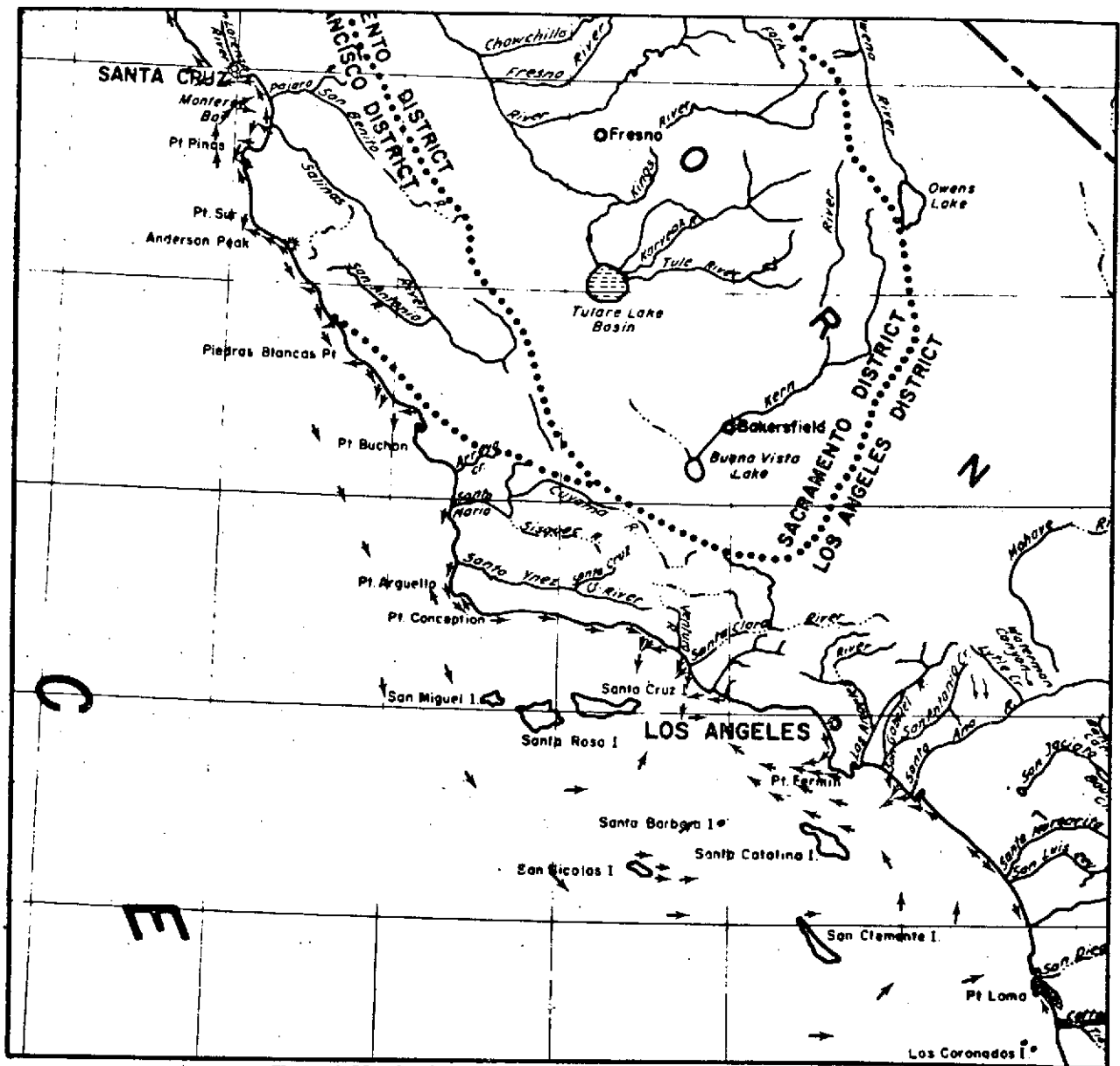
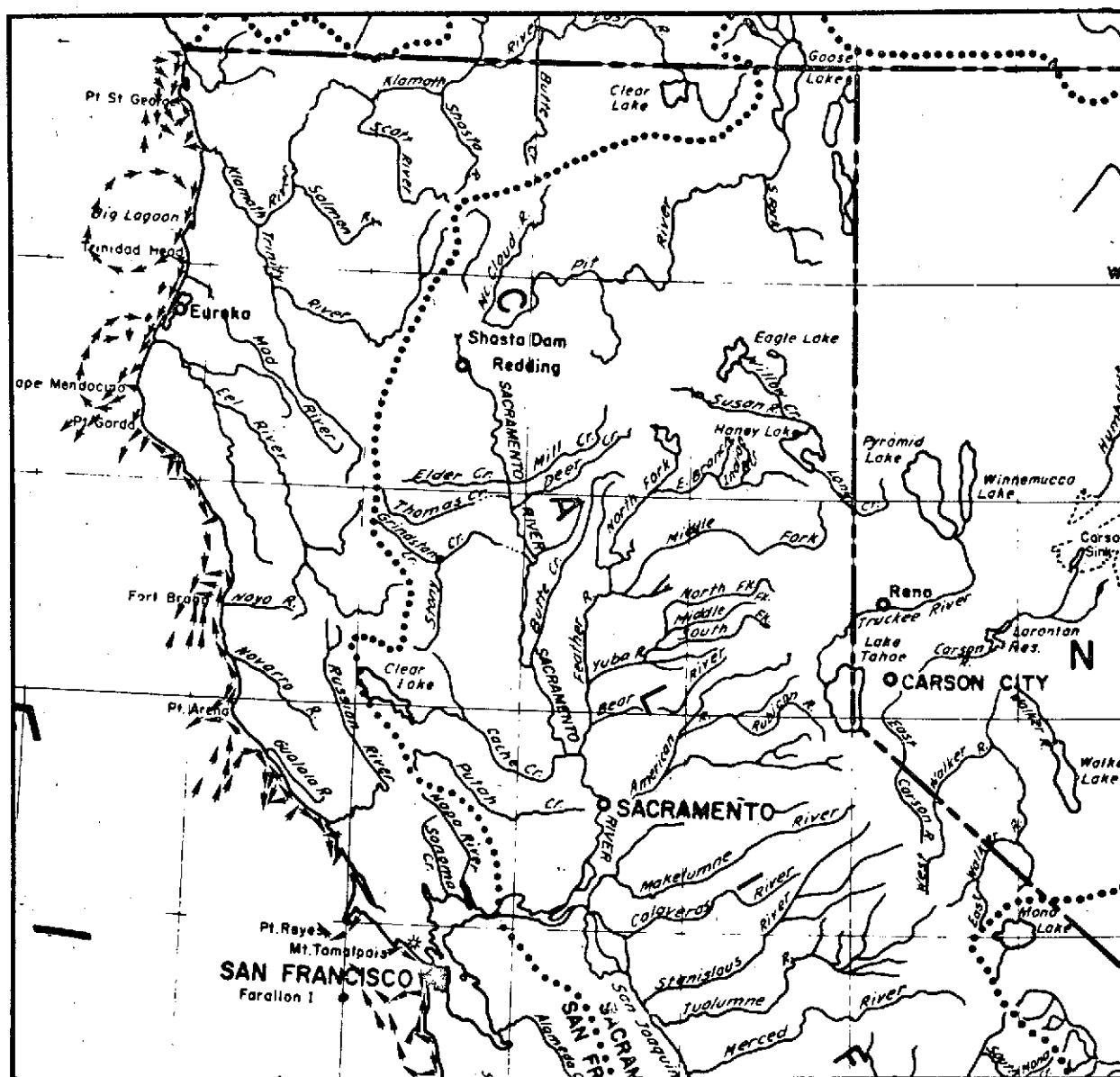


Figure 4-35. Southern California Coastal Currents - October 1972 and 1973



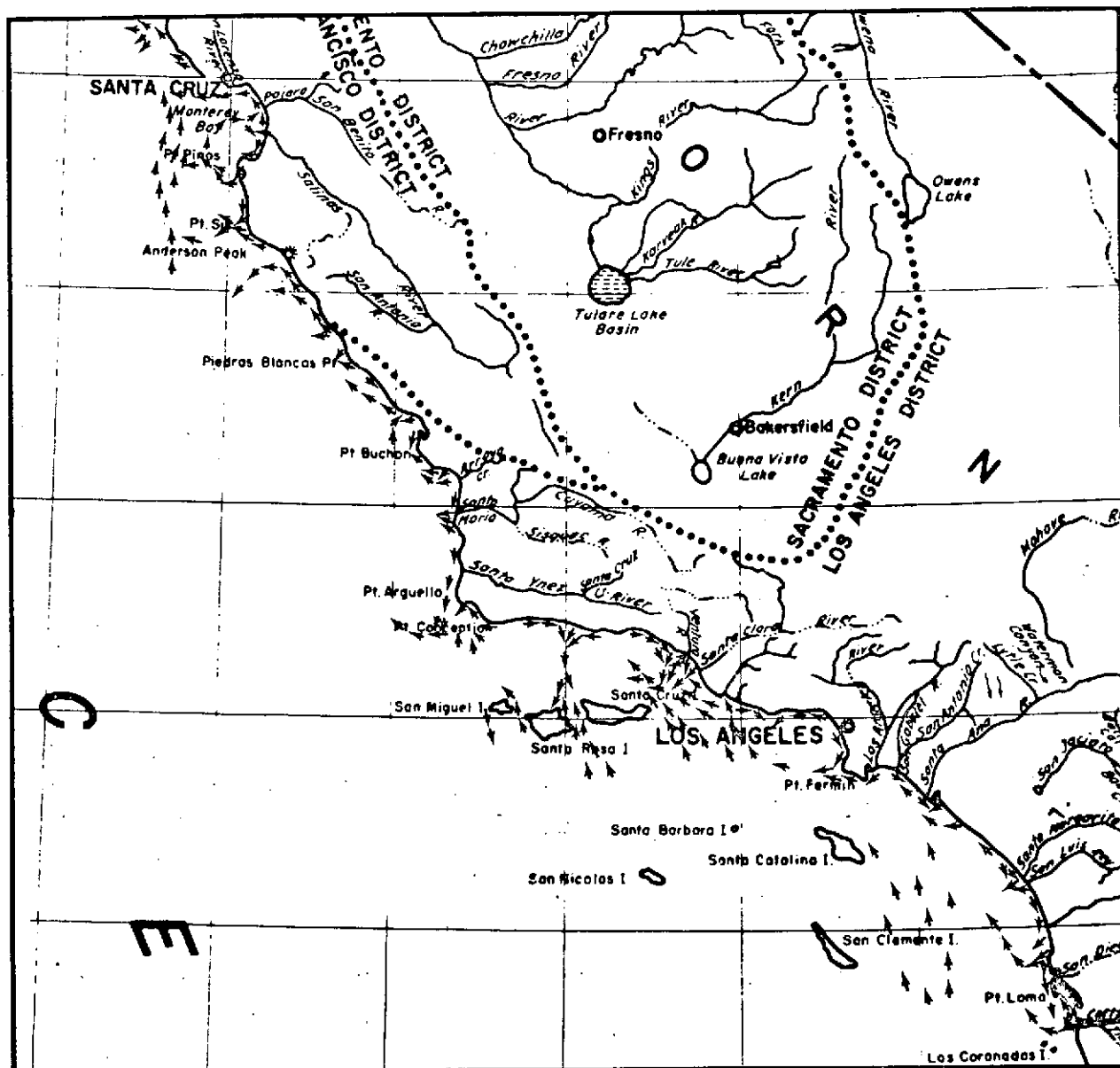


Figure 4-37. Southern California Coastal Currents - November 1972 and 1973

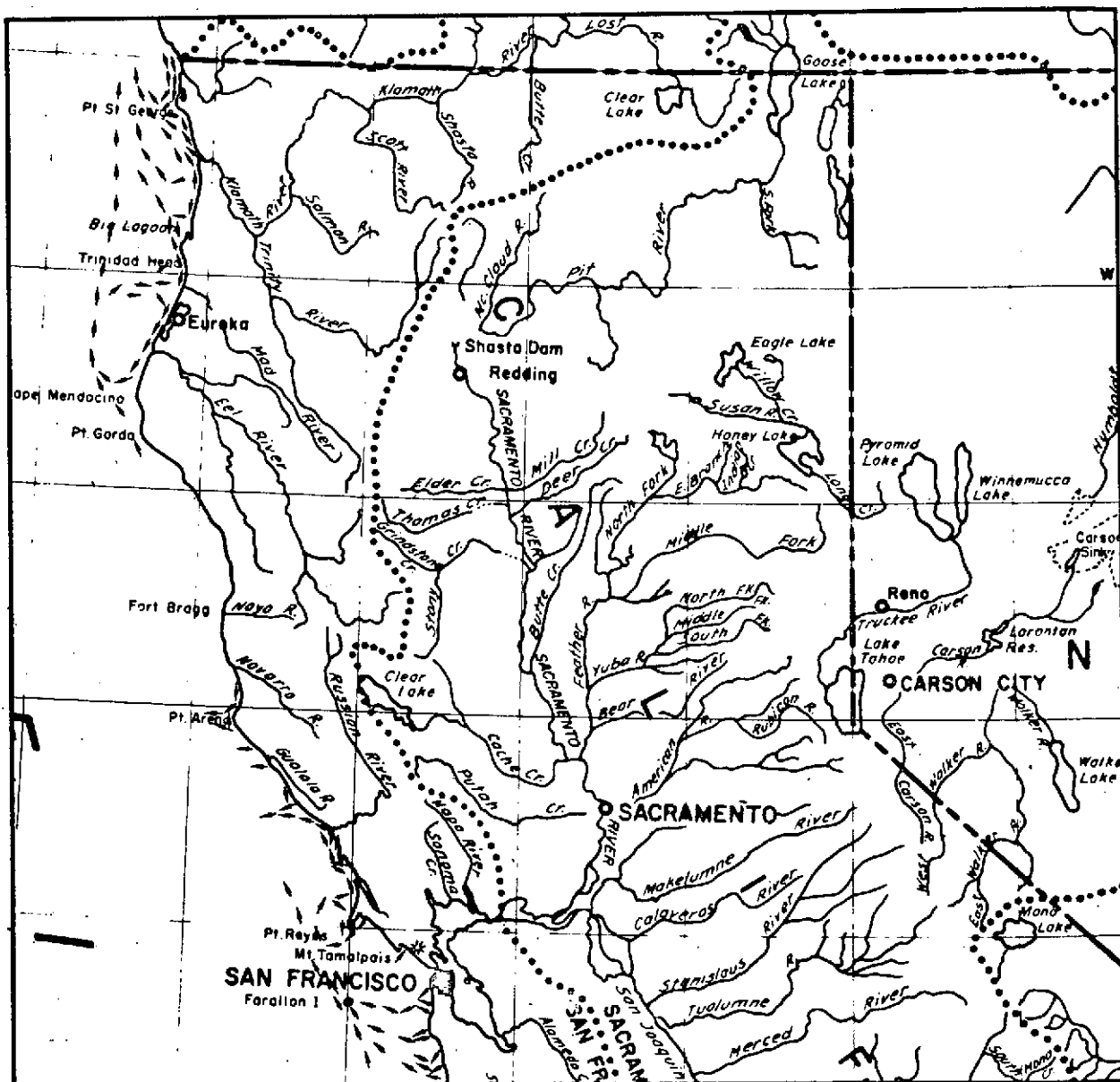


Figure 4-38. Northern California Coastal Currents - November 1972

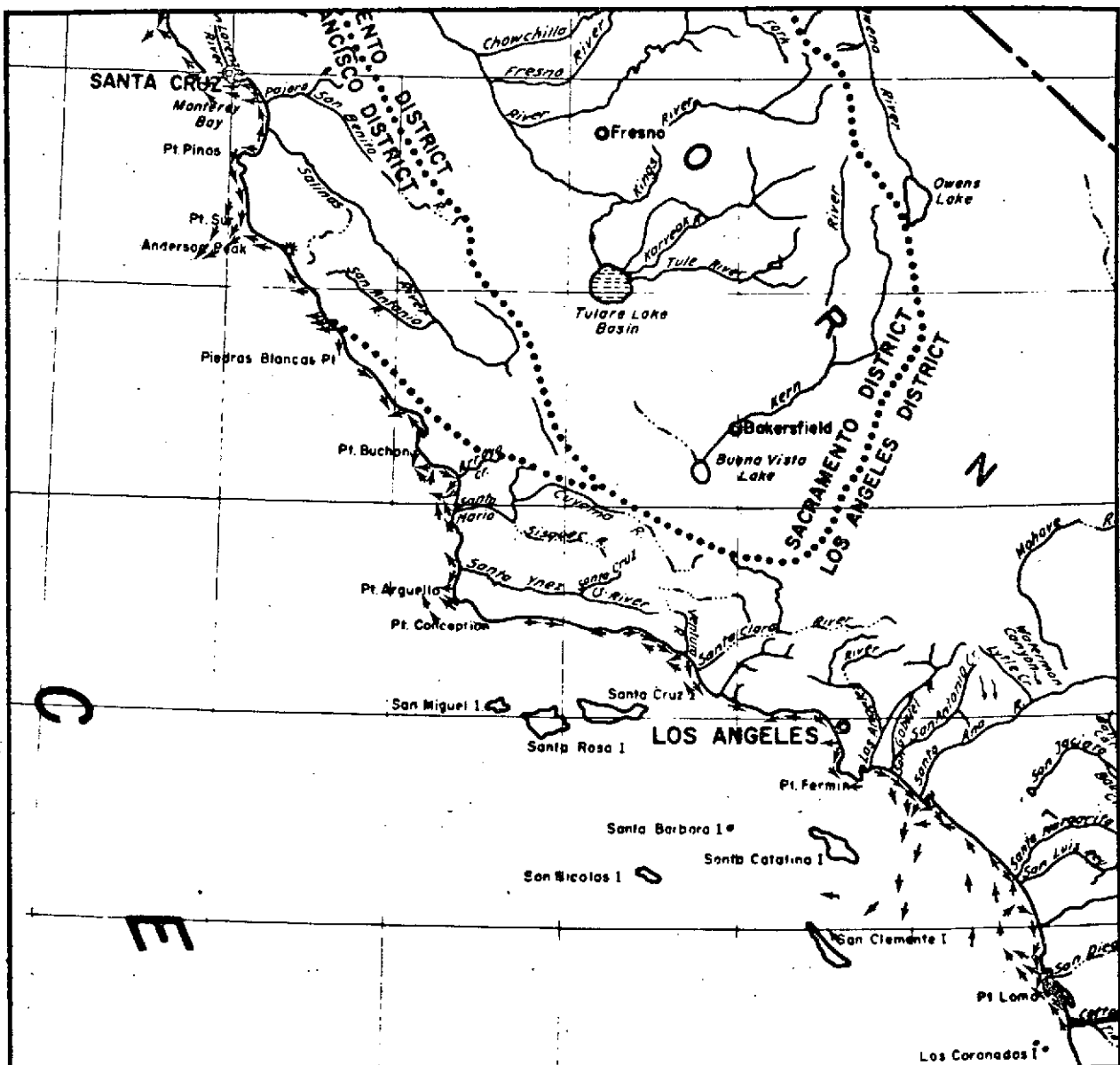


Figure 4-39. Southern California Coastal Currents - December 1972 and 1973

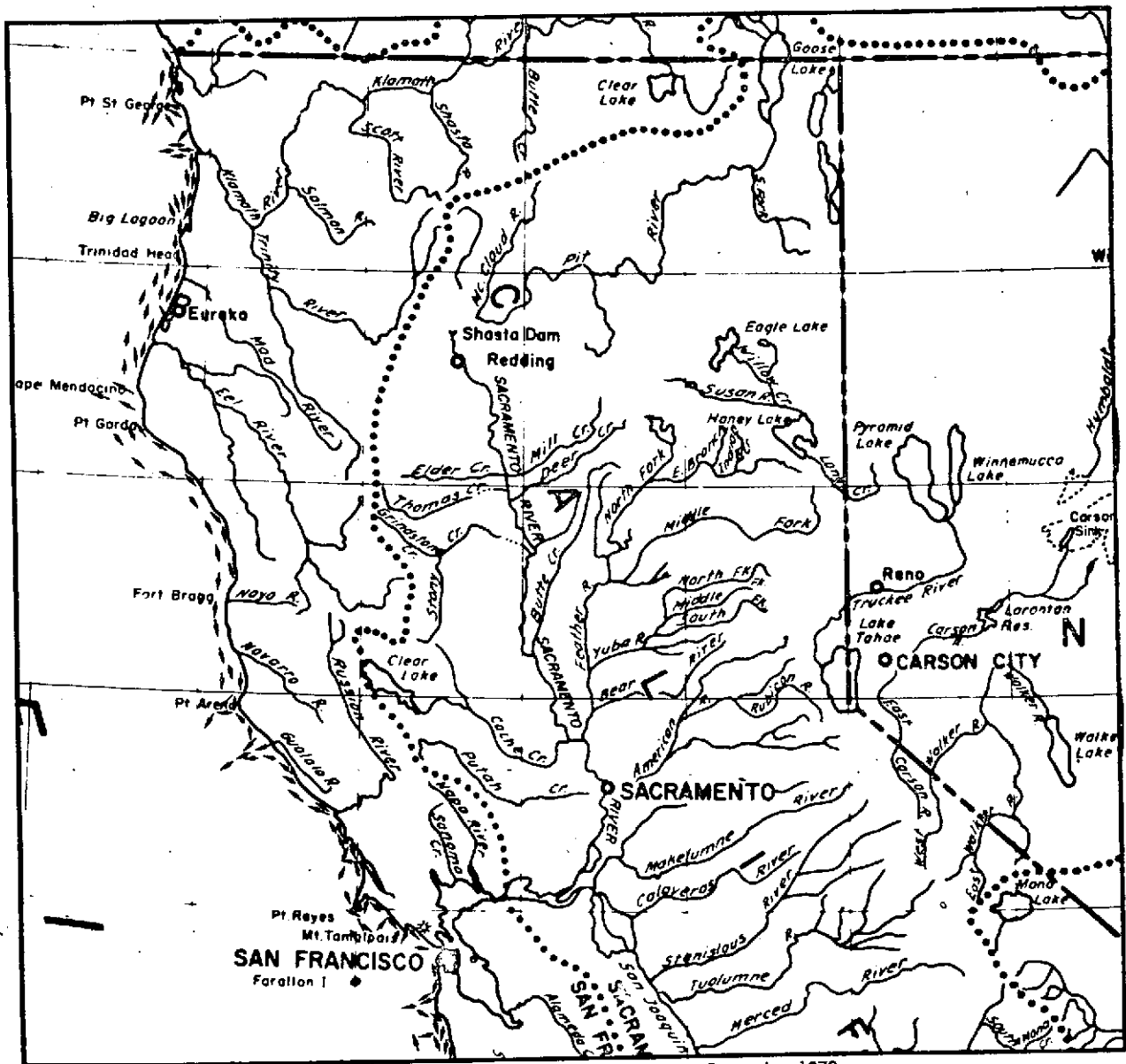


Figure 4-40. Northern California Coastal Currents - December 1973

5.0 SUSPENDED SEDIMENT ANALYSIS

5.1 APPROACH TO ERTS DENSITY VS. SUSPENDED SEDIMENT CONCENTRATION

It has been estimated that 5 million tons of sand are dumped annually into the littoral transport of Southern California by rivers and ephemeral streams. Sand-budget studies imply no net loss of sand off the shelf due to longshore drift, wave swash drift, or coastal currents. At the same time, no significant retreat or buildup of the shoreline or the volume of coastal sand dunes is observed. Shepard and Emery proposed in 1941 that this equilibrium is maintained by the entrapment of sand in submarine canyons, with subsequent down canyon flows removing the sediment to deeper water. From major rivers (i.e., the Mississippi), Scruton and Moore showed in 1953 that a surface layer of fresh turbid water may extend up to 100 km offshore. Such a sediment plume is presumably composed of silt and clay-sized particles, and larger particles absorbed to organic material. In Southern California such fresh water river plumes, according to Natland and Kuenen (1951) are restricted to less than a 2-km range offshore. Thus, subsequent experimental studies have concentrated upon the elusive canyon turbidity flows and oscillatory down-slope movement of sediment in bottom turbid layers.

From this point of view, the extent of the visible sediment plume from the Southern California rivers, in flood, as revealed by ERTS-1 is extraordinary. The sediment plume's continuous tonal values imply that they may be more significant for moving fine material beyond the "null point" line (15m depth contour) than has been heretofore supposed. They may in fact be partially responsible for maintaining the equilibrium. The attempted sediment load-film density correlation discussed in this report may provide a semi-quantitative method of evaluating this hypothesis.

A number of workers have noted that there is an apparent relationship between suspended sediment load and film density in aerial and space photos. Classical oceanographers have long used narrow band optical transmissometer data over a short path to infer sediment loads up to 1 or 10 mg/liter. Densitometric plotting of relative film densities is sufficient for temporal analysis of sediment level changes if an absolute exposure calibration is maintained on a day-to-day basis. Lacking this, relative sediment concentration estimates can be made within a given frame. In an orbital photo, due to its extreme scale, this is a significant contribution in that large dimensional current circulation and gross sediment transport can be discerned.

On a seasonal basis, stable sediment patterns are observed in ERTS-1 images to persist for several weeks with minor changes. In situ measurements of suspended sediment as a function of depth and lateral extent show these patterns to be extremely complex in three-dimensional development. Such sediment clouds with either a sharp or diffuse boundary at an intermediate depth above the bottom, will reflect or back scatter a

disproportionate amount of light, thus confounding the film density/sediment load determination. Color of the sediment cloud may be used to identify it and assign an appropriate statistical weight in the image merging program, but the morphology of the turbidity cells is complex (e.g., see Figure 5-1 which shows typical color differences in a lagoon, surf zone, and deeper ocean waters).

Along the California coast, coastal mountain ranges cause surface winds to parallel the coast in an equator-ward direction, thus producing a dominantly offshore sweep for the sun-warmed surface waters. The colder subsurface waters rise to produce both thermal and suspended sediment-type gradients.

What is of concern here is to attempt a calibration of film density in terms of absolute sediment load. Color and turbidity are very much interrelated in that the particulates which cause water to be turbid themselves selectively absorb and scatter (when small enough) visible energy. Turbidity in water results from the presence of particulates, either organic or inorganic in nature, while color can sometimes be attributed to scattering and absorption by dissolved materials or by the water molecules themselves. A basic definition of turbidity is that it is a means of expressing that optical property of a sample which results in rapid attenuation of light by scattering and absorption by particulates. Although some investigators feel that the weight-concentration of suspended matter in the given optical path is infeasible to correlate with turbidity, the basic problem is illustrated in Figure 5-1 showing normalized transmittance of several turbid coastal and ocean water types. The strongest difference in transmittance is obviously due to the scatterer type (i.e., in the lagoon, in the surf zone, or ocean). A lesser effect (i.e., a few percent per meter) is due to the specific sediment load (e.g., reference curves M3 and M5 of Figure 5-1).

On the other hand, curves such as Figures 5-2 and 5-3 indicate that this may not be correct since they show excellent agreement. Indeed, logic tells one that the concentration of particulates in the path will be the dominating factor in a long path length. Size, shape, and refractive index are possibly not as important as once thought in terms of scattering. Hence, most oceanographers utilize suspended sediment concentration (organic plus inorganic) as a measure of turbidity. In situ measurements made with a 30 cm Secchi disk, in extremely turbid San Francisco Bay waters show strong correlation of sediment loads to the 4500 Å band film density readings.

The closest ERTS band analog is at 5000 Å. Apparently, the 5000 Å band indicates the position of the sediment cloud where the mean density change of the total suspended sediment in water is on the order of 10 milligrams/liter on a volumetric average over the water column.

In deeper water, a critical hypothesis to test is if the net increase in suspended sediment contributes dominantly to the back scattered light. In this case, higher reflectances due to multiple sediment layers at varying depths would be confounded with increased back scatter due to an increase in total suspended sediment.

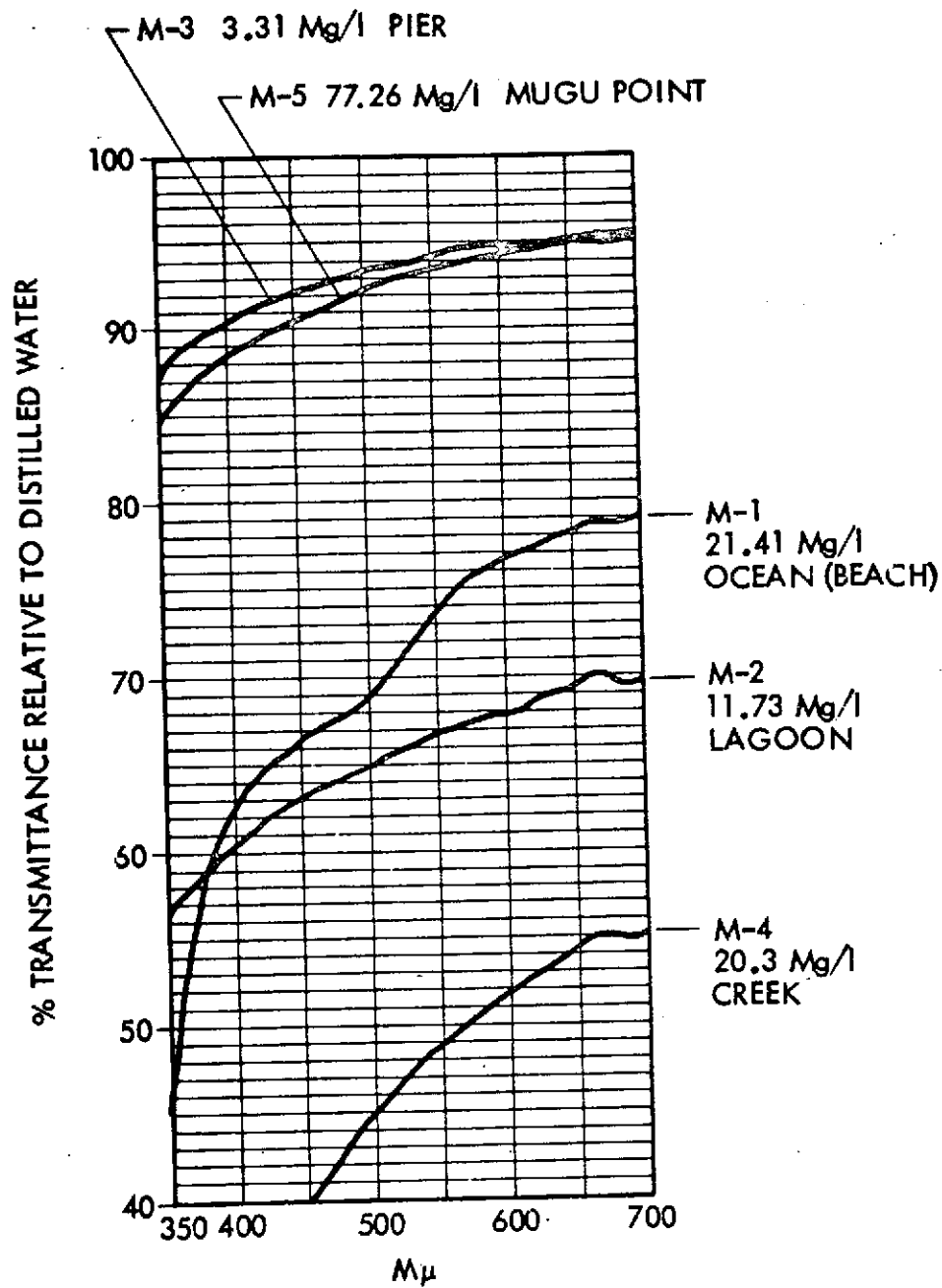


Figure 5-1. Mugu Lagoon & Ocean Water Sediment Loads and Spectral Transmittance

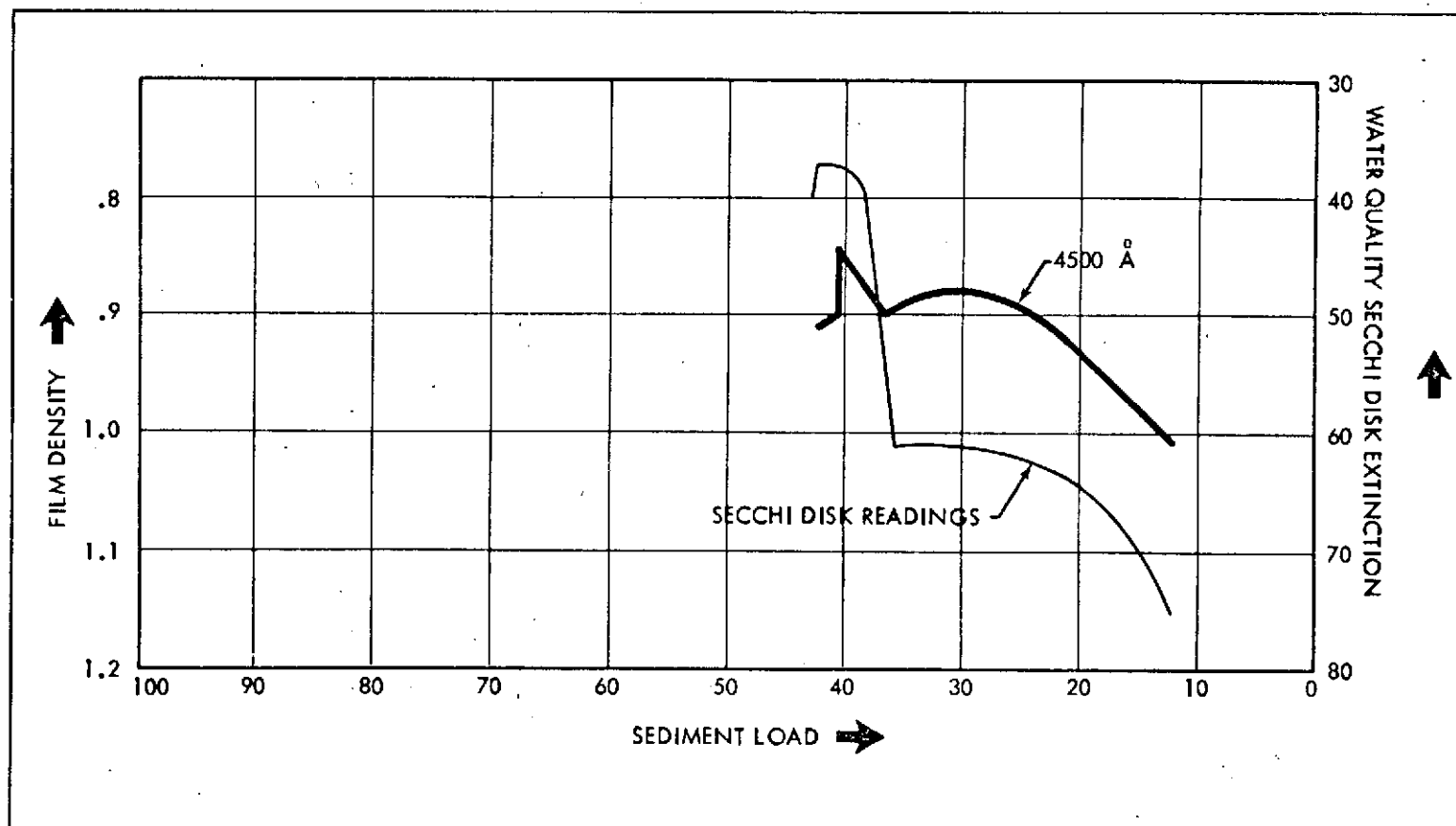


Figure 5-2. Film Density Vs. Sediment Load & Optical Extinction

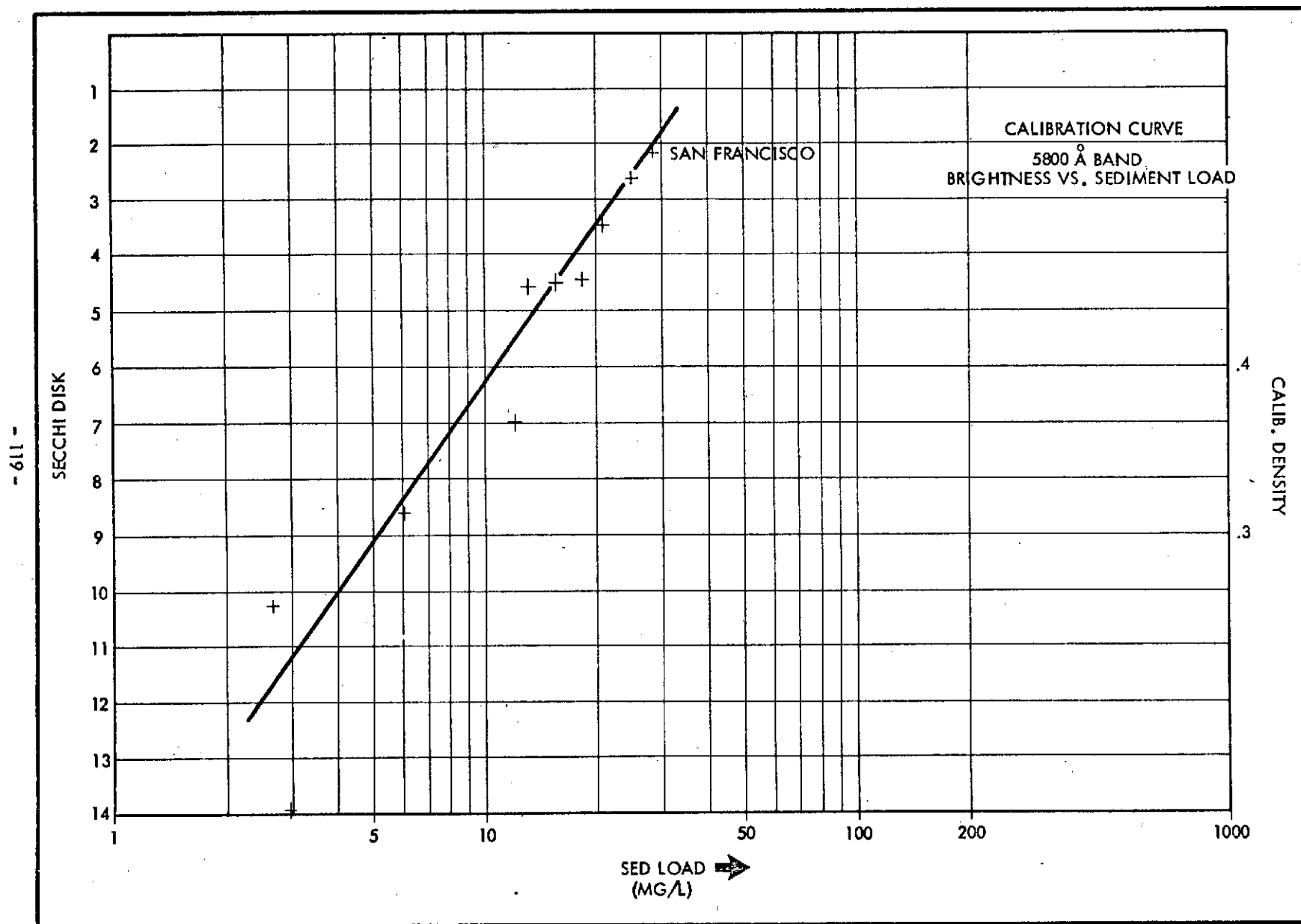
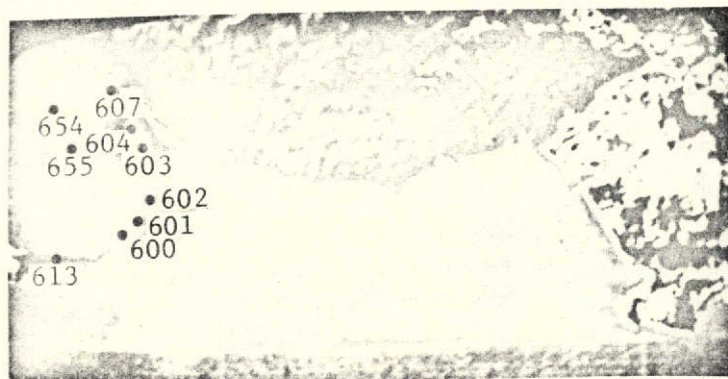


Figure 5-3. Calibration Curve for Sediment Load Vs. Film Density in Median California Coastal Waters (Film GAMMA = 1)

Figure 5-4. Attenuation of Blue-Green Light Vs. Sediment Loading
Ghovanlou, et al 1973



(NASA ERTS Frame 1108-18014-4)
8 November 1972

Sediment Load

Key: (Interpolated from Figure 5-3)

Dark Blue	-	1-2 mg/liter	} insensitivity may be due to reciprocity failures in the film
Medium Blue	-	2-3 mg/liter	
Light Blue	-	3-4 mg/liter	
Light Green	-	4-8 mg/liter	
Dark Green	-	8-15 mg/liter	

Figure 5-5. Tentative Mapping of Near-Surface Suspended
Sediment from ERTS Imagery
(Based on Drakes Values)

Since a wide range of sediment samples and simultaneous aerial photography were available from an ONR Bathymetry Study for Portuguese Bend and Inspiration Cove on Palos Verdes Peninsula near Los Angeles, they were chosen to test this hypothesis. These waters represent the "median" coastal seeing environment. Although in general, the Portuguese Bend sediment load was observed to increase with water depth, both concave and convex gradients as well as linear increased with depth were characteristic of individual stations in the raw sample data. These data ranged from a high of 44.9 mg/l to a low of 0.3 mg/l. It should also be noted that these particular data correspond to a period of runoff of terrogenous sediment due to rain during the preceding week. Comparison of film isodensity traces over the sampled area with suspended sediment anomalies at depth showed neither a significant correlation nor anticorrelation. Hence, in the absence of a more extensive sampling grid, simple volumetric averages of sediment load were computed from the water sample analysis. (These ranged from 16 to 4 mg/l.) These showed a "break" at approximately the 20-foot depth contour corresponding roughly to a 10 mg/l decrease in sediment seaward. A visible scum line was also observed in the photography in this vicinity, evidently marking the boundary between these two water types.

These data were employed to derive the film density/sediment load calibration shown in Figure 5-3. The same calibration was applied to NASA frame 1108 - 18014 -4, Figure 5-5. Initially, it was noted that the negative supplied by NASA did not have the stated densities on its stepwedge. Table 5-1 below provides the recalibration performed. Attenuation vs. sediment loading is shown on Figure 5-4.

Table 5-1. Recalibration Data

Drakes Sediment Level	
Station #	Mg/l
600	1.1
601	.56
602	2.51 (Avg)
603	3.6 (Avg)
604	15.3
613	0.5
651	4.3
654	3.1
655	4.4

Step	1108-18014-4 Negative (Reference Figure 30) January 1969	
	Density (MacBeth)	NASA
15	0.18	0.40
14	0.40	1.31
13	0.62	1.48
12	0.76	1.75
11	0.86	1.87
10	0.96	1.96
9	1.04	2.04
8	1.08	2.10
7	1.14	2.16
6	1.20	2.21

5.2 SURVEY OPERATIONS FOR SEDIMENT QUANTIFICATION

A more specific sediment/film brightness experiment was designed based upon the above results of the airborne and sea truth photographic results obtained between suspended sediment measurements in the same season (from a prior year). The objectives of this experiment were to obtain a more specific relationship between ERTS scene brightness and suspended sediment load. The site selected for this experiment was the Ventura-Anacapa area.

This site was picked for two reasons. First, the National Park Service agreed to allow collection from their patrol boat, "Conger," during the ERTS overpass. Secondly, the survey site between Ventura Harbor and Anacapa Island (Figure 5-6) represents an area of complex current activity. The Anacapa Current usually flows northwest at this site while inshore and offshore currents are southeast.

On November 21, 1973 the first combination ERTS overpass, aircraft remote sensing flight, and sea truth cruise took place. The weather was clear and the sea calm in the morning with the swell from the west 1-2 meters. At each station shown on Figure 5-6 water samples were collected for later quantitative analysis at the University of Southern California Sedimentology Laboratory. Dye markers (rhodamine) were dropped at stations 2-10 for locating aircraft imagery and determining current characteristics. Water samples were collected at stations 2-18 on the survey line and stations 19-24 around Anacapa Island. The collected data was used in analyzing the reflection levels present in the offshore area on the ERTS imagery and the computer compatible tape. All of the information was collected almost simultaneously. The aircraft data is plotted on Figure 5-8 and described in Appendix A. The support equipment is described in Appendix B.

During the next ERTS-1 orbit over this site on December 9, 1973 a similar type aircraft and sea truth survey took place. Again, the weather cooperated with a clear day and relatively little wind. The ocean stations occupied on December 9 are plotted on Figure 5-7, and the accompanying aircraft flight line on Figure 5-9. On this cruise secchi disk measurements and spectrophotometer readings were collected. The increase in wind velocity and the resulting high seas caused cancellation of spectrophotometer measurements near Anacapa Island. Assisting on the cruise were Earth Science students from California State University, Fullerton. The following table, 5-2, gives results of the sea truth collection. Analysis of this site is described in the following section, 5.3.

Table 5-2. Sea Truth Data

November 21, 1973		December 9, 1973		
Station	Conc. * Mg/l	Station	Secchi Disk Meters	Conc. * Mg/l
1	1.7	1	2.5	4.7
2	3.8	2	2.5	6.6
3	6.9	3	4.0	3.0
4	4.2	4	5.5	6.0
5	2.5	5	12.0	0.6
6	0.7	6	21.0	1.0
7	2.0	7	24.5	0.7
8	2.1	8	--	0.8
9	2.5	9	22.5	0.8
10	1.1	10	21.0	.0
11	1.4	11	22.0	0.5
12	0.9	12	24.5	0.5
13	1.1	13	23.0	0.3
14	0.5	14	24.5	0.3
15	0.7			
16	0.7			
17	0.9			
18	0.7			
19	0.3			
20	0.1			
21	1.1			
22	--			
23	0.7			
24	3.4			
25	5.5			

* Concentrations were determined at the University of Southern California Sedimentology Laboratory using the Millipore filtration technique (Drake, 1972).

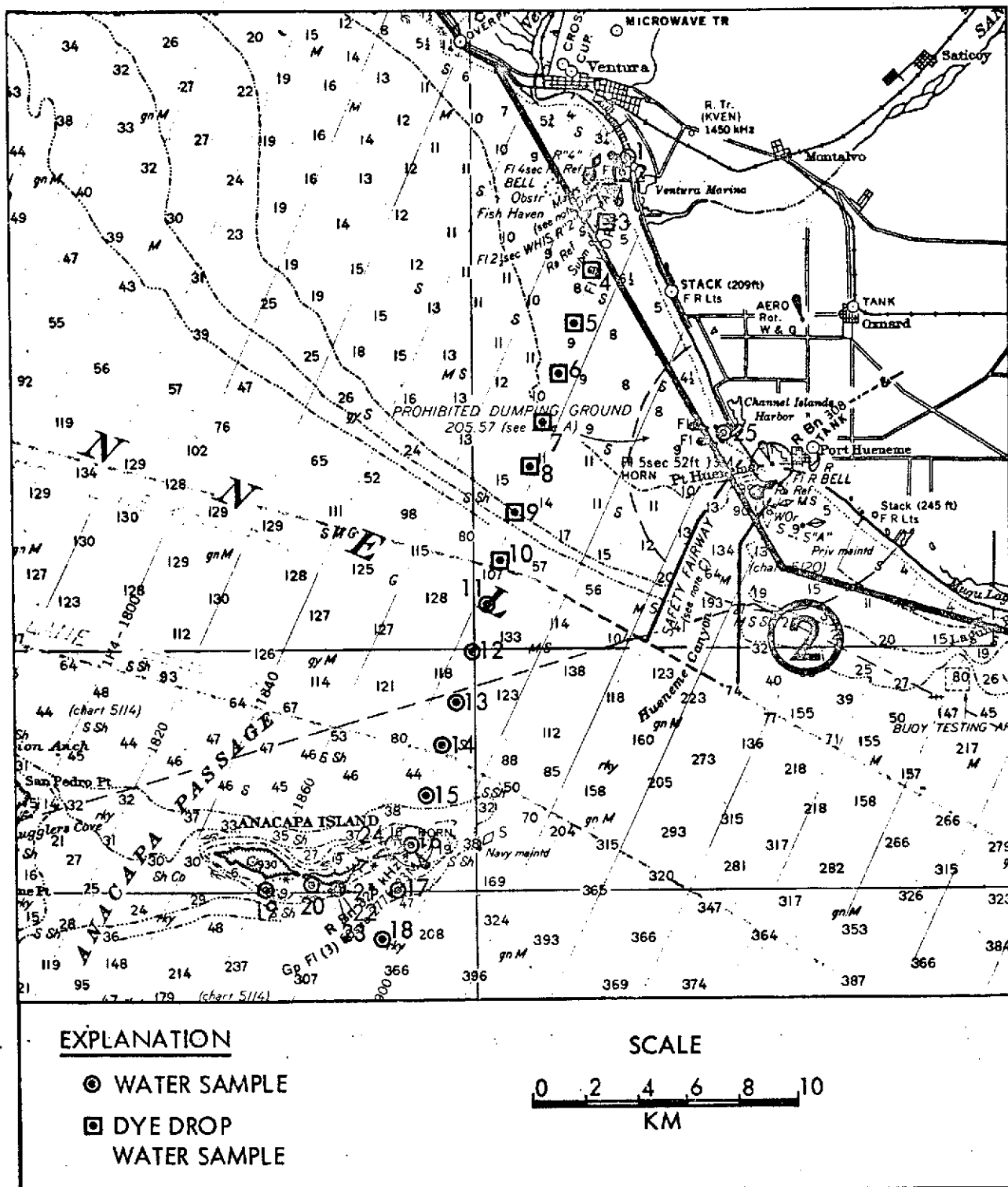


Figure 5-6. Sea Truth Stations - November 21, 1973

Ventura Harbor-Anacapa Island survey on National Park Service boat, Cougar

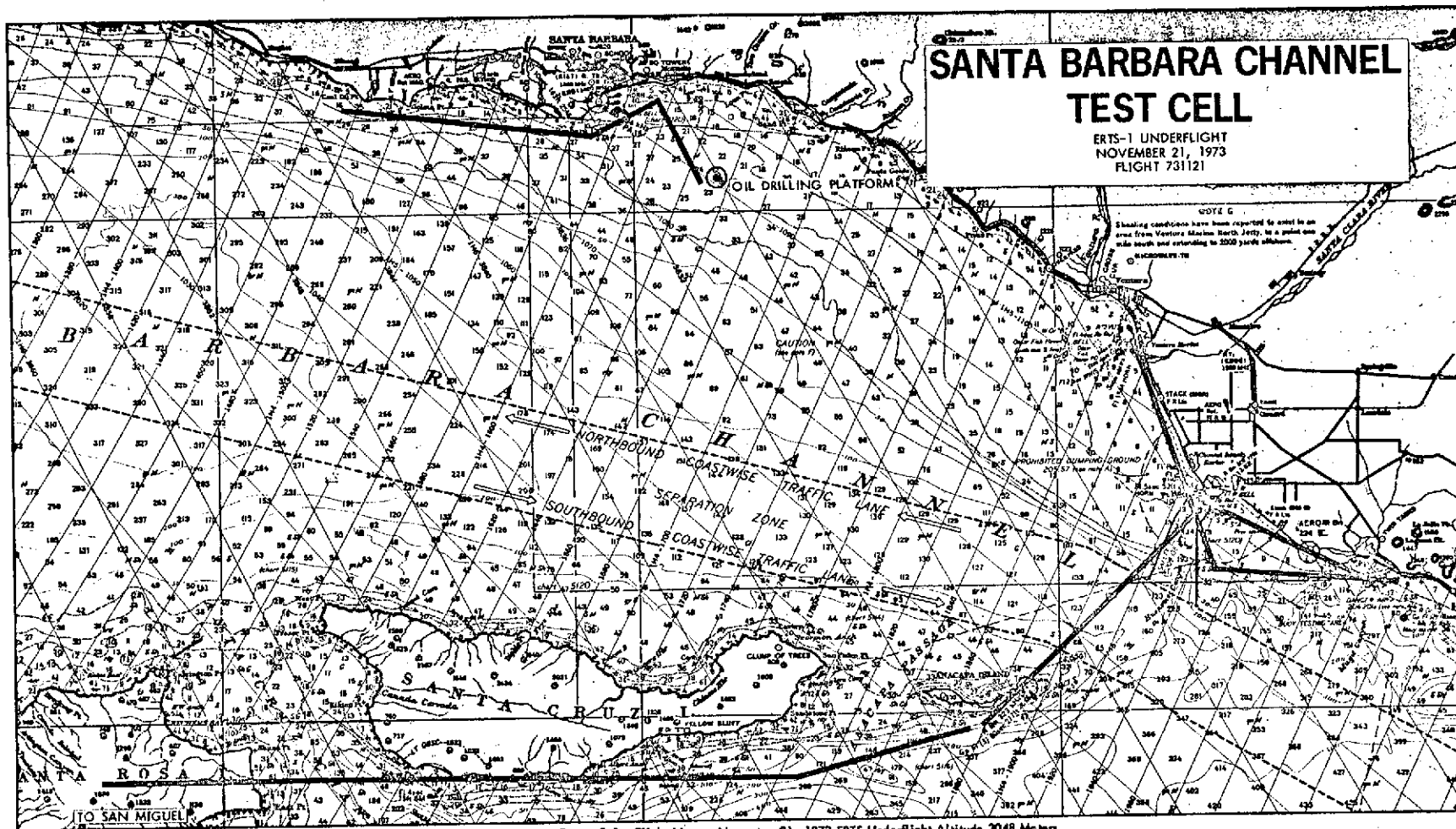


Figure 5-8. Flight Lines - November 21, 1973 ERTS Underflight Altitude 3048 Meters

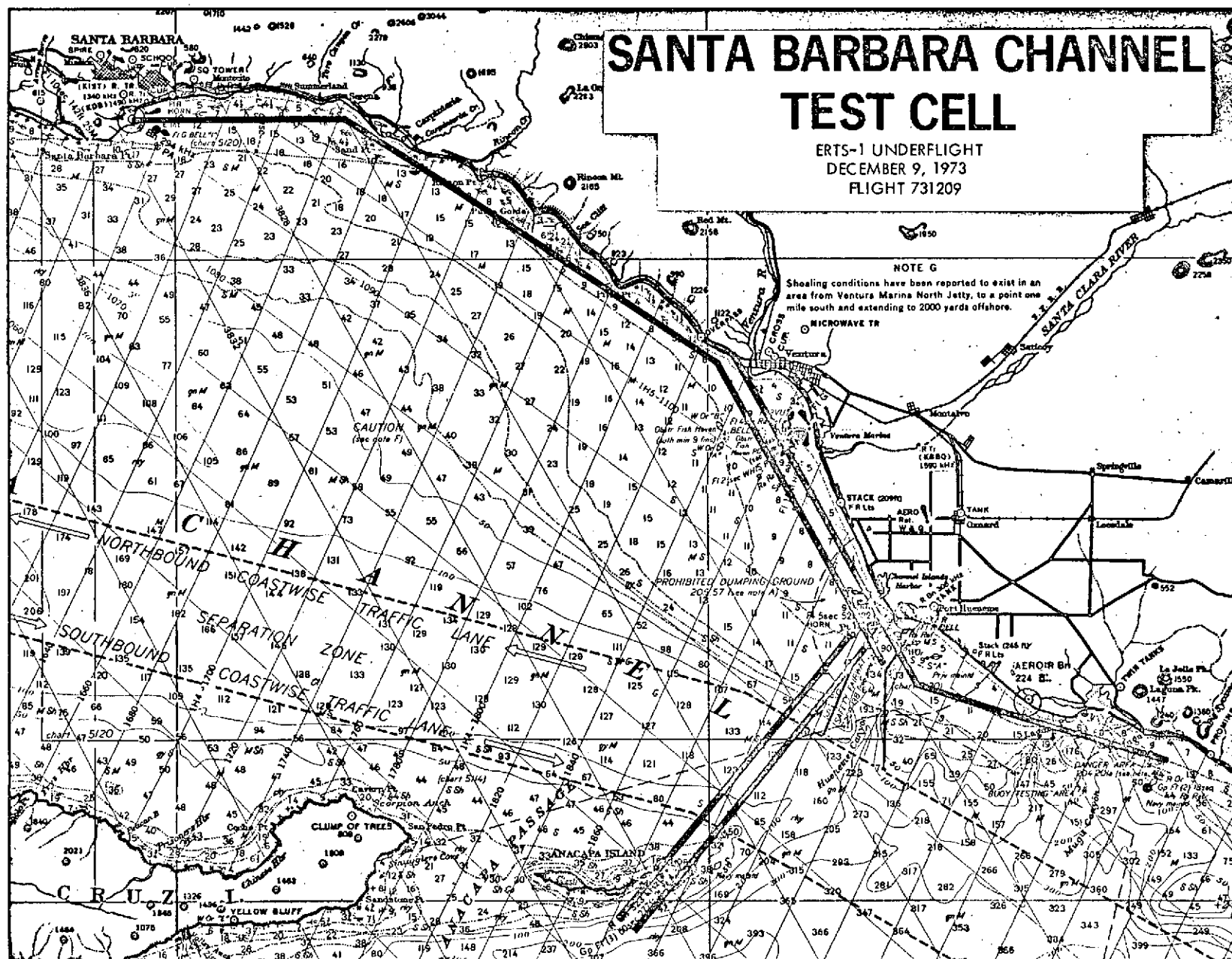


Figure 5-9. Flight Lines - December 9, 1973 ERTS Underflight Altitude 3048 Meters

5.3 EXPERIMENT ANALYSIS OF 1973 SEDIMENT DATA

The scale of the original 70 mm negative film chips provided by NASA and employed in this calibration procedure are 1:3,369,000. Scanned at an effective aperture of 50 microns, this implies that each film density value employed is at best an average over a 170 meter area. The sediment sample on the other hand represents an area of no more than a meter or so. Figure 5-10 depicts the implications of these scale mis-matches. Evidently, in at least the nearshore zone, we are seeing water mass and surface suspended sediment changes on the order of a meter or so across convergence lines, 10 to 100 meters due to eddies, and lobate mixing patterns due to wave mixing and tidal and fluvial discharge currents. Thus, we would expect a generally smoother curve for the ERTS film density line scan vs. the scatter in suspended sediment values from boat samples at intervals along the same line. Also shown as a control on the sediment values and the laboratory measurement procedure are the Secchi disk extinction depths obtained at the same time as the sediment values. The Secchi disk values more or less confirm the suspended sediment readings, but imply intermittent (random) errors in the laboratory sediment analysis technique or sampling procedure (e.g., point A in Figure 5-11). This comparison verifies, as predicted by the dimensional arguments above, that while the ERTS averaged values are quite stable with an apparent periodic variation of 1,000 m or so, the point sample sediment values are more highly variable and, in fact, least stable in the nearshore zone (e.g., Figure 5-10). This implies the requirement to average as large a number of point samples as possible. This implies combining the data from both underflights for which the Anacapa line was sampled (11/21/73 and 12/9/73). This, however, requires that a normalization procedure be applied to remove differences in color brightness due to season and atmosphere changes between the two missions, and any variations introduced by NASA in writing the ERTS film clips employed in the analysis, Figure 5-13 illustrates the difference in available light as measured at the surface between the two days, relative to the spectral sensitivity of the two MSS bands employed for the sediment analysis. Independent of variance in the water column's extinction depths for light of these wavelengths on the two days, there is a significant change in the orange-red (MSS-band-5), a difference of about 30%. The green-yellow band 4 on the other hand has almost the same integrated intensity. If this were the only change in the negatives, we could presumably calibrate directly from these curves.

The second variable requiring normalization is the apparent variance in film base density and gamma on the respective ERTS negatives since it is desired to compare sediment readings and density values for both days. To do this, all four negatives were scanned with the Joyce Loebel isodensity tracer along the Anacapa sea truth traverse line. At the same time, a calibrated reference density wedge and the density wedge imprinted on the film were scanned with a MacBeth Microdensitometer, with the following result:

Table 5-3

Comparison of ERTS-Negative Stepwedge Densities

	1	2	3	4	5	6	7
	Wedge Number						
Band 4 - ID 1504-17585 - 12/9/73	.46	.82	1.26	1.47	1.64	1.75	1.86
Band 5 - ID 1504-17585 - 12/9/73	.47	.82	1.26	1.48	1.62	1.74	1.84
Band 4 - ID 1486-17590 - 11/21/73	.74	1.27	1.64	1.80	1.92	2.00	2.08
Band 5 - ID 1486-17590 - 11/21/73	.61	1.16	1.54	1.71	1.82	1.90	1.99

Again we evidently have to account for the additional problem over solar brightness variations of density errors introduced in writing the source negatives. In view of this dual calibration problem, and the limited range of water density values shown, it was decided to perform a linear calibration to the channel 4 November 21 values employing the San Miguel Island dune fields for a bright standard and deepwater beyond the channel islands as a dark standard. All of the resulting normalized values of ERTS - negative density were then combined and plotted against the corresponding averaged suspended sediment values for both days. Figure 5-14 shows the implied dependence of normalized (to MSS Channel 4 on November 21, 1973) density to suspended sediment load. Two sediment readings were discarded, one due to contamination and the other because it yielded no sediment in a nearshore sample. The dependence out to 2 mg/l is quite good. The variance for sediment loads more than 2 mg/l is evidently greater.

There are three possible explanations. The first is that the nearshore, higher suspended sediment values have considerably more eddy structure than the offshore (lower) values and hence require a denser sea truth point sampling grid, and in fact this is verified by the aerial photography. Secondly, the higher nearshore suspended sediment values imply maximum penetration in the yellow-orange MSS band 5 and hence an inferior sensitivity to this layered structure since it is integrated through a greater depth of the water column. Conversely, in the deeper, clearer water, one would expect the channel 4, green-yellow light to penetrate to greater depths and hence be less sensitive to sediment structure. But, of course, less detailed structure is expected. Figure 5-15, showing a breakdown of the individual normalized spectral responses for each day, basically confirms these ideas.

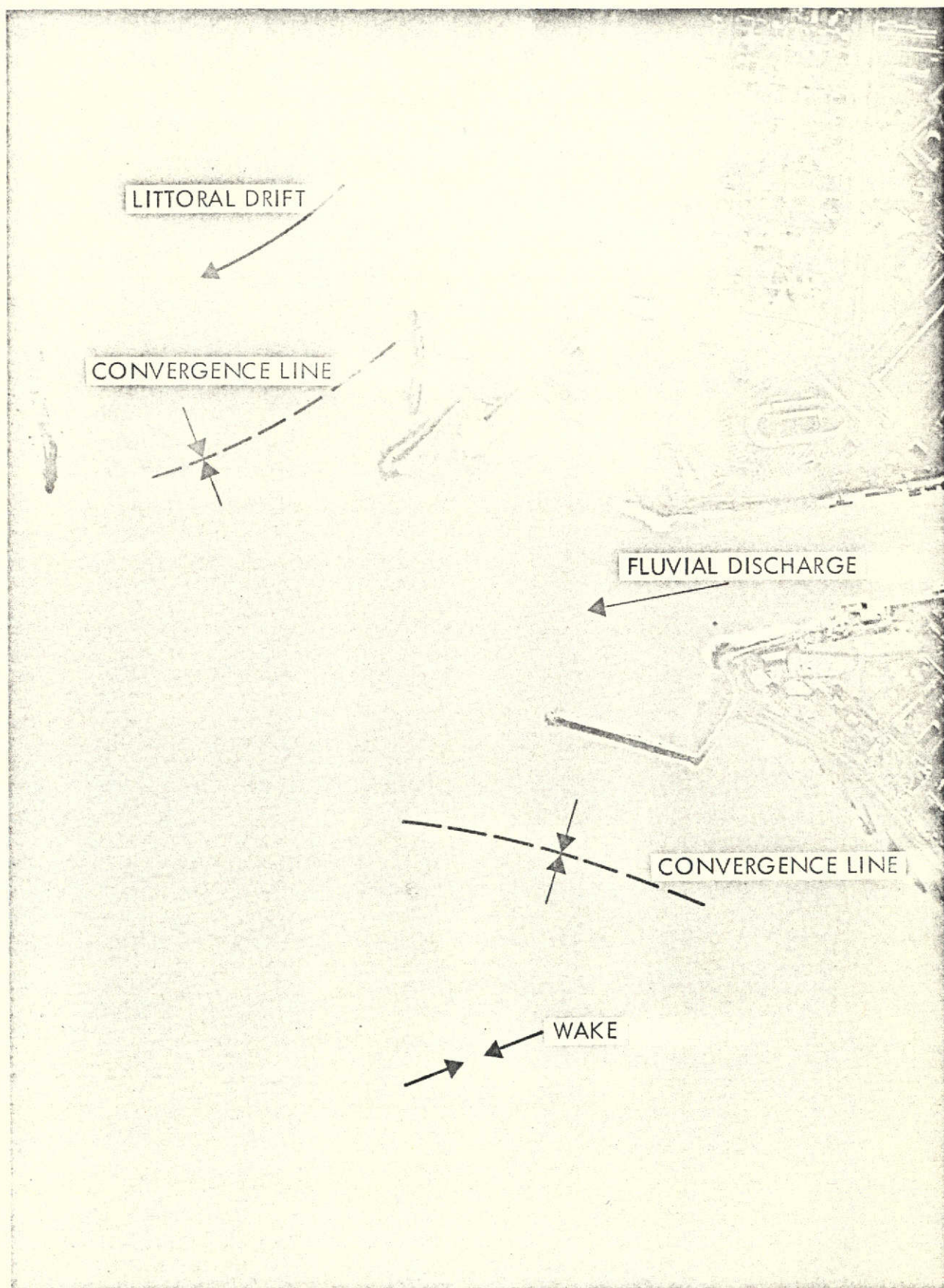


Figure 5-10. Airborne Photo Evidence of Nearshore Sediment Inhomogeneity
(Point Hueneme, 12/9/73)

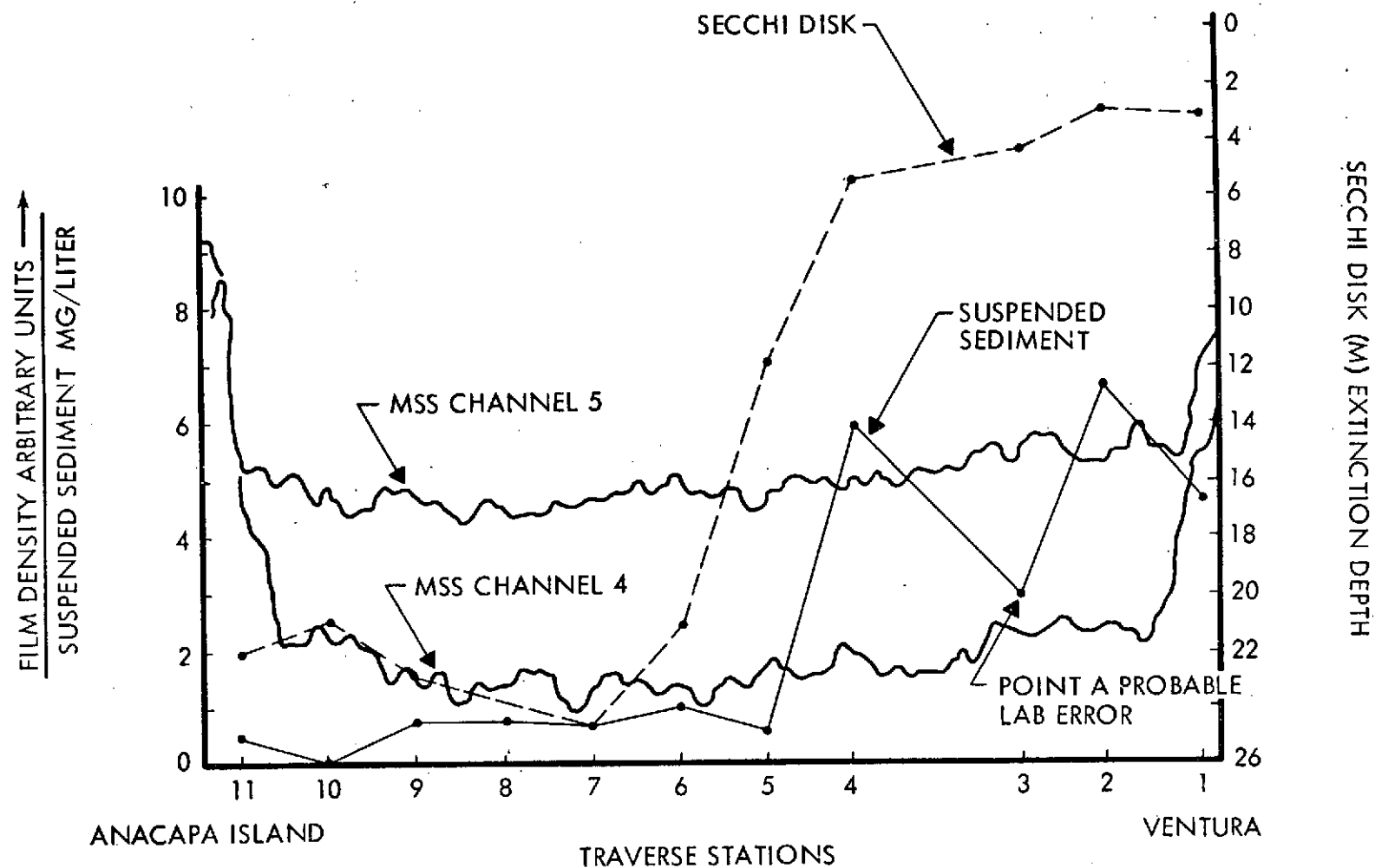


Figure 5-11. COMPARISON OF UNNORMALIZED ERTS FILM DENSITY
SEDIMENT LOAD AND EXTINCTION DEPTH.
(9 DECEMBER 1973)

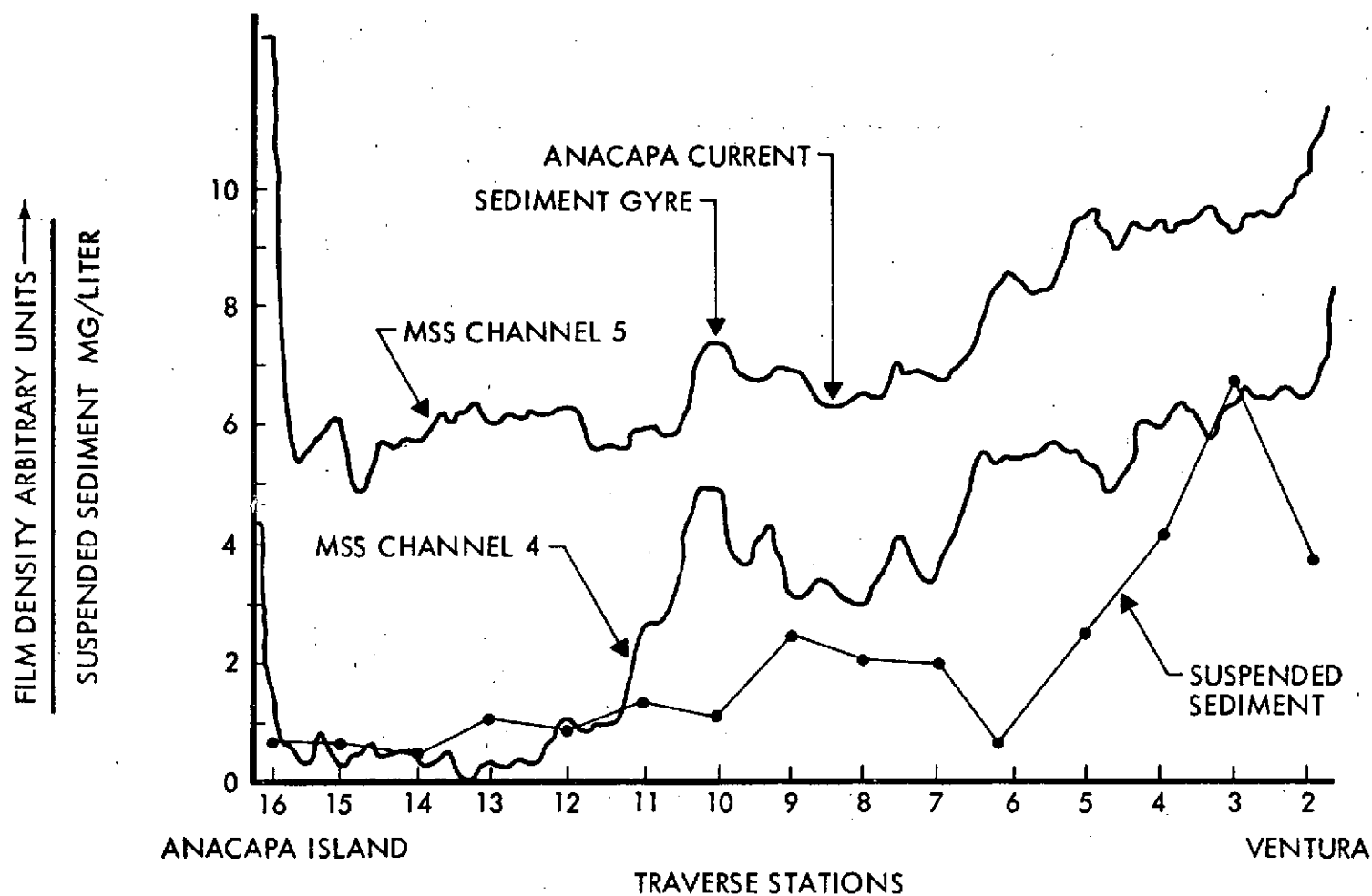


Figure 5-12. COMPARISON OF UNNORMALIZED ERTS FILM DENSITY
SEDIMENT LOAD AND EXTINCTION DEPTH.
(21 NOVEMBER 1973)

COMPARISON OF AVAILABLE LIGHT
SPECTRUM - VENTURA
(10:00 AM 12/9/73 AND 11/21/73)

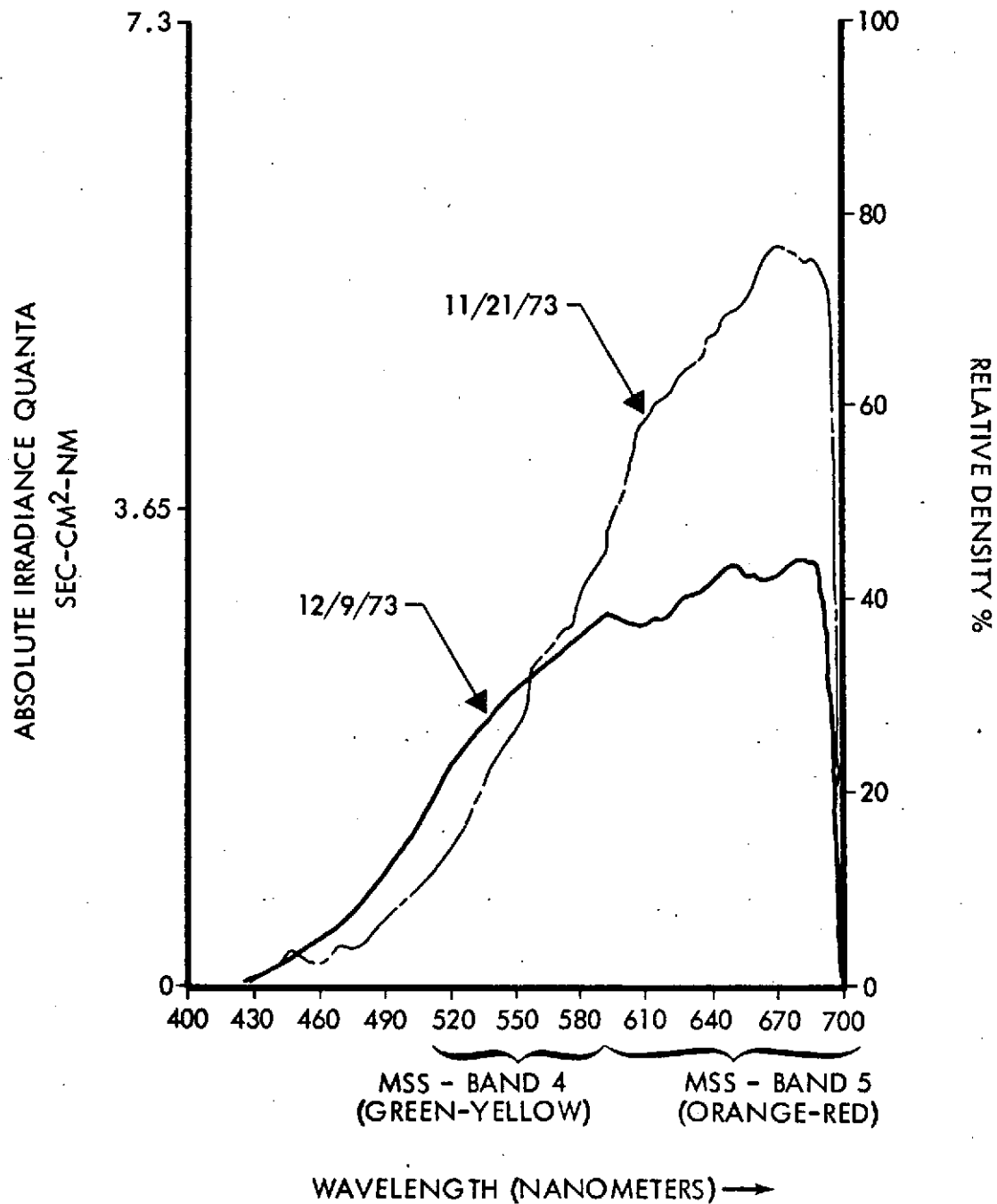


Figure 5-13. Comparison of Available Light Spectrum - Ventura
(10:00 am, 12/9/73 and 11/21/73) IRD Quanta Spectrometer

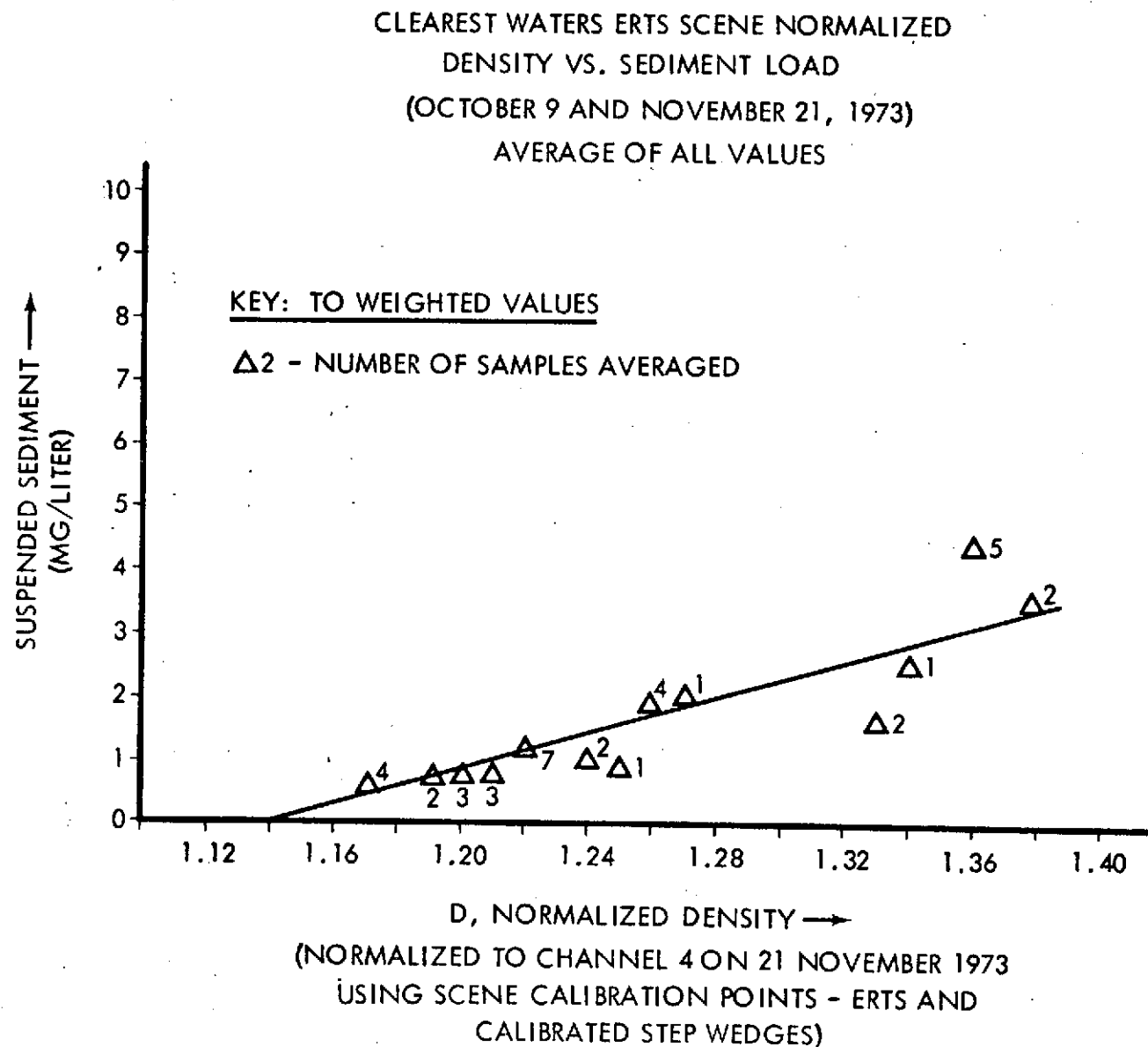


Figure 5-14. Clearest Waters ERTS Scene Normalized Density Vs. Sediment Load (10/9 and 11/21/73) Average of all Values

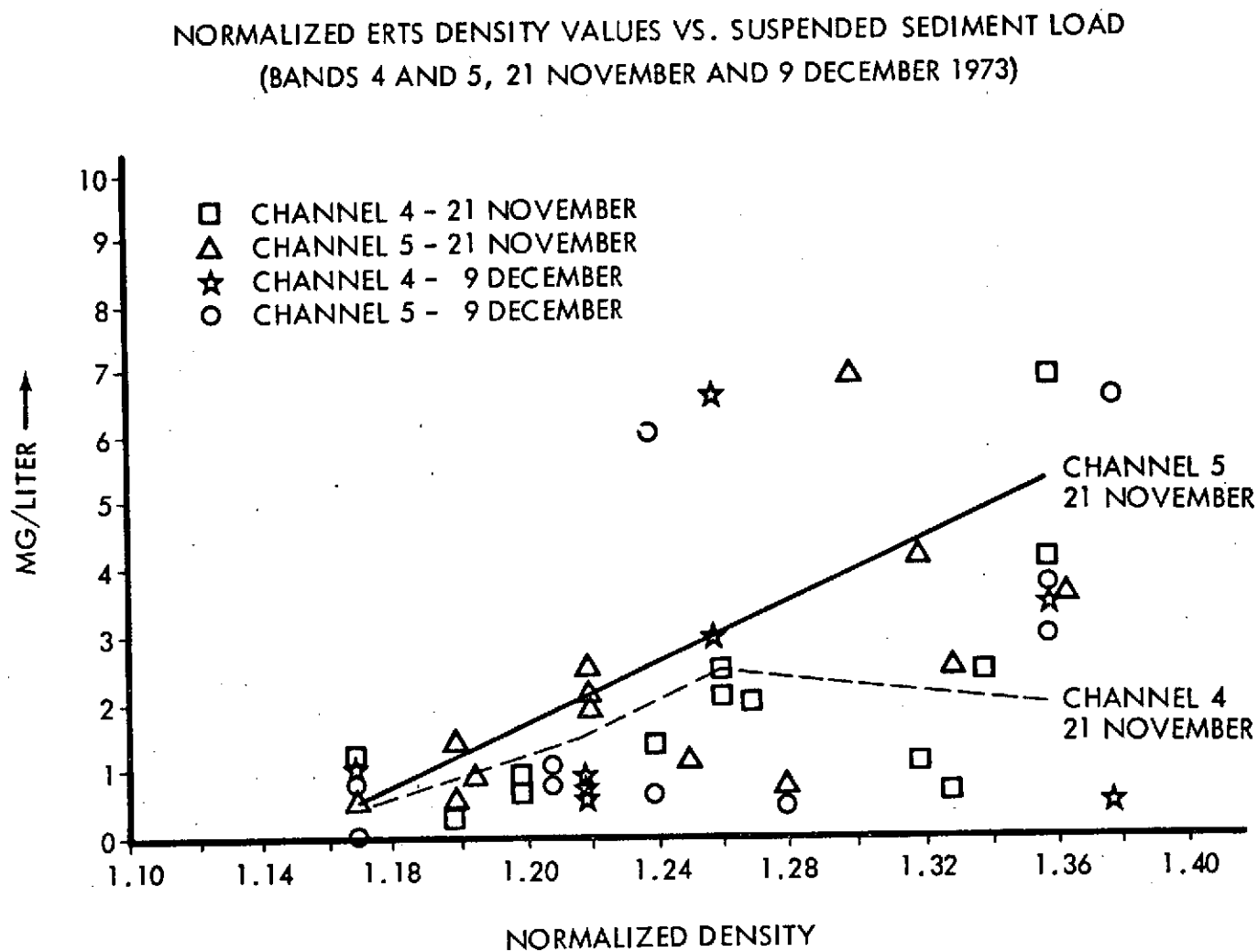


Figure 5-15. Normalized ERTS Density Values Vs. Suspended Sediment Load
(Bands 4 and 5, 11/21/73 and 12/9/73)

5.4 CONCLUSIONS

The major concern of this section is to evaluate the feasibility of establishing a sediment load/film density dependence which would permit the quantitative estimation of the amount of sediment represented by the visible sediment plumes in the ERTS photography. The field studies done are of limited extent, essentially two days of a given water type for a given season. The problem treated is complex; a different result can be expected for each combination of wavelength, sun angles, suspended particle size, type and vertical distribution in the water. However, such a dependence has already been demonstrated for these same waters from aircraft photography (Fig. 5-3, Hodder 1973) and for lab studies of east coast waters (Ghovanlou, 1973 - Figure 5-4). From both these results, it can be concluded that the desired film density/sediment load relationship exists. However, both these results are for relatively high sediment loads (5 to 50 mg/liter). The initial look at ERTS data on the other hand, where Drake's (1972) non-simultaneous sediment data were compared to like conditions ERTS film density, imply an opposite conclusion (Fig. 5-5). There seems to be no linear dependence of film density at high sediment loads above 4 mg/liter. On the other hand, the ERTS film density values do appear to relate to the lower sediment loads, where the aircraft experiments showed a lack of sensitivity.

The Anacapa Island experiments were designed to evaluate this preliminary conclusion, by providing a test cell with a high sediment gradient across a short distance. The major results of this last experiment (Fig. 5-14 - all data) suggest that indeed a quantifiable relationship can be obtained to quantify sediment load from the MSS Band 4 ERTS imagery. A more detailed evaluation, however, again indicates the bimodal nature of this relationship. As for the earlier experiment, we again find (Fig. 5-15) the least scatter in the raw data for the sediment loads below 3-4 mg/liter.

The explanation for this apparent disparity between the ERTS and aircraft results appears to lie in the different scale turbidity clouds mapped by the two systems. The ERTS satellite is apparently incapable of resolving the small scale eddies and inhomogenities recognized in the aircraft imaging, which are of course mappable when resolved. The lower density sediment variations are apparently larger dimensioned, and the "averaging" applied by sampling at the ERTS scale offers a superior fit to the large area trend in sediment variation. The aircraft imagery collected during this experiment provided detailed information on the overview that ERTS supplies. Both sources of data are required for a comprehensive evaluation of sediment transport characteristics.

6.0 CONCLUSIONS

ERTS-1 imagery, representing reflected light from the ocean, reveals beneficial near-shore processes information. The MSS channel 4 ($0.5-0.6\mu\text{m}$) imagery provided the most usable data for this study. This channel's water penetration capability of approximately 15 meters resulted in knowledge of the transitory current and sediment transport features not available by other means. MSS channel 5 ($0.6-0.7\mu\text{m}$) was used to delineate the main core of sediment plumes and to differentiate between near surface and subsurface material. The two infrared channels MSS 6 and 7 ($0.7-0.8\mu\text{m}$ and $0.8-1.1\mu\text{m}$, respectively) were utilized mainly for water land boundaries.

The nearshore processes information that were interpreted from the ERTS-1 imagery includes: 1) monthly and seasonal current patterns, 2) source and distribution of sediment transport characteristics, 3) nodal points of coastal water motion, 4) riverine discharge pulsing and offshore movement, 5) water penetration characteristics, 6) effect of wind and coastal contour on sediment transport and surface dynamics, and 7) erosional and depositional sites. This knowledge is being incorporated into ongoing Corps operational projects. The benefits from using ERTS-1 in these projects is expected to result in more efficient utilization of maintenance and engineering funds. In planning coastal projects it is necessary to obtain the most current available data on the oceanic forces affecting the areas being considered. ERTS-1 imagery presents a new, broad view, continually updated source of information which can be applied to operational projects.

From the operational standpoint, the ERTS-1 nearshore processes information can be used in the following Corps' coastal responsibilities: 1) determination of the effect of dam construction on riverine discharge; 2) cliff erosional hazard to property; 3) environmental effect of riverine outfall and effluent discharge; 4) dynamic ocean environment at proposed sites of deep water ports; 5) transport and distribution of dredge effluent; 6) oil spill distribution; and 7) erosion and deposition in the vicinity of coastal construction projects. Dredging and groin placement programs alone cost the taxpayers over \$7 million a year along the California coast. More economical utilization of these funds is expected from continually updating ERTS data.

Examples of areas which are within the Corps responsibility which were studied include: 1) critical erosion from the headlands at the entrance to Bolinas Bay, 2-3; 2) deposition and necessary continuous dredging at Channel Island Harbor and Port Hueneme, Figures 3-4 and 5-10; 3) critical erosion and groin placement at Newport Beach, Figure 2-12; 4) effluent discharge at Humboldt Bay, Figures 2-1, 2-5, 2-6; 5) possible deep water port at Moss Landing in Monterey Bay, Figures 1-5, 3-7; 6) sediment transport behind the Los Angeles Harbor breakwater, Figure 2-12; 7) Russian River discharge and basin study, Figure 2-11; and 8) loss of beach sand at Devils Slide near San Francisco, Figures 2-7, 2-9, 3-1 and 3-2.

Detailed analysis was made of suspended sediments revealed by ERTS-1 imagery of the Santa Barbara Channel. A closely coordinated aircraft and sea truth collection program supplied valuable calibration information. The result was a means of determining the quantitative suspended sediment levels is possible; valuable data in measuring accretion and erosion of beaches in that area. During the ERTS study of this area, the possibility that pesticides from the Ventura-Santa Clara Rivers were being transported to the vicinity of the Channel Islands was detected. The National Park Service has noted, in these islands, that problems with weak shell structures of Brown Pelican eggs and stillborn California Sea Lion cubs are occurring and these conditions might be attributed to pesticides being introduced into their food chain. The suspicion that pesticides from river discharges are polluting the Channel Islands is still under investigation. However, ERTS imagery definitely illustrates the riverine discharges being transported to the Channel Islands.

As a result of this study, it was possible to plot currents for monthly and seasonal periods. Along the California coast, three major detectable seasonal changes occur. The California Current flows generally southward from July to November, the Davidson Current northward from mid-November to February, and the Upwelling Current Period from February to July. Monthly plots for the coast show seasonal changes and inshore-offshore current differences. The suspended sediment acted as tracer material during analysis of the currents. Sediment transport characteristics including source, distribution, gyres, mixing, erosion and deposition were detected.

Two techniques found to be very useful in interpretation of nearshore processes were the flying spot scanner (FSS) enhancements and the computer compatible tape (CCT) processing. The FSS was used to expand or stretch the ERTS-1 density ranges which represented suspended suspensates on film and magnetic tape. The CCT's were used for discrete point density analyses, isodensity contour analyzer and mass concentration image analyses. The CCT processing techniques were also utilized in multi-channel computer processing. The ultimate result was to reveal information not detectable with the human eye or "normal" photographic processing techniques.

During the photographic processing of prints made from NASA supplied 70 mm negatives, two useful techniques resulted from several experiments to enhance ocean features. The first approach was the control of the slope of the gamma of a specific film's characteristic curve in order to increase the contrast displayed by offshore suspended material. The other photographic process that proved most useful was the use of Kodak type 2575 film. The characteristics of the film were more tailored to the contrast enhancement application in the density range of interest. This film displays an increased gamma for shorter processing times, thus simplifying the data processing work.

It is necessary to analyze nearshore processes in relationship to future coastal protection, procedures, ocean engineering projects and the design of coastal structures. In making the decisions on whether such projects should be carried out and in what way, one must define the coastal parameters, determine the importance and relationships of the processes, and correctly predict how a change in the coast will modify the nearshore environ. This ERTS-1 study represents an important new means of meeting these requirements.

7.0 RECOMMENDATIONS

1. We recommend continuation of ERTS imagery analysis of California nearshore processes for use in U. S. Army Corps of Engineers operational projects. This ERTS-1 research study has proven the usefulness of applying detectable information to the problems involved in coastal protection, harbor development, and ocean engineering projects at Moss Landing, Port Hueneme, Bolinas Bay, Newport Beach, Humboldt Bay, and Russian River. Each project requires a detailed analysis of regional and local coastal processes before management decisions can be made on construction and financing plans. ERTS imagery presents a source of continually updated information which can be applied to the transitory nearshore processes.
2. The dynamic range of the signal available for ocean and nearshore observations should be increased in spectral range and channel availability. Of the 127 digital levels available on MSS Channel 4, the majority of the nearshore processes studied were confined to a maximum 14 levels. This resulted in the need for extensive processing and density expansion (Section 3.0) that was necessary to extract information. The dynamic range might be expanded down to 4000\AA and divided by 200\AA increments.
3. The computer compatible tapes (CCT) should be processed so that the information from a single channel is on one tape rather than four. In the case of ocean investigations, it would be necessary to order only one or two tapes (i.e., MSS Channels 4 and 5) instead of the four now required to process a single scene. This would cut NASA tape costs and would result in a substantial savings to the investigator. Reformatting time on computers, individual programming and storage needs would all be reduced.
4. Although ERTS-1 was designed mainly for terrestrial investigations, we found in our study of coastal and oceanic features that it meets the minimum necessary requirements. The scale is suitable for large-scale phenomena, and the 80 meter resolution is usable. The main recommendation on design would be to increase resolution to 30 meters or less for determining coastal features such as estuary environment differentiation.
5. The recommended increase in resolution is a requirement only in the nearshore zone. Thus, a "zoom" capability requirement is implied where the coastline could be acquired and surveyed at a higher resolution than the rest of the area. The need for this improved resolution is evident from our comparison of the aircraft and ERTS images.
6. The 18-day orbit also presents a problem in studying the transitory near-shore processes. Based on the lunar tidal periodicities alone, statistical

consideration (Shannon's Theorem) would imply at least a 6-hour sampling interval and for most areas a 3-hour interval. This recommendation is coupled with that for higher resolution. Without higher resolution, sampling at 3 or 6 hour intervals will not be as meaningful in that the tidal phenomena of interest are with few exceptions (e.g., San Francisco Bay) small dimensioned.

7. Even with existing resolutions, a higher sampling frequency is implied, in that large dimension Coriolis circulation periodicities are as short as 24 hours (polar regions) and again required sampling at twice this frequency. Such sampling requirements clearly imply the use of nighttime sensors such as thermal IR and low light level sensors under full moonlight.

8.0 REFERENCES

- _____, 1966, Bolinas Channel and Lagoon, California: U. S. Army Engineering District, San Francisco, California.
- _____, 1971, Dredge disposal study for San Francisco Bay and estuary: U. S. Army Engineering District, San Francisco, California.
- _____, 1972, Use of remote sensing in the study of coastal processes: U. S. Army Engineering District, San Francisco.
- _____, 1973, The ecology of the southern California Bight, implications for water quality management: Southern California Coastal Water Research Project.
- _____, 1969, Kodak data for aerial photography: Eastman Kodak Company Publication, M-29.
- _____, 1972, Data users handbook: Goddard Space Flight Center, Document N. 71SD4249.
- Austin, Roswell W., 1972, Surface truth measurements of optical properties of the water in the Northern Gulf of California: in 4th Annual Earth Resources Program Review, V. IV, N72-29378.
- Bowerman, Frank R. and Kenneth Y. Chen, 1971, Marina del Rey: A study of environmental variables in a semi-enclosed coastal water: University of Southern California Sea Grant Program, Pub. N4-71.
- Brown, W. L., F. C. Polcyn and S. R. Stewart, 1971, A method for calculating water depth, attenuation coefficient and bottom reflectance characteristics: 7th Intl Remote Sensing Proceedings, Ann Arbor, Michigan.
- CCOFI, 1958, California Cooperative Oceanic Fisheries Investigations: Progress Report.
- Chamell, R. L., J. R. Abel, W. Manning, III, and R. H. Qualset, 1974, Utility of ERTS-1 for coastal ocean observation: The New York Bight Example: Marine Technology Soc. Jour. V. 8, No. 3
- Cook, David O. and Donn S. Gorsline, 1972, Field observation of sand transport by shoaling waves: Mar. Geol., V. 13.

- DeLong, Robert L., William G. Gilmarten and John G. Simpson, 1973, Premature births in California Sea Lions: Association with high organochlorine pollutant residue levels: Science V. 181.
- Drake, David Edward, 1972, Distribution and transport of suspended matters, Santa Barbara Channel, California, unpubl. Ph.D. dissertation: University of Southern California, Los Angeles.
- Drake, David Edward and Donn S. Gorsline, 1973, Distribution and transport of suspended particulate matter in Hueneme, Redondo, Newport and La Jolla Submarine Canyons, California: Contribution #316, Dept. of Geological Sciences, University of Southern California, Los Angeles.
- Ecker, Richard, 1973, Personal communication on study of Mad River mouth and adjacent beaches: U. S. Army Engineering District, San Francisco, California.
- Engle, J. C., 1966, The movement of beach sand: Elsevier Publishing Co.
- Fay, Remmon C., Eugene D. Michael, James A. Vallee and Genevieve G. Anderson, 1972, Southern California's deteriorating marine environment: Center for California Public Affairs, An affiliate of the Claremont College.
- Ghovanlou, A. H., G. D. Hickman, and J. E. Hogg, 1973, Laser transmission studies of east coast waters: Tech. Rpt. #2, Sparcom Inc.
- Goodell, H. G., C. M. Woolheater and K. L. Echternacht, 1972, Environmental application of remote sensing methods to coastal zone land use and marine resources management: University of Virginia, NTIS PB 214547.
- Hodder, D. T., 1973, Coastal bathymetric plotting: Space Division, Rockwell International, SD 73-SA-0131.
- Hodder, D. T. and M. C. Kolipinski, 1973, Airborne and satellite remote sensing of Anacapa Island for hydrology and aquatic biology: 13th International Technical Scientific Meeting on Space, Rome, Italy.
- Hsueh, Y. and James J. O'Brien, 1971, Steady coastal upwelling induced by an along-shore current: J. Physical Oceanography, V. 1.
- Inman, Douglas L. and Borchard M. Brush, 1973, The coastal challenge: Science, V. 181.
- Jones, James H., 1971, General circulation and water characteristics in the Southern California Bight: Southern California Coastal Water Research Project.

- Klemas, V., J. F. Borchardt and W. M. Treasure, 1973, Suspended sediment observations from ERTS-1: Remote Sensing of Environment, Ann Arbor, Mich.
- Kolpack, R. L. (editor), 1971, Biological and oceanographical survey of the Santa Barbara Channel oil spill: Vol. II, Physical, chemical and geological studies, Allen Hancock Foundation, University of Southern California, Los Angeles.
- Lawson, A. C., 1950, Sea bottom off the coast of California: Geol. Soc. American Bull., V. 61.
- Menard, H. W., 1964, Marine geology of the Pacific: McGraw Hill.
- Natland, M. L. and Kuenen, P. H., 1951, Sedimentary history of Ventura Basin, California and the actions of turbidity currents, p. 66-107 in Hough, J. L. Ed., Turbidity currents and the transportation of coarse sediments to deep water: Soc. Econ. Paleontologists and Mineralogists Spec., Pub. No. 2.
- Richardson, William S., 1971, Development of an operational system for measuring ocean surface currents from aircraft: U. S. Coast Guard Contract #DOT-CG-10, 737-A.
- Roberts, J. A., K. M. Beesmer, E. L. Geeman, 1970, Littoral transport study Crescent City, California: in Final Report on Crescent City, California, USACE, San Francisco District, August 1972.
- Ross, D. S., 1972, Water depth estimation with ERTS-1 imagery, International Imaging Systems Rpt.
- Schwartzlose, R. A., 1970, Surface currents off Southern California: California Cooperative Oceanic Fisheries Investigations, 33rd Annual Conference, Indian Wells, California.
- Schwartzlose, R. A. and Joseph L. Reid, 1972, Nearshore circulation in the California Current: California Mar. Res. Comm. CCOFI Rpt. 16.
- Skogsberg, 1936, Hydrography of Monterey Bay, California - thermal condition 1929-1933. Am. Phil. Soc. Trans., NS, V. 29.
- Scruton, P. C. and D. G. Moore, 1953, Distribution of surface turbidity off Mississippi Delta: Am. Assoc. Petroleum Geologists Bull., V. 37.
- Shepard, F. P. and K. O. Emery, 1941, Submarine topography off the California coast, canyons and tectonic interpretation: Geol. Soc. America Spec. Paper 31.
- Specht, M. R., D. Needler, and N. L. Fritz, 1973, New color film for water photography penetration: Photogrammetric Engineering, V. 39, No. 4.

Straughan, Dale (compiler), 1971, Biological and oceanographical survey of the Santa Barbara Channel Oil Spill 1969-1970: Vol. 1, Biology and Bacteriology, Allen Hancock Foundation, University of Southern California.

Swift, D. J. P., D. B. Duane and O. H. Pilkey, 1972, Shelf sediment transport: Process and pattern: Dowden, Hutchinson and Ross, Inc.

Trask, P. D., 1955, Movement of sand around southern California promontories: U. S. Army Beach Erosion Board, Tech. Mem. 76.

Wagner, R. J. and P. J. Lynch, 1972, Analytical studies of scattering and emission by the sea surface: Office of Naval Research 17608-6006-RO-00.

Williams, Jerome, 1970, Optical properties of the sea: U. S. Naval Institute.

APPENDIX A

SUMMARY OF FLIGHT OPERATIONS

A total of eleven Geoscience airborne data collection flights were conducted during the study. Six flights fulfilled contract requirements, and the additional five were performed to provide supplemental data. All flights are listed in Table A-1. The table also contains additional information pertinent to specific flights, as shown. Detailed flight logs were prepared for each data collection flight. These logs are available if more information is required. The following, however, is a series of short narratives presented to define flight operations. In addition, Figure A-1 is an aircraft flight line map. Metric altitude equivalents are 500' = 152 m, 5,000' = 1,524 m, and 10,000' = 3,048 m.

Airborne Survey of the Southern California Coast From Point Vicente to Dana Point on 12/14/72

After takeoff from L. A. International Airport at 0944 on the morning of December 14, 1972, the aircraft climbed and maintained an altitude of 10,000' A.G.L. Two calibration runs were flown over the test cell to set up the Emside and LN-3 mapping systems. A series of six data collection lines were then flown covering the coastline from Dana Point to Point Vicente. Actual data collection started at 1007 and ended at 1120. After completing this initial phase, the aircraft returned to the airport to replenish the IR detector with liquid nitrogen. A second sortie commenced at 1332 to cover an additional area. Two data runs were flown in a north-south direction providing complete thermal IR coverage of the San Gabriel River mouth. A third flight line was flown over the Bolsa Chica wetlands providing complete 70mm (Hasselblad) coverage. Table A-1 provides a summary of the instrumentation uses during this flight as well as subsequent flights.

Airborne Survey of the Santa Barbara Channel on 4/2/73

On April 2, 1973, a data collection flight of approximately two hours was conducted over the Santa Barbara test cell. Data was collected between 1030 and 1210. A total of nine flight lines were flown. From an altitude of 10,000 ft., six lines were flown in a north-south direction. The remaining three flight lines were flown at an altitude of 5,000 ft.

Airborne Survey of Monterey, San Francisco, and Santa Cruz on April 4 and 5, 1973

Sortes in the vicinities of Monterey, San Francisco, and Santa Cruz were conducted during a two-day period on April 1973. A total of 25 runs were flown. These data collection lines are shown in Figure A-1. On April 4, six runs were made from an altitude of 5,000 feet over the Monterey test cell. Data collection started at 0944 and was completed by 1022. The aircraft then climbed to an altitude of 10,000 feet.

The same flight lines were re flown between 1034 and 1054. Ten runs were made from 10,000 feet over the San Francisco test cell starting at 1112 which terminated at 1214. On April 5, a fourth sortie at 10,000 feet was flown. This mission consisted to three runs over Half Moon Bay, Santa Cruz, and the Monterey test cells. Data collection started at 0954 and terminated at 1100.

Airborne Survey of the Santa Barbara Channel on November 21, 1973

The survey of the Santa Barbara Channel Islands was conducted for approximately three hours on November 21, 1973. The aircraft maintained an altitude of 10,000 feet throughout all data acquisition runs. A total of seven runs were flown and are shown in Figure A-1. Aircraft takeoff from L. A. International was at 0930 for the first run which covered (on north heading) Mugu Lagoon to Channel Islands Harbor. The second run was started at 1010 on a west heading from Port Hueneme to Anacapa Island, and the third run on a northwest heading was flown from Santa Rose Island to San Miguel Island. The aircraft then flew east to get on a northwest heading to make the fourth run from Coal Oil Point to Santa Barbara Marina, and continuing on to the fifth data run to the Santa Barbara drilling platform. Upon completion of these five data runs, the Beechcraft turned south to cover the last two data runs from Ventura Marina to Point Mugu and Palos Verdes Peninsula to Dana Point. The aircraft then returned to L. A. International Airport at 1315.

Airborne Survey of the Santa Barbara Channel on December 9, 1973

The survey of the Santa Barbara Channel Islands was conducted for approximately three hours on December 9, 1973. The aircraft maintained an altitude of 10,000 feet throughout all data acquisition runs. A total of five runs were flown and are shown in Figure A-1. Aircraft takeoff from L. A. International Airport was at 0910 and arrived Ventura Marina at 0940 to make the first run north to Santa Barbara. Upon returning to Ventura Marina, the second run was made from Ventura Marina to Anacapa Island flying over the red dye patches released from the Geoscience Sea Truth boat. This second run was repeated from Anacapa Island to Ventura Marina. The fourth run was made from Ventura Marina to Point Mugu. Of special interest, a multicolor dye patch was released by the Corps of Engineers and was photographed at Point Mugu through a 5300, 5900 and 6400Å (+ 100Å interference filter). The final run was made south from Palos Verdes Peninsula to Newport Harbor. The aircraft returned to LAX at 1215.

Helicopter Survey of the Southern California Coast on February 15, 1973

The airborne survey of sediment plumes of selected sites along the Southern California Coast were conducted for approximately two hours on February 15, 1973. The Rockwell helicopter maintained an altitude of approximately 500 feet for all the data acquisition runs. A total of nine selected sites were photographed as shown on

Figure A-1. Takeoff from NR Seal Beach facility was at 1000 hrs. The initial run was flown in a southeastern direction covering the first five sites. The last run was flown in a northwesterly direction covering the remaining four sites.

Airborne Survey of the Santa Barbara and
Ventura Areas on February 23, 1973

An airborne survey of the Southern California Coast from Point Hueneme to Santa Barbara was conducted on February 23, 1973. Between 1031 and 1108, the area was mapped from 10,000 ft. The flight lines were re flown from 5,000 feet between 1112 and 1210. Figure A-1 shows the details of these specific data runs.

Helicopter Survey of the Southern California
Coast on March 20, 1973

A helicopter survey of sediment effluents resulting from a storm on March 19, 1973, were photographed on March 20. These features were photographed from a low altitude using 70 mm as well as 35 mm hand-held cameras. Coverage started at Dana Point ending at L. A. Harbor. Specific lines are shown in Figure A-1.

Airborne Survey of Storm Damage Along the
Southern California Coast on January 9, 1974

An aircraft, as well as a helicopter survey, was initiated on January 9, 1974, to map storm damage along the Southern California Coast. Damage resulted from storms which passed through this area on January 4-8, 1974. Areas from L. A. Harbor south to Dana Point plus Malibu Creek were covered with 70 mm and 35 mm oblique photography. Altitudes varied between 100-500 feet during data collection.

In addition, nine selected areas from Dana Point to the Ventura River mouth were photographed with a Wild RC-8. The aircraft then flew a continuous run with 70 mm coverage from Dana Point to Santa Barbara. Aerial coverage is shown on Figure A-1.

Table A-1. ERTS-1 Underflights - Geoscience

DATE OF FLIGHT	TEST CELL	FLIGHT #	ALTITUDE FEET***	SENSOR					AVAILABLE DATA ON FILM AND TAPE			
				LN-3 SCANNER	EMSIDE SCANNER	I ² S	HASSELBLAD (80 MM)	35 MM	TRI-X 2403	TAPE	MINUS BLUE (K-2)	EKTA (WRATTEN 12)
12-14-72	SAN GABRIEL RIVER BOLSA CHICA	721214*	10,000'	• •	•		• •		• •	• •	• •	• •
4-2-73	SANTA BARBARA CHANNEL	730402*	10,000' 5,000'	• •	• •	• •	• •		• •	• •	• •	• •
4-4-73	MONTEREY MONTEREY SAN FRANCISCO	730404*	5,000' 10,000' 10,000'	• • •	• • •	• • •	• • •		• • •	• • •	• • •	• • •
4-5-73	HALF MOON BAY SANTA CRUZ MONTEREY	730405*	10,000'	•			•		•		•	•
11-21-73	SANTA BARBARA CHANNEL IS. VENTURA, PT. MUGU, PALOS VERDES DANA POINT	731121*	10,000'				•				•	•
12-9-73	SANTA BARBARA CHANNEL IS. VENTURA- SANTA B., PT. MUGU, PALOS VERDES, DANA POINT	731209*	10,000'				•	•			•	•
2-15-73	SO. CAL. COAST	HELICOPTER**	500'				•	•				• (NO FILTER)
2-23-73	SANTA BARBARA VENTURA	FIXED WING**	10,000'	•	•	•	•		•	•	•	•
3-20-73	SO. CAL. COAST	HELICOPTER**	500'					•				•
1-9-74	SO. CAL. COAST	FIXED WING**	10,000'			• (RC-8)	•					• (NO FILTER)
1-9-74	SO. CAL. COAST (STORM DAMAGE)	HELICOPTER**	500'				•	•				• (NO FILTER)

* CONTRACT FLIGHTS

** OPTIONAL NON-CONTRACT FLIGHTS

*** 500' = 152 meters

5,000' = 1,524 meters

10,000' = 3,048 meters

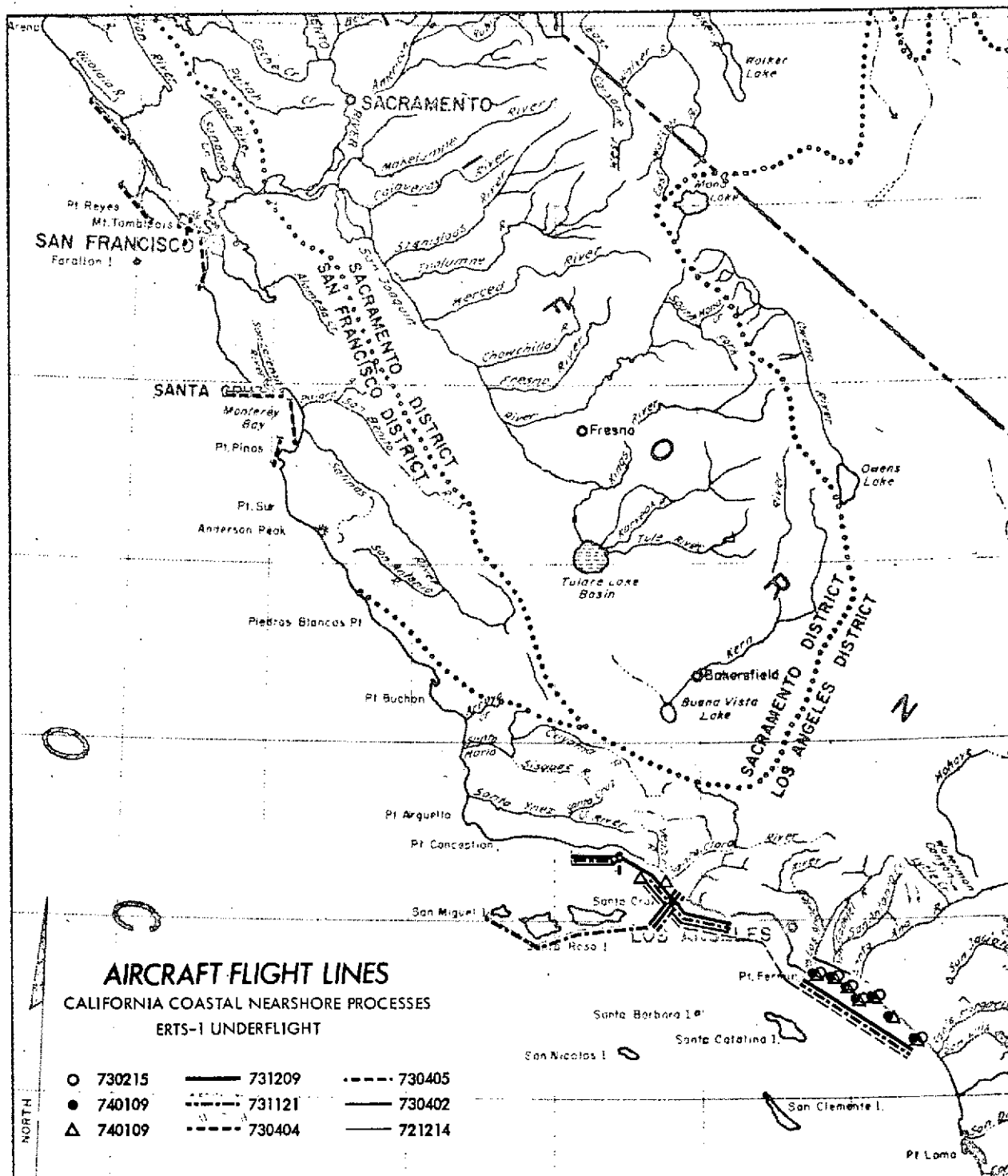


Figure A-1. ERTS-1 Underflights - Geoscience

APPENDIX B

ANCILLARY SUPPORT EQUIPMENT

The ancillary support equipment was used during aircraft flights and in enhancement and interpretation. It is variously referred to throughout the text of this report.

Multiband Camera

The International Imaging Systems (I²S) Mark I system is a four band multispectral camera. A single shutter simultaneously records four 3.5 X 3.5" spectrally filtered images onto a 9 X 9" format. The optical system consists of four Schneider Xenotar 150 mm focal length lens in conjunction with their respective bandpass filters. Image scale is maintained between the four images by selective matching of the lens/filter assemblies. The I²S system was used to collect data displaying coloration changes within concentrated sediment anomalies and river discharges, as well as detecting the movement of coastal currents (3.5" = 89 mm).

Data Color System

Spatial Data's Model 703 Data Color System is a raster scanning densitometer with a color coded display. A low noise 525-line video camera is used to scan transparencies (or hard copy prints). The camera video signal is then digitized into 32 levels with a unique color being assigned to each for display purposes. Such a system is programmable in the sense that the color range can either be shifted up or down over the total density range, expanded or compressed to encompass specific density ranges.

This density slicing technique not only allows the interpreter to interact with the system, but provides rapid quantitative evaluation of specific targets within the context of the total image. Such features as sediment plumes, river discharges, as well as other anomalies were processed displaying details with color contrast as an aid for interpretation.

Scanning Microdensitometer

The Tech Ops-Joyce Loebel device used for the ERTS-1 contract is both a scanning microdensitometer and an isodensity plotter. This system records a total of 64 levels of gray with considerably higher spatial resolution than the Data Color System. The output of the isodensitracer mode is a two-dimensional density map which is color coded. In the scanning microdensitometer mode, the quantified density values read alone along a single scan line are plotted as a line trace of density versus distance along the scan.

Preceding page blank

Both devices were used under the contract for the enhancement of imagery for the purpose of locating sediment plumes and to determine the concentration of sediment within the plumes by the different densities shown on the density plot.

Bendix Infrared and Ultraviolet Thermal Mapper

The Model TM/LN-3 Thermal Mapper used on the ERTS-1 contract underflights is an airborne single channel scanner system designed to utilize four interchangeable detector modules. The four detector modules which are currently available provide spectral coverage ranging from 0.2 to 14 microns. The bandwidth used under this contract was 8-14 micron. The data may be simultaneously recorded on magnetic tape while photographically recorded in-flight on 70 mm film. The scanner has a 2.5 milliradian instantaneous field of view which is swept through a 120° lateral scan.

This system was used in the California Coast Nearshore Processes Study for the purpose of detecting current flow by interpreting temperature differences on surface waters.

Bendix 9-Channel Scanner

The Multispectral Scanner used for the ERTS-1 contractual underflights operates in the visible/near infrared spectral band to provide remotely sensed data from an airborne platform. The scanner includes two calibration sources (a black-body reference and a skylight reference). The electronics provides for automatic reference level setting and gain stabilization. The scanner collects spectral reflectance data in 9 band widths from 0.38 to 1.2 microns. The scanner has a scan angle sweep of 120° with an instantaneous field of view of 2.5 milliradians.

The 9-channel data was used on the ERTS-1 contract for the purpose of data detecting and interpretation of surface water temperature differences to detect coastal current flow.

EDP Scanning Microscope

The EDP scanning microscope is a general purpose film scanner capable of digitizing photographic film transparencies, photographic prints as well as other specimens. Resulting data can be stored on digitally coded magnetic tape for inputting to other digital image processing equipment. However, the basic instrument also includes an integral facsimile recording system through which magnified real time recording is possible. These recordings can either be in the form of continuous tone reproductions of the sample or as density contour maps containing up to 32 contour lines. The range and contour intervals are programmable via front panel controls.

Likewise, the density and contrast of the continuous tone recordings are controllable. In addition, an edge enhancement circuit is provided. The recording can also be a combination of the available processing techniques.

Photometrics, Inc. provided an EDP system on a trial basis to support the ERTS-1 contract. ERTS frame No. 1486-17590-5 was scanned into approximately 3 million data points. Numerous magnified recordings were produced as 8-inch diameter enhancements. The 70 mm bulk negative was processed with spatial resolutions to 1 micron and density discrimination to .02 density discrimination to .02 density units. The results proved the EDP system to be a useful tool for processing ERTS data. Figure B-1 is an example of the EDP product.



Figure B-1. EDP Scan - Santa Barbara Area

ERTS-1 scene 1486-17590-5, magnification 10X, scanning aperture 200μ . Contour of scene brightness differentiation.

APPENDIX C

ERTS DATA UTILIZATION

The following reports resulted directly from the techniques and processes developed during the California Coast Nearshore Processes Study. Of basic concern in this study is to develop a handbook of remote sensing image enhancement methods, for application to U. S. Army Corps of Engineers site selection problems.

The following paper was presented at the 49th Annual Joint Meeting of the Society of Exploration Geophysicists (SEG), American Association of Petroleum Geologists (AAPG), and Society of Economic Paleontologists and Mineralogists, San Diego, California, April 26, 1974.

A COMPARISON OF SIDE-LOOKING RADAR AND ENHANCED ERTS-1 SATELLITE IMAGERY FOR TECTONIC MAPPING OF THE CARMEL BASIN IN THE CALIFORNIA COAST RANGES*

D. T. Hodder, L. V. Lewis, Geosource International, and
R. Gelnet, U. S. Army Corps of Engineers

Side-looking radar has been employed in remote areas as a pioneering reconnaissance tool for mapping tectonic and related features of subtle topographic expression, such as fault linears, beach ridges, fold structures, and drainage patterns. Even though available radar imagery (e.g. X and K band) cannot penetrate foliage canopies, the terrain following of the top of the canopy is sufficient to contour surface features. Due to the low illumination angle of the side-looking radar it is possible to exaggerate very low relief features. ERTS-1 imagery has also been employed for mapping of large-scale tectonic features, its low sun angle (10:00 am) produces shadow effects similar to those found in the radar but of lesser degree due to the relatively higher illumination angle. Further the look angle on ERTS-1 is limited to the solar zenith seasonal range at the 10:00 am overpass at a given latitude, while the radar look angle may be chosen to suit any tectonic "grain" of the terrain being studied.

This study compares ERTS-1 visible scanner imagery and airborne side-looking radar of the same area with these factors normalized to the extent practicable. The ERTS-1 image and radar mosaic (Figure C-1) are compared at a scale of 1:250,000 with similar look and solar illumination angles. The area chosen for the comparison is in a remote, seismically active part of the Santa Lucia range where the geology is both complex and largely unknown. Various digital and analog enhancement procedures are applied to the

* A wider application of these ideas and analysis methods has been presented in the Geosource report "Proposal for an Investigation of Machine Processing of Geologic Data," February 1974.

ERTS-1 visible range scanner imagery to produce a radar-like, image (viz. Figures C-1 and C-3) showing significant linear features, trending not only NW-SE along the known predominant direction of faulting but also NE-SW indicative of major cross faulting. Further, large arcuate thrusts are shown in the enhanced ERTS imagery, as well as surface multispectral reflectance changes corresponding to terrain and vegetation boundaries. These features are not as noticeable in the unenhanced imagery and compare favorably to the features mappable from the same scale radar imagery.

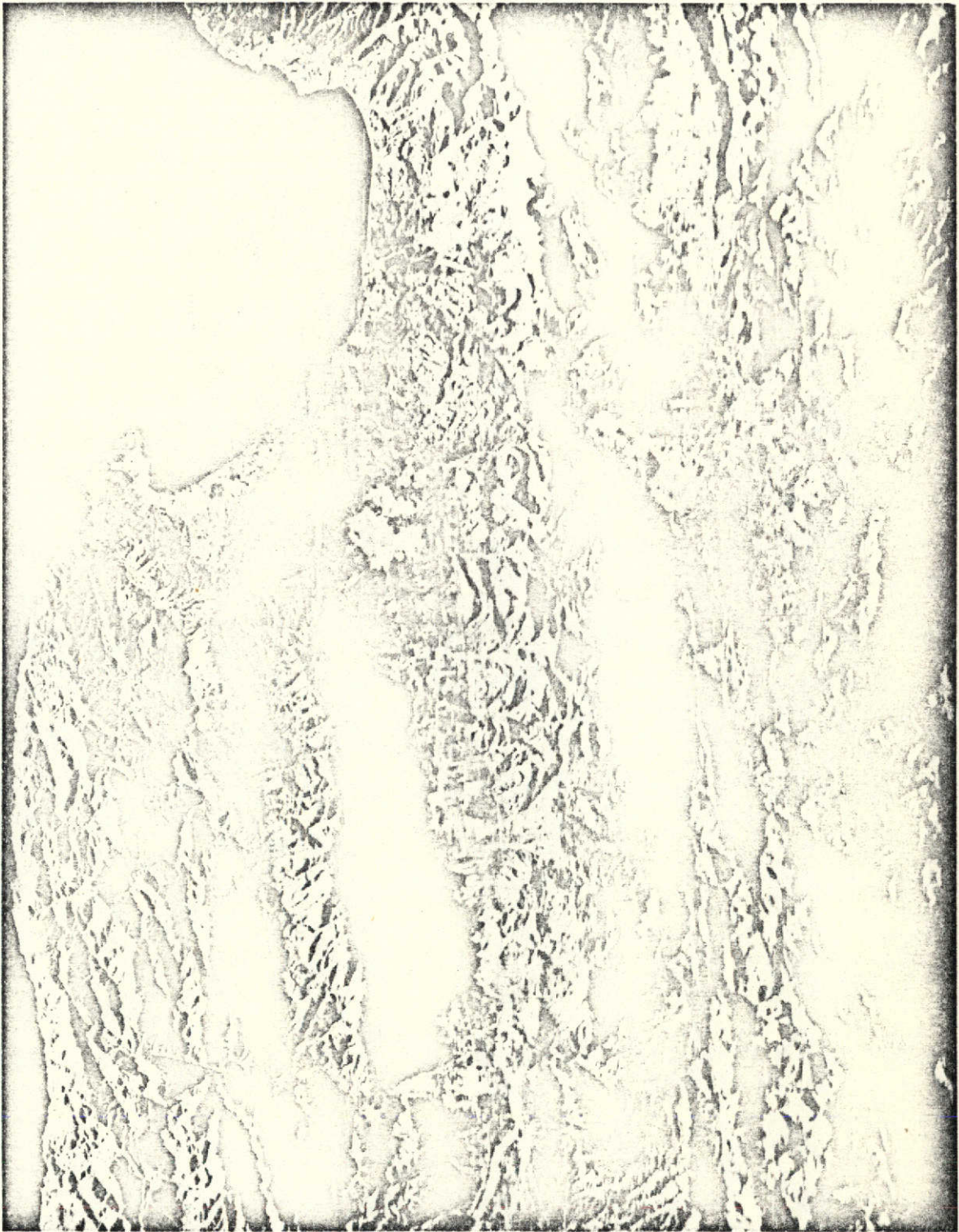


Figure C-1. X-Band Side Looking Radar Image of Monterey Bay and the Carmel Basin. Data was acquired by a military aircraft during a thunder storm period. Note that there are V/H and flight line distortions due to the flight lines "draping" the coastline, particularly in the lower portion of the image.

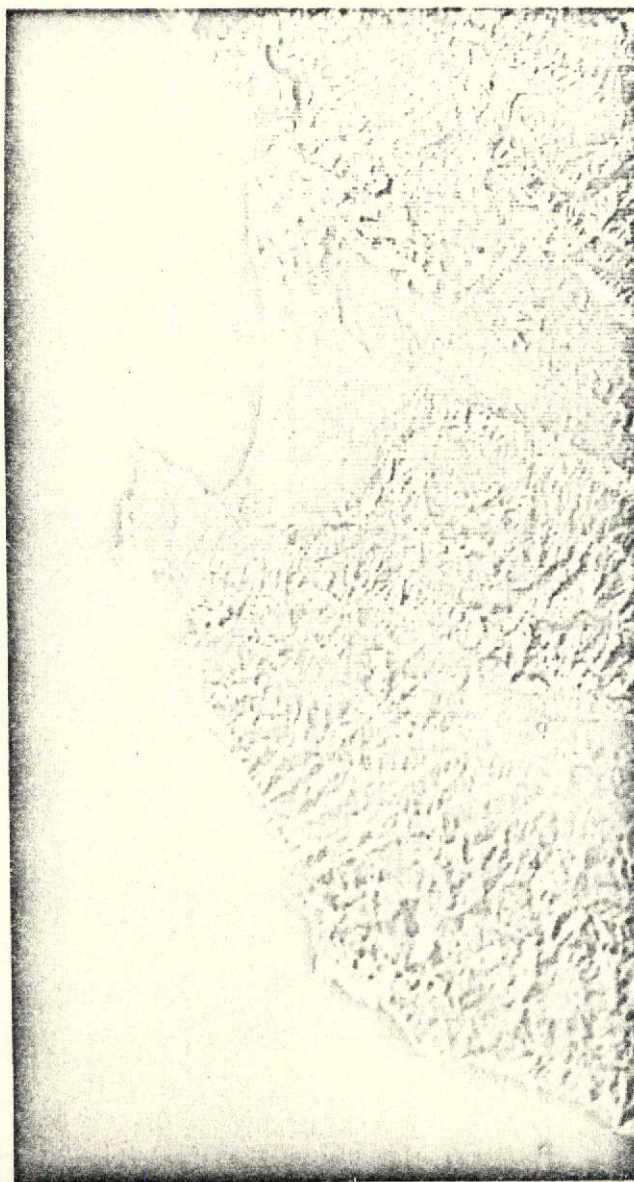


Figure C-2. Unenhanced ERTS-1 MSS Channel 5 for 22 January 1973, Monterey Bay and the Carmel Basin.

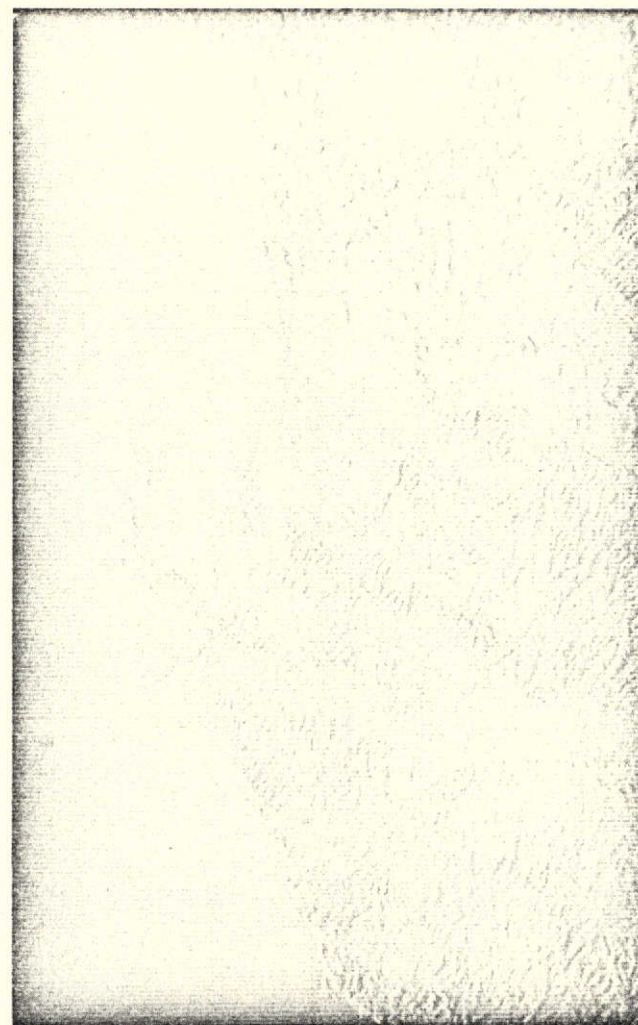


Figure C-3. Analog Derivative and Thresholding of the same MSS Channel 5 to enhance linears. The derivative is taken along a scan line to avoid enhancing the raster edge. Large areas of low contrast are suppressed to permit following linear features through various terrain patches. This enhancement clearly implies conjugate faulting to the San Andreas trend.

APPENDIX D

ATMOSPHERIC EFFECTS

The atmosphere represents an undefined transfer media which tends to mask information contained in ERTS imagery. We have made no attempt to specifically study or model the air column. However, its effect on one's ability to discern and delineate coastal processes (such as suspended sediment transport nearshore circulation patterns, extent of river effluent, etc.) can be extreme. One would expect that band 4 would penetrate deeper into water and thus show a weaker response for subsurface suspended sediment features. As noted by Klemas, 1973, East Coast investigators found considerable haze in band 4. This led them to prefer band 5 data for most nearshore processes applications. This conclusion was not reached in investigating the California coast. Band 4 data, despite its inherent haze phenomenon, proved to be superior to band 5 imagery for our application. As illustrated in the nearshore processes, Section (2), the extent and detail of sedimentary features are shown best in band 4 imagery.

It is realized that the atmospheric haze tends to attenuate signal return. Inspection of the inland features shows more contrast in band 5 than in band 4, illustrating proof of this phenomena. The water column through which band 4 data penetrates to image subsurface features also attenuates the signal in band 4. However, the fact is that band 4 is superior for nearshore applications. Two explanations are offered to account for the choice of band 4 imagery over band 5. The greater sediment extent imaged in band 4 could have resulted from the fact that suspended sediment is concentrated at a depth which exceeds the extinction depth of band 5 sensitivity. Thus, this sediment cannot be imaged in band 5. This explanation can be substantiated by inspection of Figure D-1.

The scene is a portion of Frame 1235-18075. Gray scale expansion to enhance sediment features was accomplished from CCT's data via the flying spot scanner. One notices immediately that band 4 shows great sediment detail while band 5 shows little or no sediment. The fact is that band 5 has undergone more enhancement (all land features being saturated, than band 4, yet sediment details are still not visible). The conclusion is that the sediment features were not imaged, confirming the above explanation. This being the case, the atmospheric effect was not the significant parameter. One may also conclude sediment features visible in band 5 imagery, for the most part, are surface or near-surface effluents. This statement implies that sediment in river effluents and areas of high sediment concentrations, such as found within inner bays and estuaries, would be visible in band 5. Inspection of ERTS imagery, generally, substantiates this premise.

The second explanation deals with the spectral signature of the sediment features. Laboratory analysis of sediment sampled within our region showed a peak reflectance at 4000Å. This implies that this peak matches band 4 sensitivity rather than band 5, thus further substantiating the empirical results.

In conclusion, band 4 imagery is superior to band 5 imagery for discerning and delineating sediment features along the West Coast of California. Two explanations have been offered to substantiate these findings. The explanations deal with parameters other than atmosphere effect. It is realized the atmosphere has an effect on one's ability to detect features.

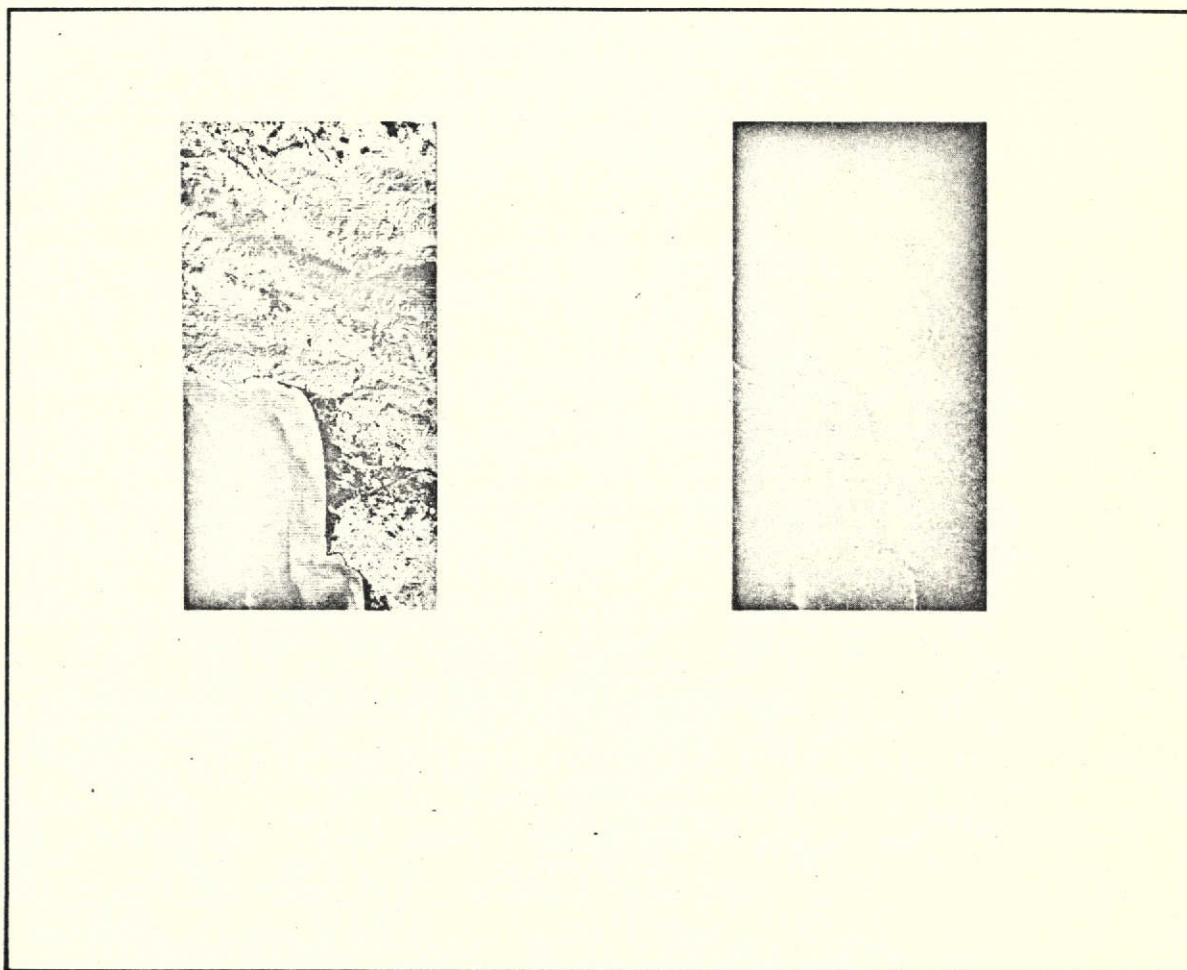


FIGURE D-1. ERTS-1 Strip 1, Block 1, Frame 1235-18075-4 and -5